

2012

# Transition metal complexes of oxazolinylboranes and cyclopentadienyl-bis(oxazolinyl)borates: Catalysts for asymmetric olefin hydroamination and acceptorless alcohol decarbonylation

Kuntal Manna  
Iowa State University

Follow this and additional works at: <https://lib.dr.iastate.edu/etd>

 Part of the [Inorganic Chemistry Commons](#)

## Recommended Citation

Manna, Kuntal, "Transition metal complexes of oxazolinylboranes and cyclopentadienyl-bis(oxazolinyl)borates: Catalysts for asymmetric olefin hydroamination and acceptorless alcohol decarbonylation" (2012). *Graduate Theses and Dissertations*. 12861.  
<https://lib.dr.iastate.edu/etd/12861>

This Thesis is brought to you for free and open access by the Iowa State University Capstones, Theses and Dissertations at Iowa State University Digital Repository. It has been accepted for inclusion in Graduate Theses and Dissertations by an authorized administrator of Iowa State University Digital Repository. For more information, please contact [digirep@iastate.edu](mailto:digirep@iastate.edu).

**Transition metal complexes of oxazolinylboranes and cyclopentadienyl-  
bis(oxazolinyl)borates: Catalysts for asymmetric olefin hydroamination and acceptorless  
alcohol decarbonylation**

by

**Kuntal Manna**

A dissertation submitted to the graduate faculty  
in partial fulfillment of the requirements for the degree of

DOCTOR OF PHILOSOPHY

Major: Inorganic Chemistry

Program of Study Committee:  
Aaron D. Sadow, Major Professor  
Marek Pruski  
Andreja Bakac  
Javier Vela  
Malika Jeffries-EL

Iowa State University

Ames, Iowa

2012

Copyright © Kuntal Manna, 2012. All rights reserved.

*Dedicated to my Family*

## Table of Contents

<b>Acknowledgements</b>	v
<b>Abstract</b>	viii
<b>Chapter 1 – Introduction</b>	1
General Introduction	1
Thesis Organization	8
References	9
<b>Chapter 2 - Neutral cyclopentadienyl-bis(oxazoliny)borato group 4 complexes as catalysts for enantioselective hydroamination of aminoolefins</b>	12
Abstract	12
Introductions	13
Results and Discussion	17
Conclusions	66
Experimental	67
References	103
<b>Chapter 3 - The desymmetrization of non-conjugated aminodienes and aminodiynes through enantioselective and diastereoselective hydroamination</b>	110
Abstract	110
Introduction	111
Results and Discussion	112
Conclusions	125
Experimental	126
References	136

<b>Chapter 4 - Concerted C–N and C–H bond formation in highly enantioselective yttrium(III)-catalyzed hydroamination: Comparison of stereinduction with zirconium analogs</b>	139
Abstract	139
Introduction	140
Results and Discussion	144
Conclusions	172
Experimental	173
References	191
<b>Chapter 5 - Acceptorless thermal decarbonylation of alcohols catalyzed by oxazolinyborato iridium complexes</b>	195
Abstract	195
Introduction	196
Results and Discussion	198
Conclusions	218
Experimental	219
References	231
<b>Chapter 6 – Conclusion</b>	235
<b>Vita</b>	238

## Acknowledgements

First and foremost, I am heartily thankful to my advisor Prof. Aaron D. Sadow, without whom this thesis would not have been possible. I am indebted to him for taking me into his group and teaching me how to appreciate science, to make molecules, and to have a vision for the future. Not only has he been an excellent teacher and mentor, but also his undaunted enthusiasm, suggestions, encouragements, and moral support inspired me to do more experiment in laboratory, and also helped to satisfy myself for my successful graduate research. I am very fortunate having an excellent advisor for my Ph.D. study. I have promised myself that I would try to be a mentor like Prof. Sadow in my future independent career.

I express my gratitude to all of my POS committee members- Prof. Andreja Bakac, Prof. Marek Pruski, Prof. Javier Vela, and Prof. Malika Jeffries-EL for their valuable support, advice, and input in my research.

Thanks to all of my past and present labmates in Sadow group: Ben Baird, Dr. James Dunne, Dr. Steven Neal, Dr. Hung-An Ho, KaKing Yan, Dr. Andrew Pawlikowski, Jiachun Su, Songchen Xu, Naresh Eedugurala, Zak Weinstein, Megan Hovey, Nicole Lampland, Aradhana Pindwal, Jacob Fleckenstein, Regina Reinig, Jing Zhu, Bradley Schmidt, Jiachun Su, Dr. Barun Jana, Stephanie Smith, and Debabrata Mukherjee for their cooperation, support and fun in last five years. Especially, I am grateful to Steven, Isaac, Kaking, James, and Andy who provided me a countless valuable suggestions and help since my first day in Sadow group. Thanks to Dr. Ho again for teaching me several introductory level courses such as golfing, snowboarding etc. I thank Marissa L. Kruse and Jessica Brown, who had conducted excellent research with me in Sadow lab. I also like to thank all other undergraduates who have worked in our lab over the years: Yitzhak, Brianna, Marlie, Tristan, Jared, Kate, Jooyoung, Rick, and Josh.

I gratefully thank all the members of CBS catalysis program in Ames laboratory. I enjoyed working as part of this great collaborative research project, and became knowledgeable with many other fields in chemistry outside of my research area. I like to thank Dr. Takeshi Kobayashi for the solid state NMR experiments of my samples. Thanks to Prof. Victor Shang-Yi Lin, Dr. Igor I. Slowing, Dr. Brian Trewyn, and their group members for our collaboration and also allowing me to access instruments within their laboratory. I also thank Prof. Marek Pruski and Prof. Jason Chen for our collaboration.

I like to thank Prof. Aaron D. Sadow, Prof. Andreja Bakac, and Prof. Arthur Winter for their invaluable lectures in CHEM courses. I thank all staffs in chemical instrument services, glass shop, and machine shop in our department. Thanks to Dr. Shu Xu, Dr. Sarah Cady, Dr. Dave Scott, and Dr. Bruce Fulton for helping me several NMR experiments in my research. Thanks to Prof. Malika Jeffries-EL for letting me use the HPLC in her laboratory. I would like to acknowledge support of all the members from Department of Chemistry, Iowa State University.

I owe my deepest gratitude to all professors and laboratory staffs in Panskura Banamali College and Indian Institute of Technology, Kanpur (IIT Kanpur) for teaching me chemistry. I gratefully thank Prof. V. Chandrasekhar at IIT Kanpur, whose guidance and encouragement influenced me significantly to be a motivated student during my graduate studies. I also express my gratitude to Prof. Mahadev Maity, Prof. Tridip Tripathy, and Prof. S. Pahari for their guidance and excellent teaching of undergraduate chemistry.

A very large thank you to my friends Saptak, Haradhan, Sujoy, Rajada, Akshay, Labakanta, Khitish, Subhas, Ajit, Amit, Parimalda, Biplabda, and Subratada. I can never forget their support and fun times we had together during my undergraduate and graduate studies. I also like to thank Pranaw Kunal, Premkumar, Raghu V Maligal Ganesh, Songchen Xu, Naresh

Eedugurala, Zak Weinstein, Ananitra Ghosh, Ramkrishna Adhikary, Prasun Mukherjee, Supratim Giri, Sayantan Bose, and Shibabrata Nandi for their help in Ames.

I am indebted to my parents for their love, constant support, encouragement, and sacrifices. I am grateful to my brother for his love and full support. I also thank all other family members with all my heart for their love. I thereby dedicate this thesis to my family.

Finally, I like to acknowledge the Ames Laboratory, the Henry Gilman Fellowship, and Iowa State University for funding and support of my research.



## Abstract

The research presented and discussed in this dissertation involves the synthesis of transition metal complexes of oxazolinylboranes and cyclopentadienyl-bis(oxazolinyl)borates, and their application in catalytic enantioselective olefin hydroamination and acceptorless alcohol decarbonylation.

Neutral oxazolinylboranes are excellent synthetic intermediates for preparing new borate ligands and also developing organometallic complexes. Achiral and optically active bis(oxazolinyl)phenylboranes are synthesized by reaction of 2-lithio-2-oxazolidine and 0.50 equiv of dichlorophenylborane. These bis(oxazolinyl)phenylboranes are oligomeric species in solid state resulting from the coordination of an oxazoline to the boron center of another borane monomer.

The treatment of chiral bis(oxazolinyl)phenylboranes with sodium cyclopentadienide provide optically active cyclopentadienyl-bis(oxazolinyl)borates  $H[PhB(C_5H_5)(Ox^R)_2]$  [ $Ox^R = Ox^{4S-iPr,Me_2}, Ox^{4R-iPr,Me_2}, Ox^{4S-tBu}$ ]. These optically active proligands react with an equivalent of  $M(NMe_2)_4$  ( $M = Ti, Zr, Hf$ ) to afford corresponding cyclopentadienyl-bis(oxazolinyl)borato group 4 complexes  $\{PhB(C_5H_4)(Ox^R)_2\}M(NMe_2)_2$  in high yields. These group 4 compounds catalyze cyclization of aminoalkenes at room temperature or below, providing pyrrolidine, piperidine, and azepane with enantiomeric excesses up to 99%. Our mechanistic investigations suggest a non-insertive mechanism involving concerted C–N/C–H bond formation in the turnover limiting step of the catalytic cycle.

Among cyclopentadienyl-bis(oxazolinyl)borato group 4 catalysts, the zirconium complex  $\{PhB(C_5H_4)(Ox^{4S-iPr,Me_2})_2\}Zr(NMe_2)_2$  ( $\{S-2\}Zr(NMe_2)_2$ ) displays highest activity and enantioselectivity. Interestingly,  $\{S-2\}Zr(NMe_2)_2$  also desymmetrizes olefin moieties of achiral

non-conjugated aminodienes and aminodiyne during cyclization. The cyclization of aminodienes catalyzed by  $\{S-2\}Zr(NMe_2)_2$  affords diastereomeric mixture of *cis* and *trans* cyclic amines with high diastereomeric ratios and excellent enantiomeric excesses. Similarly, the desymmetrization of alkyne moieties in  $\{S-2\}Zr(NMe_2)_2$ -catalyzed cyclization of aminodiyne provides corresponding cyclic imines bearing quaternary stereocenters with enantiomeric excesses up to 93%. These stereoselective desymmetrization reactions are significantly affected by concentration of the substrate, temperature, and the presence of a noncyclizable primary amine. In addition, both the diastereomeric ratios and enantiomeric excesses of the products are markedly enhanced by *N*-deuteration of the substrates.

Notably, the cationic zirconium-monoamide complex  $[\{S-2\}Zr(NMe_2)][B(C_6F_5)_4]$  obtained from neutral  $\{S-2\}Zr(NMe_2)_2$  cyclizes primary aminopentenes providing pyrrolidines with *S*-configuration; whereas  $\{S-2\}Zr(NMe_2)_2$  provides *R*-configured pyrrolidines. The yttrium complex  $\{S-2\}YCH_2SiMe_3$  also affords *S*-configured pyrrolidines by cyclization of aminopentenes, however the enantiomeric excesses of products are low. An alternative optically active yttrium complex  $\{PhB(C_5H_4)(Ox^{4*S*-*t*Bu})_2\}YCH_2SiMe_3$  ( $\{S-3\}YCH_2SiMe_3$ ) is synthesized, which displays highly enantioselective in the cyclization of aminoalkenes at room temperature affording *S*-configured cyclic amines with enantiomeric excesses up to 96%. A noninsertive mechanism involving a six-membered transition state by a concerted C–N bond formation and N–H bond cleavage is proposed for  $\{S-3\}YCH_2SiMe_3$  system based on the kinetic, spectroscopic, and stereochemical features.

In the end, a series of bis- and tris(oxazoliny)borato iridium and rhodium complexes are synthesized with bis(oxazoliny)phenylborane  $[PhB(Ox^{Me_2})_2]_n$ , tris(oxazoliny)borane  $[B(Ox^{Me_2})_3]_n$ , and tris(4,4-dimethyl-2-oxazoliny)phenylborate  $[To^M]^-$ . All these new and other

known rhodium and iridium complexes were examined in acceptorless dehydrogenative decarbonylation of primary alcohols. The catalysts survey shows that the compound  $\text{To}^{\text{M}}\text{Ir}(\eta^4\text{-C}_8\text{H}_{12})$  is the most active for the conversion of primary alcohols into alkane,  $\text{H}_2$ , and  $\text{CO}$  at  $180\text{ }^\circ\text{C}$  in toluene. Several aliphatic and aromatic primary alcohols are decarbonylated in the catalytic conditions. Furthermore,  $\text{To}^{\text{M}}\text{Ir}(\eta^4\text{-C}_8\text{H}_{12})$  is also able to decarbonylate polyols such as ethylene glycol and glycerol to syngas ( $\text{H}_2$  and  $\text{CO}$ ) at  $180\text{ }^\circ\text{C}$ .

## Chapter 1 – Introduction

### General Introduction

Since the landmark discovery of ferrocene in 1951-52,<sup>1</sup> metallocenes are one of the most developed and versatile catalyst classes used in a range of catalytic transformations such as olefin polymerizations, hydrogenations, and carbon-element bond formations.<sup>2</sup> Bent-sandwich group 3 and group 4 complexes are among these metallocene catalysts, which mediate a range of processes *via* insertion and sigma-bond metathesis pathways. If the two cyclopentadienyl ligands of a bent-sandwich complex are linked to a bridging element (*i.e.* *ansa*-metallocene), the reactivity of the metal center increases (Figure 1.1).<sup>3</sup>

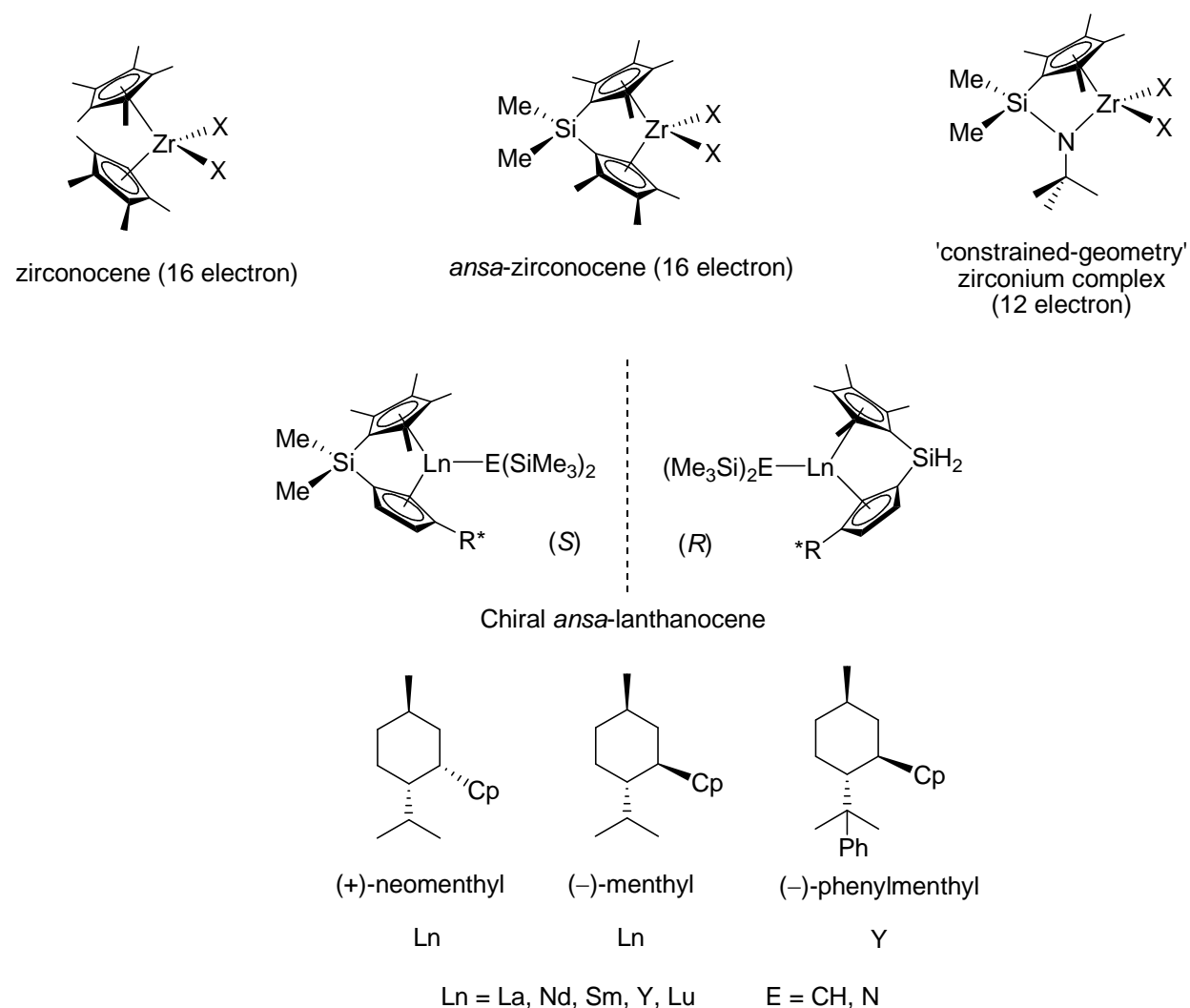


**Figure 1.1:** Group 3 & 4 bent-sandwich metallocenes and derivatives

Much of the chemistry of these bent-sandwich complexes depends on the three mutually adjacent frontier orbitals located in the wedge of the  $\text{Cp}_2\text{M}$ -fragment ( $\text{Cp} = \text{C}_5\text{H}_5$ ) (Figure 1.2).<sup>4</sup> Other modified ligands, such as mixed cyclopentadienyl-amido ligands (*i.e.* constrained geometric ligands),<sup>5</sup> or the incorporation of a borate in the ligand periphery,<sup>6</sup> also increase reactivity of the metal center because of the reduced number of electrons in its orbitals.

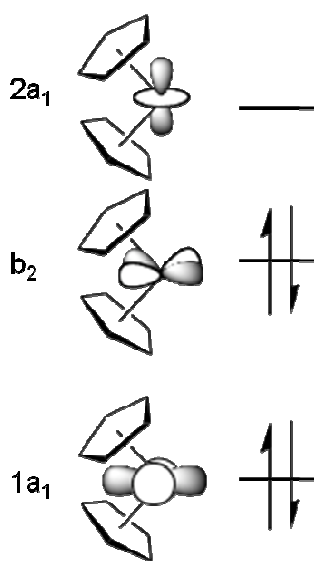
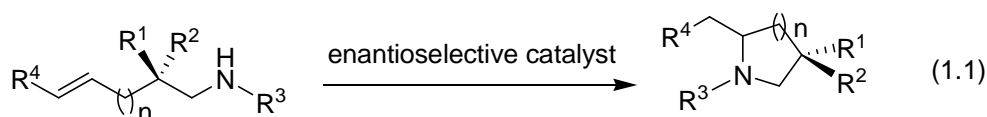


**Figure 1.2:** Frontier orbitals of  $\text{Cp}_2\text{M}$ -fragment of group 4 bent-metallocenes

Introduction of chiral substituents on the cyclopentadienyl rings affords  $C_1$ -symmetric chiral metallocenes that have been applied as catalysts for stereospecific olefin polymerization,<sup>7</sup> asymmetric hydrogenation,<sup>8,9</sup> and hydroamination<sup>8,10</sup>. Optically active metallocenes display reasonable stereospecificity in olefin polymerization,<sup>11</sup> however, they are vulnerable to undergo epimerization in many catalytic processes such as hydroamination.<sup>12</sup> Combining all these concepts and limitations of metallocenes and their derivatives, we envision that a borate-

containing, mixed Cp–L<sub>n</sub> (L<sub>n</sub> = chiral donor group) ligand could provide reactive and stereo-rigid compounds for enantioselective catalysis by reducing the effective electron count while maintaining the mutually-*cis* configuration of orbitals.

In this context, we are interested on developing highly enantioselective catalysts for hydroamination/cyclization of aminoolefins because enantioselective cyclohydroamination affords optically active nitrogen-heterocycles *via* addition of amine N–H bond across a carbon-carbon unsaturated bond in an intramolecular fashion (eq 1.1).<sup>13</sup>



Optically active nitrogen-heterocycles are important moieties in many natural products and biologically active molecules, which are valuable in chemical and pharmaceutical industries (Figure 1.3). Hence, the development of enantioselective hydroamination catalysts and understanding the reaction mechanisms are extremely important for synthesizing enantiopure cyclic amines.

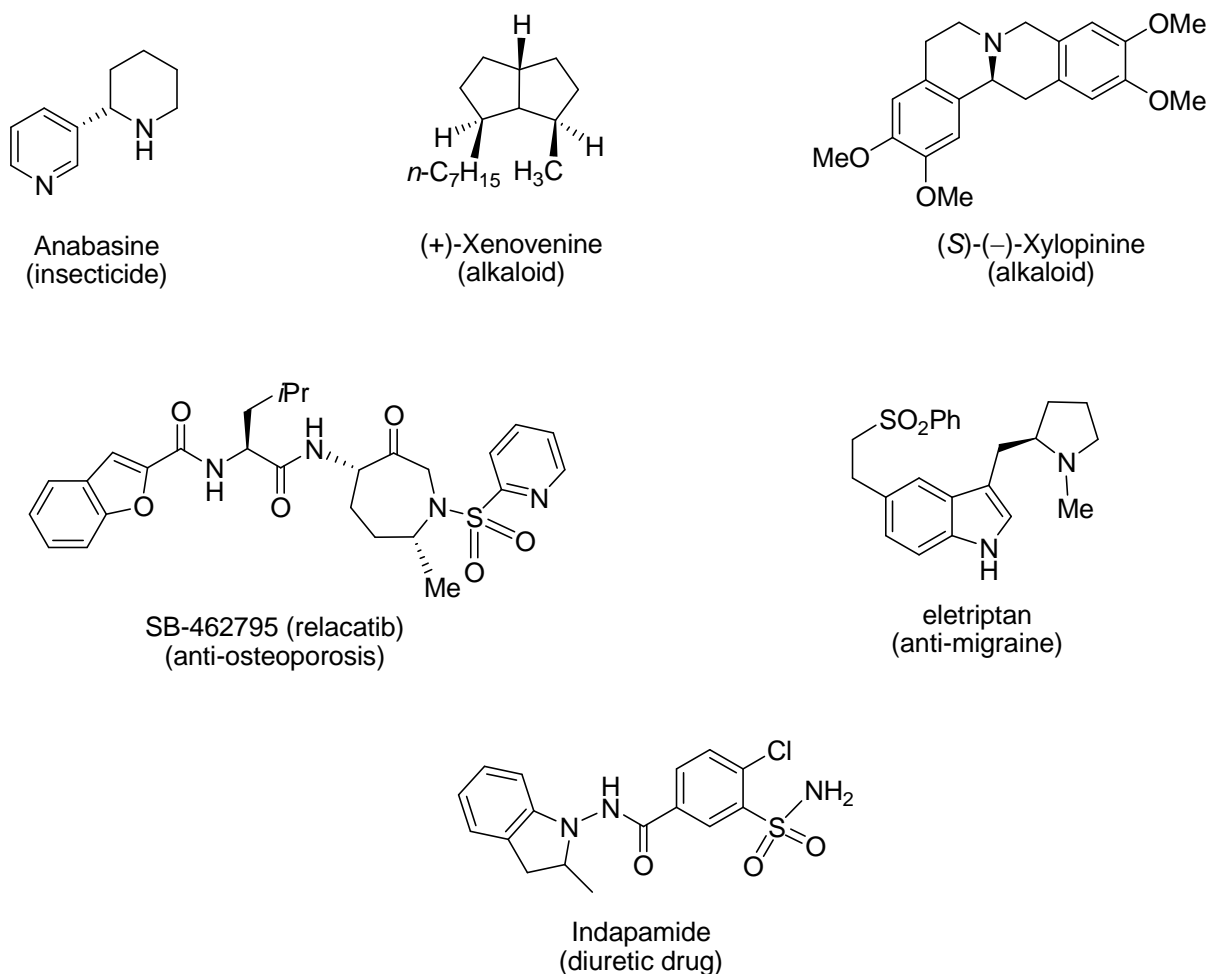


**Figure 1.3.** Selective examples of biologically active molecules containing nitrogen-heterocycles

$C_1$ -symmetric chiral lanthanocenes are the first enantioselective catalysts, which cyclize aminoolefins to cyclic amines bearing a stereocenter at 2-position with enantiomeric excesses up to 74% (Figure 1.4, i). However, these chiral lanthanocenes undergo facile epimerization under the reaction conditions *via* reversible protolytic cleavage of metal-cyclopentadienyl bonds, leading to an equilibrium mixture of diastereomeric complexes (Scheme 1.1).<sup>12</sup> Therefore, the enantioselectivity of the chiral lanthanocenes is limited by their epimeric ratio in solution.

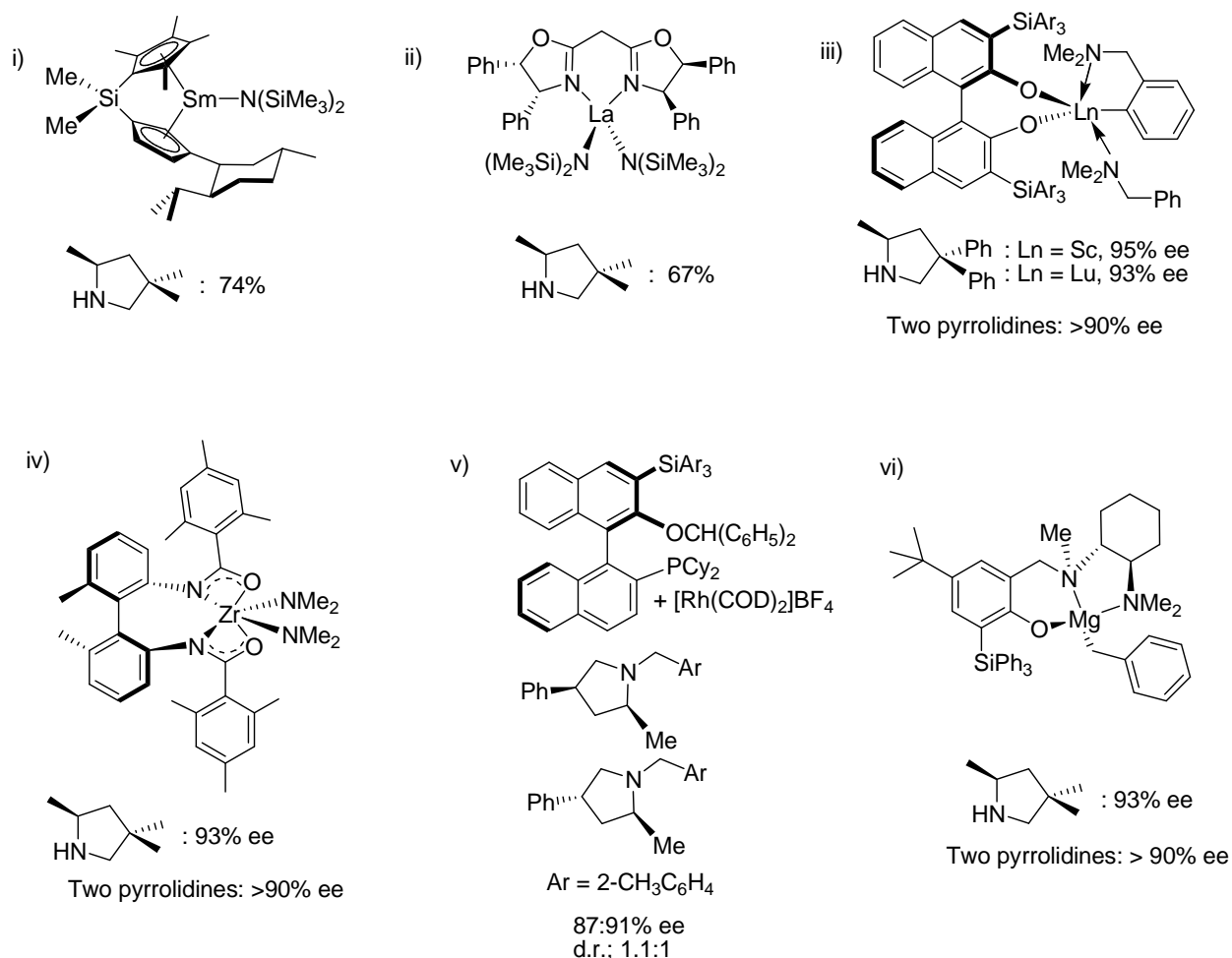
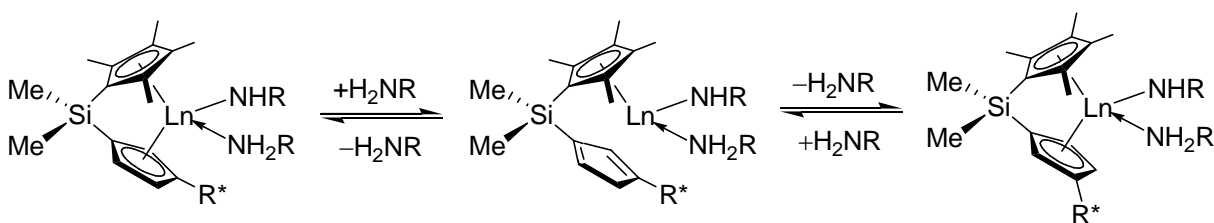


**Figure 1.4.** Selected enantioselective catalysts for hydroamination/cyclization of aminoolefins

**Scheme 1.1.** Proposed mechanism for the epimerization of chiral lanthanocene complexes during hydroamination reaction



The limitation of the chiral cyclopentadienyl based hydroamination catalysts has stimulated the development of cyclopentadienyl-free catalyst systems. Bisoxazolinato rare earth catalysts exhibit moderate enantioselectivities to afford optically active 2-methylpyrrolidines and



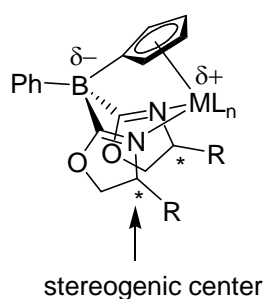
2-methylpiperidines (Figure 1.4, ii).<sup>14</sup> Several diamidobinaphthyl,<sup>15</sup> and aminothiophenolate<sup>16</sup> group 3 complexes were synthesized, which are active catalysts in hydroamination/cyclization of aminoolefins at room or higher temperatures. However, none of these catalysts provide cyclic amines with more than 90% ee. Significant improvement of enantioselectivity was observed for binaphtholate-supported scandium, yttrium, and lutetium catalysts (Figure 1.4, iii).<sup>17,18</sup> Enantiomeric excesses up to 95% were achieved using these rare-earth binaphtholate catalysts, however only two pyrrolidines having greater than 90% ee were obtained.

Besides rare-earth catalysts, several optically active cyclopentadienyl free group 4 catalysts have been developed. The cationic aminophenolate zirconium complex cyclizes only secondary aminoalkenes with enantiomeric excesses up to 82% ee.<sup>19</sup> In contrast to the cationic zirconium catalysts, neutral zirconium catalysts generally cyclize only primary aminoolefins. Chiral bis(phosphinic amido)<sup>20</sup> and binaphthalenedicarboxamide<sup>21</sup> zirconium complexes are moderate enantioselective in hydroamination/cyclization. Chiral bis(amidate)zirconium complexes exhibit significantly high enantioselectivity affording pyrrolidines up to 93% ee (Figure 1.4, iv).<sup>22</sup> Notably, group 4-catalyzed hydroamination typically requires elevated temperature (90-135 °C) and longer reaction time. Recently, several other catalyst systems have also been explored. A binaphtholate tantalum complex has been reported, and highest 81% ee was observed in cyclization of aminoalkenes.<sup>23</sup> A chiral magnesium phenoxyamine complex affords pyrrolidines with good enantioselectivity (up to 93% ee) (Figure 1.4 vi).<sup>24</sup> Additionally, several optically active pyrrolidines are obtained up to 91% ee using a binaphthyl-based rhodium catalyst (Figure 1.4, v).<sup>25,26</sup>

Nevertheless, despite significant advances, only a few hydroamination catalysts display good enantioselectivity (above 90% ee). Additionally, all these catalysts display high

enantioselectivity only for a very limited number of substrates. Furthermore, the current catalytic systems are associated with many other synthetic problems in hydroamination such as more general substrate applicability, functional group tolerance, and improve diastereoselectivity.

The potential of catalytic hydroamination reactions for preparing valuable optically active amines was the inspiration for the work described in this thesis. The necessity of stereo-rigid chiral ligand-metal systems with easily tuned steric properties of the ancillary ligand led us to develop a new class of optically active ligands, cyclopentadienyl-bis(oxazolanyl)borates.



The availability of an array of substituted enantiopure chiral oxazolines should allow for the facile synthesis of ligands with variable steric pockets.<sup>27</sup> Additionally, the stereogenic center at 4-position of oxazoline would be in close proximity to the metal center, which might create excellent stereo-induction near metal center in catalysis. The following chapters describe the development of this new ligand class, and their group 3 and group 4 complexes. Additionally, the catalytic activity of the metal complexes in stereoselective olefin hydroamination will be discussed.

## Thesis Organization

The thesis is composed of six chapters. Chapter 1 gives a general introduction of the research topic discussed in this dissertation. As the dissertation describes a diverse range of topics, the relevant literature review and references are given in the introduction of each chapter to provide an adequate understanding to the reader about the significance of the results. Majority of the materials in Chapter 2 through 5 are taken from the articles to be submitted for publication. Some of the results are already published in literature.

Chapter 2 describes the synthesis and characterization of group 4 complexes containing cyclopentadienyl-bis(oxazolanyl)borate ligands, and their catalytic activity in enantioselective cyclohydroamination of aminoolefins. Additionally, the detailed mechanistic investigations and proposed catalytic cycle of these group 4-catalyzed hydroamination have been discussed.

Chapter 3 illustrates the desymmetrizing hydroamination/cyclization of achiral dialkenyl- and dialkynylamines catalyzed by a highly enantioselective cyclopentadienyl-bis(oxazolanyl)borato zirconium(IV) complex. The effect of dilution, temperature, and isotopic perturbation on diastereoselectivity and enantioselectivity is describes in order to optimize the both diastereo- and enantioselectivity of the azacycle products.

Chapter 4 reports the catalytic activity and mechanism of cyclopentadienyl-bis(oxazolanyl)borato yttrium-catalyzed enantioselective cyclohydroamination of aminoalkenes. The stereochemical and mechanistic features of these yttrium catalysts are also compared to analogous zirconium catalysts.

Chapter 5 describes the acceptorless decarbonylation of primary alcohols and polyols to alkanes and *sys*-gas under thermal conditions catalyzed by bis- and tris(oxazolanyl)borato iridium compounds.

## References

- (1) (a) Kealy, T. J.; Pauson, P. L. *Nature* **1951**, *168*, 1039. (b) Miller, S. A.; Tebboth, J. A.; Tremaine, J. F. *J. Chem. Soc.* **1952**, 632. (c) Wilkinson, G.; Rosenblum, M.; Whiting, M. C.; Woodward, R. B. *J. Am. Chem. Soc.* **1952**, *74*, 2125.
- (2) Togni, A.; Halterman, R. L. *Metallocenes: synthesis, reactivity, applications*, Wiley-VCH, Weinheim, 1998.
- (3) Lee, H.; Desrosiers, P. J.; Guzei, I.; Rheingold, A. L.; Parkin, G. *J. Am. Chem. Soc.* **1998**, *120*, 3255-3256.
- (4) Lauher, J. W.; Hoffmann, R. *J. Am. Chem. Soc.*, **1976**, *98*, 1729-1742.
- (5) (a) Shapiro, P. J.; Bunel, E.; Schaefer, W. P.; Bercaw, J. E. *Organometallics*, **1990**, *9*, 867-869. (b) McKnight, A. L.; Waymouth, R. M. *Chem. Rev.*, **1998**, *98*, 2587-2598.
- (6) (a) Bochmann, M.; Lancaster, S. J.; Robinson, O. B. *J. Chem. Soc., Chem. Commun.*, **1995**, 2081-2082. (b) Shapiro, P. J. *Eur. J. Inorg. Chem.*, **2001**, 321-326.
- (7) (a) Erker, G.; Nolte, R.; Tsay, Y.-H.; Krüger, C. *Angew. Chem., Int. Ed. Engl.* **1989**, *28*, 628. (b) Erker, G.; Nolte, R.; Aul, R.; Wilker, S.; Krüger, C.; Noe, R. *J. Am. Chem. Soc.* **1991**, *113*, 7594.
- (8) Giardello, M. A.; Conticello, V. P.; Brard, L.; Gagne, M. R.; Marks, T. J. *J. Am. Chem. Soc.* **1994**, *116*, 10241-10254.
- (9) Conticello, V. P.; Brard, L.; Giardello, M. A.; Tsuji, Y.; Sabat, M.; Stern, C. L.; Marks, T. J. *J. Am. Chem. Soc.* **1992**, *114*, 2761-2762.
- (10) (a) Gagne', M. R.; Brard, L.; Conticello, V. P.; Giardello, M. A.; Stern, C. L.; Marks, T. J. *Organometallics* **1992**, *11*, 2003. (b) Douglass, M. R.; Ogasawara, M.; Hong, S.; Metz, M. V.; Marks, T. J. *Organometallics* **2002**, *21*, 283.

- (11) Nakayama, Y.; Shiono, T. *Molecules* **2005**, *10*, 620-633.
- (12) (a) Giardello, M. A.; Conticello, V. P.; Brard, L.; Sabat, M.; Rheingold, A. L.; Stern, C. L.; Marks, T. J. *J. Am. Chem. Soc.* **1994**, *116*, 10212-10240. (b) Giardello, M. A.; Conticello, V. P.; Brard, L.; Gagne', M. R.; Marks, T. J. *J. Am. Chem. Soc.* **1994**, *116*, 10241-10254.
- (13) (a) Hong, S.; Marks, T. J. *Acc. Chem. Res.* **2004**, *37*, 673-686. (b) Müller, T. E.; Hultsch, K. C.; Yus, M.; Foubelo, F.; Tada, M. *Chem. Rev.* **2008**, *108*, 3795-3892.
- (14) Hong, S.; Tian, S.; Metz, M. V.; Marks, T. J. *J. Am. Chem. Soc.* **2003**, *125*, 14768.
- (15) (a) Riegert, D.; Collin, J.; Daran, J.-D.; Fillebeen, T.; Schulz, E.; Lyubov, D.; Fukin, G.; Trifonov, A. *Eur. J. Inorg. Chem.* **2007**, 1159. (b) Aillaud, I.; Lyubov, D.; Collin, J.; Guillot, R.; Hannedouche, J.; Schulz, E.; Trifonov, A. *Organometallics* **2008**, *27*, 5929. (c) Hannedouche, J.; Aillaud, I.; Collin, J.; Schulz, E.; Trifonov, A. *Chem. Commun.* **2008**, 3552. (d) Aillaud, I.; Collin, J.; Hannedouche, J.; Schulz, E.; Trifonov, A. *Tetrahedron Lett.* **2010**, *51*, 4742. (e) Chapurina, Y.; Hannedouche, J.; Collin, J.; Guillot, R.; Schulz, E.; Trifonov, A. *Chem. Commun.* **2010**, *46*, 6918.
- (16) (a) Kim, J. Y.; Livinghouse, T. *Org Lett*, **2005**, *7*, 1737. (b) O'Shaughnessy, P. N.; Knight, P. D.; Morton, C.; Gillespie, K. M.; Scott, P. *Chem. Commun.* **2003**, 1770.
- (17) Gribkov, D. V.; Hultsch, K. C. *Chem. Commun.* **2004**, 730.
- (18) Gribkov, D. V.; Hultsch, K. C.; Hampel, F. *J. Am. Chem. Soc.* **2006**, *128*, 3748.
- (19) Knight, P. D.; Munslow, I.; O'Shaughnessy, P. N.; Scott, P. *Chem. Commun.* **2004**, 894-895.
- (20) Watson, D. A.; Chiu, M.; Bergman, R. G. *Organometallics* **2006**, *25*, 4731-4733.
- (21) Reznichenko, A. L.; Hultsch, K. C. *Organometallics* **2010**, *29*, 24-27.
- (22) Wood, M. C.; Leitch, D. C.; Yeung, C. S.; Kozak, J. A.; Schafer, L. L. *Angew. Chem., Int. Ed.* **2007**, *46*, 354-358.

- (23) Reznichenko, A. L.; Emge, T. J.; Audörsch, S.; Klauber, E. G.; Hultsch, K. C.; Schmidt, B. *Organometallics* **2011**, *30*, 921-924.
- (24) Zhang, X.; Emge, T. J.; Hultsch, K. C. *Angew. Chem. Int. Ed.* **2012**, *51*, 394-398.
- (25) Shen, X.; Buchwald, S. L. *Angew. Chem. Int. Ed.* **2010**, *49*, 564-567.
- (26) (a) Widenhoefer, R. A.; Han, X. *Eur. J. Org. Chem.* **2006**, 4555. (b) Hartwig, J. F. *Pure Appl. Chem.* **2004**, *76*, 507. (c) Beller, M.; Breindl, C.; Eichberger, M.; Hartung, C. G.; Seayad, J.; Thiel, O. R.; Tillack, A.; Trauthwein, H. *Synlett* **2002**, 1579.
- (27) (a) Leonard, W.R.; Romine, J.L.; Meyers, A.I. *J. Org. Chem.* **1991**, *56*, 1961-1963. (b) Kamata, K.; Agata, I.; Meyers, A. I. *J. Org. Chem.* **1998**, *63*, 3113-3116.

**Chapter 2. Neutral cyclopentadienyl-bis(oxazoliny)borato group 4 complexes as catalysts  
for enantioselective hydroamination of aminoolefins**

Modified from a paper submitted to *J. Am. Chem. Soc.*

Kuntal Manna,<sup>‡</sup> Arkady Ellern, Aaron D. Sadow<sup>\*</sup>

**Abstract**

Cs- and C<sub>1</sub>-symmetric cyclopentadienyl-bis(oxazoliny)borato group 4 complexes of type {PhB(C<sub>5</sub>H<sub>4</sub>)(Ox<sup>R</sup>)<sub>2</sub>}M(NMe<sub>2</sub>)<sub>2</sub> (M = Ti, Zr, Hf; Ox<sup>R</sup> = 4,4-dimethyl-2-oxazoline, 4*S*-isopropyl-5,5-dimethyl-2-oxazoline, 4*S*-tert-butyl-2-oxazoline, 4*R*-isopropyl-5,5-dimethyl-2-oxazoline) are highly active precatalysts for intramolecular hydroamination of aminoolefins. These group 4 complexes are synthesized by the reaction of optically active ligands H[PhB(C<sub>5</sub>H<sub>5</sub>)(Ox<sup>R</sup>)<sub>2</sub>] with an equivalent of M(NMe<sub>2</sub>)<sub>4</sub>. These compounds catalyze cyclization of aminoalkenes at room temperature or below, providing pyrrolidine, piperidine, and azepane with enantiomeric excesses up to 99%. The cyclization rate is first order dependence on both aminopentene and precatalyst. Substrate saturation on initial reaction rate was observed, which indicates the existence of reversible substrate-catalyst association preceding the turnover-limiting step in the catalytic cycle. The nonzero x-intercept in the initial rate plots that coincides with concentration of the catalyst indicates that 1.0 equiv. of substrate is required to activate the precatalyst. The observed isotopic perturbation of enantioselectivity (IPE) eliminates intramolecular [2π + 2π] cycloaddition of a metal-imido alkene intermediate as possible mechanisms for C–N bond

<sup>‡</sup> Primary researcher and author

<sup>\*</sup> Author for correspondence

formation. Primary kinetic isotope effect was measured, which indicates the cleavage of N–H/N–D bond in the turnover limiting step, and also exhibits the favor of one diastereomeric pathways over the other. Secondary aminopentene is not cyclized, however cyclization occurs in presence of non-cyclizable primary amine. The zirconium monoamide complex  $\{\text{PhB}(\text{C}_5\text{H}_4)(\text{Ox}^{4S\text{-}i\text{Pr,Me}_2})_2\}\text{ZrCl}(\text{NMe}_2)$  was synthesized and is seen to be inactive in hydroamination. The accumulated data including the rate law, the KIE, isotopic perturbation of enantioselectivity, and the KIE for the two enantiotopic pathways are less consistent with olefin insertion as possible mechanisms for C–N bond formation. A non-insertive mechanism involving concerted C–N/C–H bond formation is proposed. The cyclopentadienyl-mono(oxazolanyl)borate ligand  $\text{H}[\text{Ph}_2\text{B}(\text{C}_5\text{H}_5)(\text{Ox}^{4S\text{-}i\text{Pr,Me}_2})]$  was synthesized, and its zirconium complex was inactive in hydroamination/cyclization of aminoolefin at room temperature, which suggest the involvement of both oxazoline with the metal center to activate the precatalyst  $\{\text{PhB}(\text{C}_5\text{H}_4)(\text{Ox}^{4S\text{-}i\text{Pr,Me}_2})_2\}\text{Zr}(\text{NMe}_2)_2$ .

## Introduction

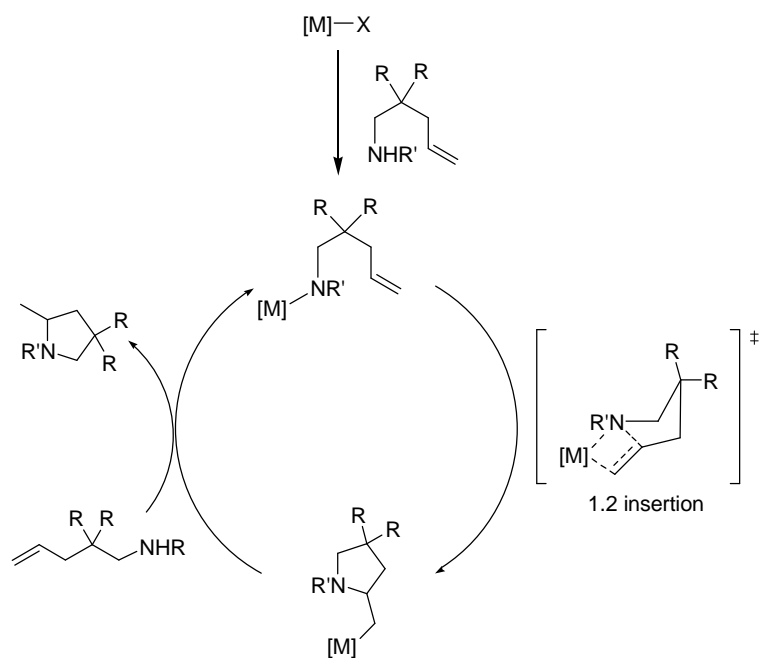
Asymmetric olefin hydroamination is a facile and promising approach for the synthesis of optically active nitrogen heterocycles, which are important in commodity and specialty chemicals, medicinal compounds, and natural products preparations.<sup>1</sup> Despite significant progresses, the synthesis of efficient, configurationally stable, and highly enantioselective catalysts is still challenging to solve synthetic problems in hydroamination such as general substrate applicability, enantioselectivity, diastereoselectivity, enantioselective intermolecular hydroamination, and anti-Markonikov additions. Products with high optical purities are limited to a few choice pyrrolidines even in the well-studied intramolecular hydroamination/cyclization;



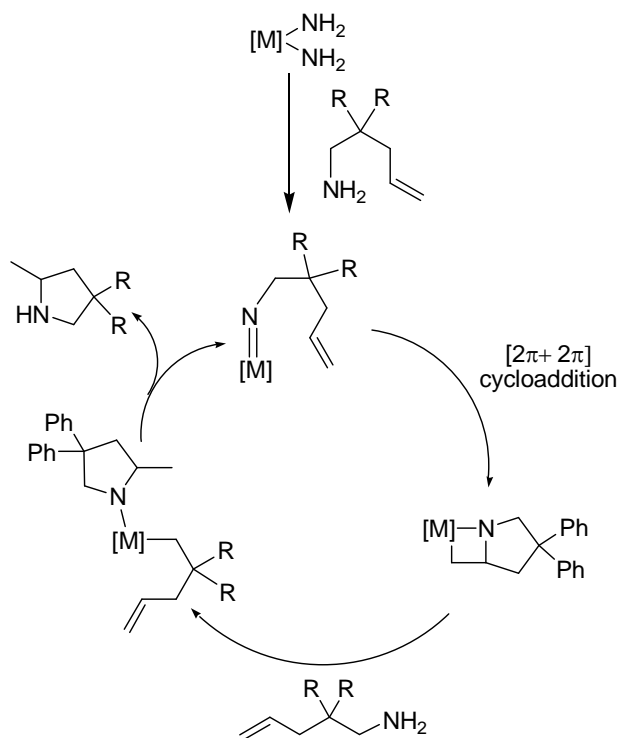
asymmetric olefin hydroaminations that afford functionalized pyrrolidines, piperidines, and homopiperidines (among *many* valuable chiral *N*-heterocycles) are not developed.

Still, great progress is highlighted by catalyst advances with metallocene-based and axially chiral lanthanide compounds,<sup>2,3,4,5,6,7,8,9,10</sup> alkali metal coordination complexes,<sup>11</sup> and C<sub>1</sub>-, C<sub>2</sub>-, and C<sub>3</sub>-symmetric alkaline earth metal catalysts.<sup>12</sup> Breakthroughs in zirconium-catalyzed alkene hydroamination include axially chiral cationic bis(aryloxy),<sup>13</sup> bis(amido),<sup>14</sup> a highly enantioselective bis(amidate),<sup>15,16</sup> and bis(carboxyamido)<sup>17</sup> complexes (or similar Ta-based systems)<sup>18</sup> as precatalysts. C<sub>1</sub>-symmetric mixed Cp\*(oxazolanyl-aryloxo)zirconium and constrained geometry-type catalysts uniquely depart from the predominant axially chiral ligand design.<sup>19</sup> A single example of a highly enantioselective late transition-metal (rhodium-based) aminopentene cyclization catalyst has been reported.<sup>20</sup> Although these systems are generally limited to pyrrolidines, highly efficient and selective intramolecular catalysts may provide strategies for addressing some of the tougher challenges in olefin hydroamination.

In this context, catalyst synthesis and screening accompanied by mechanistic tests should help advance the field. Most detailed studies involving hydroamination/cyclization mechanism have involved *d*<sup>0</sup> complexes including lanthanide,<sup>21,5d,10, 22</sup> actinide,<sup>23</sup> alkaline earth metal,<sup>24,25,26</sup> and zirconium,<sup>23,27,28,29</sup> and all of the catalytic cycles associated with these catalysts typically are proposed to have metal-amido resting states. From that point, the proposed mechanisms for C–N bond formation are remarkable divergent to include (A) olefin insertion into M–N bonds and (B) [2 $\pi$ +2 $\pi$ ] cycloaddition to metal-imido that involve four-centered transition state.

Scheme 2.1. The  $\sigma$ -bond insertive mechanism for cyclohydroamination

Scheme 2.2. Imido mechanism for cyclohydroamination



A few interesting and sometimes conflicting observations, however, provide some guidance. First, the primary-in-magnitude isotope effect suggests that the intramolecular cyclization of the metal-amidoalkene catalyst resting state is not a simple unimolecular process in almost any conversion.<sup>21,5d,27</sup> Perhaps an even more compelling observation is that *cis/trans* ratio is increased at high substrate concentration or by addition of propylamine in the diastereoselective cyclization of chiral racemic aminoalkenes by achiral catalysts; in addition, the *cis/trans* ratio is lowered by *N*-deuteration.<sup>21</sup> A second interesting observation in zirconium-catalyzed hydroamination involves primary and secondary aminoalkenes as substrates and cationic and neutral precatalysts. The cationic catalyst system  $\text{Cp}_2\text{ZrMe}_2/\text{B}(\text{C}_6\text{F}_5)_3$  is only active for secondary aminoalkenes, and the authors suggest catalyst deactivation occurs with primary amines through the formation of inactive, neutral zirconium imidoalkene species.<sup>13,30</sup> In contrast, several neutral zirconium catalysts cyclize primary but not secondary aminoalkenes; such observation is often invoked as support for a zirconium imido intermediate prior to  $[2\pi+2\pi]$  cycloaddition.

Notably, the reaction of imidozirconium compounds and olefins (Scheme 2.2) is not independently established (although  $\text{Zr}=\text{NR}$  and alkyne cycloadditions are well known).<sup>31a</sup> In fact, mixtures of an isolated zirconium-imido and alkenes returned starting materials.<sup>31b</sup> Furthermore, isolation of the immediate organometallic products (*i.e.*, a metal-alkylamine or a azametallacyclobutane) formed from either of these steps has not yet been described for a  $d^0$  or  $f^0$  metal compound. However, the vinylamine product of alkyne insertion into a hafnium-nitrogen bond was recently isolated and characterized.<sup>32</sup> In addition, a molybdenum amido and alkyne react to provide a  $d^2$  vinylamine.<sup>33</sup> Interestingly, conclusive evidence for olefin insertion into  $d^n$  metal amidos ( $n \neq 0$ ) has been provided in palladium systems.<sup>34,35</sup>

These unusual features, as well as the potential for amine synthesis, motivated our investigations of group 4-catalyzed aminoalkene cyclization using bis(oxazolanyl)cyclopentadienyl borate ligands.<sup>36,37</sup> We envisioned that  $C_1$ -symmetric cyclopentadienyl-bis(oxazolanyl)borate supported metal complexes could be highly enantioselective hydroamination catalysts, because of the close proximity of the stereogenic center of the oxazolines to the metal center. Additionally, these complexes would be non-epimerizable unlike the  $C_1$ -symmetric chiral lanthanocenes, due the lack of stereogenic center on the cyclopentadienyl ring. Herein, we report the synthesis and catalytic activity of cyclopentadienyl-bis(oxazolanyl)borate supported group 4 complexes for hydroamination/cyclization of aminoolefins, which exhibit high catalytic activity and excellent enantioselectivity (>95%) in a number of azacycles. The substrates scope, and the effect of temperature, solvents and additives to the enantioselectivity will be discussed. Our studies have attempted to address a range of synthetic and mechanistic issues, including the precatalyst conformation, the coordinating properties of the oxazoline moieties in the borate ligands, relative rate and stereoselectivity of titanium, zirconium, and hafnium based precatalysts, the valence needed for catalysis, and the effect of the oxazoline group on catalyst's stability, activity, and stereoselectivity.

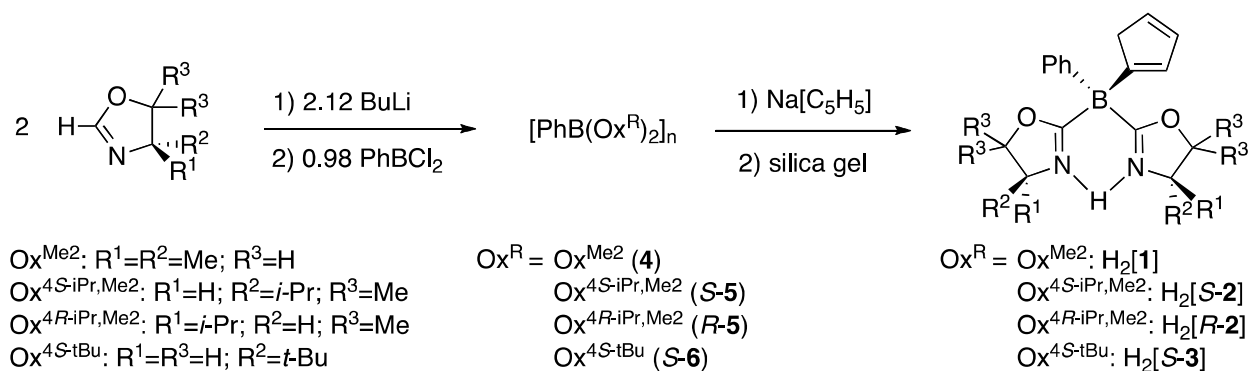
## Results and discussion

### *Synthesis and Characterization of Proligands*

Four dianionic cyclopentadienyl-bis(oxazolanyl)borates are prepared as protonated species (Scheme 2.3).<sup>10,29,36</sup> The achiral proligand  $H[PhB(C_5H_5)(Ox^{Me_2})_2]$  ( $H_2\{\mathbf{1}\}$ ;  $Ox^{Me_2} = 4,4$ -dimethyl-2-oxazolanyl), the chiral 4-isopropyl oxazolanyl  $H[PhB(C_5H_5)(Ox^{4S-iPr,Me_2})_2]$  ( $H_2\{S\text{-}\mathbf{2}\}$ );

$\text{Ox}^{4S-iPr,Me_2} = 4S\text{-isopropyl-5,5-dimethyl-2-oxazolinyl}$ ) and its readily-available enantiomer  $\text{H}[\text{PhB}(\text{C}_5\text{H}_5)(\text{Ox}^{4R-iPr,Me_2})_2]$ ; ( $\text{H}_2\{\text{R-2}\}$ ;  $\text{R-Ox}^{4R-iPr,Me_2} = 4R\text{-isopropyl-5,5-dimethyl-2-oxazolinyl}$ ), and the optically-active 4-*tert*-butyl oxazoline  $\text{H}[\text{PhB}(\text{C}_5\text{H}_5)(\text{Ox}^{4S-tBu})_2]$  ( $\text{H}_2\{\text{S-3}\}$ ;  $\text{Ox}^{4S-tBu} = 4S\text{-tert-butyl-2-oxazolinyl}$ ) are all synthesized following a similar route in two steps from the appropriate 2H-oxazolines  $2\text{H-Ox}^R$ :  $2\text{H-Ox}^{\text{Me}_2}$ ,  $2\text{H-Ox}^{4S-iPr,Me_2}$ ,  $2\text{H-Ox}^{4R-iPr,Me_2}$ ,  $2\text{H-Ox}^{4S-tBu}$  via neutral bis(oxazolinyl)phenylborane  $\text{PhB}(\text{Ox}^R)_2$  intermediates (Scheme 2.3).<sup>37</sup> These borane intermediates are critical to the overall ligand synthesis. The steric bulk of the oxazoline substituents in  $2\text{Li-Ox}^{\text{Me}_2}$ ,  $2\text{Li-Ox}^{4S-iPr,Me_2}$ ,  $2\text{Li-Ox}^{4R-iPr,Me_2}$ , and  $2\text{Li-Ox}^{4S-tBu}$  slow the addition of a third oxazoline preventing the formation of oxazolinylborates. This approach works well for the synthesis of the oligomeric bis(4,4-dimethyl-2-oxazolinyl)phenylborane  $[\text{PhB}(\text{Ox}^{\text{Me}_2})_2]_n$  (**4**). However, 4*S*-isopropyl-2-oxazoline apparently does not have sufficient bulk, and the attempted synthesis of bis(4*S*-isopropyl-2-oxazolinyl)phenylborane affords an inseparable mixture of  $\text{PhB}(\text{Ox}^{4S-iPr})_2$  and  $\text{Li}[\text{PhB}(\text{Ox}^{4S-iPr})_3]$ .<sup>36,38</sup>

**Scheme 2.3.** Synthesis of proligands  $\text{H}[\text{PhB}(\text{C}_5\text{H}_5)(\text{Ox}^R)_2]$  from achiral and chiral 2H-oxazolines.



The isolable dimethyl-substituted **4** guided our preparation of chiral derivatives, and 5,5-dimethyl-4*S*-isopropyl-oxazoline ( $2\text{H-Ox}^{4S-iPr,Me_2}$ ) was targeted to provide an optically active

oxazolinyllborane intermediate. Deprotonation of  $2\text{H-Ox}^{4S-i\text{Pr},\text{Me}2}$  with  $n\text{BuLi}$  in THF at  $-78\text{ }^\circ\text{C}$  occurs selectively at the 2-position to give the 5,5-dimethyl-4*S*-isopropyl-2-lithio-2-oxazolidine ( $2\text{Li-Ox}^{4S-i\text{Pr},\text{Me}2}$ ). Addition of 0.5 equiv. of  $\text{PhBCl}_2$  to the THF solution of  $2\text{Li-Ox}^{4S-i\text{Pr},\text{Me}2}$  is followed by stirring at room temperature for 14 h to provide bis(5,5-dimethyl-4*S*-isopropyl-2-oxazolinyll)phenylborane  $\text{PhB}(\text{Ox}^{4S-i\text{Pr},\text{Me}2})_2$  (**S-5**). The preparation of  $\text{PhB}(\text{Ox}^{4R-i\text{Pr},\text{Me}2})_2$  (**R-5**) proceeds similarly, but  $\text{PhB}(\text{Ox}^{4S-t\text{Bu}})_2$  (**S-6**) is synthesized using *tert*-butyllithium for the deprotonation of 4*S-tert*-butyl-2-oxazoline.

The crude yellow solid bis(oxazolinyll)phenylboranes contain variable amounts of LiCl, but are sufficiently pure for further synthetic work. The solid state  $^{11}\text{B}$  NMR spectroscopy indicates that  $[\text{PhB}(\text{Ox}^{\text{Me}2})_2]_n$  is a complicated mixtures of oligomeric species resulting from the coordination of an oxazoline to the boron center of another  $\text{PhB}(\text{Ox}^{\text{Me}2})_2$  monomer.<sup>37</sup> In acetonitrile- $d_3$ , solvent coordination to the boron center gave a single  $^{11}\text{B}$  NMR signal at  $-8.1$  ppm assigned to the adduct  $\text{Ph}(\text{Ox}^{\text{Me}2})_2\text{B}(\text{NCMe})$ . In non-coordinating toluene- $d_8$  solvent,  $[\text{PhB}(\text{Ox}^{\text{Me}2})_2]_n$  does not provide an observable signal  $^{11}\text{B}$  NMR spectra acquired at room temperature or at elevated temperature (350 K). However, two  $^{11}\text{B}$  NMR resonances were detected at  $-5.2$  and  $-11.0$  ppm in a spectrum acquired at 220 K. Comparison of these low temperature chemical shift values to those obtained for acetonitrile adducts of  $[\text{PhB}(\text{Ox}^{\text{Me}2})_2]_n$  suggest that intermolecular *O*-oxazoline and *N*-oxazoline coordination provides two distinct boron sites. At room temperature in non-coordinating solvent (toluene- $d_8$  or benzene- $d_6$ ), the exchange process is in the so-called intermediate regime, which obscures the signals.

The other bis(oxazolinyll)phenylboranes have similar spectroscopic properties, and  $^{11}\text{B}$  and  $^{15}\text{N}$  NMR chemical shifts and infrared C=N stretching frequencies for **4**, **S-5**, **R-5** and **S-6** are

reported in Table 2.1. The  $^{11}\text{B}$  NMR values are consistent with neutral, four-coordinate boron centers and suggest that a neutral donor (*i.e.*, acetonitrile- $d_3$ ) coordinated to the boron center.<sup>39</sup>

**Table 2.1.**  $^{11}\text{B}$ ,  $^{15}\text{N}$  NMR chemical shift and  $\nu_{\text{CN}}$  values for bis(oxazoliny)phenylboranes (**4-6**), cyclopentadienyl-bis(oxazoliny)phenylborates ( $\text{H}_2\{\mathbf{1}\}$ - $\text{H}_2\{\mathbf{3}\}$ ), and 2H-oxazolines.

Compound	$^{11}\text{B}$ NMR ( $\delta$ ) <sup>a</sup>	$^{15}\text{N}$ NMR ( $\delta$ ) <sup>a</sup>	$\nu_{\text{CN}}$ (KBr, $\text{cm}^{-1}$ )	$[\alpha]_{\text{D}}^{20}$ <sup>b</sup>
H[PhB(C <sub>5</sub> H <sub>5</sub> )(Ox <sup>Me2</sup> ) <sub>2</sub> ] (H <sub>2</sub> [ <b>1</b> ])	-15.3, -15.6, -16.0	-172	1589	n.a.
H[PhB(C <sub>5</sub> H <sub>5</sub> )(Ox <sup>4S-iPr,Me2</sup> ) <sub>2</sub> ] (H <sub>2</sub> [ <b>S-2</b> ])	-15.7 br	-179.1	1584, 1567	-62.9°
H[PhB(C <sub>5</sub> H <sub>5</sub> )(Ox <sup>4R-iPr,Me2</sup> ) <sub>2</sub> ] (H <sub>2</sub> [ <b>R-2</b> ])	-15.7 br	-179.1	1582, 1560	+63.2°
H[PhB(C <sub>5</sub> H <sub>5</sub> )(Ox <sup>4S-tBu</sup> ) <sub>2</sub> ] (H <sub>2</sub> [ <b>S-3</b> ])	-14.9, -15.3, -15.6.	-190.9	1595, 1588	-139.1°
PhB(Ox <sup>Me2</sup> ) <sub>2</sub> ( <b>4</b> )	-8.1	-147.0	1621, 1601	n.a.
PhB(Ox <sup>S-iPr,Me2</sup> ) <sub>2</sub> ( <b>S-5</b> )	-7.5	-131.6	1588	n.a.
PhB(Ox <sup>R-iPr,Me2</sup> ) <sub>2</sub> ( <b>R-5</b> )	-7.5	-131.6	1588	n.a.
PhB(Ox <sup>S-tBu</sup> ) <sub>2</sub> ( <b>S-6</b> )	-7.3	-124.3	1617, 1590	n.a.
H[Ph <sub>2</sub> B(Ox <sup>4S-iPr,Me2</sup> )(C <sub>5</sub> H <sub>5</sub> )] (H <sub>2</sub> [ <b>S-7</b> ])	-10.0, -11.5, -12.4	-155.2	1594	-55.2°
2H-Ox <sup>4S-iPr,Me2</sup>	n.a.	-143.3	1632 $\text{cm}^{-1}$	-35.2°
2H-Ox <sup>4R-iPr,Me2</sup>	n.a.	-143.3	1632 $\text{cm}^{-1}$	+34.8°
2H-Ox <sup>4S-tBu</sup>	n.a.	-148.0	1635 $\text{cm}^{-1}$	-104°

<sup>a</sup> Measured in acetonitrile- $d_3$  solvent. <sup>b</sup> Measured in benzene.

The bis(oxazoliny)phenylboranes **4-6** react with Na[C<sub>5</sub>H<sub>5</sub>] in THF to provide the desired mixed oxazoline-cyclopentadienylborates Na[PhB(C<sub>5</sub>H<sub>5</sub>)(Ox<sup>R</sup>)<sub>2</sub>]. The crude products are purified

by column chromatography to yield the proligands  $\text{H}[\text{PhB}(\text{C}_5\text{H}_5)(\text{Ox}^{\text{R}})_2]$ . These compounds are all light yellow solids that are soluble in benzene, methylene chloride, and THF.

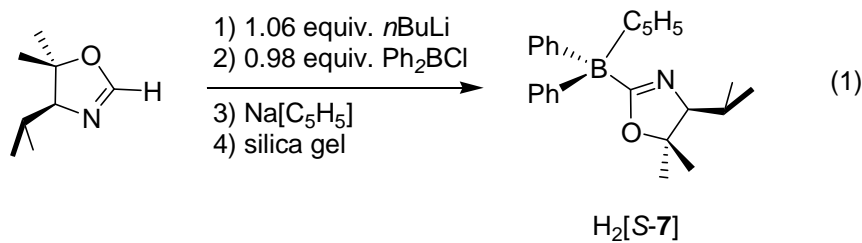
The isolated ligands **1-4** are each a mixture of three isomers, as indicated by  $^1\text{H}$  and  $^{11}\text{B}$  NMR spectroscopy (Table 2.1). The  $^1\text{H}$  NMR spectra of these mixtures were complicated by overlapping resonances in the phenyl, cyclopentadienyl, and oxazoline regions and were not useful for characterization or assessment of purity.  $^{11}\text{B}$  NMR spectroscopy is more informative, and the three resonances in the  $^{11}\text{B}$  NMR spectrum of achiral **1** are upfield compared to that of borane **4** (as an acetonitrile adduct), as expected for a boron center in an anionic four coordinated borate.<sup>39</sup> Thus, 1- $\text{C}_5\text{H}_5(\text{BR}_3)$ , 2- $\text{C}_5\text{H}_5\text{B}(\text{BR}_3)$ , and 5- $\text{C}_5\text{H}_5\text{B}(\text{BR}_3)$  connectivity accounts for the three isomers. Borylcyclopentadienyl compounds are well known to form mixtures of isomers.<sup>40</sup> In a  $^1\text{H}$ - $^{15}\text{N}$  HBQC experiment on **1**, correlations from the oxazoline methyl and methylene resonances provided an  $^{15}\text{N}$  NMR chemical shift of  $-172$  ppm (on the  $\text{CH}_3\text{NO}_2$  scale) that is 45 ppm upfield of 4,4-dimethyl-2-oxazoline ( $-127$  ppm). For comparison, the  $^{15}\text{N}$  NMR chemical shift of *N*-protonated oxazoline in  $\text{Ir}(\kappa^2\text{-(Ox}^{\text{Me}2})_2\text{BPh(Ox}^{\text{Me}2}\text{H)})(\eta^4\text{-C}_8\text{H}_{12})\text{OTf}$  is  $-206$  ppm.<sup>41</sup> In the IR spectrum of **1**, a single oxazoline-based band ( $\nu_{\text{CN}} = 1589 \text{ cm}^{-1}$ , KBr) was observed at lower energy than that of 4,4-dimethyl-2-oxazoline ( $\nu_{\text{CN}} = 1630 \text{ cm}^{-1}$ ). Thus, upfield  $^{15}\text{N}$  NMR and IR data are consistent with proton-oxazoline interactions through the imidine nitrogen, where the proton either bridges between the two nitrogen or rapidly exchanges.

In case of optically-active bis(oxazoliny)borate ligands  $\text{H}_2[\text{S-2}]$  and  $\text{H}_2[\text{R-2}]$ , only one broad  $^{11}\text{B}$  signal at  $-15.7$  ppm (232 Hz at half-height) was resolved. Again, the  $^1\text{H}$  NMR spectrum contained overlapping resonances for the isomers. The  $^{11}\text{B}$  NMR signals for  $\text{H}_2[\text{S-3}]$  were well-separated. Interestingly and in contrast to  $\text{H}_2[\text{1}]$ , two  $\nu_{\text{CN}}$  bands were detected in the



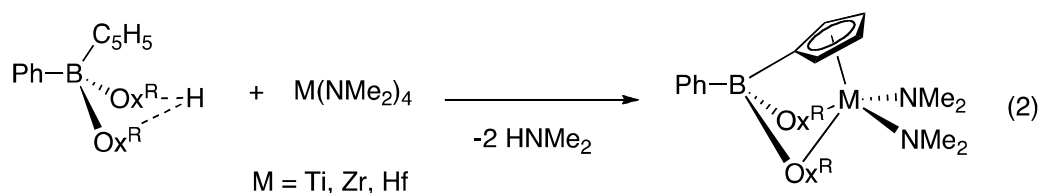
IR spectra of H<sub>2</sub>[S-2], H<sub>2</sub>[R-2], and H<sub>2</sub>[S-3]. The wavenumber for these bands appeared at lower energy by 40-50 cm<sup>-1</sup> than uncoordinated oxazoline.

A chiral cyclopentadienyl(oxazolinyl)diphenylborate, synthesized for comparison with the bis(oxazolinyl)borates **1-3**, is prepared by reaction of 2Li-Ox<sup>4*S*-iPr,Me<sup>2</sup></sup> and Ph<sub>2</sub>BCl followed by addition Na[C<sub>5</sub>H<sub>5</sub>]. Exhaustive purification by silica gel column chromatography yields H[Ph<sub>2</sub>B(C<sub>5</sub>H<sub>5</sub>)(Ox<sup>4*S*-iPr,Me<sup>2</sup></sup>)] (H<sub>2</sub>[S-7]) in modest yield. Three <sup>11</sup>B NMR resonances indicated that this cyclopentadienyl-mono(oxazoline)borate is also a mixture of three isomers. Unexpectedly, the <sup>15</sup>N NMR signal modestly shifted upfield (-155 ppm), less than H<sub>2</sub>[S-2]; the proton is shared or rapidly exchanges between two oxazolines in the latter (oxazoline:H = 2:1), whereas we expected the oxazoline in the former is fully protonated (oxazoline:H = 1:1). Presumably, the nitrogen-proton interaction is not the only variable governing the <sup>15</sup>N NMR chemical shift of these compounds.

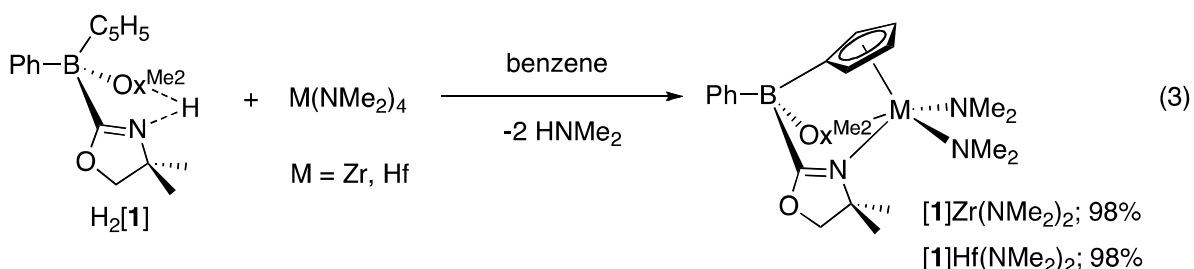


### *Synthesis and Characterization of Mixed Cyclopentadienyl-Oxazolinylborate Group 4 Compounds*

The general scheme for preparation of group 4 complexes containing mixed cyclopentadienyl-oxazolinylborate ligands involves the interaction of homoleptic dimethylamide compounds M(NMe<sub>2</sub>)<sub>4</sub> (M = Ti, Zr, Hf) with H<sub>2</sub>{**1**}, H<sub>2</sub>{S-2}, H<sub>2</sub>{R-2}, H<sub>2</sub>{S-3} and H<sub>2</sub>{**7**} (eq 2). However, the conditions for synthesis and the complex stability vary for the metal-ligand pairs.



The achiral proligand  $\text{H}_2\{\mathbf{1}\}$  and  $\text{M}(\text{NMe}_2)_4$  ( $\text{M} = \text{Zr}, \text{Hf}$ ) react rapidly in benzene at room temperature affording  $\{\text{PhB}(\text{C}_5\text{H}_4)(\text{Ox}^{\text{Me}_2})_2\}\text{Zr}(\text{NMe}_2)_2$  ( $\{\mathbf{1}\}\text{Zr}(\text{NMe}_2)_2$ ) and  $\{\text{PhB}(\text{C}_5\text{H}_4)(\text{Ox}^{\text{Me}_2})_2\}\text{Hf}(\text{NMe}_2)_2$  ( $\{\mathbf{1}\}\text{Hf}(\text{NMe}_2)_2$ ).  $^1\text{H}$  NMR spectra of micromolar-scale experiments in benzene- $d_6$  indicated that the reactions proceed to completion within 10 min. Analytically pure materials are obtained by evaporation of the benzene and  $\text{HNMe}_2$  byproduct in 98% isolated yield for both zirconium and hafnium compounds.



The spectroscopic data for  $\{\mathbf{1}\}\text{Zr}(\text{NMe}_2)_2$  and  $\{\mathbf{1}\}\text{Hf}(\text{NMe}_2)_2$  are similar (Table 2.2). Upon coordination and amine elimination, the  $^1\text{H}$  NMR multiplets associated with the three  $\text{C}_5\text{H}_5\text{B}$  isomers are replaced with two resonances assigned to  $\text{C}_5\text{H}_4\text{B}$  in a  $\text{C}_s$ -symmetric molecule. One set of oxazoline resonances was observed as two singlets for inequivalent methyl groups and two doublets for the inequivalent  $\text{CH}_2$ . This pattern did not vary in  $^1\text{H}$  NMR spectra of the zirconium and hafnium compounds, acquired at temperatures from 190 K and 300 K in toluene- $d_8$ .  $^1\text{H}$ - $^{15}\text{N}$  HMBC experiments contained a correlation between oxazoline methyl and nitrogen, and the  $^{15}\text{N}$  NMR chemical shifts for the oxazoline nitrogen in zirconium and hafnium compounds at  $-135$  and  $-132$  ppm are only slightly upfield of non-coordinated 2H-4,4-dimethyl-

2-oxazoline (−127 ppm). The  $^{15}\text{N}$  NMR chemical shift of  $\{\kappa^3\text{-PhB}(\text{Ox}^{\text{Me}_2})_3\}\text{Zr}(\text{NMe}_2)_3$  is −140 ppm, in which oxazoline coordination to Zr is unambiguous; in the current system, the small change in  $^{15}\text{N}$  NMR data of complexes *vs.* 2H-oxazoline does not distinguish two simultaneously coordinated oxazolines from one coordinated oxazoline rapidly exchanging with a pendent oxazoline. Analytically pure  $\{\mathbf{1}\}\text{Zr}(\text{NMe}_2)_2$  and  $\{\mathbf{1}\}\text{Hf}(\text{NMe}_2)_2$ , obtained from evaporation of benzene solutions, were analyzed by IR spectroscopy, and only one  $\nu_{\text{CN}}$  band was observed for each compound (both at  $1595\text{ cm}^{-1}$ ; KBr). From these data, either (a) the  $\text{C}_5\text{H}_4\text{B}$  group and both oxazolines are bonded to the metal center or (b) the  $\text{C}_5\text{H}_4\text{B}$  group and only one oxazoline is coordinated, and the pendent oxazoline and coordinated oxazoline exchange rapidly on the  $^1\text{H}$  NMR timescale in solution and the IR timescale in the solid state.

Slow diffusion of pentane into a solution of  $\{\mathbf{1}\}\text{Zr}(\text{NMe}_2)_2$  dissolved in THF and cooled to 243 K provided X-ray quality crystals of  $\{\mathbf{1}\}\text{Zr}(\text{NMe}_2)_2\text{THF}$ , in which only one oxazoline was coordinated to the zirconium center (Figure 2.1a). The coordination geometry of zirconium is described as that of a squashed 4-legged piano stool such that  $\text{Cp}_{\text{centroid}}\text{-Zr-N}(\text{NMe}_2)$ :  $125.8$  and  $135.0^\circ$   $\text{Ox}^{\text{Me}_2}$ :  $99.4^\circ$ ) and  $\text{Cp}_{\text{centroid}}\text{-Zr-O}$  ( $101.2^\circ$ ) angles. The dimethylamide groups are transoid ( $\text{N-Zr-N}$ :  $120.26^\circ$ ), as are the oxazoline and THF ligands ( $\text{N-Zr-O}$ :  $159.4^\circ$ ). The site *trans* to the cyclopentadienyl ring is unoccupied. The unit cell contains four, symmetry-related molecules ( $Z = 4$ ), but the model does not reveal close contacts between the pendent oxazoline nitrogen and the other molecules in the unit cell.

The solid-state infrared spectrum of  $\{\mathbf{1}\}\text{Zr}(\text{NMe}_2)_2\text{THF}$  revealed that this structure and the structure of  $\{\mathbf{1}\}\text{Zr}(\text{NMe}_2)_2$  are not equivalent. In particular, two  $\nu_{\text{CN}}$  stretching frequencies at  $1610\text{ cm}^{-1}$  (pendant oxazoline) and  $1533\text{ cm}^{-1}$  ( $\text{Zr-Ox}^{\text{Me}_2}$ ) were observed for crystals from THF. Furthermore, the conformation of  $\{\mathbf{1}\}\text{Zr}(\text{NMe}_2)_2\text{THF}$  in the solid state is not representative of

the solution structure. At room temperature, the signals in  $^1\text{H}$  NMR spectrum of  $\{\mathbf{1}\}\text{Zr}(\text{NMe}_2)_2\text{THF}$  were identical to those of  $\{\mathbf{1}\}\text{Zr}(\text{NMe}_2)_2$  in the absence of THF and those of THF in the absence of  $\{\mathbf{1}\}\text{Zr}(\text{NMe}_2)_2$ . Interestingly, the  $^1\text{H}$  NMR spectrum of  $\{\mathbf{1}\}\text{Zr}(\text{NMe}_2)_2\text{THF}$  at 190 K contained only two broad single resonances, one assigned to oxazoline methyl and the other to oxazoline methylene groups. The two methyl groups on each oxazoline are expected to remain chemically inequivalent at all temperatures, and a rigid structure for  $\{\mathbf{1}\}\text{Zr}(\text{NMe}_2)_2(\text{THF})$  should contain either two or four methyl signals (depending on the structure). Thus, the fluxional process is too fast on the  $^1\text{H}$  NMR timescale to resolve a rigid structure. The hafnium analog  $\{\mathbf{1}\}\text{Hf}(\text{NMe}_2)_2$  is also fluxional in the presence of 1 equiv. of THF, and the resonances (observed at room temperature) assigned to oxazoline methyl substituents and the methylene group coalesce into two broad singlets at 190 K.

**Table 2.2.**  $^{11}\text{B}$ ,  $^{15}\text{N}$  NMR chemical shifts and  $\nu_{\text{CN}}$  values for cyclopentadienyl-bis(oxazolinyl)borate group 4 complexes.

Compound	$^{11}\text{B}$ NMR ( $\delta$ ) acetonitrile- $d_3$	$^{15}\text{N}$ NMR ( $\delta$ ) acetonitrile- $d_3$	$\nu_{\text{CN}}$ (KBr, $\text{cm}^{-1}$ )	$[\alpha]_{\text{D}}^{20}$ ( $\text{C}_6\text{H}_6$ )
$\{\text{PhB}(\text{C}_5\text{H}_4)(\text{Ox}^{\text{Me}_2})_2\}\text{Zr}(\text{NMe}_2)_2$ $\{\mathbf{1}\}\text{Zr}(\text{NMe}_2)_2$ ; amorphous	-14.5	-135.4	1595	n.a.
$\{\text{PhB}(\text{C}_5\text{H}_4)(\text{Ox}^{\text{Me}_2})_2\}\text{Zr}(\text{NMe}_2)_2$ $\{\mathbf{1}\}\text{Zr}(\text{NMe}_2)_2$ ; crystallized	-14.5	n.a.	1603, 1505	n.a.
$\{\text{PhB}(\text{C}_5\text{H}_4)(\text{Ox}^{\text{Me}_2})_2\}\text{Zr}(\text{NMe}_2)_2\text{THF}$ $\{\mathbf{1}\}\text{Zr}(\text{NMe}_2)_2\text{THF}$	-14.5	n.a.	1610, 1533	n.a.
$\{\text{PhB}(\text{C}_5\text{H}_4)(\text{Ox}^{\text{Me}_2})_2\}\text{Hf}(\text{NMe}_2)_2$ $\{\mathbf{1}\}\text{Hf}(\text{NMe}_2)_2$	-14.6	-132.3	1595	n.a.
$\{\text{PhB}(\text{C}_5\text{H}_4)(\text{Ox}^{4\text{S-7Pr,Me}_2})_2\}\text{Zr}(\text{NMe}_2)_2$ $\{\text{S-2}\}\text{Zr}(\text{NMe}_2)_2$	-14.5	-152.6, -155.0	1565	-124.7°

{PhB(C <sub>5</sub> H <sub>4</sub> )(Ox <sup>4<i>R</i>-iPr,Me<sup>2</sup></sup> ) <sub>2</sub> }Zr(NMe <sub>2</sub> ) <sub>2</sub> { <i>R</i> -2}Zr(NMe <sub>2</sub> ) <sub>2</sub>	-14.5	-152.3, -155.1	1559	+122.6°
{PhB(C <sub>5</sub> H <sub>4</sub> )(Ox <sup>4<i>S</i>-iPr,Me<sup>2</sup></sup> ) <sub>2</sub> }Hf(NMe <sub>2</sub> ) <sub>2</sub> { <i>S</i> -2}Hf(NMe <sub>2</sub> ) <sub>2</sub>	-14.6	-148.8, -150.7	1559	-86.98°
{PhB(C <sub>5</sub> H <sub>4</sub> )(Ox <sup>4<i>S</i>-iPr,Me<sup>2</sup></sup> ) <sub>2</sub> }Ti(NMe <sub>2</sub> ) <sub>2</sub> { <i>S</i> -2}Ti(NMe <sub>2</sub> ) <sub>2</sub>	-14.8	-153.8, -156.1	1560	-94.71°
{PhB(C <sub>5</sub> H <sub>4</sub> )(Ox <sup>4<i>S</i>-iBu</sup> ) <sub>2</sub> }Zr(NMe <sub>2</sub> ) <sub>2</sub> { <i>S</i> -3}Zr(NMe <sub>2</sub> ) <sub>2</sub>	-14.4	-145.4, -148.1	1608, 1506	-139.13°
{PhB(C <sub>5</sub> H <sub>4</sub> )(Ox <sup>4<i>S</i>-iPr,Me<sup>2</sup></sup> ) <sub>2</sub> }ZrCl(NMe <sub>2</sub> ) { <i>S</i> -2}ZrCl(NMe <sub>2</sub> )	-16.4	-153.4, -154.9	1578, 1567	-111.4°
{Ph <sub>2</sub> B(C <sub>5</sub> H <sub>4</sub> )(Ox <sup>4<i>S</i>-iPr,Me<sup>2</sup></sup> ) <sub>2</sub> }Zr(NMe <sub>2</sub> ) <sub>2</sub> { <i>S</i> -7}Zr(NMe <sub>2</sub> ) <sub>2</sub>	-11.7	-155.2	1562	-82.02°

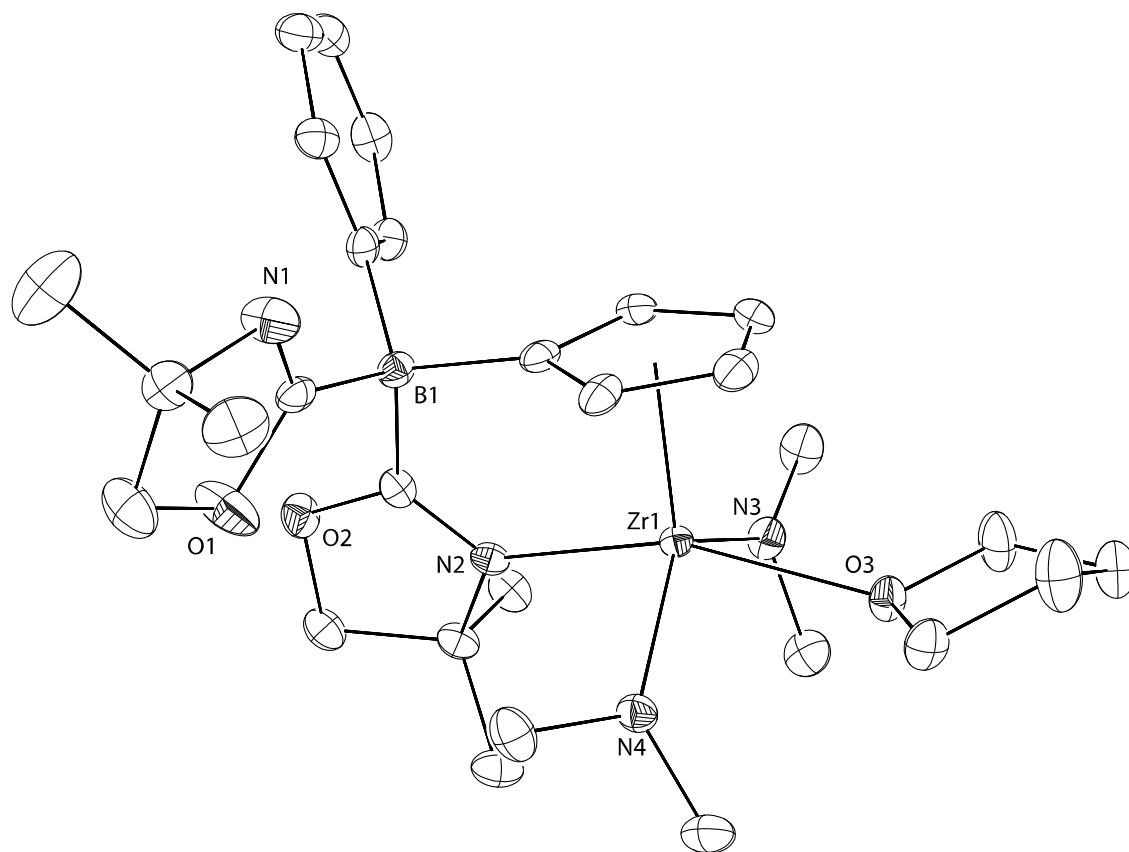


**Figure 2.1a.** ORTEP diagram of  $\{\text{PhB}(\text{C}_5\text{H}_4)(\text{Ox}^{\text{Me}_2})_2\}\text{Zr}(\text{NMe}_2)_2\text{THF}$  (**1**)  $\text{Zr}(\text{NMe}_2)_2\text{THF}$ ). Ellipsoids are plotted at 50% probability, and hydrogen atoms are not illustrated for clarity. Atomic distances (Å): Zr1–N2, 2.321(1); Zr1–N3, 2.045(1); Zr1–N4, 2.062(1); Zr1–O3, 2.415(1).

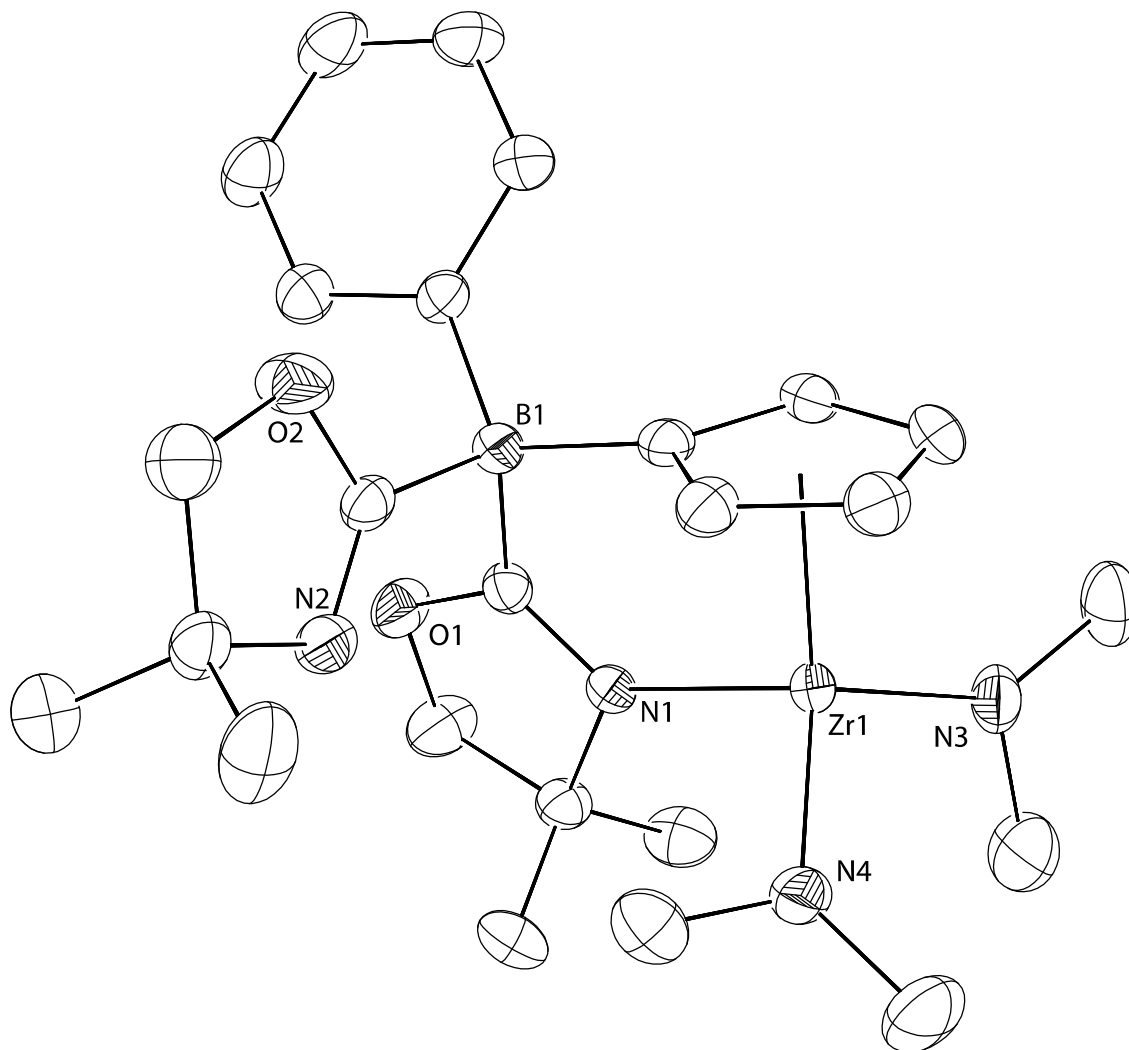


**Figure 2.1b.** ORTEP diagram of  $\{\text{PhB}(\text{C}_5\text{H}_4)(\text{Ox}^{\text{Me}_2})_2\}\text{Zr}(\text{NMe}_2)_2$  ( $\{\mathbf{1}\}\text{Zr}(\text{NMe}_2)_2$ ). Ellipsoids are plotted at 50% probability, and hydrogen atoms are not illustrated for clarity. Atomic distances (Å): Zr1–N1, 2.255(1); Zr1–N3, 2.031(2); Zr1–N4, 2.035(2).

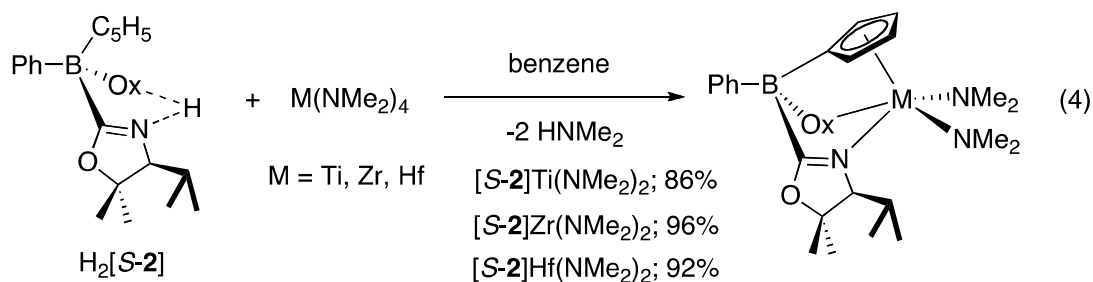
We therefore pursued THF-free, X-ray quality crystals of  $\{\mathbf{1}\}\text{Zr}(\text{NMe}_2)_2$ , which were obtained by slow diffusion of pentane into toluene solutions of  $\{\mathbf{1}\}\text{Zr}(\text{NMe}_2)_2$  cooled to 243 K. As in  $\{\mathbf{1}\}\text{Zr}(\text{NMe}_2)_2\text{THF}$ , the  $[\text{PhB}(\text{C}_5\text{H}_4)(\text{Ox}^{\text{Me}_2})_2]$  ligand bonds to Zr in the THF-free compound through the  $\text{C}_5\text{H}_4\text{B}$  and one oxazoline group (Zr1–N1, 2.25 Å), while the second

oxazoline is not coordinated to Zr (Zr1–N2, 4.31 Å). The geometry at zirconium is that of a three-legged piano stool; the  $\text{Cp}_{\text{centroid}}\text{-Zr-N}_{\text{Oxazoline}}$  angle ( $103.1^\circ$ ) is similar to that of the THF-adduct, while the  $\text{Cp}_{\text{centroid}}\text{-Zr-NMe}_2$  angles ( $110.47$  and  $122.35^\circ$ ) are smaller than in  $[\mathbf{1}]\text{Zr}(\text{NMe}_2)_2\text{THF}$ . The Zr–NMe<sub>2</sub> distances (Zr1–N3, Zr1–N4) are slightly shorter in  $[\mathbf{1}]\text{Zr}(\text{NMe}_2)_2$  than in the THF adduct (just outside of  $3\sigma$ ), and the Zr–Ox<sup>Me2</sup> distance is 0.066 Å shorter in the THF-free species. We wished to identify whether this compound would provide the same IR spectrum as the material obtained from evaporation of benzene. In fact, a spectrum of the crystalline sample (KBr) contained two bands in the IR at 1603 and 1505 cm<sup>-1</sup> assigned to  $\nu_{\text{CN}}$  stretching frequencies of non-coordinated and Zr-coordinated oxazolines. This IR data contrasts that of the material obtained by evaporation, where only one  $\nu_{\text{CN}}$  band at 1595 cm<sup>-1</sup> was observed.

In contrast, the reaction of  $\text{Ti}(\text{NMe}_2)_4$  with  $\text{H}_2\{\mathbf{1}\}$  in benzene at room temperature provides a mixture of unidentified products. The <sup>1</sup>H NMR spectrum does not have the same spectral signatures as noted above for  $\{\mathbf{1}\}\text{Zr}(\text{NMe}_2)_2$ . <sup>1</sup>H NMR spectra of reaction mixtures in benzene-*d*<sub>6</sub> or toluene-*d*<sub>8</sub> contained vinylic resonances from isomers of C<sub>5</sub>H<sub>5</sub>B; the conversion of these signals to those associated with a single C<sub>s</sub>-symmetric compound was not observed even upon heating at 120 °C. HNMe<sub>2</sub> was observed in spectra of reaction mixtures within 10 min. which indicated that some ligand substitution occurred. Four <sup>11</sup>B resonances were detected ranging from 33.6 to –14.7 ppm, and the upfield <sup>11</sup>B NMR signal also suggested that a borane was among the reaction products.

The chiral, 4*S*-isopropyl-5,5-dimethyl-2-oxazoline-based proligand  $\text{H}_2[\mathbf{S-2}]$  and  $\text{M}(\text{NMe}_2)_4$  (M = Ti, Zr, Hf) react in benzene at room temperature, providing  $\{\mathbf{S-2}\}\text{M}(\text{NMe}_2)_2$  in excellent yield (eq 4; Ti: 25 h, 86%; Zr: 7 h, 96%; Hf: 7 h, 92%).

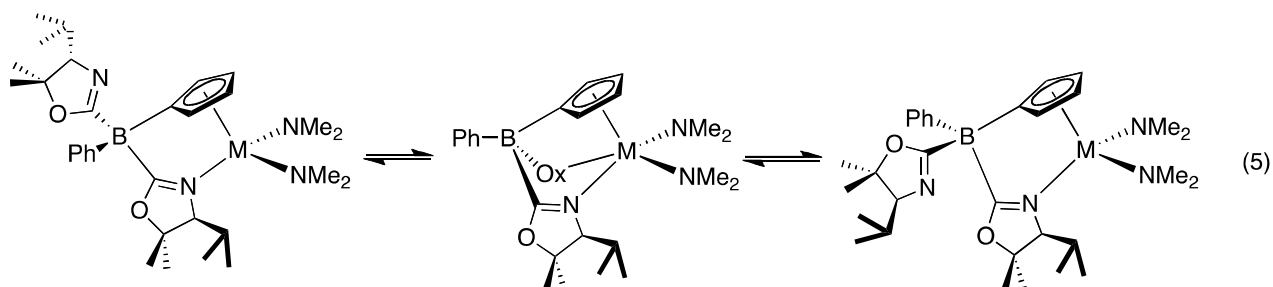




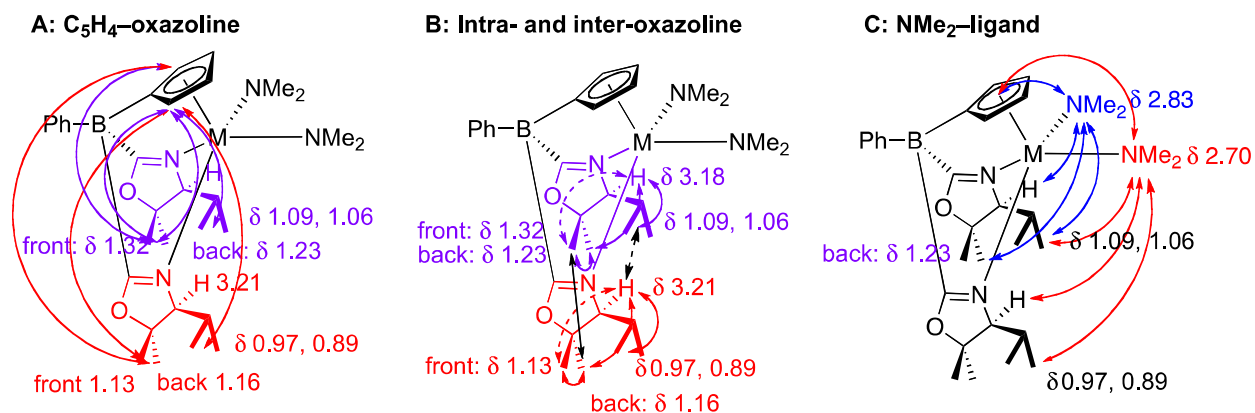
The opposite enantiomer  $\{R-2\}Zr(NMe_2)_2$  is prepared from  $H_2[R-2]$  and  $Zr(NMe_2)_4$ . As expected, the NMR and IR spectroscopic features of  $\{S-2\}Zr(NMe_2)_2$  and  $\{R-2\}Zr(NMe_2)_2$  are identical. Two sets of oxazoline resonances (*e.g.*, two septets and four doublets assigned to the isopropyl groups and four singlets for the 5-methyl groups) and four downfield multiplets ranging from 6.7 to 6.06 ppm for the cyclopentadienyl group suggested  $C_1$ -symmetric species for  $\{S-2\}Zr(NMe_2)_2$ . Two singlets are observed for the two inequivalent dimethylamide ligands. Additionally, the broad  $^{11}B$  NMR resonance at  $-15.7$  ppm resulting from overlapping signals from isomers of  $H_2[S-2]$  is replaced with a sharper signal at  $-14.5$  ppm (122 Hz at half-height). The compounds  $\{S-2\}Ti(NMe_2)_2$  and  $\{S-2\}Hf(NMe_2)_2$  have similar  $^1H$  NMR spectra. The  $C$ -stereocenters in the molecule necessarily render the two oxazolines inequivalent, so  $^1H$  NMR spectroscopy does not distinguish between zero, one, or two coordinated oxazolines. However,  $^{15}N$  NMR and IR spectroscopy suggests that both oxazolines coordinate to the metal centers in  $\{S-2\}M(NMe_2)_2$ . Two  $^{15}N$  NMR signals were observed at  $-152.6$  and  $-155.0$  in comparison to  $-143$  for  $2H-Ox^{4S-iPr,Me_2}$ . Additionally, only one CN stretching frequency was observed in the IR at  $1565\text{ cm}^{-1}$ . A  $\nu_{CN}$  associated with a non-coordinated oxazoline, based on the higher energy  $\nu_{CN}$  of  $2H-Ox^{4S-iPr,Me_2}$  ( $1632\text{ cm}^{-1}$ ), was not detected.

The solution structure was further probed with a  $^1H$ - $^1H$  NOESY experiment to identify which groups on the ancillary ligand interact with the presumed reactive sites that are occupied by  $NMe_2$  groups in  $[S-2]Zr(NMe_2)_2$ , and correlations and assignments are illustrated in Figure

2.2. First, the *S*-**2** intraligand correlations establish the metal-ligand conformations that are sufficiently populated to provide NOEs. The two sets of correlations discerned are oxazoline- $C_5H_4$  correlations and oxazoline-oxazoline correlations. Interestingly, the former correlations only involve the lateral 2- and 5- hydrogen on the  $C_5H_4$  group (Figure 2.2A) to methyl and isopropyl groups of both oxazolines. No correlations between the oxazoline and the 3- and 4- hydrogen were observed in the NOESY. The lateral correlations suggest significant population of configurations in which the zirconium-ligand interaction contains one dissociated oxazoline  $\{\eta^5-\kappa^1\text{-Ph}(\text{Ox}^{i\text{Pr},\text{Me}_2})\text{B}(\text{C}_5\text{H}_4)(\text{Ox}^{i\text{Pr},\text{Me}_2})\}\text{Zr}(\text{NMe}_2)_2$ . The significance of this conformation is further suggested by the X-ray crystal structure of **1** $\}\text{Zr}(\text{NMe}_2)_2$ . However, there are also through-space correlations between the two oxazolines that suggest both oxazolines coordinate to zirconium for on an NOE-significant timescale. Thus, we suggest that these two conformations dominate the geometry of  $\{\textit{S}\text{-2}\}\text{Zr}(\text{NMe}_2)_2$  and exchange rapidly on the NMR time scale (eq 5).



Furthermore, the intra- and inter-oxazoline correlations are useful to establish the relative orientation of the two oxazolines (Figure 2.2B). Based on these assignments and NOEs between oxazoline and  $\text{NMe}_2$  ligands, we can assign the signals for the inequivalent  $\text{NMe}_2$  groups and the overall configuration of the zirconium center (Figure 2.2C).



\*A dashed double-headed arrow represents a weak correlation

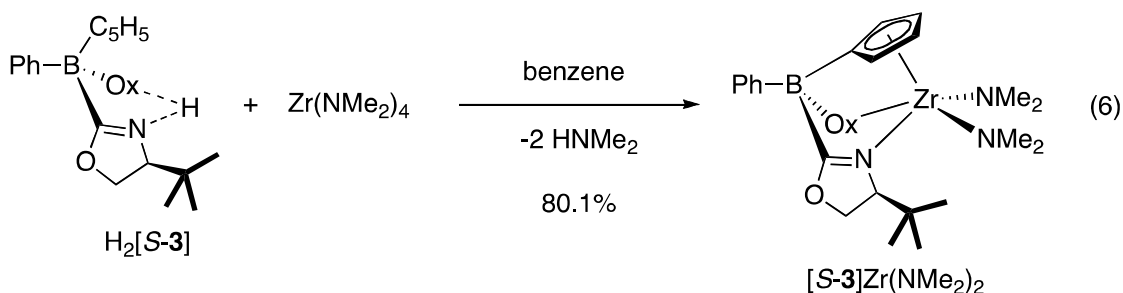
**Figure 2.2:** Through-space correlations in  $[S-2]Zr(NMe_2)_2$ .

Interestingly, the "back"  $NMe_2$  in Figure 2.2 at 2.83 ppm correlations show through-space interactions with the "back" oxazoline, whereas the "front"  $NMe_2$  at 2.70 contained correlations with resonances from both oxazoline rings. Thus, the open space between the cyclopentadiene and the "back" oxazoline is occupied by a dimethylamide group, and the other dimethylamide group is situated between the two oxazoline rings in the di-coordinated conformer.

A second optically active zirconium complex  $\{PhB(C_5H_4)(Ox^{4S-tBu})_2\}Zr(NMe_2)_2$   $\{S-3\}Zr(NMe_2)_2$  is prepared by reaction of  $H_2\{S-3\}$  and  $Zr(NMe_2)_4$  in benzene at room temperature for 20 min. In its  $^1H$  NMR spectrum, two singlet resonances at 0.85 and 0.84 ppm were assigned to *tert*-butyl substituents on two inequivalent oxazoline groups, and four downfield multiplets ranging from 6.74 to 6.09 ppm were assigned to the cyclopentadienyl group. Likewise and as in  $S-2$ , two singlets for two inequivalent dimethylamido groups were observed, and the overall pattern was consistent with  $C_1$  symmetry. In the  $^{11}B$  spectrum, a sharp resonance at  $-14.4$  ppm indicated that a single product was formed. The complex  $\{S-3\}Zr(NMe_2)_2$  decomposes in

benzene at room temperature ( $t_{1/2} = 2$  h), leading to  $\text{HNMe}_2$  and unidentified oxazolinyborate products.

In contrast,  $\{S-2\}\text{M}(\text{NMe}_2)_2$  complexes ( $\text{M} = \text{Ti}, \text{Zr}, \text{Hf}$ ) are unchanged in benzene even after 36 h at room temperature.

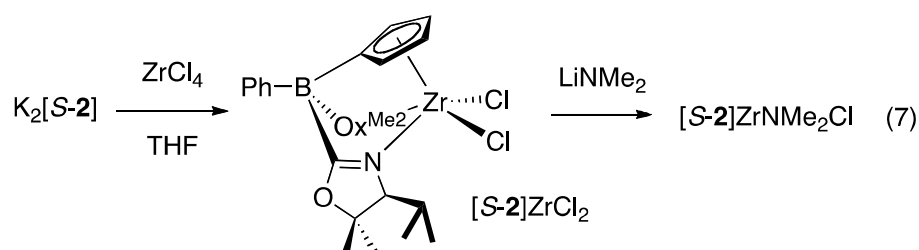


Additionally, several compounds were required to test (a) the reactive valencies required for hydroamination catalysis and (b) the nature of ancillary ligand-zirconium interaction and its impact on cyclization and enantioselectivity. The compound  $\{S-2\}\text{ZrNMe}_2\text{Cl}$  was prepared to address the former point. Reaction of  $\text{H}_2[S-2]$  and 2 equiv. of  $\text{KCH}_2\text{C}_6\text{H}_5$  affords  $\text{K}_2[S-2]$ . Reaction of  $\text{K}_2[S-2]$  and  $\text{ZrCl}_4$  in THF at room temperature provides  $\{S-2\}\text{ZrCl}_2$  within 30 min.

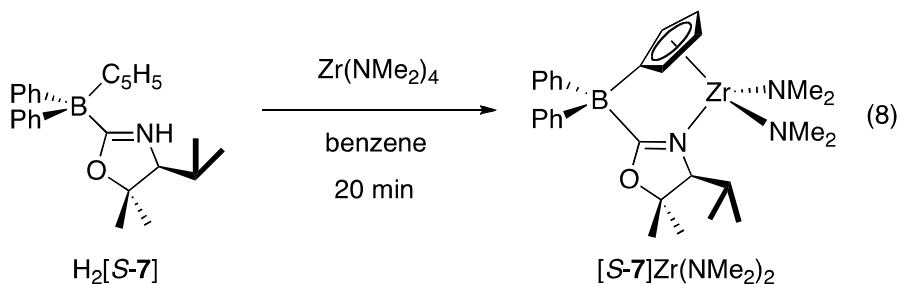
Two septets, four doublets, and four singlets in the  $^1\text{H}$  NMR spectrum (tetrahydrofuran- $d_8$ ) assigned to oxazoline isopropyl and methyl groups were consistent with inequivalent oxazolines expected for a  $C_1$ -symmetric complex. Four multiplets in the downfield region from 6.88 to 6.23 ppm were attributed to the cyclopentadienyl group in  $\{S-2\}\text{ZrCl}_2$ . The complex is unchanged in THF- $d_8$  for 7 days at room temperature, however, broad signals were observed in  $^1\text{H}$  NMR spectra of  $\{S-2\}\text{ZrCl}_2$  after the solvent was evaporated and the residue was redissolved in tetrahydrofuran- $d_8$ . Therefore, the complex  $\{S-2\}\text{ZrCl}_2$  is best prepared in situ for the synthesis of  $\{S-2\}\text{Zr}(\text{NMe}_2)\text{Cl}$ .

The desired compound  $\{S-2\}\text{Zr}(\text{NMe}_2)\text{Cl}$  is prepared by of one equiv. of  $\text{LiNMe}_2$  to  $\{S-2\}\text{ZrCl}_2$  (generated in situ). The complex was isolated by removal of volatiles from the reaction

mixture *in vacuo*, followed by benzene extraction with 79% isolated yield. A mixture of two diastereomers is formed (in 4:1 ratio as detected by  $^1\text{H}$  NMR spectroscopy of tetrahydrofuran- $d_8$  solutions) because the zirconium in  $\{S\text{-}2\}\text{Zr}(\text{NMe}_2)\text{Cl}$  is a stereocenter. The  $^1\text{H}$  NMR resonances associated with the ancillary ligand in each of the two diastereomers indicated the (expected)  $C_1$ -symmetry. Two sets of oxazoline resonances, one singlet for dimethylamido group, and four multiplets for the cyclopentadienyl group were observed for each of the  $C_1$ -symmetric diastereomers. The 4:1 diastereomeric ratio remains unchanged in THF at room temperature after 12 h.



A mono(oxazolinyl)borato zirconium  $\{S\text{-}7\}\text{Zr}(\text{NMe}_2)_2$  compound is prepared by reaction of  $\text{H}[\text{Ph}_2\text{B}(\text{C}_5\text{H}_5)(\text{Ox}^{4S\text{-}i\text{PrMe}_2})]$  ( $\text{H}_2\{S\text{-}7\}$ ) and  $\text{Zr}(\text{NMe}_2)_4$ . The treatment of isomeric mixture of  $\text{H}_2\{S\text{-}7\}$  with 1 equiv. of  $\text{Zr}(\text{NMe}_2)_4$  in benzene at room temperature formed  $\{S\text{-}7\}\text{Zr}(\text{NMe}_2)_2$  after 20 min with 92% isolated yield. The  $^1\text{H}$  NMR spectrum of  $\{S\text{-}7\}\text{Zr}(\text{NMe}_2)_2$  in benzene is constant at room temperature over at least 12 h.



One set of oxazoline resonances (*i.e.*, one septet and two doublets assigned to the isopropyl groups and two singlets for the 5-methyl groups), two singlets for two inequivalent

dimethylamido groups, and four downfield multiplets for the cyclopentadienyl group suggest a  $C_1$ -symmetric species for  $\{S-7\}Zr(NMe_2)_2$ . The  $^1H$  NMR pattern did not change at variable temperatures ranging from 190 K and 320 K in toluene- $d_8$ . Additionally, three  $^{11}B$  NMR resonance at  $-10.0$ ,  $-11.5$  and  $-12.4$  ppm from isomers of  $H_2[S-7]$  is converted to a single resonance at  $-11.7$  ppm. In infrared, one  $\nu_{CN}$  at  $1562\text{ cm}^{-1}$  for  $\{S-7\}Zr(NMe_2)_2$  indicates that the oxazoline is coordinated to the zirconium center.

### *Catalytic Hydroamination/Cyclization of Aminoalkenes*

The bis(oxazolynyl)cyclopentadienylborate-coordinated bis(amido) group 4 compounds  $\{1\}Zr(NMe_2)_2$ ,  $\{1\}Hf(NMe_2)_2$ ,  $\{S-2\}Zr(NMe_2)_2$ ,  $\{S-2\}Hf(NMe_2)_2$ ,  $\{S-2\}Ti(NMe_2)_2$ ,  $\{R-2\}Zr(NMe_2)_2$ , and  $\{S-3\}Zr(NMe_2)_2$  catalyze the cyclization of aminoalkenes to give racemic and optically-enriched pyrrolidine, piperidine, azepane, and indoline products at room temperature (Tables 2.3-2.5). These tables are organized by substrate type: Table 2.3 gives conditions for cyclization of aminopentenes **8a-13a** that have aliphatic or aromatic 3,3-disubstitution; Table 2.4 contains 6 and 7-membered rings from substrates **14a-17a**; Table 2.5 contains cyclizations of substrates **18a-23a** that give indoline, halogenated, acetal, and internal alkenes. In contrast,  $\{S-2\}Zr(NMe_2)Cl$  and  $\{S-7\}Zr(NMe_2)_2$  are not precatalysts for cyclization of aminoalkenes under the conditions tested.

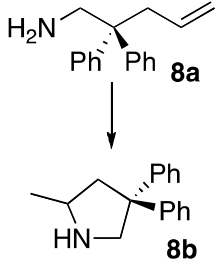
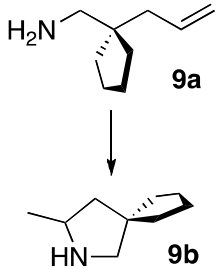
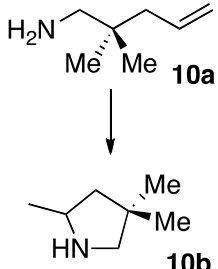
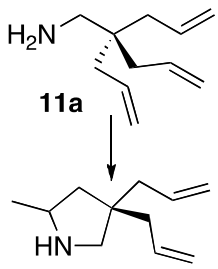
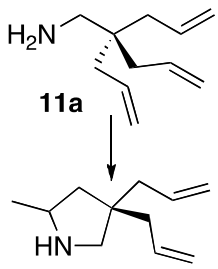
The general rates of cyclization depend on the metal center, ancillary ligand, and substrate. Some general trends (for which exceptions) are summarized as follows. The metal center affects the reaction rate following the trend  $Zr > Hf \gg Ti$ . For example, the apparent reaction rate (based on time required for conversion to 95%) for cyclization of aminopentene **8a** is greater for  $\{1\}Zr(NMe_2)_2$  than  $\{1\}Hf(NMe_2)_2$  (Table 2.3, entries 1 and 2).  $\{S-2\}Zr(NMe_2)_2$  is

a significantly more effective precatalyst than  $\{S-2\}\text{Hf}(\text{NMe}_2)_2$ , and in many cases only starting materials were detected in mixtures of  $\{S-2\}\text{Ti}(\text{NMe}_2)_2$  and aminopentenes (allowed to stand at room temperature for extended times). In fact, only three of the most highly reactive substrates diphenyl **8a**, tris(allyl) **11a** and cyclohexyl **12a** are cyclized by  $\{S-2\}\text{Ti}(\text{NMe}_2)_2$  at room temperature with appreciable conversion.

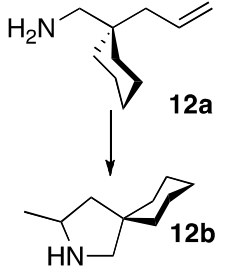
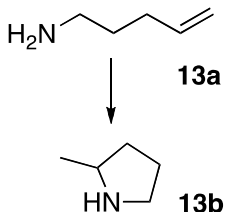
For zirconium diamide catalysts, the oxazoline substituents on the ancillary ligand affect hydroamination rates, generally following the trend  $\{S-2\}\text{Zr}(\text{NMe}_2)_2 > \{\mathbf{1}\}\text{Zr}(\text{NMe}_2)_2 > \{S-3\}\text{Zr}(\text{NMe}_2)_2$ . For example, diphenyl substrate **8a** is cyclized to pyrrolidine **8b** in 1.25 h by  $\{S-2\}\text{Zr}(\text{NMe}_2)_2$ , 11 h by  $\{\mathbf{1}\}\text{Zr}(\text{NMe}_2)_2$ , and 18 by  $\{S-3\}\text{Zr}(\text{NMe}_2)_2$  (Table 3, entries 3, 1, and 14). This trend applies to the formation of most pyrrolidine, azepane, and indoline products found in Tables 2.3–2.5. However, achiral 4,4-dimethyl-2-oxazoline-based  $\{\mathbf{1}\}\text{Zr}(\text{NMe}_2)_2$  is a more active catalyst than  $\{S-2\}\text{Zr}(\text{NMe}_2)_2$  for unsubstituted aminopentene **13a** (Table 2.3, entries 46 and 47) and aminohexenes **14a** and **15a** (Table 2.4, entries 1 and 2; entries 5 and 6); the unsubstituted aminopentene is readily cyclized by  $\{\mathbf{1}\}\text{Zr}(\text{NMe}_2)_2$  at room temperature, but  $\{S-2\}\text{Hf}(\text{NMe}_2)_2$ ,  $\{S-2\}\text{Ti}(\text{NMe}_2)_2$ , and  $\{S-3\}\text{Zr}(\text{NMe}_2)_2$  are not precatalysts for this cyclization, and  $\{S-2\}\text{Zr}(\text{NMe}_2)_2$  requires temperatures of 110 °C for only a few turnovers.

**Table 2.3.** Catalytic cyclization of aminopentenes with achiral and optically active group 4 compounds coordinated by mixed cyclopentadienyl bis(oxazolinyl)borato ligands.<sup>a</sup>

Reactant to Product	Entry	Precatalyst	Solvent	Time (h)	Yield (%)	ee (%) <sup>b</sup>
	1	$\{\mathbf{1}\}\text{Zr}(\text{NMe}_2)_2$	$\text{C}_6\text{D}_6$	11	90	racemic
	2	$\{\mathbf{1}\}\text{Hf}(\text{NMe}_2)_2$	$\text{C}_6\text{D}_6$	24	29	racemic
	3	$\{S-2\}\text{Zr}(\text{NMe}_2)_2$	$\text{C}_6\text{D}_6$	1.25	95	93 (R)
	4	$\{S-2\}\text{Zr}(\text{NMe}_2)_2$	$\text{C}_6\text{D}_6$	6	95 <sup>c</sup>	93 (R)
	5	$\{S-2\}\text{Zr}(\text{NMe}_2)_2$	THF- <i>d</i> <sub>8</sub>	5	95	95 (R)
	6	$\{S-2\}\text{Zr}(\text{NMe}_2)_2$	$\text{CD}_2\text{Cl}_2$	5	95	93 (R)

	7	{ <i>S</i> -2}Zr(NMe <sub>2</sub> ) <sub>2</sub>	C <sub>7</sub> D <sub>8</sub>	5 d	98 <sup>e</sup>	98 ( <i>R</i> ) <sup>f</sup>	
	8	{ <i>R</i> -2}Zr(NMe <sub>2</sub> ) <sub>2</sub>	C <sub>6</sub> D <sub>6</sub>	1.25	95	93 ( <i>S</i> )	
	9	{ <i>S</i> -2}Hf(NMe <sub>2</sub> ) <sub>2</sub>	C <sub>6</sub> D <sub>6</sub>	5	97	91 ( <i>R</i> )	
	10	{ <i>S</i> -2}Hf(NMe <sub>2</sub> ) <sub>2</sub>	C <sub>7</sub> D <sub>8</sub>	15	98 <sup>d</sup>	96 ( <i>R</i> ) <sup>f</sup>	
	11	{ <i>S</i> -2}Hf(NMe <sub>2</sub> ) <sub>2</sub>	CD <sub>2</sub> Cl <sub>2</sub>	15	96 <sup>d</sup>	94 ( <i>R</i> )	
	12	{ <i>S</i> -2}Hf(NMe <sub>2</sub> ) <sub>2</sub>	THF- <i>d</i> <sub>8</sub>	20	98 <sup>d</sup>	96 ( <i>R</i> ) <sup>f</sup>	
	13	{ <i>S</i> -2}Ti(NMe <sub>2</sub> ) <sub>2</sub>	C <sub>6</sub> D <sub>6</sub>	5 d	93	76 ( <i>R</i> )	
	14	{ <i>S</i> -3}Zr(NMe <sub>2</sub> ) <sub>2</sub>	C <sub>6</sub> D <sub>6</sub>	18	95	93 ( <i>R</i> )	
		15	{ <b>1</b> }Zr(NMe <sub>2</sub> ) <sub>2</sub>	C <sub>6</sub> D <sub>6</sub>	11	88	racemic
		16	{ <i>S</i> -2}Zr(NMe <sub>2</sub> ) <sub>2</sub>	C <sub>6</sub> D <sub>6</sub>	4	88	92 ( <i>R</i> )
		17	{ <i>R</i> -2}Zr(NMe <sub>2</sub> ) <sub>2</sub>	C <sub>6</sub> D <sub>6</sub>	4	88	92 ( <i>S</i> )
		18	{ <i>S</i> -2}Hf(NMe <sub>2</sub> ) <sub>2</sub>	C <sub>6</sub> D <sub>6</sub>	20	90	94 ( <i>R</i> )
		19	[ <i>S</i> -2]Hf(NMe <sub>2</sub> ) <sub>2</sub>	C <sub>7</sub> D <sub>8</sub>	8	85 <sup>d</sup>	95 ( <i>R</i> ) <sup>f</sup>
		20	{ <i>S</i> -2}Ti(NMe <sub>2</sub> ) <sub>2</sub>	C <sub>6</sub> D <sub>6</sub>	48	0	-
21		{ <i>S</i> -3}Zr(NMe <sub>2</sub> ) <sub>2</sub>	C <sub>6</sub> D <sub>6</sub>	11	77	88 ( <i>R</i> )	
	22	{ <b>1</b> }Zr(NMe <sub>2</sub> ) <sub>2</sub>	C <sub>6</sub> D <sub>6</sub>	11	85	racemic	
	23	{ <i>S</i> -2}Zr(NMe <sub>2</sub> ) <sub>2</sub>	C <sub>6</sub> D <sub>6</sub>	7	89	89	
	24	{ <i>S</i> -2}Zr(NMe <sub>2</sub> ) <sub>2</sub>	C <sub>7</sub> D <sub>8</sub>	8 d	95 <sup>e</sup>	93	
	25	{ <i>S</i> -2}Hf(NMe <sub>2</sub> ) <sub>2</sub>	C <sub>6</sub> D <sub>6</sub>	20	90	87	
	26	{ <i>S</i> -2}Ti(NMe <sub>2</sub> ) <sub>2</sub>	C <sub>6</sub> D <sub>6</sub>	72	0	-	
	27	{ <i>S</i> -3}Zr(NMe <sub>2</sub> ) <sub>2</sub>	C <sub>6</sub> D <sub>6</sub>	48	20	-	
		28	{ <b>1</b> }Zr(NMe <sub>2</sub> ) <sub>2</sub>	C <sub>6</sub> D <sub>6</sub>	11	98	racemic
29		{ <i>S</i> -2}Zr(NMe <sub>2</sub> ) <sub>2</sub>	C <sub>6</sub> D <sub>6</sub>	0.75	98	93 ( <i>R</i> )	
30		{ <i>S</i> -2}Zr(NMe <sub>2</sub> ) <sub>2</sub>	CD <sub>2</sub> Cl <sub>2</sub>	1	98	94 ( <i>R</i> )	
31		{ <i>S</i> -2}Zr(NMe <sub>2</sub> ) <sub>2</sub>	THF- <i>d</i> <sub>8</sub>	1.25	96	94 ( <i>R</i> )	
32		{ <i>S</i> -2}Hf(NMe <sub>2</sub> ) <sub>2</sub>	C <sub>6</sub> D <sub>6</sub>	5	98	90 ( <i>R</i> )	
33		{ <i>S</i> -2}Hf(NMe <sub>2</sub> ) <sub>2</sub>	C <sub>7</sub> D <sub>8</sub>	20	90 <sup>[d]</sup>	96 ( <i>R</i> ) <sup>f</sup>	
34		{ <i>S</i> -2}Ti(NMe <sub>2</sub> ) <sub>2</sub>	C <sub>6</sub> D <sub>6</sub>	5 d	90	82 ( <i>R</i> )	
35		{ <i>S</i> -3}Zr(NMe <sub>2</sub> ) <sub>2</sub>	C <sub>6</sub> D <sub>6</sub>	30	97	88 ( <i>R</i> )	
		36	{ <b>1</b> }Zr(NMe <sub>2</sub> ) <sub>2</sub>	C <sub>6</sub> D <sub>6</sub>	11	92	racemic
	37	{ <i>S</i> -2}Zr(NMe <sub>2</sub> ) <sub>2</sub>	C <sub>6</sub> D <sub>6</sub>	1.25	96	90 ( <i>R</i> )	
	38	{ <i>S</i> -2}Zr(NMe <sub>2</sub> ) <sub>2</sub>	C <sub>6</sub> D <sub>6</sub>	6.5	92 <sup>c</sup>	90 ( <i>R</i> )	
	39	{ <i>S</i> -2}Zr(NMe <sub>2</sub> ) <sub>2</sub>	C <sub>7</sub> D <sub>8</sub>	10	94 <sup>d</sup>	91 ( <i>R</i> )	



	40	{ <i>S</i> -2}Zr(NMe <sub>2</sub> ) <sub>2</sub>	THF- <i>d</i> <sub>8</sub>	11	92 <sup>d</sup>	94 ( <i>R</i> )
	41	{ <i>S</i> -2}Zr(NMe <sub>2</sub> ) <sub>2</sub>	CD <sub>2</sub> Cl <sub>2</sub>	10	95 <sup>d</sup>	93 ( <i>R</i> )
	42	{ <i>R</i> -2}Zr(NMe <sub>2</sub> ) <sub>2</sub>	C <sub>6</sub> D <sub>6</sub>	1.25	96	90 ( <i>S</i> )
	43	{ <i>S</i> -2}Hf(NMe <sub>2</sub> ) <sub>2</sub>	C <sub>6</sub> D <sub>6</sub>	5	95	93 ( <i>R</i> )
	44	{ <i>S</i> -2}Ti(NMe <sub>2</sub> ) <sub>2</sub>	C <sub>6</sub> D <sub>6</sub>	5 d	75	83 ( <i>R</i> )
	45	{ <i>S</i> -3}Zr(NMe <sub>2</sub> ) <sub>2</sub>	C <sub>6</sub> D <sub>6</sub>	30	92	87 ( <i>R</i> )
	46	{ <b>1</b> }Zr(NMe <sub>2</sub> ) <sub>2</sub>	C <sub>6</sub> D <sub>6</sub>	15	90	racemic
	47	{ <i>S</i> -2}Zr(NMe <sub>2</sub> ) <sub>2</sub>	C <sub>6</sub> D <sub>6</sub>	15	24 <sup>g</sup>	-
	48	{ <i>S</i> -2}Hf(NMe <sub>2</sub> ) <sub>2</sub>	C <sub>6</sub> D <sub>6</sub>	48	0	-
	49	{ <i>S</i> -2}Ti(NMe <sub>2</sub> ) <sub>2</sub>	C <sub>6</sub> D <sub>6</sub>	48	0	-
	50	{ <i>S</i> -3}Zr(NMe <sub>2</sub> ) <sub>2</sub>	C <sub>6</sub> D <sub>6</sub>	48	0	-

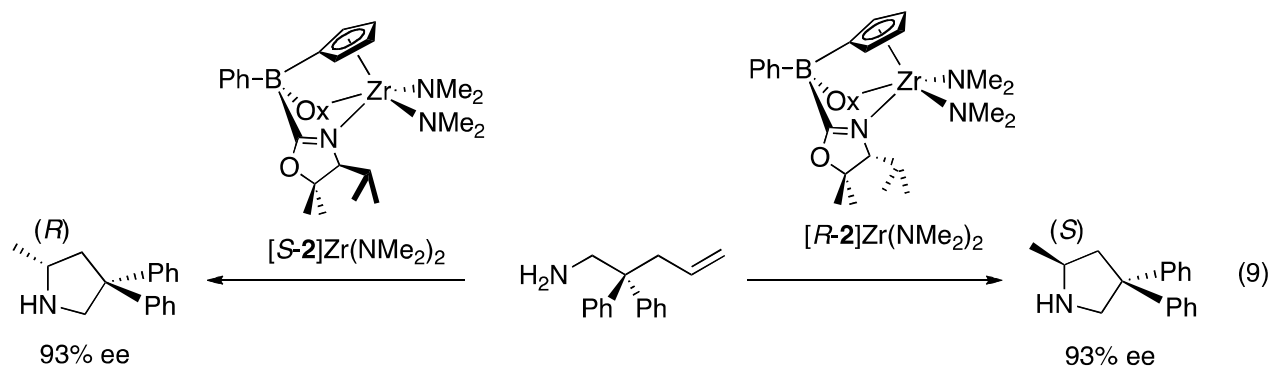
<sup>a</sup> Reaction conditions: 10 mol % catalyst, r.t. unless noted. <sup>b</sup> % ee ( $\pm 0.5\%$ ) was determined by <sup>1</sup>H and/or <sup>19</sup>F NMR spectroscopy by integration of the spectra of Mosher amide derivatives. The absolute configuration assignments are based on literature reports.<sup>5d,15a</sup> <sup>c</sup> 2 mol % catalyst. <sup>d</sup> Reaction performed at 0 °C. <sup>e</sup> Reaction performed at -30 °C. <sup>f</sup> % ee measured by <sup>19</sup>F NMR of Mosher amides derivatives and HPLC of benzoylamide derivatives. <sup>g</sup> Reaction performed at 110 °C.

The enantioselectivities were determined by integration of <sup>19</sup>F NMR spectra of trifluoromethylamide derivatives. For samples with the highest % ee, the result was checked with HPLC using a chiral stationary phase; the two methods invariably provided the same value within error. Racemic products were obtained from {**1**}Zr(NMe<sub>2</sub>) for spectroscopic and chromatographic comparison with optically active heterocycles.

Several generalizations about the influence of ancillary ligand, metal center, solvent, and temperature on enantioselectivity for most substrates can be identified. Overall, this group 4 system provides pyrrolidines with excellent optical purities. For example, diphenylaminopentene is cyclized at room temperature to *R*-configured 2-Me-pyrrolidine with 93% ee by {*S*-2}Zr(NMe<sub>2</sub>)<sub>2</sub> (Table 2.3, entry 3) and 91% ee by {*S*-2}Hf(NMe<sub>2</sub>)<sub>2</sub> (Table 2.3, entry 9), and 93% ee by {*S*-3}Zr(NMe<sub>2</sub>)<sub>2</sub> (Table 2.3, entry 14). Impressively, the enantioselectivities of reactions catalyzed by {*S*-2}Zr(NMe<sub>2</sub>)<sub>2</sub> are high for a range of substrates that include functional groups on five membered rings and seven-membered rings (Tables 2.3 – 2.5). In the series of

pyrrolidines, spiro-cyclohexyl-pyrrolidine **12b** (90%), cyclopentyl-pyrrolidine **9b** (92%), dimethyl-pyrrolidine **10b** (89%), and trisallyl-pyrrolidine **11b** (93%) are obtained at room temperature using  $\{S-2\}Zr(NMe_2)_2$  (Table 2.3). Furthermore, while the reaction rate is sensitive to the substrate and catalyst concentration, however the enantioselectivity is not. For example, 2-10 mol %  $\{[S-2]Zr(NMe_2)_2$  provides **8b** pyrrolidine with 93% ee at all catalyst loadings, but the apparent turnover rate decreases significantly as catalyst concentration decreases (Table 2.3; entries 3 and 4).

In general,  $\{S-2\}Zr(NMe_2)_2$ ,  $\{S-2\}Hf(NMe_2)_2$  and  $\{S-3\}Zr(NMe_2)_2$  provide products with better optical purities than the titanium-based precatalyst  $\{S-2\}Ti(NMe_2)_2$ . The 4*S*-isopropyl-5,5-dimethyl-2-oxazoline ligands *S-2* and *R-2* often give pyrrolidines with higher % enantiomeric excess than 4*S*-tert-butyl-2-oxazoline ligand *S-3*. For example, tris(allyl)methylamine is cyclized by  $\{S-2\}Zr(NMe_2)_2$  to give 4,4-diallyl-2-methyl-pyrrolidine in 93% ee, whereas  $\{S-3\}Zr(NMe_2)_2$  affords the product in 88% ee. Similar effects are observed with the cyclopentyl substrate (92% vs. 88%) and cyclohexyl substrate (90% vs. 87%), while diphenyl pyrrolidine forms with equivalent % ee with  $\{S-2\}Zr(NMe_2)_2$  and  $\{S-3\}Zr(NMe_2)_2$ . As expected, the mirror-image precatalyst  $\{R-2\}Zr(NMe_2)_2$  gives equivalent reactivity and enantioselectivity as  $\{S-2\}Zr(NMe_2)_2$ , but provides the products with the opposite absolute configuration. Thus, an additional advantage of valine-derived ligands vs. *tert*-leucine is that both enantiomers are readily available for the former.



The hafnium precatalyst  $\{S-2\}Hf(NMe_2)_2$  is also highly enantioselective, and the examples here are the first in which hafnium complex affords hydroamination products with optical purities  $>90\%$ . In fact,  $\{S-2\}Hf(NMe_2)_2$  provides pyrrolidines with higher enantioselectivity than  $\{S-2\}Zr(NMe_2)_2$  for about half of the aminoalkenes that were tested. In particular,  $\{S-2\}Hf(NMe_2)_2$  gives higher % ee in benzene- $d_6$  at room temperature for cyclopentylpyrrolidine (**9b**, 94% ee) and cyclohexylpyrrolidine (**12b**, 93% ee). Under these conditions, diphenylpyrrolidine, trimethylpyrrolidine, and diallylpyrrolidine are formed with greater optical purities in reactions catalyzed by  $\{S-2\}Zr(NMe_2)_2$  than  $\{S-2\}Hf(NMe_2)_2$ . The enantiomeric excesses were always lowest with  $\{S-2\}Ti(NMe_2)_2$  as the precatalyst, regardless of the substrate. Thus, the effect of metal center on hydroamination enantioselectivity follows the trend  $Zr \approx Hf > Ti$  for this mixed cyclopentadienyl-bis(oxazolinyl)borate group 4 system.

Aside from slight variations, in general the pyrrolidine products' optical purities are high in benzene, toluene, methylene chloride, and THF. The apparent turnover rate is diminished in THF or methylene chloride compared to benzene or toluene, however, the enantioselectivity is enhanced. With the  $\{S-2\}Zr(NMe_2)_2$ -catalyzed cyclization of the diphenyl substrate **8a** as a representative example, benzene- $d_6$  and methylene chloride- $d_2$  solvents the same enantioselectivity (93% ee), although the reaction is faster in benzene- $d_6$ . Higher enantiomeric

excess is obtained in THF at room temperature (95%; Table 2.3, entry 5) and conditions of lower temperature ( $-30\text{ }^{\circ}\text{C}$ ) in toluene- $d_8$  solvent provide the product with 98% ee (Table 2.3, entry 7).

In fact, the asymmetric induction is significantly enhanced at lower temperatures, although in several cases long reaction times are needed. For example,  $\{S\text{-}2\}\text{Zr}(\text{NMe}_2)_2$  catalyzes the formation of 4,4-dimethyl-pyrrolidine **10b** at  $-30\text{ }^{\circ}\text{C}$  with 93% enantiomeric excess, whereas the product is formed with only 89% ee at room temperature (Table 2.3, entries 23 and 24). A similar trend is also observed for  $\{S\text{-}2\}\text{Hf}(\text{NMe}_2)_2$ , which mediates the formation of diallylpyrrolidine with 96% ee at  $0\text{ }^{\circ}\text{C}$  compared to 90% ee at room temperature (Table 2.3, entries 32 and 33).

These trends established for more common pyrrolidine products suggest that  $\{S\text{-}2\}\text{Zr}(\text{NMe}_2)_2$  is a highly effective and enantioselective group 4 catalyst for the cyclization of additional amino alkenes. Some minor optimizations, per substrate, could involve the hafnium catalyst, solvent modification, or temperature control as additional substrates are tested.

Typically, cyclizations of aminohexenes and aminoheptenes have proven more difficult than the aminopentenes described above. In fact, the rates of cyclization of aminohexene **14a** and **15a**, as catalyzed by  $\{S\text{-}2\}\text{Zr}(\text{NMe}_2)_2$ , are significantly decreased with respect to the aminopentenes. Additionally, the enantiomeric excesses of the 2-methylpiperidines products are significantly lower than the 2-methylpyrrolidines. The conversion and rate of the hafnium precatalyst  $\{S\text{-}2\}\text{Hf}(\text{NMe}_2)_2$  is superior to the zirconium catalyst for piperidine formation, although elevated temperature is required.

Although cyclization of aminoheptenes is also slower than the catalytic conversions of aminopentenes, azepanes are obtained with high enantiomeric excesses. The cyclization of aminoheptene substrates is catalyzed by  $\{1\}\text{Zr}(\text{NMe}_2)_2$  to give the racemic products and by  $\{S\text{-}$

$2\}$ Zr(NMe<sub>2</sub>)<sub>2</sub>, providing optically active homopiperidines, at room temperature (Table 2.4, entries 9). However, hafnium complex  $\{S-2\}$ Hf(NMe<sub>2</sub>)<sub>2</sub>, the titanium compound  $\{S-2\}$ Ti(NMe<sub>2</sub>)<sub>2</sub>, and the tert-butyl-oxazolinylborate zirconium complex  $\{S-3\}$ Zr(NMe<sub>2</sub>)<sub>2</sub> are not effective at room or elevated temperatures.

**Table 2.4.** Catalytic hydroamination/cyclization of aminohexenes and aminoheptenes.<sup>a</sup>

Reactant to Product	Entry	Precatalyst	solvent	Time (h)	Yield (%)	ee (%) <sup>b</sup>
	1	$\{1\}$ Zr(NMe <sub>2</sub> ) <sub>2</sub>	C <sub>6</sub> D <sub>6</sub>	11	87	racemic
	2	$\{S-2\}$ Zr(NMe <sub>2</sub> ) <sub>2</sub>	C <sub>6</sub> D <sub>6</sub>	40	48	31 <sup>c</sup>
	3	$\{S-2\}$ Hf(NMe <sub>2</sub> ) <sub>2</sub>	C <sub>6</sub> D <sub>6</sub>	30	85 <sup>d</sup>	26 <sup>c</sup>
	4	$\{S-3\}$ Zr(NMe <sub>2</sub> ) <sub>2</sub>	C <sub>6</sub> D <sub>6</sub>	48	80	29 <sup>c</sup>
	5	$\{1\}$ Zr(NMe <sub>2</sub> ) <sub>2</sub>	C <sub>6</sub> D <sub>6</sub>	4 d	95	racemic
	6	$\{S-2\}$ Zr(NMe <sub>2</sub> ) <sub>2</sub>	C <sub>6</sub> D <sub>6</sub>	4 d	65	46
	7	$\{S-2\}$ Hf(NMe <sub>2</sub> ) <sub>2</sub>	C <sub>6</sub> D <sub>6</sub>	20	89 <sup>d</sup>	18
	8	$\{1\}$ Zr(NMe <sub>2</sub> ) <sub>2</sub>	C <sub>6</sub> D <sub>6</sub>	5 d	56	racemic
	9	$\{S-2\}$ Zr(NMe <sub>2</sub> ) <sub>2</sub>	C <sub>6</sub> D <sub>6</sub>	5 d	73	91
	10	$\{1\}$ Zr(NMe <sub>2</sub> ) <sub>2</sub>	C <sub>6</sub> D <sub>6</sub>	4 d	76 d.r. = 5.6:1	racemic
	11	$\{S-2\}$ Zr(NMe <sub>2</sub> ) <sub>2</sub>	C <sub>6</sub> D <sub>6</sub>	4 d	85 d.r. = 3.8:1	94, 90

<sup>a</sup> Reaction conditions: 10 mol % catalyst, r.t. unless noted. <sup>b</sup> % ee ( $\pm 0.5\%$ ) was determined by <sup>1</sup>H and/or <sup>19</sup>F NMR spectra of Mosher amide derivatives. <sup>c</sup> % ee verified by HPLC. <sup>d</sup> 85 °C.

The highly enantioselectivity in amino pentene cyclizations motivated further study of the formation of other five-membered rings. The precatalysts  $\{S-2\}$ Zr(NMe<sub>2</sub>)<sub>2</sub> and  $\{S-2\}$ Hf(NMe<sub>2</sub>)<sub>2</sub> cyclize *ortho*-allylaniline at room temperature to generate optically active 2-

methyl-indoline with 95% and 94% ee respectively (Table 2.5, entries 2 & 3). 2-Substituted indolines are important subunits in drug candidates including as eletriptan, indapamide, muscarine receptor agonists and antagonists.<sup>42</sup> Previously described syntheses of highly enantioenriched (>90%) indoline subunit bearing a stereogenic center at the 2-position rely on either catalytic asymmetric hydrogenation of indoles, or the kinetic resolution of racemic mixture of indoles. Therefore, complexes  $\{S-2\}Zr(NMe_2)_2$  and  $\{S-2\}Hf(NMe_2)_2$  are promising precatalysts for preparation of optically active indoline building blocks from aniline derivatives. Two other reported hydroamination catalysts can provide 2-methyl indoline from ortho-allylaniline with moderate enantioselectivity.<sup>14,20</sup>

This series of group 4 precatalysts are active in methylene chloride and THF, suggesting that substrates containing halogen and ether functionality. We therefore investigated cyclizations of aminopentenes containing these functional groups. Quite promisingly, high enantioselectivity is obtained for the intramolecular hydroamination of 2,2-diethoxy-aminopentene **19a** ( $\{S-2\}Zr(NMe_2)_2$ , 97% ee;  $\{S-2\}Hf(NMe_2)_2$ , 96% ee; Table 2.5, entries 6 and 7). The achiral precatalyst  $\{1\}Zr(NMe_2)_2$  mediates the cyclization at approximately the same rate as  $\{S-2\}Zr(NMe_2)_2$ , but neither the 4*S*-tert-butyl-oxazolinylborate-based  $\{S-3\}Zr(NMe_2)_2$  nor titanium-based precatalyst is effective.

2-Allyl-2-(4-bromophenyl)pent-4-enylamine **20a** is cyclized by  $\{1\}Zr(NMe_2)_2$  to a 2:1 diastereomeric mixture of *cis* and *trans* pyrrolidines at room temperature. The assignment of the major isomer as *cis* is supported by NOE experiments in benzene-*d*<sub>6</sub> in which irradiation of the 2-methyl signal of the major isomer (1.00 ppm) results in decreased intensity of the *ortho*- and *meta*-phenyl resonances at 7.27 ppm and 6.69 ppm. Interestingly, the optically active precatalyst  $\{S-2\}Zr(NMe_2)_2$  is more efficient (full conversion in 20 min), gives better diastereoselectivity

(*cis:trans* = 4:1), and provides the products with exceedingly high enantioselectivity (*cis*: 97% ee; *trans*: 95% ee). The diastereomeric ratio (*trans:cis* = 2:1) as well as the optical purity of the major enantiomer (at 93% ee) are lower with the hafnium catalyst [*S-2*]Hf(NMe<sub>2</sub>)<sub>2</sub>. Even higher optical purities are obtained with by [*S-3*]Zr(NMe<sub>2</sub>)<sub>2</sub> (Table 2.5, entries 13), although the diastereomeric ratio is 1:1.2 (favoring the *trans* isomer) and the reaction time is two days. Finally and impressively, both diastereomers are obtained in 99% ee after cyclization at -30 °C in toluene with [*S-2*]Zr(NMe<sub>2</sub>)<sub>2</sub> as the precatalyst. However at that temperature, the diastereomeric ratio (*cis:trans*) decreases to 1:1.3 (with the *trans* isomer slightly favored).

Similar effects are observed in the cyclization of 4-aminomethyl-4-methyl-hepta-1,6-diene, in that the fastest cyclization rates is obtained with {*S-2*}Zr(NMe<sub>2</sub>)<sub>2</sub> as the precatalyst and the highest diastereoselectivity is obtained with {*S-2*}Hf(NMe<sub>2</sub>)<sub>2</sub>. The enantioselectivity is slightly better with {*S-2*}Zr(NMe<sub>2</sub>)<sub>2</sub> whereas the diastereoselectivity for cyclization is slightly better with {*S-3*}Zr(NMe<sub>2</sub>)<sub>2</sub>. Although diastereoselectivity for bis(allyl)amine substrates is poor, the enantioselectivity is high. Although the absolute configuration of the stereocenters in these molecules are not established by X-ray crystallography, inspection of HPLC traces of benzoyl derivatives and <sup>19</sup>F NMR spectra of Mosher amide derivatives suggest that the stereocenter obtained from C–N bond formation with {*S-2*}Zr(NMe<sub>2</sub>)<sub>2</sub> is *R* for both diastereomers for both methyl and *para*-bromophenyl substrates. In particular, Mosher-amide derivative of **S-8b** structurally characterized by X-ray crystallography.<sup>5d</sup>

*R* enantiomer elutes before the *S* enantiomer from a Regis (*S,S*)-Whelk O1 column HPLC column; additionally the peak from the *R* enantiomer is sharp whereas a broad band is apparent from the *S* isomer.<sup>2d,43</sup> In the mixtures of diastereomers obtained from cyclization of substrates **20a** and **21a** by {*S-2*}Zr(NMe<sub>2</sub>)<sub>2</sub>, four peaks were observed in the HPLC that appear in pairs.

The two peaks associated with the major *R* enantiomers elute together and earlier than the *S* disfavored enantiomers, following the same elution trend established with the pyrrolidines, whose absolute configurations are determined either by crystallographically<sup>5d</sup> or optical rotation.<sup>2a,2b,2d</sup>

These early bands are narrow, whereas the disfavored enantiomers of the diastereomeric pairs are broad. Likewise, in the <sup>19</sup>F NMR spectra of the Mosher amides of 2-methyl-pyrrolidines **20b** and **21b**, the *R,R*-pyrrolidine Mosher amide resonances are upfield and sharp whereas the *S,R*-pyrrolidine Mosher amides resonances are broad and downfield. In the <sup>19</sup>F NMR spectra of **20b** and **21b** acquired at 60 °C, two sharp, upfield singlets were observed as the major species present (**20b**: -73.73 and -70.83; **21b**: -70.83 and -71.07); the minor species were detected as a pair of broad downfield signals (**20b**: -69.98 ppm and -69.89 ppm; **21b**: -70.15 ppm and -70.04 ppm in chloroform-*d*). From consistent the relative peak positions and signal shape for the *R* enantiomers and the tendency of {*S*-2}Zr(NMe<sub>2</sub>)<sub>2</sub> to provide the *R* enantiomer of **21a** and **21b** substrates, we assign the configurations of the major enantiomers of the two diastereomers as 2*R* for bromophenyl and methyl substrates.

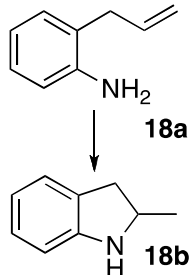
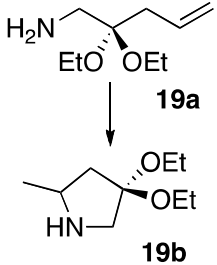
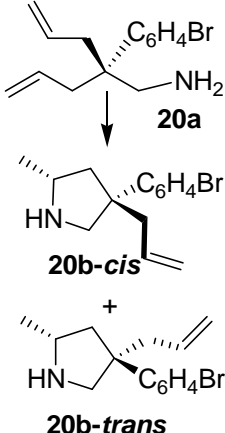
In case of cyclization of substrate containing internal alkene **22a** only {**1**}Zr(NMe<sub>2</sub>)<sub>2</sub> and {*S*-2}Zr(NMe<sub>2</sub>)<sub>2</sub> are seen to be active precatalysts providing racemic and enantio-enriched pyrrolidines respectively. 2-ethyl-pyrrolidine with 89% ee is obtained using {*S*-2}Zr(NMe<sub>2</sub>)<sub>2</sub> (Table 2.5, entries 19).

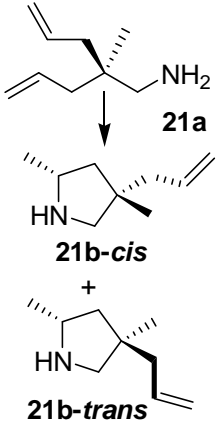
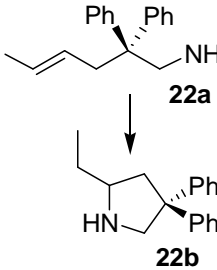
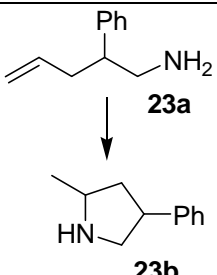
The turnover rate diminished with decreasing the steric bulk on the backbone of aminopentene, following the commonly cited Thorp-Ingold effect. The rate of cyclization of mono-phenyl aminopentene (Table 2.5, entries 22) is decreased significantly compare to the



substrate diphenyl substrate (Table 2.3, entries 3), and as noted above the parent aminopentene is not efficiently cyclized by any of these chiral oxazolinylborate catalysts.

**Table 2.5** Catalytic hydroamination/cyclization of aminoalkenes

Reactant to Product <sup>[a]</sup>	Entry	Precatalyst	Solvent	Time (h)	Yield (%) <sup>b</sup>	ee (%) <sup>[c]</sup>
 <b>18a</b> ↓ <b>18b</b>	1	{ <b>1</b> }Zr(NMe <sub>2</sub> ) <sub>2</sub>	C <sub>6</sub> D <sub>6</sub>	72	90	racemic
	2	{ <i>S</i> - <b>2</b> }Zr(NMe <sub>2</sub> ) <sub>2</sub>	C <sub>6</sub> D <sub>6</sub>	3 d	92	95
	3	{ <i>S</i> - <b>2</b> }Hf(NMe <sub>2</sub> ) <sub>2</sub>	C <sub>6</sub> D <sub>6</sub>	5 d	80	94
	4	{ <i>S</i> - <b>3</b> }Zr(NMe <sub>2</sub> ) <sub>2</sub>	C <sub>6</sub> D <sub>6</sub>	72	0	-
 <b>19a</b> ↓ <b>19b</b>	5	{ <b>1</b> }Zr(NMe <sub>2</sub> ) <sub>2</sub>	C <sub>6</sub> D <sub>6</sub>	30	90	racemic
	6	{ <i>S</i> - <b>2</b> }Zr(NMe <sub>2</sub> ) <sub>2</sub>	C <sub>6</sub> D <sub>6</sub>	30	90	97
	7	{ <i>S</i> - <b>2</b> }Hf(NMe <sub>2</sub> ) <sub>2</sub>	C <sub>6</sub> D <sub>6</sub>	5 d	90	96
	8	{ <i>S</i> - <b>3</b> }Zr(NMe <sub>2</sub> ) <sub>2</sub>	C <sub>6</sub> D <sub>6</sub>	5 d	15	-
 <b>20a</b> ↓ <b>20b-cis</b> + <b>20b-trans</b>	9	{ <b>1</b> }Zr(NMe <sub>2</sub> ) <sub>2</sub>	C <sub>6</sub> D <sub>6</sub>	20	100	racemic
	10	{ <i>S</i> - <b>2</b> }Zr(NMe <sub>2</sub> ) <sub>2</sub>	C <sub>6</sub> D <sub>6</sub>	0.33	100	97, 95
	11	{ <i>S</i> - <b>2</b> }Zr(NMe <sub>2</sub> ) <sub>2</sub>	C <sub>7</sub> D <sub>8</sub>	2 d	100 <sup>d</sup> , 1:1.3	d.r. = 99, 99 <sup>[e]</sup>
	12	{ <i>S</i> - <b>2</b> }Hf(NMe <sub>2</sub> ) <sub>2</sub>	C <sub>6</sub> D <sub>6</sub>	3	90	93, 95.6
	13	{ <i>S</i> - <b>3</b> }Zr(NMe <sub>2</sub> ) <sub>2</sub>	C <sub>6</sub> D <sub>6</sub>	48	100	d.r. = 2:1 96, 98

	14	{ <b>1</b> }Zr(NMe <sub>2</sub> ) <sub>2</sub>	C <sub>6</sub> D <sub>6</sub>	30	85	racemic
	15	{ <i>S</i> - <b>2</b> }Zr(NMe <sub>2</sub> ) <sub>2</sub>	C <sub>6</sub> D <sub>6</sub>	0.5	98	93, 92
	16	{ <i>S</i> - <b>2</b> }Hf(NMe <sub>2</sub> ) <sub>2</sub>	C <sub>6</sub> D <sub>6</sub>	20	90	87, 63
	17	{ <i>S</i> - <b>3</b> }Zr(NMe <sub>2</sub> ) <sub>2</sub>	C <sub>6</sub> D <sub>6</sub>	30	85	92, 91
	18	{ <b>1</b> }Zr(NMe <sub>2</sub> ) <sub>2</sub>	C <sub>6</sub> D <sub>6</sub>	4 d	20	racemic
	19	{ <i>S</i> - <b>2</b> }Zr(NMe <sub>2</sub> ) <sub>2</sub>	C <sub>6</sub> D <sub>6</sub>	4 d	85	89
	20	{ <i>S</i> - <b>2</b> }Hf(NMe <sub>2</sub> ) <sub>2</sub>	C <sub>6</sub> D <sub>6</sub>	4 d	15	-
	21	{ <b>1</b> }Zr(NMe <sub>2</sub> ) <sub>2</sub>	C <sub>6</sub> D <sub>6</sub>	20	95	racemic
	22	{ <i>S</i> - <b>2</b> }Zr(NMe <sub>2</sub> ) <sub>2</sub>	C <sub>6</sub> D <sub>6</sub>	15	95	66, 57
	23	{ <i>S</i> - <b>2</b> }Hf(NMe <sub>2</sub> ) <sub>2</sub>	C <sub>6</sub> D <sub>6</sub>	24	90, d.r. = 2.5:1	65, 58
	24	{ <i>S</i> - <b>2</b> }Zr(NMe <sub>2</sub> ) <sub>2</sub>	C <sub>6</sub> D <sub>6</sub>	48	20	-

<sup>a</sup> Reaction conditions: 10 mol % catalyst, r.t. unless noted. <sup>b</sup> ratio of diastereomers defined as *cis/trans*. <sup>c</sup> % ee ( $\pm 0.5\%$ ) was determined by <sup>1</sup>H and/or <sup>19</sup>F NMR spectra of Mosher amide derivatives. <sup>d</sup> -30 °C. <sup>e</sup> % ee verified by HPLC.

### Spectroscopic and Kinetics Features of Catalytic Reactions

The olefin hydroamination reactions catalyzed by {*S*-**2**}Zr(NMe<sub>2</sub>)<sub>2</sub> are unique among current group 4 systems in terms of the mild conditions of conversion (room temperature to -30 °C), their broadly high enantioselectivity, and the relative insensitivity of enantioselectivity to solvent choice. We have collected additional data to characterize some of the kinetic and stereochemical features of our system for comparison to other group 4 catalysts, to rule out possible catalytic pathways, and possibly identify the features that provide high rates and high

enantioselectivity. We have also investigated effects of ancillary ligand modifications on cyclization rates, and along with the kinetic data, provide a mechanistic hypothesis that we believe best explains the currently available data.

**a. Reaction time course and its kinetic features.**  $\text{HNMe}_2$  is observed by  $^1\text{H}$  NMR spectroscopy to upon addition of the aminoalkenes to the precatalyst. The active catalyst is not directly observed at room temperature by in situ  $^1\text{H}$  NMR spectroscopy of the reaction mixture. However, the active species is formed at room temperature within one minute after addition of aminoalkenes to metal diamides, based on the appearance of product in the  $^1\text{H}$  NMR spectrum of the reaction mixture.

In situ  $^1\text{H}$  NMR spectra of a mixture of 1.0 equiv. of *C*-(1-allyl-cyclohexyl)-methylamine (**12a**) and  $\{S\text{-}2\}\text{Zr}(\text{NMe}_2)_2$  at 230 K in toluene- $d_8$  contained resonances assigned to  $\text{HNMe}_2$  (2.20 ppm), new olefinic resonances (5.81 and 5.10 ppm) associated with transformation but not cyclization of **12a** (5.69 and 4.99 ppm at 230 K), and ancillary ligand resonances. Signals at 2.82 ppm are assigned to the remaining  $\text{Zr}(\text{NMe}_2)$ . Peaks from **12a** and the  $\{S\text{-}2\}\text{Zr}(\text{NMe}_2)_2$  starting material are not visible in this mixture. Upon warming to room temperature, the resonances in the olefinic region are no longer observed.

Reaction of  $\{S\text{-}2\}\text{Zr}(\text{NMe}_2)_2$  and two equiv. of **12a** at 230 K also provides  $\text{HNMe}_2$ . The  $^1\text{H}$  NMR signals previously assigned to  $\text{ZrNMe}_2$  were absent from the spectra, as were resonances assigned to **12a**. However the  $^1\text{H}$  NMR spectrum of the reaction mixture was complicated by broad overlapping resonances in the phenyl and cyclopentadienyl regions, and structural assignment was not possible. Similarly broad resonances for  $\{S\text{-}2\}\text{Zr}$ -species were

observed in catalytic reaction mixtures at low temperature, therefore assignment of the structure of a catalytic resting state is not possible at this point.

Instead, the reaction pathway was characterized using kinetic studies. The concentrations of the "cyclohexyl" substrate *C*-(1-allyl-cyclohexyl)-methylamine (**12a**) and the cyclized "spiro" product 3-methyl-2-aza-spiro[4,5]decane (**12b**) were monitored by <sup>1</sup>H NMR spectroscopy over the course of the catalytic conversion. Plots of ln[**12a**] vs. time are linear (up to 75-82% conversion), and this is consistent with first-order dependence on substrate concentration. Using the first 75% of the reaction, a series of pseudo-first order rate constant ( $k_{\text{obs}}$ ) are obtained for a range of initial concentrations of the precatalyst {*S*-**2**}Zr(NMe<sub>2</sub>)<sub>2</sub>. A linear relationship between  $k_{\text{obs}}$  and [{*S*-**2**}Zr(NMe<sub>2</sub>)<sub>2</sub>] provides the empirical rate law:  $-\text{d}[\mathbf{12a}]/\text{dt} = k'_{\text{obs}}[\mathbf{12a}]^1[\{\mathbf{S-2}\}\text{Zr}(\text{NMe}_2)_2]^1$  ( $k'_{\text{obs}} = 0.085 \text{ M}^{-1}\text{s}^{-1}$ ; 21 °C).

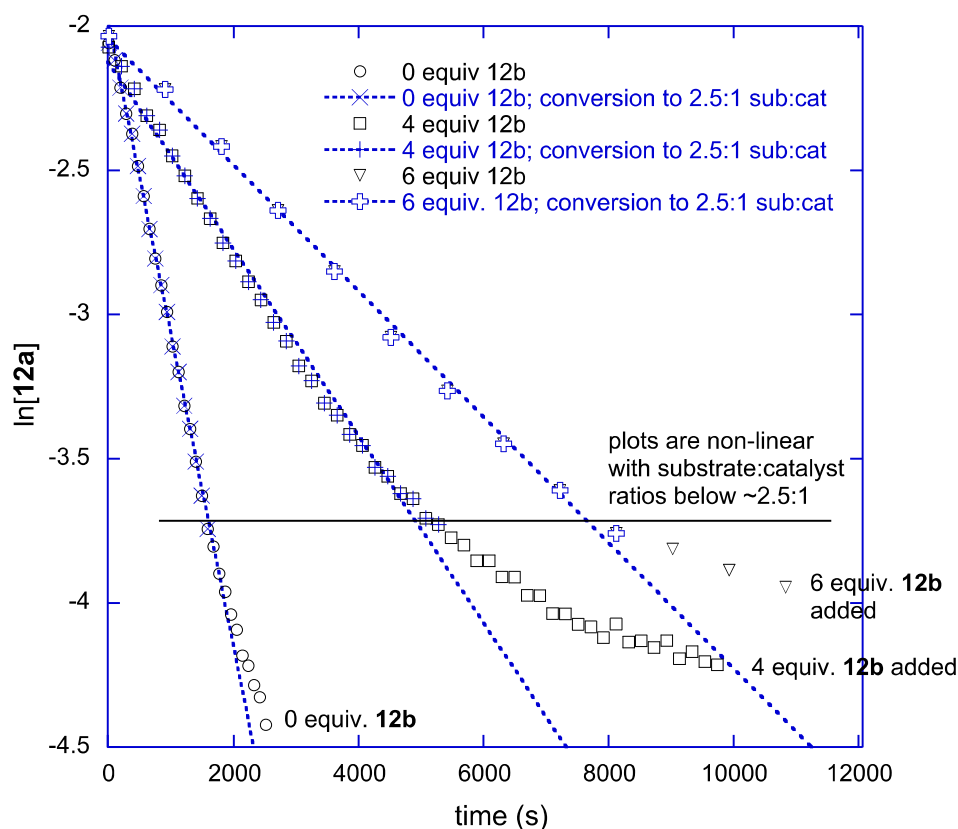


**Figure 2.3.** Plots of  $\ln[12a]$  versus time for the  $\{S-2\}Zr(NMe_2)_2$  catalyzed conversion of **12a** into pyrrolidine **12b**. Three experiments are illustrated, in which  $[\{S-2\}Zr(NMe_2)_2] = 9.7$  mM and 0, 4, and 6 equiv. of the product **12b**, are added prior to conversion. Linear least-squares best fits for  $\sim 2.5$  half-lives corresponds to conversion to substrate:catalyst ratio = 2.5:1 for the three data sets.

However, after two half lives, the reaction rate decreases to a greater degree than expected for a first-order reaction. Similar observations have been reported in other early-metal-catalyzed aminoolefin cyclizations (although typically these showed zero-order substrate concentration dependence), and the non-linearity was attributed to product inhibition.<sup>2b,23,28,5d</sup>

Recently, however, Schafer pointed out that the curvature might result from a change in rate law.<sup>28</sup> We therefore pursued this point further. Cyclization rates of **12a** catalyzed by  $[S-$

$2\text{]Zr(NMe}_2)_2$  were measured with 4 equiv. and 6 equiv. of product **12b** (using 90% ee material) relative to catalyst, and pseudo-first order rate constants (0 equiv **12b**:  $k_{\text{obs}} = 1.08 \times 10^{-3} \text{ s}^{-1}$ ; 4 equiv **12b**:  $k_{\text{obs}} = 0.32 \times 10^{-3} \text{ s}^{-1}$ ; 6 equiv **12b**:  $k_{\text{obs}} = 0.22 \times 10^{-3} \text{ s}^{-1}$ ) were smaller in the presence of **12b** (measured with equivalent catalyst concentration  $\{S\text{-}2\}\text{Zr(NMe}_2)_2$ ). Thus, kinetic experiments indicate that addition of product results in slower conversion (without a change in rate law) consistent with product inhibition.

Interestingly, even in the presence of 6 equiv. of **12b**, plots of  $\ln[\mathbf{12a}]$  vs. time are linear for only ~75% conversion. In general, the  $\ln[\mathbf{12a}]$  vs. time plots deviate from first-order substrate dependence at a ratio of  $[\text{substrate}]/[\text{catalysts}]$  of ~2.5. This apparent effect may be related to the requirement that two molecules of **12a** are required for catalytic turnover (see the initial rates experiments below). Thus, these experiments suggest that the curvature in first-order plots results from a change in mechanism at low substrate concentration. Furthermore, the product inhibition suggest that initial rate measurements, where **12b** is minimized, might better describe the substrate dependence of the catalytic reaction.

An additional observable that can provide insight into possible mechanism change is the enantioselectivity, which is often sensitive to catalyst structure and mechanism. Therefore, the % ee was monitored as a function of conversion, and this is plotted in Figure 2.4. Notably, this plot shows that the % ee is constant from 35-70% conversion, and the enantioselectivity begins to decrease above 75% conversion. Furthermore, the lower enantioselectivity occurs at the same % conversion at which the rate appears to deviate from first order. However, we should note that at equivalent and full conversion, the observed % ee is invariant over experiments in which the total volume (and thus, the concentration) of the reaction mixture is varied.

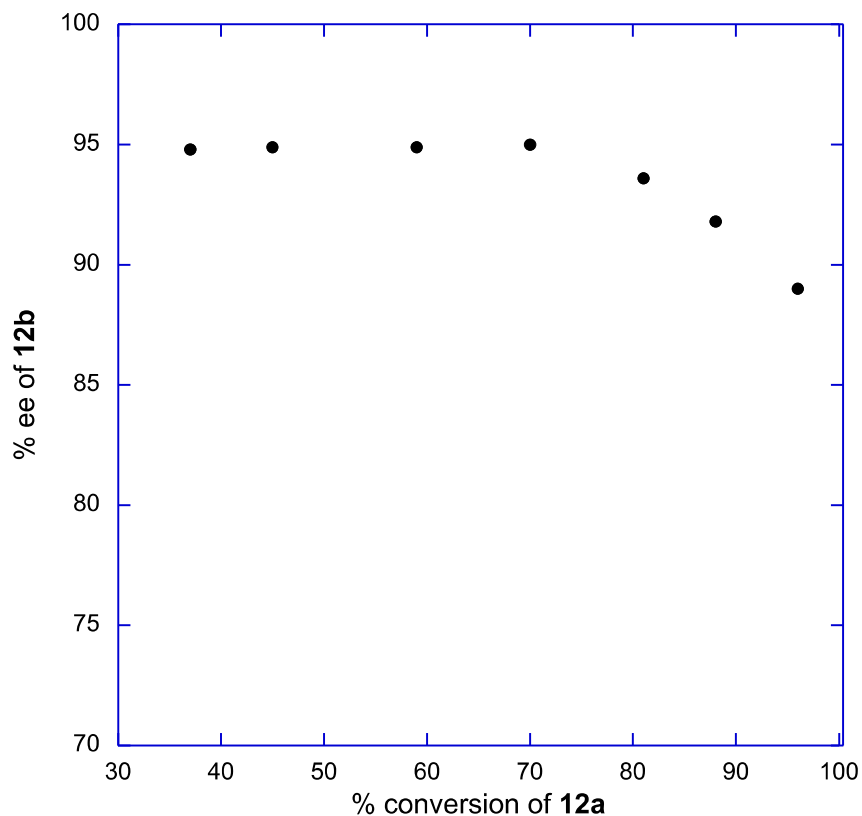


**Figure 2.4.** Plot showing the correlation of enantiomeric excess of pyrrolidine product **12b** with catalytic conversion of substrate **12a**.

Still, most mechanistic studies of early-transition metal, lanthanide, and actinide-catalyzed hydroamination/cyclization have probed the kinetic features (isotope effects, temperature-dependence) based on some percentage of catalytic conversion. The same is done here for comparison to other hydroamination systems, using  $\sim 2.5$  half-lives of data. Conversion of *C*-(1-allyl-cyclohexyl)-methylamine-ND<sub>2</sub> (**12a-d<sub>2</sub>**), catalyzed by [*S*-2]Zr(NMe<sub>2</sub>)<sub>2</sub>, is much slower than conversion **12a** itself. Linear least squares best fits of plots of  $k_{\text{obs}}^{(\text{D})}$  versus catalyst concentration provide the second-order rate constant  $k'_{\text{obs}}^{(\text{D})}$  and the large  $k'_{\text{obs}}^{(\text{H})}/k'_{\text{obs}}^{(\text{D})}$  value (3.5) that is consistent with a primary isotope effect (*i.e.*, an N–H or N–D bond is broken in the transition state of the turnover-limiting step; Figure 2.5).

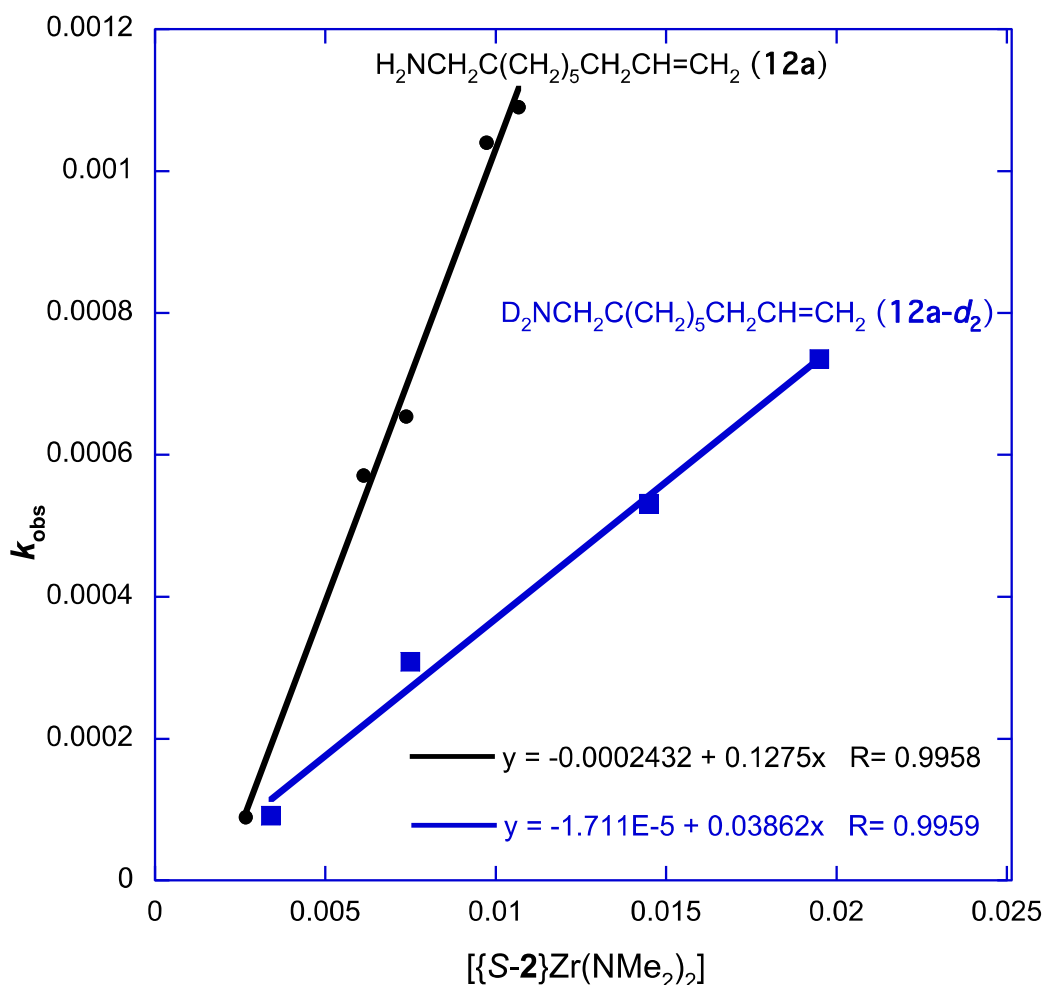


**Figure 2.5.** Plots of pseudo first order rate constants ( $k_{obs}$ ) vs. catalyst concentration. Reactions were performed at 295 K in toluene- $d_8$ .

In addition, hydroamination mechanisms are often kinetically characterized using transition-state theory. Second-order rate constants ( $k'_{obs}$ ) for cyclization of **12a** were measured at temperatures from 266 K to 314 K (Figure 2.6). The plot of  $\ln(k'_{obs}/T)$  vs.  $1/T$  from these data provides the values of activation parameters:  $\Delta H^\ddagger = 11.01 \text{ kcal}\cdot\text{mol}^{-1}$  and  $\Delta S^\ddagger = -18.3 \text{ cal}\cdot\text{mol}^{-1}\text{K}^{-1}$ .



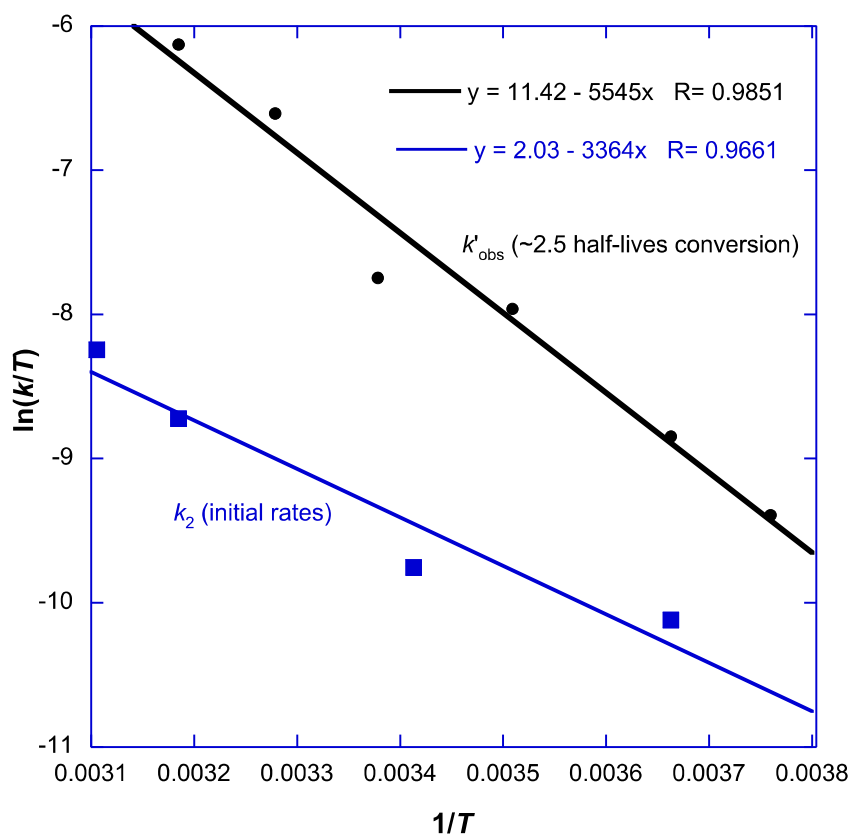


**Figure 2.6.** Plots of  $\ln(k'_{\text{obs}}/T)$  vs.  $1/T$  and  $\ln(k_2/T)$  vs.  $1/T$ .

**b. Initial rates.** The effects of product inhibition should be minimized at the initial portion of the reaction. This potential simplification motivated investigations of the instantaneous rate dependence on substrate concentration for the first 20-35% of the catalytic conversion. Linear least squares best fit of curves obtained from **[12a]** vs. time provide the initial rate  $(d[\mathbf{12a}]/dt)_{\text{ini}}$ . For a series of experiments, **[12a]** was varied from 0.0098 to 0.154 M as  $[\{\mathbf{S-2}\}\text{Zr}(\text{NMe}_2)_2]$  (5.39 mM) and temperature (23 °C) were kept constant to provide a set of data that describe the rate dependence on substrate concentration (Figure 2.7).

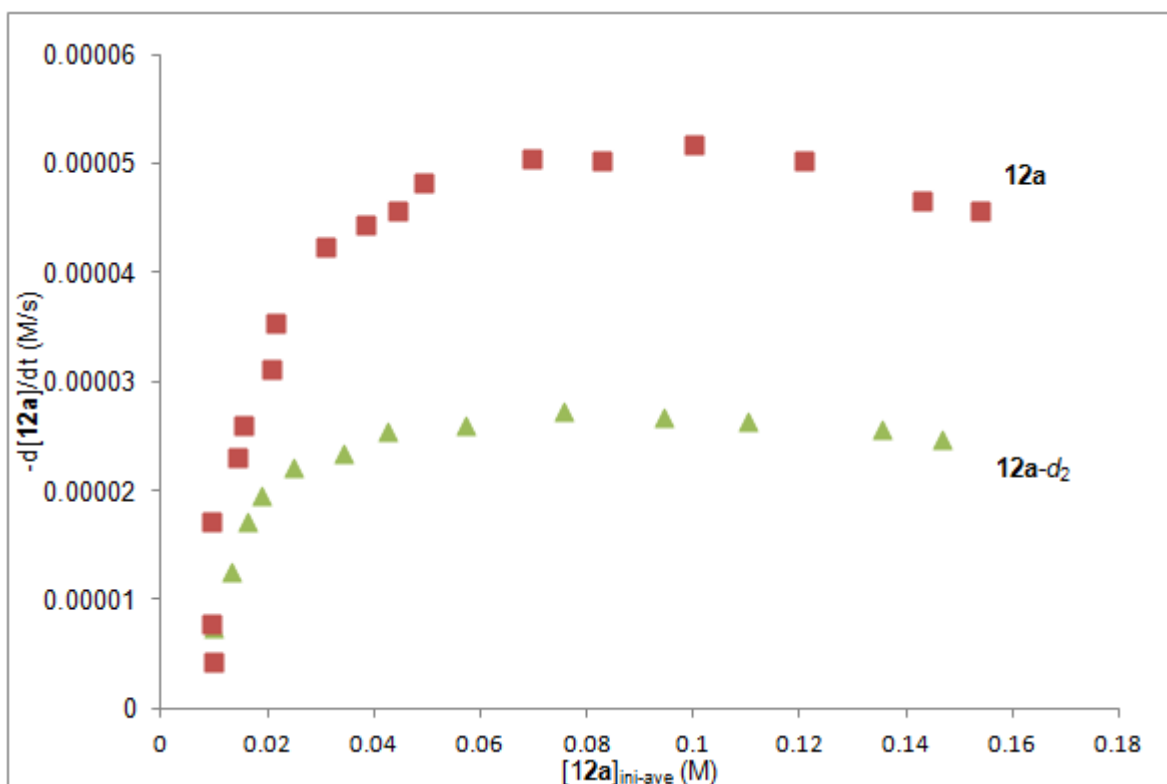


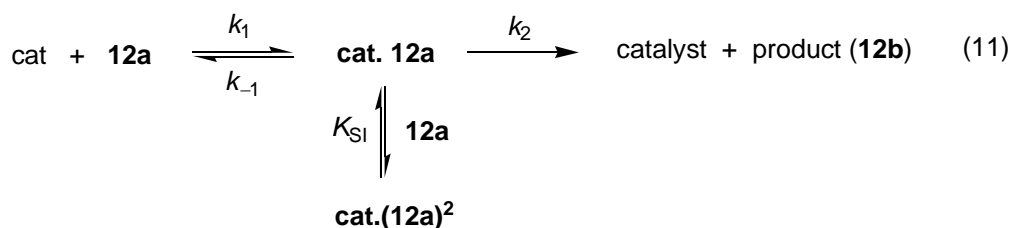
**Figure 2.7.** Plot of initial cyclization rate of  $(-d[12a]/dt)_{ini}$  vs.  $[substrate]_{ini}$  for **12a** (■) and **12a-d<sub>2</sub>** (▲), measured in toluene-*d*<sub>8</sub>, 23 °C. The curves represent nonlinear least-squares fit (eq 10).

At low concentrations (0.0098 to 0.07 M), the average initial substrate conversion rates increase linearly as the substrate concentration increases; however, at higher substrate concentrations (70 mM), the initial rates approaches a maximum and eventually do not increase with further increases in substrate concentration. A slight decrease of the initial rate is observed at  $[12a] > 70$  mM. Experiments that probe initial rate dependence on substrate concentration performed at 273, 314, and 322 K, as well as using *N*-deuterated substrate **12a-d<sub>2</sub>**, provide similar curves. As can be seen in Figure 2.7, the initial rate plots also contains a non-zero x-intercept that coincides with precatalyst concentration, which suggests that 1 equiv. of substrate is required before one catalytic cycle can be completed. That statement is an approximation, in fact, because the low temperature experiments with 1:1 substrate to catalyst indicate that

cyclization can occur at that low ratio. However, as suggested by the  $\ln[\text{substrate}]$  vs. time plots, the reaction rate drops precipitously at low substrate concentrations.

The non-linear rate dependence on concentration indicates that the rates of the elementary reaction steps are inequivalently influenced by substrate concentration; the results is that changing substrate concentration modifies the contribution of the elementary steps to the rate of catalysis. Nonlinear least-squares regression analysis of the data in Figure 2.7 provides good correlation with eq 10, which includes the rate constant  $k_2$  for the irreversible step, the catalyst formation constant  $K'$  ( $\{k_{-1} + k_2\}/k_1$ ), and the substrate inhibition constant  $K_{SI}$ . The form of the rate equation resembles the Michaelis-Menten equation, with the addition of a reversible substrate inhibition step (eq 10).<sup>44</sup> Additionally, the substrate concentration in eq 10 is modified by the approximated requirement that one equiv. of substrate **12a** is needed to convert  $[S-2]Zr(NMe_2)_2$  precatalyst into the active catalyst, giving the terms  $\{[12a]-[S-2]Zr(NMe_2)_2\}$  in eq 10.

$$\frac{-d[12a]}{dt} = \frac{k_2\{[S-2]Zr(NMe_2)_2\} \{[12a] - [S-2]Zr(NMe_2)_2\}}{K' + \{[12a] - [S-2]Zr(NMe_2)_2\} + K_{SI}\{[12a] - [S-2]Zr(NMe_2)_2\}^2} \quad (10)$$

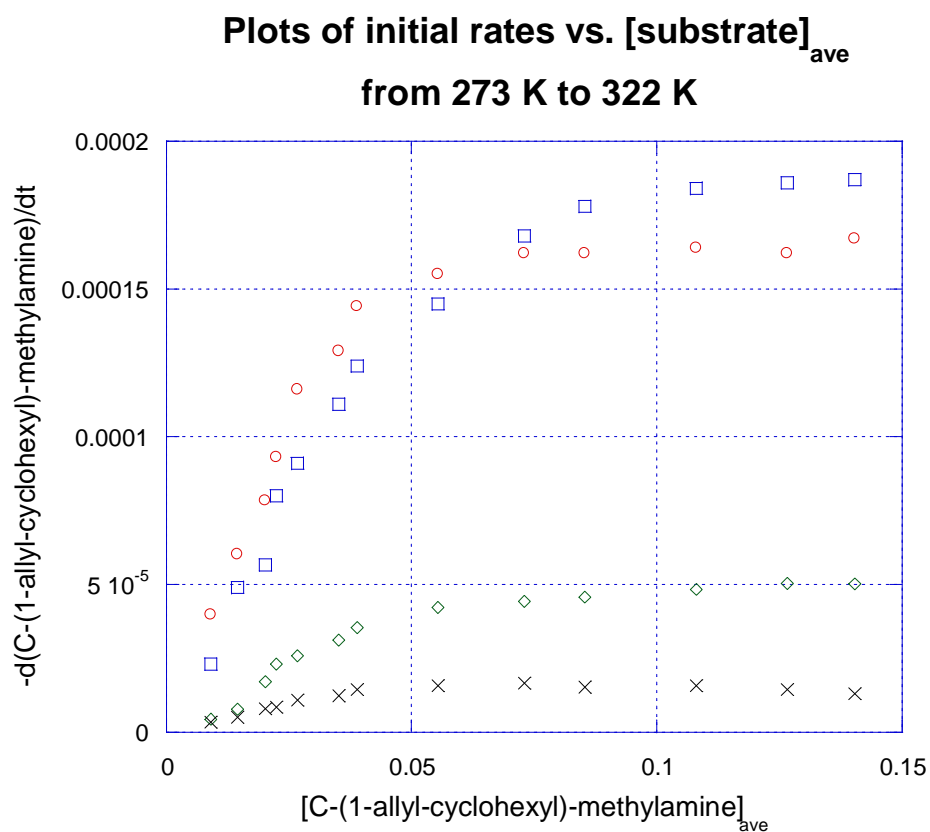


The rate law in equation 10 corresponds to the reaction mechanism shown in the following equation 11, which shows reversible substrate and catalyst association followed by an irreversible step. The three parameters obtained from the curve fit are  $k_2$  ( $1.7 \pm 0.3 \times 10^{-2} \text{ s}^{-1}$ ),  $K'$  ( $2.8 \pm 0.7 \times 10^{-2} \text{ M}$ ), and  $K_{SI}$  ( $5 \pm 2 \text{ M}^{-1}$ ). The composition of the catalytic species can be partly

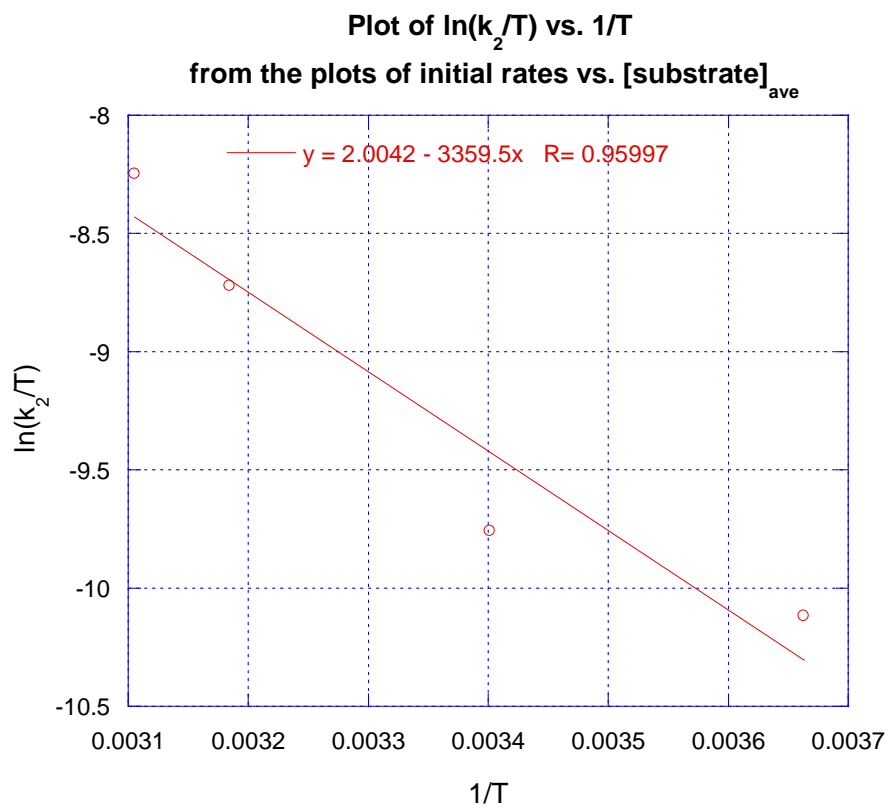
assessed from this kinetics analysis. The interaction of substrate and catalyst in a 1:1 ratio provides the active catalyst that is likely  $[\text{Zr}(\text{NHR})(\text{NMe}_2)]$  (*catalyst initiation*; NHR = amidoalkene). The equilibrium step ( $k_1/k_{-1}$ ) involves reversible interaction of catalyst with substrate giving  $[\text{Zr}(\text{NHR})_2]$  and  $\text{HNMe}_2$ .

**c. Isotope effects.** The primary kinetic isotope effect was also verified by actual rate constant  $k_2$  obtained from the saturation kinetic plots using **12a-d<sub>2</sub>**. The initial rate increased with increase of  $[\text{12a-d}_2]_{\text{ini}}$  until a saturation was observed similar to the proteo-analog (**12a**). A nonlinear least-squares fit ( $R = 0.099$ ) of  $-\text{d}(\text{12a-d}_2)/\text{dt}_{\text{ini}}$  vs.  $[\text{12a-d}_2]_{\text{ini}}$  at 23 °C provides a saturation curve, with the value of  $(k_2)_{\text{D}} = 7.3 \times 10^{-3} \text{ s}^{-1}$ . The value of  $k_2^{(\text{H})}/k_2^{(\text{D})}$  from the initial rate plots (Figure 2.7) is 2.3 (0.5), indicates that N–H bond is involved in the turnover-limiting step. Significant increase of isotope effect was observed at 0 °C. The value of  $k_2^{(\text{H})}/k_2^{(\text{D})}$  measured from initial rate plots at 0 °C is 4.5.

**d. Activation parameters.** The second order rate constant include the substrate binding constant as shown in the plot of initial rate and also in rate law. Therefore, it is necessary to determine the actual values of the activation parameters using  $k_2$  obtained from saturation kinetics, which exclude the substrate binding constant.  $k_2^{(\text{H})}$  values were determined from the initial rate plots at 273 K, 294 K, 314 K, and 322 K (Figure 2.8). The plot of  $\ln(k_2/T)$  vs.  $1/T$  provide  $\Delta H^\ddagger = 6.7 \text{ kcal}\cdot\text{mol}^{-1}$  and  $\Delta S^\ddagger = -43 \text{ cal}\cdot\text{mol}^{-1}\text{K}^{-1}$  (Figure 2.9).



**Figure 2.8.** Plots of initial rates of cyclization  $-d[\mathbf{12a}]/dt$  vs.  $[\mathbf{12a}]_{\text{ave}}$  for cyclization of  $\mathbf{12a}$  by  $\{S\text{-}2\}\text{Zr}(\text{NMe}_2)_2$  (0.0054 M) at 273 K, 294 K, 314 K, and 322 K. The curves represent non-linear least-squares regression analysis of the data to the equation:  $-d[\text{substrate}]/dt = k_2[\text{catalyst}][\text{substrate}]/\{K' + [\text{substrate}] + K_{\text{SI}}[\text{substrate}]_2\}$ .

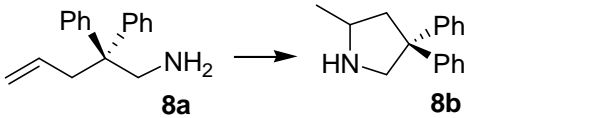
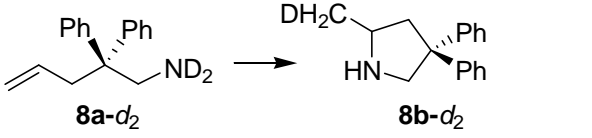
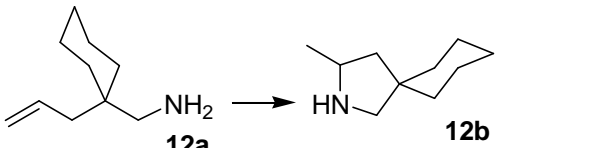


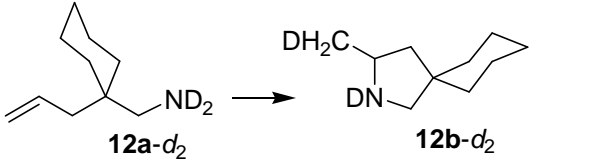
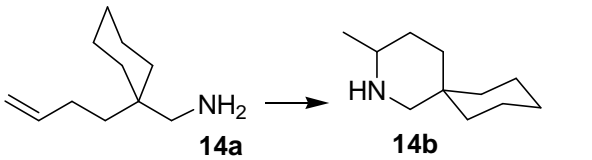
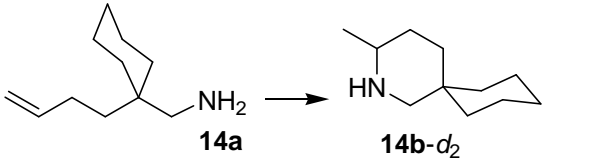
**Figure 2.9.** Plot showing a linear correlation between  $\ln(k_2/T)$  vs.  $1/T$  from initial rates plots at 273 K, 294 K, 314 K, and 322 K. From this plot,  $\Delta H^\ddagger = 6.7 \text{ kcal}\cdot\text{mol}^{-1}$  and  $\Delta S^\ddagger = -43 \text{ cal}\cdot\text{mol}^{-1} \text{ K}^{-1}$  are calculated.

**e. Significant isotope effects on enantioselectivity.** Significant isotopic perturbation on stereoselectivity was observed in hydroamination/cyclization of proteo- and deuterio-aminoalkenes using precatalyst  $\{S-2\}Zr(NMe_2)_2$ ,  $\{R-2\}Zr(NMe_2)_2$ ,  $\{S-2\}Hf(NMe_2)_2$ , and  $\{S-3\}Zr(NMe_2)_2$ . The cyclizations of deuterated aminoolefins provide deuterio-pyrrolidines with ee values, which are systematically and significantly higher than the values for the corresponding proteo-analogs. The ee values for deuterio-heterocycles (**8a-d<sub>2</sub>**, 95%; **12a-d<sub>2</sub>**, 97%; **14a-d<sub>2</sub>**, 46%) are higher compared to the corresponding proteo-heterocycles (**8a**, 93%; **12a**, 90%; **14a-d<sub>2</sub>**, 31%) for  $\{S-2\}Zr(NMe_2)_2$ . Similarly, in case of Hf-precatalyst  $\{S-2\}Hf(NMe_2)_2$ , the ee values for deuterio-heterocycles (**8a-d<sub>2</sub>**, 96%; **12a-d<sub>2</sub>**, 97%; **14a-d<sub>2</sub>**, 44%) are higher compared to the corresponding proteo-heterocycles (**8a**, 91%; **12a**, 93%; **14a-d<sub>2</sub>**, 26%).

For  $\{S-2\}Zr(NMe_2)_2$ , the isotope effect for the favored diastereomeric pathways ( $k_H^R/k_D^R$ ) is 2.2(5) and for the unfavored diastereomers ( $k_H^S/k_D^S$ ) is 7.7(1) (from  $k'_H/k'_D$ ). Thus, *N*-deuteration slows the *S*-diastereomeric pathways by a greater extent than the *R*-pathways.

**Table 2.6.** Effect of *N*-d<sub>2</sub> substitution on % ee in enantioselective hydroamination catalyzed by Zr- and Hf-catalysts<sup>a</sup>

Catalysts:	$\{S-2\}$ Zr(NMe <sub>2</sub> ) <sub>2</sub>	$\{R-2\}$ Zr(NMe <sub>2</sub> ) <sub>2</sub>	$\{S-2\}$ Hf(NMe <sub>2</sub> ) <sub>2</sub>	$\{S-3\}$ Zr(NMe <sub>2</sub> ) <sub>2</sub>
 <p><b>8a</b> → <b>8b</b></p>	93 ( <i>R</i> )	93 ( <i>S</i> )	91 ( <i>R</i> )	93 ( <i>R</i> )
 <p><b>8a-d<sub>2</sub></b> → <b>8b-d<sub>2</sub></b></p>	95 ( <i>R</i> ), 97 ( <i>R</i> ) <sup>b</sup>	95 ( <i>S</i> )	96 ( <i>R</i> )	96 ( <i>R</i> )
 <p><b>12a</b> → <b>12b</b></p>	90 ( <i>R</i> )	90 ( <i>S</i> )	93 ( <i>R</i> )	86 ( <i>R</i> )

 <p><b>12a-d<sub>2</sub></b> → <b>12b-d<sub>2</sub></b></p>	97 (R), 98 (R) <sup>c</sup>	97 (S)	97 (R)	91 (R)
 <p><b>14a</b> → <b>14b</b></p>	31 (R)	31 (S)	26 (R)	-
 <p><b>14a</b> → <b>14b-d<sub>2</sub></b></p>	46 (R)	46 (S)	44 (R)	-

<sup>a</sup> Reaction Conditions: 23 °C, C<sub>6</sub>D<sub>6</sub>, >95% yield. <sup>b</sup> 0 °C in toluene or THF. <sup>c</sup> -30 °C in THF.

**f. Ancillary ligand-metal interactions during catalysis.** The high enantioselectivity of the C<sub>1</sub>-symmetric chiral cyclopentadienyl-bis(oxazolinyl)borate zirconium precatalyst can be rationalized due to the presence of non-epimerizable chiral oxazoline based ancillary ligand. The stereogenic center is in close proximity of the nitrogen coordinating center on the oxazoline as well as to the metal center in the precatalyst, which provide excellent stereochemical induction around the metal center. However, the coordination geometry of the zirconium center during the catalysis might have an important role in high activity and enantioselectivity for cyclization of aminoalkenes, which is unknown to this point. To probe the coordination geometry of the zirconium catalyst during hydroamination, the catalytic activity of complex {Ph<sub>2</sub>B(C<sub>5</sub>H<sub>4</sub>)(Ox<sup>4*S*-iPr,Me<sub>2</sub>})}Zr(NMe<sub>2</sub>)<sub>2</sub> ({*S*-7}Zr(NMe<sub>2</sub>)<sub>2</sub>) is compared to the precatalyst {PhB(C<sub>5</sub>H<sub>4</sub>)(Ox<sup>4*S*-iPr,Me<sub>2</sub>})<sub>2</sub>}Zr(NMe<sub>2</sub>)<sub>2</sub> ({*S*-2}Zr(NMe<sub>2</sub>)<sub>2</sub>). Notably, {*S*-7}Zr(NMe<sub>2</sub>)<sub>2</sub> is not a precatalyst for hydroamination/cyclization of aminoalkenes. Diphenyl-aminopentene (**8a**) or diphenyl-aminohexene (**15a**) is not cyclized by 10 mol% of {*S*-7}Zr(NMe<sub>2</sub>)<sub>2</sub> in benzene at room temperature over 4 days and even after heating at 140 °C for 2 days. The inactivity of {*S*-7}Zr(NMe<sub>2</sub>)<sub>2</sub> in hydroamination/cyclization contrasts to the high activity of {PhB(C<sub>5</sub>H<sub>4</sub>)(Ox<sup>4*S*-</sup></sup></sup>



$^{iPr,Me_2}_2\}Zr(NMe_2)_2$  at room temperature. This comparison study indicates that the coordination of two oxazolines is required to activate the precatalyst for hydroamination.

**g. Valencies Required at Metal.** To investigate the valency required at metal center of  $\{PhB(C_5H_4)(Ox^{4S-iPr,Me_2})_2\}Zr(NMe_2)_2$  for hydroamination, the catalytic activity of a similar model complex  $\{PhB(C_5H_4)(Ox^{4S-iPr,Me_2})_2\}ZrCl(NMe_2)$  [ $\{S-2\}ZrCl(NMe_2)$ ] is tested in hydroamination/cyclization.  $\{S-2\}ZrCl(NMe_2)$  has a single readily aminolyzable amido site (single available valency). This complex is inert to cyclize both primary and secondary aminopentenes. Addition of one equiv of 2,2-diphenylaminopentene (**8a**) to the benzene solution of  $\{S-2\}ZrCl(NMe_2)$  provided the complex  $\{PhB(C_5H_4)(Ox^{4S-iPr,Me_2})_2\}ZrCl(NHCH_2C(Ph_2)CH_2CHCH_2)$ . However, no cyclization of aminopentene was observed at room temperature and even at higher temperature up to 150 °C. In contrast, the constrained geometry complex (CGC)  $(Cp^*SiMe_2N^tBu)Zr(NMe_2)Cl$ , having a single readily aminolyzable amido site (single available valency), is a competent catalyst for cyclohydroamination.<sup>23</sup>  $(Cp^*SiMe_2N^tBu)Zr(NMe_2)Cl$  cyclizes aminopentene significantly faster than  $(Cp^*SiMe_2N^tBu)Zr(NMe_2)_2$  and insertive pathway has been proposed.

**h. Cyclization of secondary aminopentene in presence of primary amine.** Secondary aminopentene is not cyclized in presence of 10 mol % of zirconium precatalyst  $\{S-2\}Zr(NMe_2)_2$  in toluene. Addition of 1.0, 2.0 of N-methyl-2,2-diphenyl-4-penten-1-amine to the toluene solution of  $\{S-2\}Zr(NMe_2)_2$  form the corresponding mono- or bis amido complexes. No formation of pyrrolidine was observed at room temperature and even upon heating at 90, 120 or 160 °C for 2 days. However, addition of two equiv of noncyclizable primary amine such as amylamine or propylamine with respect to the precatalyst leads to cyclization of N-methyl-2,2-diphenyl-4-

penten-1-amine at room temperature with 24% conversion. The conversion is not improved even after addition of variable amounts of amine additives or performing the reaction at high temperature.

### ***Mechanism and Catalytic Cycle***

The first order rate dependences on both the substrate and catalyst are observed for the cyclization of *C*-(1-allyl-cyclohexyl)-methylamine (**12a**) using precatalyst {*S*-**2**}Zr(NMe<sub>2</sub>)<sub>2</sub>. The primary kinetic isotope effect suggests that the cleavage of N–H or N–D bond is involved in the turnover-limiting step. The significant isotopic perturbation on enantioselectivity suggests that N–H/N–D bond cleavage also significantly affects the configuration of the new stereocenter; *i.e.* the C–N bond formation occurs in the turnover-limiting step.

The substrate saturation on initial rates (Figure 2.7) indicates reversible substrate-catalyst association followed by turnover-limiting step in the catalytic cycle. The nonzero x-intercept in the initial rate plots that coincides with concentration of the catalyst also indicates that 1.0 equiv of substrate is required to activate the precatalyst.

Importantly, the zirconium center of the active catalyst requires two active valencies for cyclization of aminoalkenes as {*S*-**2**}ZrCl(NMe<sub>2</sub>) is inert in cyclization of primary and secondary aminopentenes. This experiment suggests that the active catalyst contains two amidoalkene moieties. Additionally, the cyclization of secondary aminopentene by {*S*-**2**}Zr(NMe<sub>2</sub>)<sub>2</sub> in presence of catalytic amount of noncyclizable primary amine suggests the necessity of NH-proton for C–N bond formation.

The positive effect of *N*-deuteration on the enantiomeric excess of the product and the cyclization of secondary aminopentene in presence of primary amine additive rule out the

[2 $\pi$ +2 $\pi$ ] cycloaddition of a Zr-imidoalkene species in the catalytic cycle because the metal-imido moiety is lack of NH (or ND).

Additionally, our accumulated data including the kinetic isotope effect, the kinetic isotope effect for the two enantiotopic pathways, the requirement that substrate/precatalyst should be >2 for catalytic turnover, the cyclization of secondary aminopentene in presence of primary amine additive, and the inactivity of {*S*-**2**}ZrCl(NMe<sub>2</sub>) in cyclization disfavor insertion-based mechanism, rather suggest a proton-assisted noninsertive pathway for C–N bond formation.

To investigate the nature of the turnover-limiting step, the temperature dependence of the cyclization rate of *C*-(1-allyl-cyclohexyl)-methylamine (**12a**) was measured using both the second order rate constant  $k_{\text{obs}}$ , as well as the actual rate constant  $k_2$  obtained from saturation kinetics at different temperature. The values of activation parameters using  $k_{\text{obs}}$  were  $\Delta H^\ddagger = 11.01 \text{ kcal}\cdot\text{mol}^{-1}$  and  $\Delta S^\ddagger = -18.3 \text{ cal}\cdot\text{mol}^{-1}\text{K}^{-1}$ , calculated from Eyring plot  $\ln(k_{\text{obs}}/T)$  vs.  $1/T$  (Figure 2.6). These values of activation parameters were significantly different compared to those obtained from the plots ( $\ln k_2/T$  vs.  $1/T$ ) i.e.  $\Delta H^\ddagger = 6.7 \text{ kcal}\cdot\text{mol}^{-1}$  and  $\Delta S^\ddagger = -43 \text{ cal}\cdot\text{mol}^{-1}\text{K}^{-1}$  (Figure 2.9). The marked differences of  $\Delta H^\ddagger$  and  $\Delta S^\ddagger$  values for the two Eyring plots suggest that the Eyring analysis of multiple steps in catalytic cycles can be greatly affected by equilibrium steps in the mechanism. Nevertheless, the large and negative  $\Delta S^\ddagger$  value suggests a highly ordered transition state.

C–N bond formation establishes the configuration of the new stereocenter, whereas the new C–H bond is not attached to the stereogenic carbon. However, the stereochemical relationship between the N–H and the C–N bond suggests that C–N and C–H bond formation and N–H bond cleavage occur in a concerted fashion during the cyclization step. Given that an

N–H bond is broken during the turnover-limiting step and the catalytic intermediate contains two NHR ligands, we propose a six-center transition state in which N–H transfer from one amide to the terminal methylene of the other amidoalkene is concerted with intraligand C–N bond formation. The two participating ligands are proposed to be two amido groups because only two reactive valent sites are available, kinetics indicate that two substrates interact with the catalyst in the turnover limiting step, and the addition of a third substrate, presumably as a coordinated amine, inhibits the cyclization. This proposal is related to the observation that the nonzero-x intercept of the initial rate plot that is coincide with [substrate] (Figure 2.7), which indicate at least one equiv. of substrate is necessary to activate the precatalyst. Finally, this mechanism is also consistent with the fact that secondary aminoalkenes are not cyclized, unless a primary amine is present to form an amido that can transfer a proton.

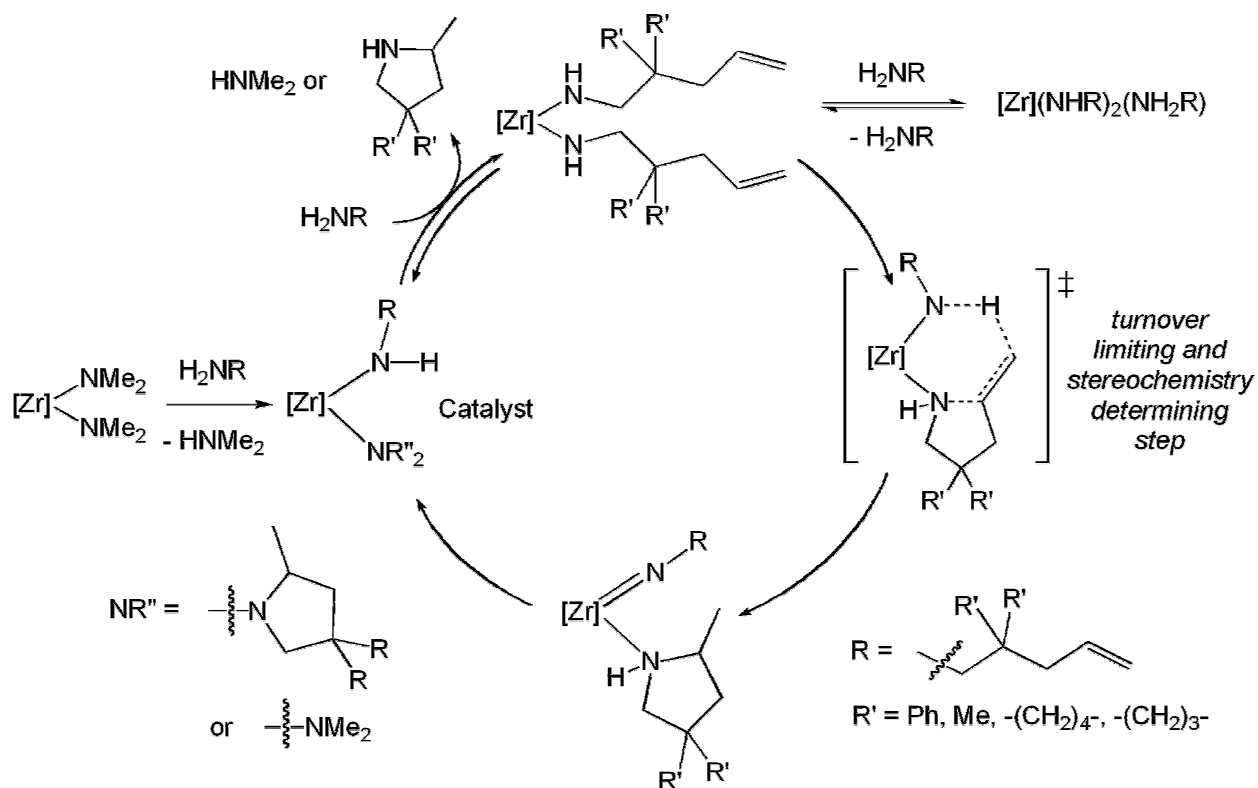


**Figure 2.10. Proposed new catalytic cycle for hydroamination of aminoalkenes as catalyzed by {S-2}Zr(NMe<sub>2</sub>)<sub>2</sub>.**

### Conclusions

Cyclopentadienyl-bis(oxazoliny)borate supported zirconium and hafnium diamide precatalysts are highly active and enantioselective precatalysts for hydroamination/cyclization of aminoolefins. The catalytic activity was observed at room temperature or even at  $-30\text{ }^{\circ}\text{C}$ . The precatalysts provide nitrogen heterocycles with very high enantiomeric excesses up to 99%. Enantioselectivities are high with varying substituents of aminopentenes and also in the presence of oxo- and halogen-functional groups. The reaction rate was first order dependence on both substrate and precatalyst. Substrate saturation on initial rate was detected. The activation parameters of saturation kinetics are not the same as overall catalytic activation parameters. Therefore, the activation parameters of catalytic cycles can disguise individual steps and can be uninformative. A non-insertive mechanism involving concerted C–N/C–H bond formation was proposed based on the kinetics, primary isotope effects, isotopic perturbation of enantioselectivity, and the investigation of intermediates. The inactivity of cyclopentadienyl-mono(oxazoliny)borate zirconium complex in hydroamination/cyclization suggests that the coordination of two oxazolines is required to activate the cyclopentadienyl-bis(oxazoliny)borato zirconium precatalyst.

## Experiment

**General Procedures.** All reactions were performed under a dry argon atmosphere using standard Schlenk techniques or under a nitrogen atmosphere in a glove box unless otherwise indicated. Dry, oxygen-free solvents were used throughout. Benzene, toluene, pentane and tetrahydrofuran were degassed by sparging with nitrogen, filtered through activated alumina columns, and stored under N<sub>2</sub>. Benzene-*d*<sub>6</sub>, toluene-*d*<sub>8</sub> and tetrahydrofuran-*d*<sub>8</sub> were vacuum transferred from Na/K alloy and stored under N<sub>2</sub> in a glove box. sodium cyclopentadienide,<sup>45</sup> diphenylchloroborane,<sup>46</sup> Zr(NMe<sub>2</sub>)<sub>4</sub>,<sup>47</sup> Hf(NMe<sub>2</sub>)<sub>4</sub>,<sup>48</sup> 2,2-diphenyl-4-penten-1-amine (**8a**),<sup>2d</sup> C-(1-allyl-cyclopentyl)-methylamine (**9a**),<sup>4c</sup> 2,2-dimethyl-4-penten-1-amine (**10a**),<sup>49</sup> 2,2-bis(2-propenyl)-4-pentenylamine (**11a**),<sup>15a</sup> C-(1-allyl-cyclohexyl)-methylamine (**12a**),<sup>4c</sup> 4-penten-1-amine (**13a**),<sup>5d</sup> 1-(3-butenyl-cyclohexyl)methylamine (**14a**),<sup>49</sup> 2,2-diphenyl-5-hexen-1-amine (**15a**),<sup>25a</sup> 2-diphenyl-1-amino-6-heptene (**16a**),<sup>21b</sup> *ortho*-allylaniline (**18a**),<sup>50</sup> 2-allyl-2-methylpent-4-enylamine (**21a**),<sup>11a</sup> 2,2-diphenyl-1-amino-4-hexene (**22a**),<sup>51</sup> 2-phenyl-4-penten-1-amine (**23a**),<sup>51</sup> and tetrakis(trimethylsilyl)silane<sup>52</sup> were prepared by published procedures. All aminoalkenes were distilled from CaH<sub>2</sub>, degassed and stored with freshly activated 4 Å molecular sieves in a glove box prior to use. All other chemicals used here are commercially available. (+)-(*S*)- $\alpha$ -methoxy- $\alpha$ -(trifluoromethyl)phenylacetyl chloride (*S*-Mosher's chloride) was obtained from Alfa-Aesar (>98%, (+)-137.3). Ti(NMe<sub>2</sub>)<sub>4</sub> and all other starting materials were purchased from Aldrich. <sup>1</sup>H, <sup>13</sup>C{<sup>1</sup>H}, <sup>11</sup>B, and <sup>19</sup>F{<sup>1</sup>H} NMR spectra were collected either on a Bruker DRX-400 spectrometer, Bruker Avance III 700 spectrometer or an Agilent MR 400 spectrometer. <sup>15</sup>N chemical shifts were determined by <sup>1</sup>H-<sup>15</sup>N HMBC experiments either on a Bruker Avance III 700 spectrometer or on a Bruker Avance III 600 spectrometer. <sup>15</sup>N chemical shifts were originally referenced to liquid NH<sub>3</sub> and recalculated to the CH<sub>3</sub>NO<sub>2</sub> chemical shift

scale by adding  $-381.9$  ppm.  $^{11}\text{B}$  NMR spectra were referenced to an external sample of  $\text{BF}_3 \cdot \text{Et}_2\text{O}$ . Accurate mass ESI mass spectrometry was performed using an Agilent QTOF 6530 equipped with the Jet Stream ESI source. An Agilent ESI test mix was used for tuning and calibration. Accurate mass data was obtained in the positive ion mode using a reference standard with ions at 121.05087 and 922.00979. The mass resolution (FWHM) was maintained at 18,000. Elemental analysis was performed using a Perkin-Elmer 2400 Series II CHN/S by the Iowa State Chemical Instrumentation Facility.  $[\alpha]_{\text{D}}$  values were measured on a ATAGO AP-300 polarimeter at  $23$  °C.

**[PhB(Ox<sup>Me2</sup>)<sub>2</sub>]**. A 100 mL Schlenk flask was charged with 4,4-dimethyl-2-oxazoline (1.0 mL, 9.48 mmol), which was then degassed by three freeze-pump-thaw cycles. The degassed oxazoline was dissolved in 50 mL of tetrahydrofuran and the flask was cooled to  $-78$  °C. Using a syringe, *n*BuLi (4.0 mL, 10.0 mmol) was added to the cold solution and the resultant solution was stirred for 45 min at  $-78$  °C. Dichlorophenylborane (0.619 mL, 4.72 mmol) was added drop wise via syringe into the flask and the solution was stirred for 1 h at  $-78$  °C. Then, the solution was allowed to gradually warm to room temperature. After stirring for 14 h at room temperature, the solvent was removed under reduced pressure to afford a light yellow solid. The resultant solid was extracted with benzene and pump off the solvent *in vacuo* to yield PhB(Ox<sup>Me2</sup>)<sub>2</sub> as a yellow solid (1.27 g, 4.47 mmol, 94.3%).  $^1\text{H}$  NMR (acetonitrile-*d*<sub>3</sub>, 400 MHz):  $\delta$  7.42 (d,  $^3J_{\text{HH}} = 7.2$  Hz, 2 H, *ortho*-C<sub>6</sub>H<sub>5</sub>), 7.13 (m, 2 H, *meta*-C<sub>6</sub>H<sub>5</sub>), 7.05 (m, 1 H, *para*-C<sub>6</sub>H<sub>5</sub>), 3.64 (d, 2 H,  $^2J_{\text{HH}} = 8.0$  Hz,  $\overline{\text{CNCMe}_2\text{CH}_2\text{O}}$ ), 3.57 (d, 2 H,  $^2J_{\text{HH}} = 8.0$  Hz,  $\overline{\text{CNCMe}_2\text{CH}_2\text{O}}$ ), 1.26 (s, 6 H,  $\overline{\text{CNCMe}_2\text{CH}_2\text{O}}$ ), 1.17 (s, 6 H,  $\overline{\text{CNCMe}_2\text{CH}_2\text{O}}$ ).  $^{13}\text{C}\{^1\text{H}\}$  NMR (acetonitrile-*d*<sub>3</sub>, 150 MHz):  $\delta$

183.00 (br,  $\overline{\text{CNCMe}_2\text{CH}_2\text{O}}$ ), 132.86 (*ortho*-C<sub>6</sub>H<sub>5</sub>), 127.58 (*meta*-C<sub>6</sub>H<sub>5</sub>), 125.99 (*para*-C<sub>6</sub>H<sub>5</sub>), 77.79 ( $\overline{\text{CNCMe}_2\text{CH}_2\text{O}}$ ), 67.44 ( $\overline{\text{CNCMe}_2\text{CH}_2\text{O}}$ ), 28.71 ( $\overline{\text{CNCMe}_2\text{CH}_2\text{O}}$ ). <sup>11</sup>B NMR (acetonitrile-*d*<sub>3</sub>, 128 MHz):  $\delta$  -8.1. <sup>15</sup>N{<sup>1</sup>H} NMR (acetonitrile-*d*<sub>3</sub>, 71 MHz):  $\delta$  -147.0 ( $\overline{\text{CNCMe}_2\text{CH}_2\text{O}}$ ). IR (KBr, cm<sup>-1</sup>): 3069 w, 3046 w, 2964 s, 2930 s, 2872 m, 1621 s, 1601 s, 1462 s, 1432 s, 1384 m, 1346 w, 1260 s, 1194 s, 1126 m, 1083 w, 993 s, 970 s, 886 m, 703 s. Calcd for C<sub>16</sub>H<sub>21</sub>BN<sub>2</sub>O<sub>2</sub>: C, 67.63; H, 7.45, N, 9.86. Found: C, 64.69; H, 7.51; N, 8.26. Mp: 133-137 °C.

**H[PhB(C<sub>5</sub>H<sub>5</sub>)(Ox<sup>Me2</sup>)<sub>2</sub>]**. A Schlenk flask was charged with PhB(Ox<sup>Me2</sup>)<sub>2</sub> (3.00 g, 10.5 mmol) and Na[C<sub>5</sub>H<sub>5</sub>] (0.581 g, 6.59 mmol) in the glove box. The flask was attached to a Schlenk manifold, and THF (150 mL) was added *via* cannula addition to form a yellow solution. The flask was sealed and the resulting solution was stirred overnight. The solution was filtered to remove a precipitate that appeared overnight, and then the solvent was removed under reduced pressure to afford a brownish yellow solid. This crude product was purified by silica gel column chromatography (Hexane:EtOAc:Et<sub>3</sub>N = 12:7:1; R<sub>f</sub> = 0.50) to afford 3.13 g of H[PhB(C<sub>5</sub>H<sub>5</sub>)(Ox<sup>Me2</sup>)<sub>2</sub>] (4.95 mmol, 47.1%) as a mixture of three isomers. The light yellow solid was dissolved in benzene and stirred over P<sub>2</sub>O<sub>5</sub> to dry without any reduction in yield. <sup>1</sup>H NMR (acetonitrile-*d*<sub>3</sub>, 400 MHz):  $\delta$  7.14-7.04 (m, 5 H, C<sub>6</sub>H<sub>5</sub>), 6.61-6.16 (m, 3 H, C<sub>5</sub>H<sub>5</sub>-*sp*<sup>2</sup>), 4.09-4.00 (m, 4 H,  $\overline{\text{CNCMe}_2\text{CH}_2\text{O}}$ ), 2.90-2.88 (m, 2 H, C<sub>5</sub>H<sub>5</sub>-*sp*<sup>3</sup>), 1.35-1.34 (m, 12 H,  $\overline{\text{CNCMe}_2\text{CH}_2\text{O}}$ ). <sup>13</sup>C{<sup>1</sup>H} NMR (acetonitrile-*d*<sub>3</sub>, 150 MHz):  $\delta$  190.50 ( $\overline{\text{CNCMe}_2\text{CH}_2\text{O}}$ ), 158.8 (br, *ipso*-C<sub>5</sub>H<sub>5</sub>), 141.90 (C<sub>5</sub>H<sub>5</sub>-*sp*<sup>2</sup>), 140.85 (C<sub>5</sub>H<sub>5</sub>-*sp*<sup>2</sup>), 134.96 (C<sub>5</sub>H<sub>5</sub>-*sp*<sup>2</sup>), 134.74 (C<sub>5</sub>H<sub>5</sub>-*sp*<sup>2</sup>), 134.65 (*ortho*-C<sub>6</sub>H<sub>5</sub>), 134.37 (C<sub>5</sub>H<sub>5</sub>-*sp*<sup>2</sup>), 134.30 (C<sub>5</sub>H<sub>5</sub>-*sp*<sup>2</sup>), 131.81 (C<sub>5</sub>H<sub>5</sub>-*sp*<sup>2</sup>), 129.71 (C<sub>5</sub>H<sub>5</sub>-*sp*<sup>2</sup>), 128.51 (C<sub>5</sub>H<sub>5</sub>-*sp*<sup>2</sup>), 128.34 (*meta*-C<sub>6</sub>H<sub>5</sub>), 126.48 (C<sub>5</sub>H<sub>5</sub>-*sp*<sup>2</sup>), 126.24 (*para*-C<sub>6</sub>H<sub>5</sub>), 81.31 (



$\overline{\text{CNCMe}_2\text{CH}_2\text{O}}$ ), 64.71 ( $\overline{\text{CNCMe}_2\text{CH}_2\text{O}}$ ), 64.68 ( $\overline{\text{CNCMe}_2\text{CH}_2\text{O}}$ ), 47.45 ( $\text{C}_5\text{H}_5\text{-}sp^3$ ), 43.48 ( $\text{C}_5\text{H}_5\text{-}sp^3$ ), 28.47 ( $\overline{\text{CNCMe}_2\text{CH}_2\text{O}}$ ), 28.35 ( $\overline{\text{CNCMe}_2\text{CH}_2\text{O}}$ ).  $^{11}\text{B}$  NMR (acetonitrile- $d_3$ , 128 MHz):  $\delta$  -15.27, -15.63, -15.99.  $^{15}\text{N}\{^1\text{H}\}$  NMR (benzene- $d_6$ , 71 MHz):  $\delta$  -172 ( $\overline{\text{CNCMe}_2\text{CH}_2\text{O}}$ ). IR (KBr,  $\text{cm}^{-1}$ ): 3080 w, 3056 w, 3028 w, 2969 m, 2929 w, 2887 w, 1589 s (C=N), 1461 s, 1429 s, 1416 s, 1383 m, 1365 m, 1345 w, 1318 s, 1265 m, 1195 s, 1138 w, 1090 w, 1064 w, 1022 w, 965 s, 934 s, 891 s. Anal. Calcd for  $\text{C}_{21}\text{H}_{27}\text{BO}_2\text{N}_2$ : C, 72.01; H, 7.77; N, 8.00. Found: C, 71.99; H, 7.99; N, 7.84. mp 152-154 °C.

$\{\text{PhB}(\text{C}_5\text{H}_4)(\text{Ox}^{\text{Me}_2})_2\}\text{Zr}(\text{NMe}_2)_2$ . In the glove box,  $\text{H}[\text{PhB}(\text{C}_5\text{H}_5)(\text{Ox}^{\text{Me}_2})_2]$  (0.250 g, 0.714 mmol) and  $\text{Zr}(\text{NMe}_2)_4$  (0.193 g, 0.721 mmol) were placed in a 100 mL Schlenk round bottom flask. The solids were dissolved in benzene (50 mL), and the solution was stirred for 2 h. All volatile materials were removed under reduced pressure to afford a light yellow oil, which was washed with pentane to obtain a light yellow powder of  $\{\text{PhB}(\text{C}_5\text{H}_4)(\text{Ox}^{\text{Me}_2})_2\}\text{Zr}(\text{NMe}_2)_2$  (0.367 g, 0.696 mmol, 97.6%).  $^1\text{H}$  NMR (benzene- $d_6$ , 400 MHz):  $\delta$  8.21 (d,  $^3J_{\text{HH}} = 7$  Hz, 2 H, *ortho*- $\text{C}_6\text{H}_5$ ), 7.52 (t,  $^3J_{\text{HH}} = 7$  Hz, 2 H, *meta*- $\text{C}_6\text{H}_5$ ), 7.32 (t,  $^3J_{\text{HH}} = 7$  Hz, 1 H, *para*- $\text{C}_6\text{H}_5$ ), 6.52 (m, 2 H,  $\text{C}_5\text{H}_4$ ), 6.15 (m, 2 H,  $\text{C}_5\text{H}_4$ ), 3.64 (d, 2 H,  $^2J_{\text{HH}} = 8.0$  Hz,  $\overline{\text{CNCMe}_2\text{CH}_2\text{O}}$ ), 3.56 (d, 2 H,  $^2J_{\text{HH}} = 8.0$  Hz,  $\overline{\text{CNCMe}_2\text{CH}_2\text{O}}$ ), 2.69 (s, 12 H,  $\text{NMe}_2$ ), 1.11 (s, 6 H,  $\overline{\text{CNCMe}_2\text{CH}_2\text{O}}$ ), 1.01 (s, 6 H,  $\overline{\text{CNCMe}_2\text{CH}_2\text{O}}$ ).  $^{13}\text{C}\{^1\text{H}\}$  NMR (benzene- $d_6$ , 100 MHz):  $\delta$  194.65 ( $\overline{\text{CNCMe}_2\text{CH}_2\text{O}}$ ), 151.5 (br, *ipso*- $\text{C}_6\text{H}_5$ ), 143.01 (*ipso*- $\text{C}_5\text{H}_4$ ), 135.11 (*ortho*- $\text{C}_6\text{H}_5$ ), 127.67 (*meta*- $\text{C}_6\text{H}_5$ ), 125.47 (*para*- $\text{C}_6\text{H}_5$ ), 122.61 ( $\text{C}_5\text{H}_4$ ), 113.66 ( $\text{C}_5\text{H}_4$ ), 78.91 ( $\overline{\text{CNCMe}_2\text{CH}_2\text{O}}$ ), 67.16 ( $\overline{\text{CNCMe}_2\text{CH}_2\text{O}}$ ), 43.94 ( $\text{NMe}_2$ ), 28.91 ( $\overline{\text{CNCMe}_2\text{CH}_2\text{O}}$ ), 28.50 ( $\overline{\text{CNCMe}_2\text{CH}_2\text{O}}$ ).  $^{15}\text{N}\{^1\text{H}\}$  NMR (benzene- $d_6$ , 71 MHz):  $\delta$  -135.4 ( $\overline{\text{CNCMe}_2\text{CH}_2\text{O}}$ );  $\text{Zr}(\text{NMe}_2)_2$  was not detected.  $^{11}\text{B}$  NMR (benzene- $d_6$ , 128

MHz):  $\delta$ -14.51. IR (KBr,  $\text{cm}^{-1}$ ): 3064 w, 3040 w, 2962 s, 2927 s, 2863 s, 2819 s, 2771 s, 1595 s (C=N), 1491 s, 1461 s, 1444 w, 1429 m, 1369 m, 1360 m, 1283 s, 1249 s, 1195 s, 1165 s, 1139 s, 1118 s, 1050 s, 1037 w, 989 w, 963 s, 942 s, 927 s, 886 w, 871 w, 837 m, 815 m, 796 m, 783 w, 732 s, 705 s, 688 s. Anal. Calcd for  $\text{C}_{25}\text{H}_{37}\text{BK}_2\text{O}_2\text{N}_4$ : C, 56.91; H, 7.07; N, 10.62. Found: C, 57.26; H, 6.99; N, 9.87. m.p. 107-110 °C, dec.

**{PhB(C<sub>5</sub>H<sub>4</sub>)(Ox<sup>Me2</sup>)<sub>2</sub>}Hf(NMe<sub>2</sub>)<sub>2</sub>**. A procedure analogous to that described for {PhBC<sub>5</sub>H<sub>4</sub>(Ox<sup>Me2</sup>)<sub>2</sub>}Zr(NMe<sub>2</sub>)<sub>2</sub>, using H[PhB(C<sub>5</sub>H<sub>5</sub>)(Ox<sup>Me2</sup>)<sub>2</sub>] (0.250 g, 0.714 mmol) and Hf(NMe<sub>2</sub>)<sub>4</sub> (0.256 g, 0.721 mmol), provides {PhB(C<sub>5</sub>H<sub>4</sub>)(Ox<sup>Me2</sup>)<sub>2</sub>}Hf(NMe<sub>2</sub>)<sub>2</sub> as a light orange solid. Yield: 0.430 g (0.699 mmol, 97.9 %). <sup>1</sup>H NMR (benzene-*d*<sub>6</sub>, 400 MHz):  $\delta$  8.21 (d, <sup>3</sup>J<sub>HH</sub> = 7 Hz, 2 H, *ortho*-C<sub>6</sub>H<sub>5</sub>), 7.52 (t, <sup>3</sup>J<sub>HH</sub> = 7 Hz, 2 H, *meta*-C<sub>6</sub>H<sub>5</sub>), 7.32 (t, <sup>3</sup>J<sub>HH</sub> = 7 Hz, 1 H, *para*-C<sub>6</sub>H<sub>5</sub>), 6.46 (m, 2 H, C<sub>5</sub>H<sub>4</sub>), 6.12 (m, 2 H, C<sub>5</sub>H<sub>4</sub>), 3.65 (d, 2 H, <sup>2</sup>J<sub>HH</sub> = 8.0 Hz,  $\overline{\text{CNCMe}_2\text{CH}_2\text{O}}$ ), 3.57 (d, 2 H, <sup>2</sup>J<sub>HH</sub> = 8.0 Hz,  $\overline{\text{CNCMe}_2\text{CH}_2\text{O}}$ ), 2.74 (s, 12 H, NMe<sub>2</sub>), 1.12 (s, 6 H,  $\overline{\text{CNCMe}_2\text{CH}_2\text{O}}$ ), 1.00 (s, 6 H,  $\overline{\text{CNCMe}_2\text{CH}_2\text{O}}$ ). <sup>13</sup>C{<sup>1</sup>H} NMR (benzene-*d*<sub>6</sub>, 400 MHz):  $\delta$  198.36 ( $\overline{\text{CNCMe}_2\text{CH}_2\text{O}}$ ), 150.75 (*ipso*-C<sub>6</sub>H<sub>5</sub>), 140.61 (*ipso*-C<sub>5</sub>H<sub>4</sub>), 134.79 (*ortho*-C<sub>6</sub>H<sub>5</sub>), 127.46 (*meta*-C<sub>6</sub>H<sub>5</sub>), 125.22 (*para*-C<sub>6</sub>H<sub>5</sub>), 120.88 (C<sub>5</sub>H<sub>4</sub>), 112.49 (C<sub>5</sub>H<sub>4</sub>), 78.91 ( $\overline{\text{CNCMe}_2\text{CH}_2\text{O}}$ ), 67.07 ( $\overline{\text{CNCMe}_2\text{CH}_2\text{O}}$ ), 43.77 (s, NMe<sub>2</sub>), 28.51 ( $\overline{\text{CNCMe}_2\text{CH}_2\text{O}}$ ), 27.90 ( $\overline{\text{CNCMe}_2\text{CH}_2\text{O}}$ ). <sup>15</sup>N{<sup>1</sup>H} NMR (benzene-*d*<sub>6</sub>, 71 MHz):  $\delta$  -132.3 ( $\overline{\text{CNCMe}_2\text{CH}_2\text{O}}$ ). <sup>11</sup>B NMR (benzene-*d*<sub>6</sub>, 128 MHz):  $\delta$  -14.6. IR (KBr,  $\text{cm}^{-1}$ ): 3064 w, 3042 w, 3012 w, 2962 s, 2928 m, 2868 s, 2853 s, 2821 s, 2773 s, 1595 m (C=N), 1549 w, 1483 s, 1462 s, 1446 m, 1429 m, 1370 m, 1361 m, 1287 s, 1251 s, 1203 s, 1195 s, 1183 s, 1166 m, 1138 m, 1051 m, 1037 w, 963 s, 936 s, 908 w. Anal. Calcd for

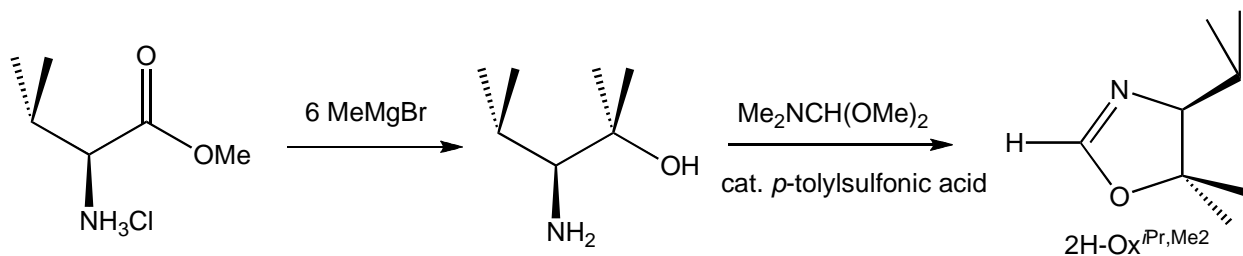
$C_{25}H_{37}BO_2N_4Hf(C_6H_6)_{0.5}$ : C, 51.43; H, 6.17; N, 8.57. Found: C, 51.17; H, 6.20; N, 8.40. Mp: 90-95 °C, dec.

**{PhB(C<sub>5</sub>H<sub>4</sub>)(Ox<sup>Me<sub>2</sub>)<sub>2</sub>)<sub>2</sub>Zr(NMe<sub>2</sub>)<sub>2</sub>THF}</sup>**. Slow diffusion of pentane into a THF solution of **2** at -30 °C provided analytically pure, X-ray quality crystals of {PhB(η<sup>5</sup>-C<sub>5</sub>H<sub>4</sub>)(Ox<sup>Me<sub>2</sub>)<sub>2</sub>)<sub>2</sub>Zr(NMe<sub>2</sub>)<sub>2</sub>THF}. The room temperature NMR spectroscopic data for **4** is identical to that of the THF-free species in addition to resonances due to uncoordinated THF. The structural difference is observed in the IR and in the analytical data. IR (KBr, cm<sup>-1</sup>): 3063 w, 3042 m, 2995 m, 2966 s, 2930s, 2862 s, 2819 s, 2768 s, 1610 s (CN), 1533 s (CN), 1488 m, 1461 m, 1429 m, 1367 w, 1356 w, 1281 s, 1243 s, 1196 s, 1180 s, 1149 m, 1135 m, 1059 s, 1048 s, 1035 m, 1021 m, 991 s, 964 s, 950 s, 937 s, 873 s, 863 s, 817 s, 799 s, 774 w, 732 s, 704 s. Anal. Calcd for C<sub>29</sub>H<sub>45</sub>BO<sub>3</sub>N<sub>4</sub>Zr: C, 58.08; H, 7.56; N, 9.34. Found: C, 57.88; H, 7.51; N, 9.10.</sup>

**L-Valine methyl ester hydrochloride.**<sup>52</sup> Thionyl chloride (47.6 mL, 0.65 mol, 1.10 equiv) was added drop wise over 2 h to methanol (300 mL) in a three-necked flask cooled in ice-salt bath and connected to an oil bubbler. L-Valine (70.0 g, 0.600 mol) was added in one portion to the solution, and the mixture was heated at 55 °C to dissolve all of the solids. The solution was then heated for 1 h. The solvent and excess reagents were removed by distillation. The resulting white solid was dried *in vacuo* for several hours and then dissolved in minimal amount of methanol (90 mL). The methanol solution was poured into Et<sub>2</sub>O (900 mL), and then recrystallized at -30 °C. The solid was collected, washed with cold Et<sub>2</sub>O, and dried *in vacuo* to give the L-Valine methyl ester hydrochloride as white solid (90.7 g, 90.5%). The <sup>1</sup>H NMR spectrum (given below) matches the literature values.<sup>52</sup> <sup>1</sup>H NMR (300 MHz, chloroform-*d*): δ 8.91 (br, 3 H,

$\text{HCl}\cdot\text{NH}_2\text{CH}(\text{CHMe}_2)\text{CO}_2\text{Me}$ ), 3.93 (d,  $^3J_{\text{HH}} = 4.5$  Hz, 1 H,  $\text{HCl}\cdot\text{NH}_2\text{CH}(\text{CHMe}_2)\text{CO}_2\text{Me}$ ), 3.84 (s, 3 H,  $\text{HCl}\cdot\text{NH}_2\text{CH}(\text{CHMe}_2)\text{CO}_2\text{Me}$ ), 2.47 (m, 1 H,  $\text{HCl}\cdot\text{NH}_2\text{CH}(\text{CHMe}_2)\text{CO}_2\text{Me}$ ), 1.16 (vt, 6 H,  $\text{HCl}\cdot\text{NH}_2\text{CH}(\text{CHMe}_2)\text{CO}_2\text{Me}$ ).

**2S-Amino-1,1,3-trimethylbutanol.** A solution of methylmagnesium bromide (180 mL, 3.0 M in  $\text{Et}_2\text{O}$ , 0.540 mol, 6.0 equiv) was diluted with  $\text{Et}_2\text{O}$  (500 mL). L-Valine methyl ester hydrochloride (15.0 g, 0.0896 mol) was added in portions over 1 h. The mixture was allowed to stir at room temperature overnight. Saturated aqueous  $[\text{NH}_4][\text{Cl}]$  was added in a drop wise fashion to quench the reaction. The white solid was separated from the diethyl ether solution, and the organic solution was dried over  $\text{Na}_2\text{SO}_4$ . The solid was dissolved in 300 mL saturated  $[\text{NH}_4][\text{Cl}]$  aqueous solution, and another 300 mL of distilled water was added. This aqueous solution was extracted with  $\text{Et}_2\text{O}$  ( $4 \times 200$  mL). The organic extracts were combined and dried over  $\text{Na}_2\text{SO}_4$ . The two organic solutions were filtered, combined, and evaporated under reduced pressure. The crude product was distilled (96 °C, 40 mm Hg) to afford 2S-Amino-1,1,3-trimethylbutanol as a clear, colorless oil (4.96 g, 42.3%) that is spectroscopically identical to the literature.<sup>53</sup>  $^1\text{H}$  NMR (300 MHz, chloroform-*d*):  $\delta$  2.41 (d,  $^3J_{\text{HH}} = 2.7$  Hz, 1 H,  $\text{NH}_2\text{CH}(\text{CHMe}_2)\text{CMe}_2\text{OH}$ ), 1.93 (m, 1 H,  $\text{NH}_2\text{CH}(\text{CHMe}_2)\text{CMe}_2\text{OH}$ ), 1.20 (s, 3 H,  $\text{NH}_2\text{CH}(\text{CHMe}_2)\text{CMe}_2\text{OH}$ ), 1.12 (s, 3 H,  $\text{NH}_2\text{CH}(\text{CHMe}_2)\text{CMe}_2\text{OH}$ ), 0.97 (d,  $^3J_{\text{HH}} = 7.2$  Hz, 3 H,  $\text{NH}_2\text{CH}(\text{CHMe}_2)\text{CMe}_2\text{OH}$ ), 0.88 (d,  $^3J_{\text{HH}} = 6.6$  Hz, 3 H,  $\text{NH}_2\text{CH}(\text{CHMe}_2)\text{CMe}_2\text{OH}$ ).



**4S-Isopropyl-5,5-dimethyl-2-oxazoline.** A modification of Meyers' procedure for 2-H oxazoline synthesis using 2S-Amino-1,1,3-trimethylbutanol was implemented.<sup>54</sup> DMF-DMA (13.7 mL, 103.3 mmol, 1.2 equiv) was added to degassed 2S-amino-1,1,3-trimethylbutanol (11.1 g, 84.7 mmol). This mixture was allowed to reflux at 75 °C for 7 h. The volatiles were removed under reduced pressure, and the mixture was triturated with hexane (4 × 30 mL). Then *p*-toluenesulfonic acid monohydrate (26.5 mg, 0.14 mmol, 0.0017 equiv) and hexane (40 mL) were added, and an addition funnel with approximately 40 mL of molecular sieves inside was placed on top of the flask, and a condenser was placed on top of the funnel. The solution was heated at 90 °C at reflux for 24 h and the condensed liquids washed over the sieves as the reaction proceeded. The reaction mixture was washed with saturated aqueous NaHCO<sub>3</sub> solution (30 mL) and then with brine (50 mL). The aqueous solutions were combined, back-extracted with Et<sub>2</sub>O (25 mL × 6), and then the organic extracts were combined with the organic solution and dried over Na<sub>2</sub>SO<sub>4</sub> overnight and filtered. Concentration of the filtrate gave a dark red oil which was distilled to provide 8.11 g (57.4 mmol, 68%) of 4S-isopropyl-5,5-dimethyl-2-oxazoline as a clear, colorless oil. Bp: 85 °C, 18 mm Hg. <sup>1</sup>H NMR (300 MHz, chloroform-*d*): δ 6.74 (s, 1 H, CHNC(CHMe<sub>2</sub>)HMe<sub>2</sub>O), 3.23 (d, <sup>3</sup>J<sub>HH</sub> = 8.4 Hz, 1 H, CHNC(CHMe<sub>2</sub>)HMe<sub>2</sub>O), 1.80 (m, 1 H, CHNC(CHMe<sub>2</sub>)HMe<sub>2</sub>O), 1.45 (s, 3 H, CHNC(CHMe<sub>2</sub>)HMe<sub>2</sub>O), 1.29 (s, 3 H, CHNC(CHMe<sub>2</sub>)HMe<sub>2</sub>O), 1.08 (d, <sup>3</sup>J<sub>HH</sub> = 6.6 Hz, 3 H, CHNC(CHMe<sub>2</sub>)HMe<sub>2</sub>O), 0.98 (d, <sup>3</sup>J<sub>HH</sub> = 6.6 Hz, 3 H, CHNC(CHMe<sub>2</sub>)HMe<sub>2</sub>O). <sup>13</sup>C{<sup>1</sup>H} NMR (benzene-*d*<sub>6</sub>, 150 MHz): δ 152.74 (CHNC(CHMe<sub>2</sub>)HMe<sub>2</sub>O), 85.17 (CNC(CHMe<sub>2</sub>)HMe<sub>2</sub>O), 80.07 (CNC(CHMe<sub>2</sub>)HMe<sub>2</sub>O), 29.56 (CNC(CHMe<sub>2</sub>)HMe<sub>2</sub>O), 29.48 (CNC(CHMe<sub>2</sub>)HMe<sub>2</sub>O), 21.53, 21.48, 21.20 (CNC(CHMe<sub>2</sub>)HMe<sub>2</sub>O, CNC(CHMe<sub>2</sub>)HMe<sub>2</sub>O). <sup>15</sup>N{<sup>1</sup>H} NMR (benzene-*d*<sub>6</sub>, 71 MHz): δ -143.3. IR (KBr, cm<sup>-1</sup>): 3069 w, 2973 s, 2874 m, 1686 w, 1632 s (CN), 1471 m, 1462 m, 1386

m, 1372 m, 1336 w, 1304 w, 1272 w, 1243 w, 1202 w, 1172 m, 1134 m, 1114 m, 1082 s, 1015 m, 934 m, 894 m, 856 w, 813 w, 769 w.  $[\alpha]_D^{20} = -35.2$  (C<sub>6</sub>H<sub>6</sub>).

**PhB(Ox<sup>4*S*-iPr,Me<sub>2</sub></sup>)<sub>2</sub>**. A 100 mL Schlenk flask was charged with 4*S*-isopropyl-5,5-dimethyl-2-oxazoline (0.500 g, 3.54 mmol) and tetrahydrofuran (50 mL), and the flask was cooled to -78 °C. Using a syringe, 2.50 M *n*BuLi (1.50 mL, 3.75 mmol) was added, and the solution was stirred for 1 h at -78 °C. Dichlorophenylborane (0.23 mL, 1.75 mmol) was slowly added, and the solution was stirred for 1 h at -78 °C and then allowed to gradually warm to ambient temperature. After stirring for 14 h at room temperature, the solvent was removed under reduced pressure to afford a light yellow solid. The solid was extracted with benzene, and the solvent was evaporated to yield [PhB(Ox<sup>4*S*-iPr,Me<sub>2</sub></sup>)<sub>2</sub>] as a light yellow, impure solid (0.60 g, 1.63 mmol) that appears to contain variable quantities of LiCl. This mixture is sufficiently pure, however, for further synthetic work and was used as obtained from the benzene extraction. <sup>1</sup>H NMR (tetrahydrofuran-*d*<sub>8</sub>, 400 MHz):  $\delta$  7.45 (d, <sup>3</sup>*J*<sub>HH</sub> = 7.6 Hz, 2 H, *ortho*-C<sub>6</sub>H<sub>5</sub>), 6.97 (m, 2 H, *meta*-C<sub>6</sub>H<sub>5</sub>), 6.87 (m, 1 H, *para*-C<sub>6</sub>H<sub>5</sub>), 3.22 (d, <sup>3</sup>*J*<sub>HH</sub> = 4.8 Hz, 2 H, CNC*i*PrHMe<sub>2</sub>O), 3.20 (d, <sup>3</sup>*J*<sub>HH</sub> = 4.8 Hz, 1 H, CNC*i*PrHMe<sub>2</sub>O), 1.79 (m, 1 H, CNC(CHMe<sub>2</sub>)HMe<sub>2</sub>O), 1.23-0.85 (24 H, CNC(CHMe<sub>2</sub>)HMe<sub>2</sub>O). <sup>13</sup>C{<sup>1</sup>H} NMR (tetrahydrofuran-*d*<sub>8</sub>, 150 MHz):  $\delta$  185.47 (br, CNC*i*PrHMe<sub>2</sub>O), 150.50 (br, *ipso*-C<sub>6</sub>H<sub>5</sub>), 133.42 (*ortho*-C<sub>6</sub>H<sub>5</sub>), 126.37 (*meta*-C<sub>6</sub>H<sub>5</sub>), 124.69 (*para*-C<sub>6</sub>H<sub>5</sub>), 82.66 (CNC*i*PrHMe<sub>2</sub>O), 82.61 (CNC*i*PrHMe<sub>2</sub>O), 79.81 (CNC*i*PrHMe<sub>2</sub>O), 79.45 (CNC*i*PrHMe<sub>2</sub>O), 30.38, 30.09, 30.07, 29.92, 22.11 br, 21.58, 21.50 (overlapping CNC(CHMe<sub>2</sub>)HMe<sub>2</sub>O, CNC*i*PrHMe<sub>2</sub>O, and CNC(CHMe<sub>2</sub>)HMe<sub>2</sub>O). <sup>11</sup>B NMR (THF-*d*<sub>8</sub>, 128 MHz):  $\delta$  -7.5. IR (KBr, cm<sup>-1</sup>): 3070 w, 3046 w, 2963 s, 2932 s, 2872 m, 1588 s (CN), 1466

m, 1432 m, 1386 m, 1371 s, 1277 w, 1242 s, 1193 m, 1176 m, 1146 s, 1120 m, 1096 m, 1023 s, 993 m, 943 m, 879 m, 849 m, 802 m, 762 w, 741 w, 726 w. Mp: 101-106 °C.

**H[PhB(C<sub>5</sub>H<sub>5</sub>)(Ox<sup>4*S*-iPr,Me<sub>2</sub></sup>)<sub>2</sub>]**. A Schlenk flask was charged with [PhB(Ox<sup>4*S*-iPr,Me<sub>2</sub></sup>)<sub>2</sub>] (0.580 g, 1.57 mmol) and [NaC<sub>5</sub>H<sub>5</sub>] (0.082 g, 0.931 mmol). Addition of THF (60 mL) provided a yellow solution that was stirred overnight. A precipitate formed after 12 h, and the solution was filtered. Solvent was removed under reduced pressure to afford a light yellow solid. This crude product was purified by silica gel column chromatography (hexane:EtOAc:Et<sub>3</sub>N = 9:1:1; R<sub>f</sub> = 0.58) to afford an off-white solid of H[PhB(C<sub>5</sub>H<sub>5</sub>)(Ox<sup>4*S*-iPr,Me<sub>2</sub></sup>)<sub>2</sub>] as a mixture of isomers. The product was dissolved in benzene and stirred over P<sub>2</sub>O<sub>5</sub> to remove residual water, giving 0.210 g of H[PhB(C<sub>5</sub>H<sub>5</sub>)(Ox<sup>4*S*-iPr,Me<sub>2</sub></sup>)<sub>2</sub>] (0.482 mmol, 51.8%). <sup>1</sup>H NMR (acetonitrile-*d*<sub>3</sub>, 400 MHz): δ 7.71-7.0 (m, 5 H, C<sub>6</sub>H<sub>5</sub>), 6.67-6.18 (m, 3 H, C<sub>5</sub>H<sub>5</sub>), 3.39-3.25 (m, 2 H, CNC*i*PrH*C*Me<sub>2</sub>O), 2.89-2.88 (m, 2 H, C<sub>5</sub>H<sub>5</sub>), 1.89-1.78 (m, 2 H, CNC(CHMe<sub>2</sub>)H*C*Me<sub>2</sub>O), 1.47-0.94 (24 H, CNC(CHMe<sub>2</sub>)H*C*Me<sub>2</sub>O). <sup>13</sup>C{<sup>1</sup>H} NMR (acetonitrile-*d*<sub>3</sub>, 150 MHz): δ 133.48 (*ortho*-C<sub>6</sub>H<sub>5</sub>), 129.06 (*meta*-C<sub>6</sub>H<sub>5</sub>), 128.22 (*para*-C<sub>6</sub>H<sub>5</sub>), 141.17 (C<sub>5</sub>H<sub>5</sub>; 10 *sp*<sup>2</sup> resonances for 3 isomers observed), 140.99 (C<sub>5</sub>H<sub>5</sub>), 135.25 (C<sub>5</sub>H<sub>5</sub>), 134.76 (C<sub>5</sub>H<sub>5</sub>), 134.20 (C<sub>5</sub>H<sub>5</sub>), 133.91 (C<sub>5</sub>H<sub>5</sub>), 133.83 (C<sub>5</sub>H<sub>5</sub>), 131.28 (C<sub>5</sub>H<sub>5</sub>), 128.90 (C<sub>5</sub>H<sub>5</sub>), 128.37 (C<sub>5</sub>H<sub>5</sub>), 94.11 (CNC*i*PrH*C*Me<sub>2</sub>O), 66.67 (CNC*i*PrH*C*Me<sub>2</sub>O), 47.52 (C<sub>5</sub>H<sub>5</sub>-*sp*<sup>3</sup>), 43.18 (C<sub>5</sub>H<sub>5</sub>-*sp*<sup>3</sup>), 30.24 (CNC(CHMe<sub>2</sub>)H*C*Me<sub>2</sub>O), 29.26 (CNC(CHMe<sub>2</sub>)H*C*Me<sub>2</sub>O), 29.92, 29.68, 22.09, 22.04, 21.81, 21.77, 21.38, 21.26 (CNC(CHMe<sub>2</sub>)H*C*Me<sub>2</sub>O). <sup>11</sup>B NMR (acetonitrile-*d*<sub>3</sub>, 128 MHz): δ -15.7 (overlapping resonances). IR (KBr, cm<sup>-1</sup>): 3084 w, 3066 w, 3025 w, 2971 s, 2927 m, 2870 m, 1584 s (CN), 1567 s (CN), 1486 w, 1466 m, 1432 w, 1403 s, 1396 s, 1376 m, 1370 m, 1356 w, 1347 w, 1330 w, 1302 w, 1244w, 1225 w, 1212 m, 1177 w, 1146 m, 1096 w, 1068 w, 1027 m, 999 w, 993 w,

956 m, 942 m, 890 m, 852 w, 813 w. Anal. Calcd for  $C_{27}H_{39}BN_2O_2$ : C, 74.65; H, 9.05; N, 6.45. Found: C, 74.29; H, 9.28; N, 6.74. Mp: 78-83 °C.  $[\alpha]_D^{20} = -62.9$  ( $C_6H_6$ ).

**$\{PhB(C_5H_4)(Ox^{4S-iPr,Me_2})_2\}Zr(NMe_2)_2$ .** A Schlenk flask was charged with  $H[PhB(C_5H_5)(Ox^{4S-iPr,Me_2})_2]$  (0.100 g, 0.230 mmol) and  $[Zr(NMe_2)_4]$  (0.061 g, 0.228 mmol). The solids were dissolved in benzene (15 mL), and the resulting solution was stirred for 8 h. After filtration, the volatile materials were evaporated to give a light yellow gel which was triturated with pentane affording  $\{PhB(C_5H_4)(Ox^{4S-iPr,Me_2})_2\}Zr(NMe_2)_2$  as an off-white analytically pure solid (0.135 g, 0.221 mmol, 96.0%).  $^1H$  NMR (benzene- $d_6$ , 400 MHz):  $\delta$  8.09 (d,  $^3J_{HH} = 7.2$  Hz, 2 H, *ortho*- $C_6H_5$ ), 7.50 (m, 2 H, *meta*- $C_6H_5$ ), 7.29 (m, 1 H, *para*- $C_6H_5$ ), 6.76 (m, 1 H,  $C_5H_4$ ), 6.59 (m, 1 H,  $C_5H_4$ ), 6.25 (m, 1 H,  $C_5H_4$ ), 6.06 (m, 1 H,  $C_5H_4$ ), 3.24 (d, 2 H,  $^3J_{HH} = 5.6$  Hz, CNCiPrH $CM_e_2$ O), 3.20 (d, 2 H,  $^3J_{HH} = 5.6$  Hz, CNCiPrH $CM_e_2$ O), 2.80 (s, 6 H, NMe $_2$ ), 2.68 (s, 6 H, NMe $_2$ ), 1.73 (m, 2 H, CNC(CHMe $_2$ )H $CM_e_2$ O), 1.34 (s, 3 H, CNCiPrH $CM_e_2$ O), 1.24 (s, 3 H, CNCiPrH $CM_e_2$ O), 1.18 (s, 3 H, CNCiPrH $CM_e_2$ O), 1.14 (s, 3 H, CNCiPrH $CM_e_2$ O), 1.12 (d,  $^3J_{HH} = 6.8$  Hz, 3 H, CNC(CHMe $_2$ )H $CM_e_2$ O), 1.09 (d,  $^3J_{HH} = 6.8$  Hz, 3 H, CNC(CHMe $_2$ )H $CM_e_2$ O), 0.97 (d,  $^3J_{HH} = 6.8$  Hz, 3 H, CNC(CHMe $_2$ )H $CM_e_2$ O), 0.89 (d,  $^3J_{HH} = 6.8$  Hz, 3 H, CNC(CHMe $_2$ )H $CM_e_2$ O).  $^{13}C\{^1H\}$  NMR (benzene- $d_6$ , 150 MHz):  $\delta$  197.01 (br, CNCiPrHCH $_2$ O), 194.29 (br, CNCiPrHCH $_2$ O), 151.50 (br, *ipso*- $C_6H_5$ ), 135.10 (*ortho*- $C_6H_5$ ), 127.51 (*meta*- $C_6H_5$ ), 125.26 (*para*- $C_6H_5$ ), 123.47 ( $C_5H_4$ ), 122.83 ( $C_5H_4$ ), 113.93 ( $C_5H_4$ ), 113.64 ( $C_5H_4$ ), 85.08 (CNCiPrH $CM_e_2$ O), 84.84 (CNCiPrH $CM_e_2$ O), 79.05 (CNCiPrH $CM_e_2$ O), 78.89 (CNCiPrH $CM_e_2$ O), 44.51 (NMe $_2$ ), 42.95 (NMe $_2$ ), 30.44 (CNC(CHMe $_2$ )H $CM_e_2$ O), 30.27 (CNC(CHMe $_2$ )H $CM_e_2$ O), 30.24 (CNCiPrH $CM_e_2$ O), 30.02 (CNCiPrH $CM_e_2$ O), 21.96 (CNCiPrH $CM_e_2$ O), 21.81 (CNCiPrH $CM_e_2$ O), 20.70 (CNC(CHMe $_2$ )H $CM_e_2$ O), 20.47



(CNC(CHMe<sub>2</sub>)HMe<sub>2</sub>O), 20.37 (CNC(CHMe<sub>2</sub>)HMe<sub>2</sub>O), 20.18 (CNC(CHMe<sub>2</sub>)HMe<sub>2</sub>O). <sup>11</sup>B NMR (benzene-*d*<sub>6</sub>, 128 MHz): δ -14.5. <sup>15</sup>N{<sup>1</sup>H} NMR (benzene-*d*<sub>6</sub>, 71 MHz): δ -152.6, -155.0 (CNC<sup>*i*</sup>PrHMe<sub>2</sub>O). IR (KBr, cm<sup>-1</sup>): 3043 w, 3068 w, 2967 s, 2930 s, 2873 s, 2772 w, 1565 m (CN), 1489 w, 1467 s, 1431 w, 1388 m, 1369 m, 1260 s, 1194 s, 1142 s, 1093 s, 1054 s, 1023 s, 947 s, 884 w, 855 w, 804 s, 734 s, 703 s. Anal. Calcd for C<sub>31</sub>H<sub>49</sub>BN<sub>4</sub>O<sub>2</sub>Zr: C, 60.86; H, 8.07; N, 9.16. Found: C, 60.63; H, 8.48; N, 9.34. Mp: 68-73 °C, dec. [α]<sub>D</sub><sup>20</sup> = -124.7 (C<sub>6</sub>H<sub>6</sub>).

**{PhB(C<sub>5</sub>H<sub>4</sub>)(Ox<sup>4S-*i*Pr,Me<sub>2</sub>)<sub>2</sub>)<sub>2</sub>Hf(NMe<sub>2</sub>)<sub>2</sub>}</sup>**. A round bottom Schlenk flask was charged with H[PhB(C<sub>5</sub>H<sub>5</sub>)(Ox<sup>4S-*i*Pr,Me<sub>2</sub>)<sub>2</sub>]<sub>2</sub> (0.125 g, 0.287 mmol) and Hf(NMe<sub>2</sub>)<sub>4</sub> (0.101 g, 0.287 mmol). The solids were dissolved in benzene (20 mL), and the resulting solution was stirred for 7-8 h. After filtration, the volatile materials were removed *in vacuo* to give a light yellow gel which was triturated with pentane giving {PhB(C<sub>5</sub>H<sub>4</sub>)(Ox<sup>4S-*i*Pr,Me<sub>2</sub>)<sub>2</sub>)<sub>2</sub>Hf(NMe<sub>2</sub>)<sub>2</sub>} as a off white solid (0.185 g, 0.265 mmol, 92.0%). <sup>1</sup>H NMR (benzene-*d*<sub>6</sub>, 400 MHz): δ 8.06 (d, <sup>3</sup>J<sub>HH</sub> = 7.2 Hz, 2 H, *ortho*-C<sub>6</sub>H<sub>5</sub>), 7.46 (m, 2 H, *meta*-C<sub>6</sub>H<sub>5</sub>), 7.26 (m, 1 H, *para*-C<sub>6</sub>H<sub>5</sub>), 6.64 (m, 1 H, C<sub>5</sub>H<sub>4</sub>), 6.55 (m, 1 H, C<sub>5</sub>H<sub>4</sub>), 6.23 (m, 1 H, C<sub>5</sub>H<sub>4</sub>), 6.00 (m, 1 H, C<sub>5</sub>H<sub>4</sub>), 3.26 (d, 2 H, <sup>2</sup>J<sub>HH</sub> = 5.6 Hz, CNC<sup>*i*</sup>PrHMe<sub>2</sub>O), 3.23 (d, 2 H, <sup>2</sup>J<sub>HH</sub> = 5.6 Hz, CNC<sup>*i*</sup>PrHMe<sub>2</sub>O), 2.84 (s, 6 H, NMe<sub>2</sub>), 2.76 (s, 6 H, NMe<sub>2</sub>), 1.74 (m, 2 H, CNC(CHMe<sub>2</sub>)HMe<sub>2</sub>O), 1.35 (s, 3 H, CNC<sup>*i*</sup>PrHMe<sub>2</sub>O), 1.24 (s, 3 H, CNC<sup>*i*</sup>PrHMe<sub>2</sub>O), 1.19 (s, 3 H, CNC<sup>*i*</sup>PrHMe<sub>2</sub>O), 1.15 (s, 3 H, CNC<sup>*i*</sup>PrHMe<sub>2</sub>O), 1.11 (d, <sup>3</sup>J<sub>HH</sub> = 6.8 Hz, 3 H, CNC(CHMe<sub>2</sub>)HMe<sub>2</sub>O), 1.07 (d, <sup>3</sup>J<sub>HH</sub> = 6.8 Hz, 3 H, CNC(CHMe<sub>2</sub>)HMe<sub>2</sub>O), 0.99 (d, <sup>3</sup>J<sub>HH</sub> = 6.8 Hz, 3 H, CNC(CHMe<sub>2</sub>)HMe<sub>2</sub>O), 0.89 (d, <sup>3</sup>J<sub>HH</sub> = 6.8 Hz, 3 H, CNC(CHMe<sub>2</sub>)HMe<sub>2</sub>O). <sup>13</sup>C{<sup>1</sup>H} NMR (benzene-*d*<sub>6</sub>, 100 MHz): δ 151.36 (*ipso*-C<sub>6</sub>H<sub>5</sub>), 135.07 (*ortho*-C<sub>6</sub>H<sub>5</sub>), 127.52 (*meta*-C<sub>6</sub>H<sub>5</sub>), 125.28 (*para*-C<sub>6</sub>H<sub>5</sub>), 122.43 (C<sub>5</sub>H<sub>4</sub>), 121.55 (C<sub>5</sub>H<sub>4</sub>), 113.38 (C<sub>5</sub>H<sub>4</sub>), 112.62 (C<sub>5</sub>H<sub>4</sub>), 85.31 (CNC(CHMe<sub>2</sub>)HMe<sub>2</sub>O), 79.02 (CNC(CHMe<sub>2</sub>)HMe<sub>2</sub>O), 44.20</sup></sup>

(NMe<sub>2</sub>), 42.71 (NMe<sub>2</sub>), 30.51 (CNC(CHMe<sub>2</sub>)HMe<sub>2</sub>O), 30.38 (CNC(CHMe<sub>2</sub>)HMe<sub>2</sub>O), 30.32 (CNC(CHMe<sub>2</sub>)HMe<sub>2</sub>O), 30.08 (CNC(CHMe<sub>2</sub>)HMe<sub>2</sub>O), 22.02 (CNC(CHMe<sub>2</sub>)HMe<sub>2</sub>O), 21.84 (CNC(CHMe<sub>2</sub>)HMe<sub>2</sub>O), 20.42 (CNC(CHMe<sub>2</sub>)HMe<sub>2</sub>O), 20.32 (CNC(CHMe<sub>2</sub>)HMe<sub>2</sub>O), 20.00 (CNC(CHMe<sub>2</sub>)HMe<sub>2</sub>O). <sup>15</sup>N NMR (benzene-*d*<sub>6</sub>, 71 MHz):  $\delta$  -148.83, -150.66. <sup>11</sup>B NMR (benzene-*d*<sub>6</sub>, 128 MHz):  $\delta$  -14.6. IR (KBr, cm<sup>-1</sup>): 3071 m, 3044 m, 2967 s, 2932 s, 2870 s, 2822 s, 2770 s, 1559 s (CN), 1469 s, 1433 m, 1393 m, 1373 m, 1353 w, 1246 m, 1195 m, 1145 s, 1105 w, 1048 m, 1021 m, 946 s, 882 w, 856 w, 807 s, 769 w, 740 s, 703 s. Anal. Calcd for C<sub>31</sub>H<sub>49</sub>BN<sub>4</sub>O<sub>2</sub>Hf: C, 53.26; H, 7.07; N, 8.01. Found: C, 52.78; H, 7.32; N, 8.04. [ $\alpha$ ]<sub>D</sub> = -86.98° (C<sub>6</sub>H<sub>6</sub>). Mp: 60-65 °C, dec.

**{PhB(C<sub>5</sub>H<sub>4</sub>)(Ox<sup>4*S*-iPr,Me<sub>2</sub></sup>)<sub>2</sub>}Ti(NMe<sub>2</sub>)<sub>2</sub>**. A round bottom Schlenk flask was charged with H[PhB(C<sub>5</sub>H<sub>5</sub>)(Ox<sup>4*S*-iPr,Me<sub>2</sub></sup>)<sub>2</sub>] (0.050 g, 0.115 mmol) and Ti(NMe<sub>2</sub>)<sub>4</sub> (0.026 g, 0.115 mmol). The solids were dissolved in benzene (5 mL), and the resulting solution was stirred for 25 h. After filtration, the volatile materials were removed *in vacuo* to give a red gel which was triturated with pentane giving {PhB(C<sub>5</sub>H<sub>4</sub>)(Ox<sup>4*S*-iPr,Me<sub>2</sub></sup>)<sub>2</sub>}Ti(NMe<sub>2</sub>)<sub>2</sub> as a off white solid (0.056 g, 0.099 mmol, 86.1%). <sup>1</sup>H NMR (benzene-*d*<sub>6</sub>, 400 MHz):  $\delta$  7.73 (d, <sup>3</sup>J<sub>HH</sub> = 7.2 Hz, 2 H, *ortho*-C<sub>6</sub>H<sub>5</sub>), 7.39 (m, 2 H, *meta*-C<sub>6</sub>H<sub>5</sub>), 7.21 (m, 1 H, *para*-C<sub>6</sub>H<sub>5</sub>), 6.88 (m, 2 H, C<sub>5</sub>H<sub>4</sub>), 6.70 (m, 1 H, C<sub>5</sub>H<sub>4</sub>), 6.59 (m, 1 H, C<sub>5</sub>H<sub>4</sub>), 3.12 (s, 6 H, NMe<sub>2</sub>), 3.10 (s, 6 H, NMe<sub>2</sub>), 3.03 (d, 2 H, <sup>2</sup>J<sub>HH</sub> = 5.6 Hz, CNC<sup>*i*</sup>PrHMe<sub>2</sub>O), 2.97 (d, 2 H, <sup>2</sup>J<sub>HH</sub> = 5.6 Hz, CNC<sup>*i*</sup>PrHMe<sub>2</sub>O), 1.82 (m, 1 H, CNC(CHMe<sub>2</sub>)HMe<sub>2</sub>O), 1.70 (m, 1 H, CNC(CHMe<sub>2</sub>)HMe<sub>2</sub>O), 1.23-0.77 (24 H, CNC(CHMe<sub>2</sub>)HMe<sub>2</sub>O). <sup>13</sup>C{<sup>1</sup>H} NMR (benzene-*d*<sub>6</sub>, 100 MHz):  $\delta$  195.50 (br, CNC<sup>*i*</sup>PrHMe<sub>2</sub>O), 152.97 (*ipso*-C<sub>6</sub>H<sub>5</sub>), 135.18 (*ortho*-C<sub>6</sub>H<sub>5</sub>), 134.91 (*meta*-C<sub>6</sub>H<sub>5</sub>), 133.46 (*para*-C<sub>6</sub>H<sub>4</sub>), 127.41 (C<sub>5</sub>H<sub>4</sub>), 125.38 (C<sub>5</sub>H<sub>4</sub>), 125.35 (C<sub>5</sub>H<sub>4</sub>), 84.79 (CNC(CHMe<sub>2</sub>)HMe<sub>2</sub>O), 84.49

(CNC(CHMe<sub>2</sub>)HMe<sub>2</sub>O), 79.28 (CNC(CHMe<sub>2</sub>)HMe<sub>2</sub>O), 78.92 (CNC(CHMe<sub>2</sub>)HMe<sub>2</sub>O), 44.38 (NMe<sub>2</sub>), 39.32 (NMe<sub>2</sub>), 31.51 (CNC(CHMe<sub>2</sub>)HMe<sub>2</sub>O), 31.41 (CNC(CHMe<sub>2</sub>)HMe<sub>2</sub>O), 30.63 (CNC(CHMe<sub>2</sub>)HMe<sub>2</sub>O), 30.11 (CNC(CHMe<sub>2</sub>)HMe<sub>2</sub>O), 22.23 (CNC(CHMe<sub>2</sub>)HMe<sub>2</sub>O), 22.19 (CNC(CHMe<sub>2</sub>)HMe<sub>2</sub>O), 21.72 (CNC(CHMe<sub>2</sub>)HMe<sub>2</sub>O), 20.53 (CNC(CHMe<sub>2</sub>)HMe<sub>2</sub>O), 20.49 (CNC(CHMe<sub>2</sub>)HMe<sub>2</sub>O), 20.29 (CNC(CHMe<sub>2</sub>)HMe<sub>2</sub>O). <sup>11</sup>B NMR (benzene-*d*<sub>6</sub>, 128 MHz):  $\delta$  -14.8. <sup>15</sup>N NMR (benzene-*d*<sub>6</sub>, 71 MHz):  $\delta$  -153.8, -156.1. IR (KBr, cm<sup>-1</sup>): 3041 w, 2969 s, 2931 m, 2872 m, 2847 m, 2766 m, 1560 s (CN), 1468 m, 1433 w, 1409 w, 1389 w, 1368 m, 1245 m, 1226 m, 1193 m, 1147 s, 1050 m, 1020 m, 988 m, 941 s, 894 w, 811 w, 740 w, 703 m, 678 m. Anal. Calcd for C<sub>31</sub>H<sub>49</sub>BN<sub>4</sub>O<sub>2</sub>Ti: C, 65.50; H, 8.69; N, 9.86. Found: C, 59.91; H, 8.84; N, 9.51. [ $\alpha$ ]<sub>D</sub> = -94.71° (C<sub>6</sub>H<sub>6</sub>). Mp: 89-93 °C.

#### 4R-isopropyl-5,5-dimethyl-2-oxazoline.

**D-Valine methyl ester hydrochloride.** Thionyl chloride (23.8 mL, 0.33 mol, 0.55 equiv) was added drop wise over 2 h to methanol (150 mL) in a three-necked flask cooled in ice-salt bath and connected to an oil bubbler. D-Valine (35.0 g, 0.300 mol) was added in one portion to the solution, and the mixture was heated at 55 °C to dissolve all of the solids. The solution was then heated for 1 h. The solvent and excess reagents were removed by distillation. The resulting white solid was dried *in vacuo* for several hours and then dissolved in minimal amount of methanol (45 mL). The methanol solution was poured into Et<sub>2</sub>O (500 mL), and then recrystallized at -30 °C. The solid was collected, washed with cold Et<sub>2</sub>O, and dried *in vacuo* to give the D-Valine methyl ester hydrochloride as white solid (45.4 g, 90.5 %). <sup>1</sup>H NMR (300 MHz, chloroform-*d*):  $\delta$  8.91 (br, 3 H, HCl·NH<sub>2</sub>CH(CHMe<sub>2</sub>)CO<sub>2</sub>Me), 3.93 (d, <sup>3</sup>J<sub>HH</sub> = 4.5 Hz, 1 H,

HCl·NH<sub>2</sub>CH(CHMe<sub>2</sub>)CO<sub>2</sub>Me), 3.84 (s, 3 H, HCl·NH<sub>2</sub>CH(CHMe<sub>2</sub>)CO<sub>2</sub>Me), 2.47 (m, 1 H, HCl·NH<sub>2</sub>CH(CHMe<sub>2</sub>)CO<sub>2</sub>Me), 1.16 (vt, 6 H, HCl·NH<sub>2</sub>CH(CHMe<sub>2</sub>)CO<sub>2</sub>Me).

**2R-Amino-1,1,3-trimethylbutanol.** A solution of methylmagnesium bromide (180 mL, 3.0 M in Et<sub>2</sub>O, 0.540 mol, 6.0 equiv) was diluted with Et<sub>2</sub>O (500 mL). D-Valine methyl ester hydrochloride (15.0 g, 0.0896 mol) was added in portions over 1 h. The mixture was allowed to stir at room temperature overnight. Saturated aqueous [NH<sub>4</sub>][Cl] was added in a drop wise fashion to quench the reaction. The white solid was separated from the diethyl ether solution, and the organic solution was dried over Na<sub>2</sub>SO<sub>4</sub>. The solid was dissolved in 300 mL saturated [NH<sub>4</sub>][Cl] aqueous solution, and another 300 mL of distilled water was added. This aqueous solution was extracted with Et<sub>2</sub>O (4 × 200 mL). The organic extracts were combined and dried over Na<sub>2</sub>SO<sub>4</sub>. The two organic solutions were filtered, combined, and evaporated under reduced pressure. The crude product was distilled (96 °C, 40 mm Hg) to afford to afford 2S-Amino-1,1,3-trimethylbutanol as a clear, colorless oil (4.96 g, 42.3%). <sup>1</sup>H NMR (300 MHz, chloroform-*d*): δ 2.41 (d, <sup>3</sup>J<sub>HH</sub> = 2.7 Hz, 1 H, NH<sub>2</sub>CH(CHMe<sub>2</sub>)CMe<sub>2</sub>OH), 1.93 (m, 1 H, NH<sub>2</sub>CH(CHMe<sub>2</sub>)CMe<sub>2</sub>OH), 1.20 (s, 3 H, NH<sub>2</sub>CH(CHMe<sub>2</sub>)CMe<sub>2</sub>OH), 1.12 (s, 3 H, NH<sub>2</sub>CH(CHMe<sub>2</sub>)CMe<sub>2</sub>OH), 0.97 (d, <sup>3</sup>J<sub>HH</sub> = 7.2 Hz, 3 H, NH<sub>2</sub>CH(CHMe<sub>2</sub>)CMe<sub>2</sub>OH), 0.88 (d, <sup>3</sup>J<sub>HH</sub> = 6.6 Hz, 3 H, NH<sub>2</sub>CH(CHMe<sub>2</sub>)CMe<sub>2</sub>OH).

**4R-Isopropyl-5,5-dimethyl-2-oxazoline.** DMF-DMA (13.7 mL, 103.3 mmol, 1.2 equiv) was added to degassed 2R-amino-1,1,3-trimethylbutanol (11.1 g, 84.7 mmol). This mixture was allowed to reflux at 75 °C for 7 h. The volatiles were removed under reduced pressure, and the mixture was triturated with hexane (4 × 30 mL). Then *p*-toluenesulfonic acid monohydrate (26.5

mg, 0.14 mmol, 0.0017 equiv) and hexane (40 mL) were added, and an addition funnel with approximately 40 mL of molecular sieves inside was placed on top of the flask, and a condenser was placed on top of the funnel. The solution was heated at 90 °C at reflux for 24 h and the condensed liquids washed over the sieves as the reaction proceeded. The reaction mixture was washed with saturated aqueous NaHCO<sub>3</sub> solution (30 mL) and then with brine (50 mL). The aqueous solutions were combined, back-extracted with Et<sub>2</sub>O (25 mL × 6), and then the organic extracts were combined with the organic solution and dried over Na<sub>2</sub>SO<sub>4</sub> overnight and filtered. Concentration of the filtrate gave a dark red oil which was distilled to provide 8.11 g (57.4 mmol, 68%) of 4*R*-isopropyl-5,5-dimethyl-2-oxazoline as a clear, colorless oil. Bp: 85 °C, 18 mm Hg. <sup>1</sup>H NMR (400 MHz, chloroform-*d*): δ 6.73 (d, <sup>3</sup>J<sub>HH</sub> = 6.4 Hz, 1 H, CHNC(CHMe<sub>2</sub>)HMe<sub>2</sub>O), 3.23 (dd, <sup>3</sup>J<sub>HH</sub> = 8.4 Hz, <sup>4</sup>J<sub>HH</sub> = 2.0 Hz, 1 H, CHNC(CHMe<sub>2</sub>)HMe<sub>2</sub>O), 1.78 (m, 1 H, CHNC(CHMe<sub>2</sub>)HMe<sub>2</sub>O), 1.43 (s, 3 H, CHNC(CHMe<sub>2</sub>)HMe<sub>2</sub>O), 1.28 (s, 3 H, CHNC(CHMe<sub>2</sub>)HMe<sub>2</sub>O), 1.06 (d, <sup>3</sup>J<sub>HH</sub> = 6.4 Hz, 3 H, CHNC(CHMe<sub>2</sub>)HMe<sub>2</sub>O), 0.97 (d, <sup>3</sup>J<sub>HH</sub> = 6.4 Hz, 3 H, CHNC(CHMe<sub>2</sub>)HMe<sub>2</sub>O). <sup>13</sup>C{<sup>1</sup>H} NMR (benzene-*d*<sub>6</sub>, 176 MHz): δ 152.72 (CHNC(CHMe<sub>2</sub>)HMe<sub>2</sub>O), 85.17 (CNC(CHMe<sub>2</sub>)HMe<sub>2</sub>O), 80.07 (CNC(CHMe<sub>2</sub>)HMe<sub>2</sub>O), 29.55 (CNC(CHMe<sub>2</sub>)HMe<sub>2</sub>O), 29.48 (CNC(CHMe<sub>2</sub>)HMe<sub>2</sub>O), 21.52, 21.47, 21.21 (overlapping CNC(CHMe<sub>2</sub>)HMe<sub>2</sub>O and CNC(CHMe<sub>2</sub>)HMe<sub>2</sub>O). <sup>15</sup>N NMR (benzene-*d*<sub>6</sub>, 71 MHz): δ -143.4. IR (KBr, cm<sup>-1</sup>): 3069 w, 2974 s, 2874 m, 1632 s (CN), 1471 m, 1462 m, 1386 m, 1372 s, 1336 w, 1303 w, 1272 w, 1243 w, 1202 w, 1172 m, 1134 m, 1114 s, 1082 s, 1015 m, 984 w, 936 m, 894 w, 856 w 813 w. [α]<sub>D</sub><sup>20</sup> = (+) 37.7 (C<sub>6</sub>H<sub>6</sub>).

**H[PhB(C<sub>5</sub>H<sub>5</sub>)(Ox<sup>4*R*-iPr,Me<sub>2</sub></sup>)<sub>2</sub>]**. A 100 mL Schlenk flask was charged with 4*R*-isopropyl-5,5-dimethyl-2-oxazoline (0.400 g, 2.83 mmol) and tetrahydrofuran (30 mL), and the flask was cooled to  $-78$  °C. Using a syringe, 2.50 M *n*BuLi (1.20 mL, 2.98 mmol) was added, and the solution was stirred for 1 h at  $-78$  °C. Dichlorophenylborane (0.23 mL, 1.40 mmol) was slowly added to the flask, and the solution was stirred for 1 h at  $-78$  °C and then allowed to gradually warm to room temperature. After stirring for 14 h at room temperature, the solvent was removed under reduced pressure to afford a light yellow solid. The solid was extracted with benzene and the solvent was evaporated to yield PhB(Ox<sup>4*R*-iPr,Me<sub>2</sub></sup>)<sub>2</sub> as a light yellow solid (0.50 g, 1.36 mmol). <sup>1</sup>H NMR (tetrahydrofuran-*d*<sub>8</sub>, 400 MHz):  $\delta$  7.45 (d, <sup>3</sup>*J*<sub>HH</sub> = 7.6 Hz, 2 H, *ortho*-C<sub>6</sub>H<sub>5</sub>), 6.98 (m, 2 H, *meta*-C<sub>6</sub>H<sub>5</sub>), 6.87 (m, 1 H, *para*-C<sub>6</sub>H<sub>5</sub>), 3.19 (d, <sup>3</sup>*J*<sub>HH</sub> = 4.8 Hz, 2 H, CNC(CHMe<sub>2</sub>)HMe<sub>2</sub>O), 3.17 (d, <sup>3</sup>*J*<sub>HH</sub> = 4.8 Hz, 2 H, CNCiPrHMe<sub>2</sub>O), 1.73 (m, 2 H, CNC(CHMe<sub>2</sub>)HMe<sub>2</sub>O), 1.22-0.95 (24 H, CNC(CHMe<sub>2</sub>)HMe<sub>2</sub>O). <sup>11</sup>B NMR (tetrahydrofuran-*d*<sub>8</sub>, 128 MHz):  $\delta$  -7.2. IR (KBr, cm<sup>-1</sup>): 3071 w, 3046 w, 2961 s, 2932 s, 2872 m, 1588 s (CN), 1466 m, 1432 m, 1386 m, 1371 s, 1277 w, 1242 s, 1193 m, 1176 m, 1146 s, 1120 m, 1096 m, 1023 s, 995 m, 943 m, 879 m, 849 m, 802 m, 759 w.

A Schlenk flask was charged with PhB(Ox<sup>4*R*-iPr,Me<sub>2</sub></sup>)<sub>2</sub> (0.500 g, 1.36 mmol) and Na[C<sub>5</sub>H<sub>5</sub>] (0.070 g, 0.799 mmol). Addition of THF (40 mL) provided a yellow solution that was stirred overnight. A precipitate formed after 12 h, and the solution was filtered. Solvent was removed under reduced pressure to afford a light yellow solid. This crude product was purified by silica gel column chromatography (hexane:EtOAc:Et<sub>3</sub>N = 9:1:1; *R*<sub>f</sub> = 0.58) to afford an off-white solid of H[PhB(C<sub>5</sub>H<sub>5</sub>)(Ox<sup>4*R*-iPr,Me<sub>2</sub></sup>)<sub>2</sub>] as a mixture of isomers. The product was dissolved in benzene and stirred over P<sub>2</sub>O<sub>5</sub> to remove residual water, affording 0.140 g of H[PhB(C<sub>5</sub>H<sub>5</sub>)(Ox<sup>4*R*-iPr,Me<sub>2</sub></sup>)<sub>2</sub>] (0.321 mmol, 40.5%). <sup>1</sup>H NMR (acetonitrile-*d*<sub>3</sub>, 400 MHz):  $\delta$  7.71-7.00 (m, 5 H, C<sub>6</sub>H<sub>5</sub>), 6.67-

6.19 (m, 3 H, C<sub>5</sub>H<sub>5</sub>), 3.39-3.25 (m, 2 H, CNC<sup>i</sup>PrH<sub>2</sub>CM<sub>2</sub>O), 2.89-2.88 (m, 2 H, C<sub>5</sub>H<sub>5</sub>), 1.84 (m, 2 H, CNC(CHMe<sub>2</sub>)H<sub>2</sub>CM<sub>2</sub>O), 1.47-0.94 (24 H, CNC(CHMe<sub>2</sub>)H<sub>2</sub>CM<sub>2</sub>O). <sup>13</sup>C{<sup>1</sup>H} NMR (acetonitrile-*d*<sub>3</sub>, 176 MHz): δ 133.46 (*ortho*-C<sub>6</sub>H<sub>5</sub>), 129.10 (*meta*-C<sub>6</sub>H<sub>5</sub>), 128.24 (*para*-C<sub>6</sub>H<sub>5</sub>), 141.27 (C<sub>5</sub>H<sub>5</sub>; 10 *sp*<sup>2</sup> resonances for 3 isomers observed), 140.99 (C<sub>5</sub>H<sub>4</sub>), 135.25 (C<sub>5</sub>H<sub>5</sub>), 134.75 (C<sub>5</sub>H<sub>5</sub>), 134.20 (C<sub>5</sub>H<sub>5</sub>), 133.85 (C<sub>5</sub>H<sub>5</sub>), 133.83 (C<sub>5</sub>H<sub>5</sub>), 131.28 (C<sub>5</sub>H<sub>5</sub>), 128.90 (C<sub>5</sub>H<sub>5</sub>), 128.40 (C<sub>5</sub>H<sub>5</sub>), 94.11 (CNC<sup>i</sup>PrH<sub>2</sub>CM<sub>2</sub>O), 66.67 (CNC<sup>i</sup>PrH<sub>2</sub>CM<sub>2</sub>O), 47.49 (C<sub>5</sub>H<sub>5</sub>-*sp*<sup>3</sup>), 43.18 (C<sub>5</sub>H<sub>5</sub>-*sp*<sup>3</sup>), 30.25 (CNC(CHMe<sub>2</sub>)H<sub>2</sub>CM<sub>2</sub>O), 29.26 (CNC(CHMe<sub>2</sub>)H<sub>2</sub>CM<sub>2</sub>O), 29.91, 29.68, 22.09, 22.06, 21.80, 21.77, 21.38, 21.27 (CNC(CHMe<sub>2</sub>)H<sub>2</sub>CM<sub>2</sub>O). <sup>11</sup>B NMR (acetonitrile-*d*<sub>3</sub>, 128 MHz): δ -15.6 sh. IR (KBr, cm<sup>-1</sup>): 3069 m, 3047 m, 2972 s, 2932 s, 2875 s, 1582 s (CN), 1560 s (CN), 1470 m, 1433 m, 1394 s, 1375 s, 1353 m, 1335 w, 1313 w, 1276 m, 1262 m, 1246 m, 1198 m, 1177 m, 1148 m, 1104 m, 1047 m, 1030 s, 1005 m, 990 w, 958 m, 943 m, 863 m, 881 m, 802 s, 765 m, 741 s, 703 s, 680 m. Anal. Calcd for C<sub>27</sub>H<sub>39</sub>BN<sub>2</sub>O<sub>2</sub>: C, 74.65; H, 9.05; N, 6.45. Found: C, 74.77; H, 8.84; N 6.06. [α]<sub>D</sub><sup>20</sup> = (+) 63.2 (C<sub>6</sub>H<sub>6</sub>). Mp: 80-85 °C.

**{PhB(C<sub>5</sub>H<sub>4</sub>)(Ox<sup>4*R*-iPr,Me<sub>2</sub>)<sub>2</sub>})<sub>2</sub>Zr(NMe<sub>2</sub>)<sub>2</sub>}</sup>**. A round bottom Schlenk flask was charged with H[PhB(C<sub>5</sub>H<sub>5</sub>)(Ox<sup>4*R*-iPr,Me<sub>2</sub>)<sub>2</sub>}] (0.120 g, 0.275 mmol) and Zr(NMe<sub>2</sub>)<sub>4</sub> (0.074 g, 0.275 mmol). The solids were dissolved in benzene (15 mL), and the resulting solution was stirred for 7 h. After filtration, the volatile materials were removed in vacuo to give a light yellow gel which was triturated with pentane giving {PhB(C<sub>5</sub>H<sub>4</sub>)(Ox<sup>4*R*-iPr,Me<sub>2</sub>)<sub>2</sub>})<sub>2</sub>Zr(NMe<sub>2</sub>)<sub>2</sub> as a off white solid (0.154 g, 0.252 mmol, 91.4%). <sup>1</sup>H NMR (benzene-*d*<sub>6</sub>, 400 MHz): δ 8.09 (d, <sup>3</sup>J<sub>HH</sub> = 7.2 Hz, 2 H, *ortho*-C<sub>6</sub>H<sub>5</sub>), 7.49 (m, 2 H, *meta*-C<sub>6</sub>H<sub>5</sub>), 7.29 (m, 1 H, *para*-C<sub>6</sub>H<sub>5</sub>), 6.76 (m, 1 H, C<sub>5</sub>H<sub>4</sub>), 6.58 (m, 1 H, C<sub>5</sub>H<sub>4</sub>), 6.25 (m, 1 H, C<sub>5</sub>H<sub>4</sub>), 6.07 (m, 1 H, C<sub>5</sub>H<sub>4</sub>), 3.24 (d, 2 H, <sup>3</sup>J<sub>HH</sub> = 5.6 Hz, CNC<sup>i</sup>PrH<sub>2</sub>CM<sub>2</sub>O), 3.20 (d, 2 H, <sup>3</sup>J<sub>HH</sub> = 5.6 Hz, CNC<sup>i</sup>PrH<sub>2</sub>CM<sub>2</sub>O), 2.80 (s, 6 H, NMe<sub>2</sub>), 2.68 (s, 6 H, NMe<sub>2</sub>), 1.73</sup></sup>

(m, 2 H, CNC(CHMe<sub>2</sub>)HMe<sub>2</sub>O), 1.33 (s, 3 H, CNC<sup>i</sup>PrHMe<sub>2</sub>O), 1.24 (s, 3 H, CNC<sup>i</sup>PrHMe<sub>2</sub>O), 1.18 (s, 3 H, CNC<sup>i</sup>PrHMe<sub>2</sub>O), 1.14 (s, 3 H, CNC<sup>i</sup>PrHMe<sub>2</sub>O), 1.12 (d, <sup>3</sup>J<sub>HH</sub> = 6.8 Hz, 3 H, CNC(CHMe<sub>2</sub>)HMe<sub>2</sub>O), 1.09 (d, <sup>3</sup>J<sub>HH</sub> = 6.8 Hz, 3 H, CNC(CHMe<sub>2</sub>)HMe<sub>2</sub>O), 0.97 (d, <sup>3</sup>J<sub>HH</sub> = 6.8 Hz, 3 H, CNC(CHMe<sub>2</sub>)HMe<sub>2</sub>O), 0.89 (d, <sup>3</sup>J<sub>HH</sub> = 6.8 Hz, 3 H, CNC(CHMe<sub>2</sub>)HMe<sub>2</sub>O). <sup>13</sup>C{<sup>1</sup>H} NMR (benzene-*d*<sub>6</sub>, 176 MHz): δ 196.92 (br, CNC<sup>i</sup>PrHCH<sub>2</sub>O), 194.35 (br, CNC<sup>i</sup>PrHCH<sub>2</sub>O), 151.53 (br, *ipso*-C<sub>6</sub>H<sub>5</sub>), 135.13 (*ortho*-C<sub>6</sub>H<sub>5</sub>), 127.51 (*meta*-C<sub>6</sub>H<sub>5</sub>), 125.26 (*para*-C<sub>6</sub>H<sub>5</sub>), 123.49 (C<sub>5</sub>H<sub>4</sub>), 122.83 (C<sub>5</sub>H<sub>4</sub>), 113.93 (C<sub>5</sub>H<sub>4</sub>), 113.64 (C<sub>5</sub>H<sub>4</sub>), 85.08 (CNC<sup>i</sup>PrHMe<sub>2</sub>O), 84.81 (CNC<sup>i</sup>PrHMe<sub>2</sub>O), 79.11 (CNC<sup>i</sup>PrHMe<sub>2</sub>O), 78.87 (CNC<sup>i</sup>PrHMe<sub>2</sub>O), 44.51 (NMe<sub>2</sub>), 42.95 (NMe<sub>2</sub>), 30.44 (CNC(CHMe<sub>2</sub>)HMe<sub>2</sub>O), 30.27 (CNC(CHMe<sub>2</sub>)HMe<sub>2</sub>O), 30.24 (CNC<sup>i</sup>PrHMe<sub>2</sub>O), 30.02 (CNC<sup>i</sup>PrHMe<sub>2</sub>O), 21.96 (CNC<sup>i</sup>PrHMe<sub>2</sub>O), 21.83 (CNC<sup>i</sup>PrHMe<sub>2</sub>O), 20.69 (CNC(CHMe<sub>2</sub>)HMe<sub>2</sub>O), 20.46 (CNC(CHMe<sub>2</sub>)HMe<sub>2</sub>O), 20.37 (CNC(CHMe<sub>2</sub>)HMe<sub>2</sub>O), 20.17 (CNC(CHMe<sub>2</sub>)HMe<sub>2</sub>O). <sup>11</sup>B NMR (benzene-*d*<sub>6</sub>, 128 MHz): δ -14.5. <sup>15</sup>N NMR (benzene-*d*<sub>6</sub>, 71 MHz): δ -152.3, -155.1 (CNC<sup>i</sup>PrHMe<sub>2</sub>O). IR (KBr, cm<sup>-1</sup>): 3071 w, 3045 w, 2966 s, 2931 s, 2869 s, 2768 s, 1559 s (CN), 1471 m, 1433 m, 1393 m, 1374 m, 1353 m, 1276 m, 1261 m, 1244 m, 1177 m, 1147 s, 1105 m, 1047 s, 1030 m, 1021 m, 990 w, 940 s, 881 m, 864 w, 804 s, 770 w, 741 s, 703 s, 680 w. Anal. Calcd for C<sub>31</sub>H<sub>49</sub>BN<sub>4</sub>O<sub>2</sub>Zr: C, 60.86; H, 8.07; N, 9.16. Found: C, 60.45; H, 7.97; N, 8.86. [α]<sub>D</sub><sup>20</sup> = 122.6 (C<sub>6</sub>H<sub>6</sub>). Mp: 66-71 °C.

{PhB(C<sub>5</sub>H<sub>4</sub>)(Ox<sup>4*S*-*t*Bu</sup>)<sub>2</sub>}Zr(NMe<sub>2</sub>)<sub>2</sub>. H[PhB(C<sub>5</sub>H<sub>5</sub>)(Ox<sup>4*S*-*t*Bu</sup>)<sub>2</sub>] (0.100 g, 0.246 mmol) and Zr(NMe<sub>2</sub>)<sub>4</sub> (0.066 g, 0.246 mmol) were dissolved in benzene (5 mL), and the solution was stirred for 20 min. Quick evaporation of the volatile materials yielded a light yellow powder of {PhB(C<sub>5</sub>H<sub>4</sub>)(Ox<sup>4*S*-*t*Bu</sup>)<sub>2</sub>}Zr(NMe<sub>2</sub>)<sub>2</sub> {**S-3**}Zr(NMe<sub>2</sub>)<sub>2</sub> (0.115 g, 0.197 mmol, 80.1%). This material



was stored at  $-30\text{ }^{\circ}\text{C}$ .  $^1\text{H}$  NMR (benzene- $d_6$ , 400 MHz):  $\delta$  8.10 (d,  $^3J_{\text{HH}} = 7.2\text{ Hz}$ , 2 H, *ortho*- $\text{C}_6\text{H}_5$ ), 7.49 (t,  $^3J_{\text{HH}} = 7.6\text{ Hz}$ , 2 H, *meta*- $\text{C}_6\text{H}_5$ ), 7.30 (t,  $^3J_{\text{HH}} = 7.2\text{ Hz}$ , 1 H, *para*- $\text{C}_6\text{H}_5$ ), 6.74 (m, 1 H,  $\text{C}_5\text{H}_4$ ), 6.50 (m, 1 H,  $\text{C}_5\text{H}_4$ ), 6.28 (m, 1 H,  $\text{C}_5\text{H}_4$ ), 6.09 (m, 1 H,  $\text{C}_5\text{H}_4$ ), 3.83 (m, 2 H,  $\text{CNCt-BuHCH}_2\text{O}$ ), 3.64 (m, 2 H,  $\text{CNCt-BuHCH}_2\text{O}$ ), 3.49 (m, 2 H,  $\text{CNCt-BuHCH}_2\text{O}$ ), 2.75 (s, 6 H,  $\text{NMe}_2$ ), 2.65 (s, 6 H,  $\text{NMe}_2$ ), 0.85 (s, 9 H,  $\text{CNCt-BuHCH}_2\text{O}$ ), 0.84 (s, 9 H,  $\text{CNCt-BuHCH}_2\text{O}$ ).  $^{13}\text{C}\{^1\text{H}\}$  NMR (benzene- $d_6$ , 100 MHz):  $\delta$  196.84 (br,  $\text{CNCt-BuHCH}_2\text{O}$ ), 153.22 (*ipso*- $\text{C}_6\text{H}_5$ ), 135.22 (*ortho*- $\text{C}_6\text{H}_5$ ), 127.54 (*meta*- $\text{C}_6\text{H}_5$ ), 125.42 (*para*- $\text{C}_6\text{H}_5$ ), 122.87 ( $\text{C}_5\text{H}_4$ ), 122.75 ( $\text{C}_5\text{H}_4$ ), 114.37 ( $\text{C}_5\text{H}_4$ ), 114.17 ( $\text{C}_5\text{H}_4$ ), 76.16 ( $\text{CNCt-BuHCH}_2\text{O}$ ), 74.74 ( $\text{CNCt-BuHCH}_2\text{O}$ ), 69.25 ( $\text{CNCt-BuHCH}_2\text{O}$ ), 68.16 ( $\text{CNCt-BuHCH}_2\text{O}$ ), 44.55 ( $\text{NMe}_2$ ), 43.36 ( $\text{NMe}_2$ ), 34.15 ( $\text{CNC(CMe}_3\text{)HCH}_2\text{O}$ ), 28.90 ( $\text{CNC(CMe}_3\text{)HCH}_2\text{O}$ ), 26.59 ( $\text{CNC(CMe}_3\text{)HCH}_2\text{O}$ ), 26.40 ( $\text{CNC(CMe}_3\text{)HCH}_2\text{O}$ ).  $^{11}\text{B}$  NMR (benzene- $d_6$ , 128 MHz):  $\delta$   $-14.4$ .  $^{15}\text{N}$  NMR (benzene- $d_6$ , 41 MHz):  $\delta$   $-145.4$ ,  $-148.1$ . (oxazoline). IR (KBr,  $\text{cm}^{-1}$ ): 3067 w, 3042 w, 2954 s, 2904 s, 2866 s, 2820 m, 2770 m, 1608 m (CN), 1506 m (CN), 1479 s, 1465 m, 1430 w, 1391 m, 1362 m, 1243 m, 1191 s, 1135 s, 1053 s, 967 s, 941 s, 848 w, 809 m, 727 m, 703 m. Anal. Calcd for  $\text{C}_{29}\text{H}_{45}\text{BN}_4\text{O}_2\text{Zr}$ : C, 59.67; H, 7.77; N, 9.60. Found: C, 59.19; H, 7.42; N, 9.13. Mp:  $128\text{-}133\text{ }^{\circ}\text{C}$ .  $[\alpha]_{\text{D}}^{20} = -103.93^{\circ}$  ( $\text{C}_6\text{H}_6$ ).

**$\{\text{PhB}(\text{C}_5\text{H}_4)(\text{Ox}^{\text{Me}_2})_2\}\text{Zr}(\text{NMe}_2)(\text{NHNMe}_2)$ .** In a glove box, a vial was charged with  $\text{PhB}(\text{C}_5\text{H}_4)(\text{Ox}^{\text{Me}_2})_2\}\text{Zr}(\text{NMe}_2)_2$  (0.300 g, 0.569 mmol). The solid was dissolved in 10 mL benzene. To the solution, 43  $\mu\text{L}$  *N,N'*-dimethylhydrazine (0.569 mmol) was added using a micro-lit syringe, and the resulting solution mixture was stirred for 15 min at room temperature. The mixture was filtered and extracted with 5 mL benzene. All the volatiles were removed under vacuo to afford  $\{\text{PhB}(\text{C}_5\text{H}_4)(\text{Ox}^{\text{Me}_2})_2\}\text{Zr}(\text{NMe}_2)(\text{NHNMe}_2)$  as a off-white solid (0.290 g, 0.534

mmol, 94%).  $^1\text{H}$  NMR (benzene- $d_6$ , 400 MHz):  $\delta$  8.20 (d,  $^3J_{\text{HH}} = 6.4$  Hz, 2 H, *ortho*-C<sub>6</sub>H<sub>5</sub>), 7.49 (t,  $^3J_{\text{HH}} = 7.2$  Hz, 2 H, *meta*-C<sub>6</sub>H<sub>5</sub>), 7.29 (t,  $^3J_{\text{HH}} = 6.4$  Hz, 1 H, *para*-C<sub>6</sub>H<sub>5</sub>), 6.59 (m, 2 H, C<sub>5</sub>H<sub>4</sub>), 6.42 (m, 2 H, C<sub>5</sub>H<sub>4</sub>), 6.25 (m, 2 H, C<sub>5</sub>H<sub>4</sub>), 6.09 (m, 2 H, C<sub>5</sub>H<sub>4</sub>), 4.22 (NHNMe<sub>2</sub>), 3.68-3.59 (m, 4 H,  $\overline{\text{CNCMe}_2\text{CH}_2\text{O}}$ ), 2.82 (s, 6 H, NMe<sub>2</sub>), 2.08 (s, 3H, NHNMe<sub>2</sub>), 2.02 (s, 3 H, NHNMe<sub>2</sub>), 1.16 (s, 3 H,  $\overline{\text{CNCMe}_2\text{CH}_2\text{O}}$ ), 1.11 (s, 3 H,  $\overline{\text{CNCMe}_2\text{CH}_2\text{O}}$ ), 1.10 (s, 3 H,  $\overline{\text{CNCMe}_2\text{CH}_2\text{O}}$ ), 1.05 (s, 3 H,  $\overline{\text{CNCMe}_2\text{CH}_2\text{O}}$ ).  $^{13}\text{C}\{^1\text{H}\}$  NMR (benzene- $d_6$ , 100 MHz):  $\delta$  198.42 ( $\overline{\text{CNCMe}_2\text{CH}_2\text{O}}$ ), 152.06 (br, *ipso*-C<sub>6</sub>H<sub>5</sub>), 143.67 (*ipso*-C<sub>5</sub>H<sub>4</sub>), 135.22 (*ortho*-C<sub>6</sub>H<sub>5</sub>), 127.52 (*meta*-C<sub>6</sub>H<sub>5</sub>), 125.22 (*para*-C<sub>6</sub>H<sub>5</sub>), 119.89 (C<sub>5</sub>H<sub>4</sub>), 118.97 (C<sub>5</sub>H<sub>4</sub>), 115.67 (C<sub>5</sub>H<sub>4</sub>), 111.88 (C<sub>5</sub>H<sub>4</sub>), 78.99 ( $\overline{\text{CNCMe}_2\text{CH}_2\text{O}}$ ), 78.30 ( $\overline{\text{CNCMe}_2\text{CH}_2\text{O}}$ ), 67.59 ( $\overline{\text{CNCMe}_2\text{CH}_2\text{O}}$ ), 67.24 ( $\overline{\text{CNCMe}_2\text{CH}_2\text{O}}$ ), 54.26 (NHNMe<sub>2</sub>), 53.71 (NHNMe<sub>2</sub>), 49.20 (NMe<sub>2</sub>), 29.10 ( $\overline{\text{CNCMe}_2\text{CH}_2\text{O}}$ ), 29.06 ( $\overline{\text{CNCMe}_2\text{CH}_2\text{O}}$ ), 29.04 ( $\overline{\text{CNCMe}_2\text{CH}_2\text{O}}$ ), 27.96 ( $\overline{\text{CNCMe}_2\text{CH}_2\text{O}}$ ).  $^{11}\text{B}$  NMR (benzene- $d_6$ , 128 MHz):  $\delta$  -15.7.  $^{15}\text{N}$  NMR (benzene- $d_6$ , 71 MHz):  $\delta$  -133.4 (NHNMe<sub>2</sub>), -134.3 ( $\overline{\text{CNCMe}_2\text{CH}_2\text{O}}$ ), -139.8 ( $\overline{\text{CNCMe}_2\text{CH}_2\text{O}}$ ), -179.9 (NHNMe<sub>2</sub>). IR (KBr, cm<sup>-1</sup>): 3308 m, 3088 w, 3066 w, 3041 w, 2994 m, 2961 s, 2926 s, 2892 s, 2863 s, 2817 m, 2769 m, 1602 m (CN), 1514 s (CN), 1489 w, 1461 s, 1430 w, 1367 w, 1358 w, 1281 s, 1265 w, 1248 m, 1196 s, 1159 s, 1122 m, 1050 s, 1034 m, 994 s, 966 s, 946 s, 909 w, 871 w, 847 w, 802 s, 732 s, 703 s, 680 m, 661 w. Anal. Calcd for C<sub>25</sub>H<sub>38</sub>BO<sub>2</sub>N<sub>5</sub>Zr: C, 55.33; H, 7.06; N, 12.91. Found: C, 55.30; H, 6.85; N, 12.12. Mp: 106-111 °C.

**K<sub>2</sub>[PhB(C<sub>5</sub>H<sub>4</sub>)(Ox<sup>4*S*-iPr,Me<sub>2</sub>)<sub>2</sub>]</sup>**. A round bottom Schlenk flask was charged with H[PhB(C<sub>5</sub>H<sub>4</sub>)(Ox<sup>4*S*-iPr,Me<sub>2</sub>)<sub>2</sub>]] (0.122 g, 0.280 mmol) and PhCH<sub>2</sub>K (0.072 g, 0.553 mmol). The solids were dissolved in THF (6 mL), and the resulting yellow solution was stirred for 3 h. The</sup>

volatile materials were removed and dry *in vacuo* to give  $K_2[PhB(C_5H_4)(Ox^{4S-iPr,Me_2})_2]$  as a yellow solid (0.140 g, 0.274 mmol, 97.9%).  $^1H$  NMR (tetrahydrofuran- $d_8$ , 400 MHz):  $\delta$  7.63 (d,  $^3J_{HH} = 7.2$  Hz, 2 H, *ortho*- $C_6H_5$ ), 6.95 (t,  $^3J_{HH} = 7.2$  Hz, 2 H, *meta*- $C_6H_5$ ), 6.78 (t,  $^3J_{HH} = 7.2$  Hz, 1 H, *para*- $C_6H_5$ ), 5.60 (m, 2 H,  $C_5H_4$ ), 5.44 (m, 2 H,  $C_5H_4$ ), 3.02 (m, 2 H,  $^3J_{HH} = 5.6$  Hz,  $CNC^iPrHMe_2O$ ), 1.73 (m, 2 H,  $CNC(CHMe_2)HMe_2O$ ), 1.32 (s, 3 H,  $CNC^iPrHMe_2O$ ), 1.22 (s, 3 H,  $CNC^iPrHMe_2O$ ), 1.21 (s, 3 H,  $CNC^iPrHMe_2O$ ), 1.15 (s, 3 H,  $CNC^iPrHMe_2O$ ), 1.01 (d,  $^3J_{HH} = 6.4$  Hz, 6 H,  $CNC(CHMe_2)HMe_2O$ ), 0.93 (d,  $^3J_{HH} = 6.4$  Hz, 6 H,  $CNC(CHMe_2)HMe_2O$ ).  $^{13}C\{^1H\}$  NMR (tetrahydrofuran- $d_8$ , 100 MHz):  $\delta$  189.90 ( $CNC(CHMe_2)HCH_2O$ ), 161.24 (*ipso*- $C_6H_5$ ), 134.43 (*ortho*- $C_6H_5$ ), 126.85 (*meta*- $C_6H_5$ ), 122.81 (*para*- $C_6H_5$ ), 112.10 ( $C_5H_4$ ), 104.48 ( $C_5H_4$ ), 82.11 ( $CNC(CHMe_2)HMe_2O$ ), 81.79 ( $CNC(CHMe_2)HMe_2O$ ), 81.11 ( $CNC(CHMe_2)HMe_2O$ ), 80.93 ( $CNC(CHMe_2)HMe_2O$ ), 31.04 ( $CNC(CHMe_2)HMe_2O$ ), 30.61 ( $CNC(CHMe_2)HMe_2O$ ) overlapped, 22.37 ( $CNC(CHMe_2)HMe_2O$ ), overlapped 21.96 ( $CNC(CHMe_2)HMe_2O$ ), 21.90 ( $CNC(CHMe_2)HMe_2O$ ).  $^{11}B$  NMR (tetrahydrofuran- $d_8$ , 128 MHz):  $\delta$  -15.2.  $^{15}N$  NMR (tetrahydrofuran- $d_8$ , 71 MHz):  $\delta$  -153.4 (one  $^{15}N$  cross peak was observed). IR (KBr,  $cm^{-1}$ ): 3044 w, 2967 s, 2931 s, 2872 m, 1583 s, 1467 m, 1430 w, 1384 m, 1367 m, 1331 w, 1245 m, 1199 m, 1176 m, 1134 s, 1094 s, 1042 m, 1019 m, 984 w, 941 m, 884 s, 856 m, 790 w, 737 m, 707 s. Anal. Calcd for  $C_{27}H_{37}BK_2N_2O_2$ : C, 63.51; H, 7.30; N, 5.49. Found: C, 63.11; H, 7.61; N, 5.28. Mp: 138-143 °C, dec.

$\{PhB(C_5H_4)(Ox^{4S-iPr,Me_2})_2\}ZrCl(NMe_2)$ . In a glove box, a vial was charged with  $K_2[PhB(C_5H_4)(Ox^{4S-iPr,Me_2})_2]$  (0.150 g, 0.294 mmol) and  $ZrCl_4$  (0.070 g, 0.300 mmol). The solids were dissolved in THF (10 mL), and the resulting solution was stirred for 1 h at room

temperature to afford  $\{\text{PhB}(\text{C}_5\text{H}_4)(\text{Ox}^{4S-i\text{Pr,Me}_2})_2\}\text{ZrCl}_2$ . Unfortunately, the complex could not be isolated. The complex decomposes upon removal of solvent THF.  $^1\text{H}$  NMR (tetrahydrofuran- $d_8$ , 400 MHz):  $\delta$  7.46 (d,  $^3J_{\text{HH}} = 6.4$  Hz, 2 H, *ortho*- $\text{C}_6\text{H}_5$ ), 7.03 (m, 2 H, *meta*- $\text{C}_6\text{H}_5$ ), 6.95 (m, 1 H, *para*- $\text{C}_6\text{H}_5$ ), 6.88 (m, 2 H,  $\text{C}_5\text{H}_4$ ), 6.66 (m, 2 H,  $\text{C}_5\text{H}_4$ ), 6.57 (m, 2 H,  $\text{C}_5\text{H}_4$ ), 6.23 (m, 2 H,  $\text{C}_5\text{H}_4$ ), 3.63 (m, 2 H,  $\text{CNC}^i\text{PrH}(\text{CMe}_2\text{O})$ ), 1.63 (m, 2 H,  $\text{CNC}(\text{CHMe}_2)\text{H}(\text{CMe}_2\text{O})$ ), 1.45 (s, 3 H,  $\text{CNC}^i\text{PrH}(\text{CMe}_2\text{O})$ ), 1.39 (s, 3 H,  $\text{CNC}^i\text{PrH}(\text{CMe}_2\text{O})$ ), 1.35 (s, 3 H,  $\text{CNC}^i\text{PrH}(\text{CMe}_2\text{O})$ ), 1.08 (s, 3 H,  $\text{CNC}^i\text{PrH}(\text{CMe}_2\text{O})$ ), 1.06 (d,  $^3J_{\text{HH}} = 7.2$  Hz, 3 H,  $\text{CNC}(\text{CHMe}_2)\text{H}(\text{CMe}_2\text{O})$ ), 0.98 (d,  $^3J_{\text{HH}} = 7.2$  Hz, 3 H,  $\text{CNC}(\text{CHMe}_2)\text{H}(\text{CMe}_2\text{O})$ ), 0.94 (d,  $^3J_{\text{HH}} = 7.2$  Hz, 3 H,  $\text{CNC}(\text{CHMe}_2)\text{H}(\text{CMe}_2\text{O})$ ), 0.85 (d,  $^3J_{\text{HH}} = 7.2$  Hz, 3 H,  $\text{CNC}(\text{CHMe}_2)\text{H}(\text{CMe}_2\text{O})$ ).  $^{11}\text{B}$  NMR (tetrahydrofuran- $d_8$ , 128 MHz):  $\delta$  -15.7.

$\{\text{PhB}(\text{C}_5\text{H}_4)(\text{Ox}^{4S-i\text{Pr,Me}_2})_2\}\text{ZrCl}(\text{NMe}_2)$  was synthesized using THF solution of  $\{\text{PhB}(\text{C}_5\text{H}_4)(\text{Ox}^{4S-i\text{Pr,Me}_2})_2\}\text{ZrCl}_2$  prepared in situ.  $\text{LiNMe}_2$  (0.015 g, 0.294 mmol) was added to the THF solution of  $\{\text{PhB}(\text{C}_5\text{H}_4)(\text{Ox}^{4S-i\text{Pr,Me}_2})_2\}\text{ZrCl}_2$  and stir for 1 h at room temperature. All the volatile materials were removed in vacuo, and the residue was extracted with benzene. Removal of solvent in vacuo provided  $\{\text{PhB}(\text{C}_5\text{H}_4)(\text{Ox}^{4S-i\text{Pr,Me}_2})_2\}\text{ZrCl}(\text{NMe}_2)$  as a light yellow solid (0.141 g, 0.233 mmol, 79.3%), which was a mixture of two diastereomers in 4:1 ratio.  $^1\text{H}$  NMR (tetrahydrofuran- $d_8$ , 400 MHz):  $\delta$  7.38 (d,  $^3J_{\text{HH}} = 6.8$  Hz, 2 H, *ortho*- $\text{C}_6\text{H}_5$ ), 7.06 (m, 2 H, *meta*- $\text{C}_6\text{H}_5$ ), 6.96 (t,  $^3J_{\text{HH}} = 6.8$  Hz, 1 H, *para*- $\text{C}_6\text{H}_5$ ), 6.19 (m, 1 H,  $\text{C}_5\text{H}_4$ ), 6.15 (m, 1 H,  $\text{C}_5\text{H}_4$ ), 6.07 (m, 1 H,  $\text{C}_5\text{H}_4$ ), 5.84 (m, 1 H,  $\text{C}_5\text{H}_4$ ), 3.86 (m, 2 H,  $\text{CNC}^i\text{PrH}(\text{CMe}_2\text{O})$ ), 2.93 (s,  $\text{NMe}_2$ ), 1.72 (m, 2 H,  $\text{CNC}(\text{CHMe}_2)\text{H}(\text{CMe}_2\text{O})$ ), 1.32 (s, 3 H,  $\text{CNC}^i\text{PrH}(\text{CMe}_2\text{O})$ ), 1.59-1.19 (24 H,  $\text{CNC}(\text{CHMe}_2)\text{H}(\text{CMe}_2\text{O})$ ).  $^{13}\text{C}\{^1\text{H}\}$  NMR (tetrahydrofuran- $d_8$ , 100 MHz):  $\delta$  189.59 ( $\text{CNC}(\text{CHMe}_2)\text{H}(\text{CMe}_2\text{O})$ ), 161.55 (*ipso*- $\text{C}_6\text{H}_5$ ), 134.12 (*ortho*- $\text{C}_6\text{H}_5$ ), 130.42 (*meta*- $\text{C}_6\text{H}_5$ ), 128.13 (*para*- $\text{C}_6\text{H}_5$ ), 126.53 ( $\text{C}_5\text{H}_4$ ), 122.49 ( $\text{C}_5\text{H}_4$ ), 111.78 ( $\text{C}_5\text{H}_4$ ), 104.16 ( $\text{C}_5\text{H}_4$ ), 81.79 ( $\text{CNC}(\text{CHMe}_2)\text{H}(\text{CMe}_2\text{O})$ ), 81.48 ( $\text{CNC}(\text{CHMe}_2)\text{H}(\text{CMe}_2\text{O})$ ), 80.79 ( $\text{CNC}(\text{CHMe}_2)\text{H}(\text{CMe}_2\text{O})$ ),

80.61 (CNC(CHMe<sub>2</sub>)HMe<sub>2</sub>O), 30.72 (CNC(CHMe<sub>2</sub>)HMe<sub>2</sub>O), 30.31  
 (CNC(CHMe<sub>2</sub>)HMe<sub>2</sub>O, overlapped), 30.29 (CNC(CHMe<sub>2</sub>)HMe<sub>2</sub>O), 30.24  
 (CNC(CHMe<sub>2</sub>)HMe<sub>2</sub>O), 22.04 (CNC(CHMe<sub>2</sub>)HMe<sub>2</sub>O, overlapped), 21.64  
 (CNC(CHMe<sub>2</sub>)HMe<sub>2</sub>O), 21.58 (CNC(CHMe<sub>2</sub>)HMe<sub>2</sub>O). <sup>11</sup>B NMR (tetrahydrofuran-*d*<sub>8</sub>, 128  
 MHz):  $\delta$  -16.4. <sup>15</sup>N NMR (tetrahydrofuran-*d*<sub>8</sub>, 71 MHz):  $\delta$  -153.4, -154.9. IR (KBr, cm<sup>-1</sup>):  
 3059 w, 2958 s, 2924 m, 2878 m, 1578 s (CN), 1567 s (CN), 1484 w, 1459 m, 1428 w, 1380 w,  
 1361 m, 1342 w, 1290 m, 1250 m, 1190 m, 1120 s, 1056 w, 1037 m, 1017 w, 966 s, 936 w,  
 876m, 824 s, 792 w, 777 m, 747 s, 731 s, 704 m, 661 w. Anal. Calcd for C<sub>29</sub>H<sub>43</sub>BClN<sub>3</sub>O<sub>2</sub>Zr: C,  
 57.75; H, 7.19; N, 6.97. Found: C, 57.56; H, 6.49; N, 6.81. Mp: 123-127 °C, dec.  $[\alpha]_D^{20} = -$   
 111.4°.

**H[Ph<sub>2</sub>B(C<sub>5</sub>H<sub>4</sub>)(Ox<sup>4*S*-iPr,Me<sub>2</sub></sup>)]**. A 100 mL Schlenk flask was charged with 4*S*-isopropyl-5,5-  
 dimethyl-2-oxazoline (0.500 g, 3.54 mmol) and THF (40 mL), and the flask was cooled to -78  
 °C. Using a syringe, 2.50 M *n*BuLi (1.20 mL, 2.98 mmol) was added, and the solution was  
 stirred for 1 h at -78 °C. A THF (20 mL) solution of Ph<sub>2</sub>BCl (0.708 g, 3.54 mmol) in another  
 Schlenk flask was slowly added to the flask containing lithium oxazolidate, and the solution was  
 stirred for 1 h at -78 °C and then allowed to slowly warm to room temperature. After stirring for  
 12 h at room temperature, the solvent was removed under reduced pressure to afford crude  
 Ph<sub>2</sub>B(Ox<sup>4*S*-iPr,Me<sub>2</sub></sup>) as a light yellow solid.

The Ph<sub>2</sub>B(Ox<sup>4*S*-iPr,Me<sub>2</sub></sup>) dissolved in 40 mL THF and Na[C<sub>5</sub>H<sub>5</sub>] (0.312 g, 3.54 mmol) was  
 added. The resultant solution was stirred overnight at room temperature. The solution was  
 filtered. Solvent was removed under reduced pressure to afford a yellow solid. This crude  
 product was purified by silica gel column chromatography to afford an light yellow solid of

H[Ph<sub>2</sub>B(C<sub>5</sub>H<sub>5</sub>)(Ox<sup>4*S*-iPr,Me<sub>2</sub>)</sup>)] as a mixture of isomers. The product was dissolved in benzene and stirred over P<sub>2</sub>O<sub>5</sub> to remove residual water, affording 0.120 g of H[Ph<sub>2</sub>B(C<sub>5</sub>H<sub>5</sub>)(Ox<sup>4*S*-iPr,Me<sub>2</sub>)</sup>)] (0.323 mmol, 10.7%). <sup>1</sup>H NMR (acetonitrile-*d*<sub>3</sub>, 400 MHz): δ 7.70-7.12 (m, 10 H, C<sub>6</sub>H<sub>5</sub>), 6.48-6.32 (m, 3 H, C<sub>5</sub>H<sub>5</sub>), 3.83 (d, <sup>3</sup>J<sub>HH</sub> = 6.4 Hz, 1 H, CNCiPrHCM<sub>2</sub>O), 2.91 (m, 2 H, C<sub>5</sub>H<sub>5</sub>), 1.84 (m, 1 H, CNC(CHMe<sub>2</sub>)HCM<sub>2</sub>O), 1.47-0.98 (12 H, CNC(CHMe<sub>2</sub>)HCM<sub>2</sub>O). <sup>13</sup>C{<sup>1</sup>H} NMR (acetonitrile-*d*<sub>3</sub>, 150 MHz): δ 135.53 (*ortho*-C<sub>6</sub>H<sub>5</sub>), 129.69 (*meta*-C<sub>6</sub>H<sub>5</sub>), 128.03 (*para*-C<sub>6</sub>H<sub>5</sub>), 142.17 (C<sub>5</sub>H<sub>5</sub>; 10 *sp*<sup>2</sup> resonances for 3 isomers observed), 141.95 (C<sub>5</sub>H<sub>5</sub>), 136.26 (C<sub>5</sub>H<sub>5</sub>), 134.92 (C<sub>5</sub>H<sub>5</sub>), 134.25 (C<sub>5</sub>H<sub>5</sub>), 133.85 (C<sub>5</sub>H<sub>5</sub>), 133.23 (C<sub>5</sub>H<sub>5</sub>), 131.87 (C<sub>5</sub>H<sub>5</sub>), 128.23 (C<sub>5</sub>H<sub>5</sub>), 128.57 (C<sub>5</sub>H<sub>5</sub>), 95.09 (CNCiPrHCM<sub>2</sub>O), 67.07 (CNCiPrHCM<sub>2</sub>O), 48.34 (C<sub>5</sub>H<sub>5</sub>-*sp*<sup>3</sup>), 43.22 (C<sub>5</sub>H<sub>5</sub>-*sp*<sup>3</sup>), 31.25 (CNC(CHMe<sub>2</sub>)HCM<sub>2</sub>O), 29.77, 22.19, 21.61, 21.29 (CNC(CHMe<sub>2</sub>)HCM<sub>2</sub>O). <sup>11</sup>B NMR (acetonitrile-*d*<sub>3</sub>, 128 MHz): δ -10.0, -11.5, -12.4. IR (KBr, cm<sup>-1</sup>): 3087 w, 3069 w, 3035 w, 2982 s, 2870 m, 1594 s (CN), 1474 w, 1467 m, 1424 w, 1396 s, 1370 m, 1352 m, 1347 w, 1311 m, 1302 w, 1244w, 1227 w, 1215 m, 1167 w, 1145 m, 1096 w, 1027 m, 999 w, 956 m, 942 m, 853 w, 829 w. Anal. Calcd for C<sub>25</sub>H<sub>30</sub>BNO: C, 80.86; H, 8.14; N, 3.77. Found: C, 80.25; H, 7.73; N, 3.51. Mp: 67-72 °C. [α]<sub>D</sub><sup>20</sup> = -55.2° (C<sub>6</sub>H<sub>6</sub>).

**{Ph<sub>2</sub>B(C<sub>5</sub>H<sub>4</sub>)(Ox<sup>4*S*-iPr,Me<sub>2</sub>)</sup> }Zr(NMe<sub>2</sub>)<sub>2</sub>.** In a glove box, a vial was charged with H[Ph<sub>2</sub>B(C<sub>5</sub>H<sub>5</sub>)(Ox<sup>4*S*-iPr,Me<sub>2</sub>)</sup>)] (0.040 g, 0.108 mmol) and Zr(NMe<sub>2</sub>)<sub>4</sub> (0.029 g, 0.108 mmol). The solids were dissolved in benzene (4 mL), and the resulting solution was stirred for 20 min. The volatile materials were evaporated to afford {Ph<sub>2</sub>B(C<sub>5</sub>H<sub>4</sub>)(Ox<sup>4*S*-iPr,Me<sub>2</sub>)</sup> }Zr(NMe<sub>2</sub>)<sub>2</sub> as an off-white solid (0.054 g, 0.098 mmol, 91.5%). <sup>1</sup>H NMR (benzene-*d*<sub>6</sub>, 400 MHz): δ 8.16 (d, <sup>3</sup>J<sub>HH</sub> = 6.8 Hz, 2 H, *ortho*-C<sub>6</sub>H<sub>5</sub>), 8.06 (d, <sup>3</sup>J<sub>HH</sub> = 7.2 Hz, 2 H, *ortho*-C<sub>6</sub>H<sub>5</sub>), 7.46 (t, <sup>3</sup>J<sub>HH</sub> = 7.6 Hz, 2 H, *meta*-C<sub>6</sub>H<sub>5</sub>), 7.34 (t, <sup>3</sup>J<sub>HH</sub> = 7.6 Hz, 2 H, *meta*-C<sub>6</sub>H<sub>5</sub>), 7.27 (m, 1 H, *para*-C<sub>6</sub>H<sub>5</sub>), 7.17 (m, 1 H, *para*-

C<sub>6</sub>H<sub>5</sub>), 6.64 (m, 1 H, C<sub>5</sub>H<sub>4</sub>), 6.55 (m, 1 H, C<sub>5</sub>H<sub>4</sub>), 6.23 (m, 1 H, C<sub>5</sub>H<sub>4</sub>), 6.01 (m, 1 H, C<sub>5</sub>H<sub>4</sub>), 3.24 (d, 1 H, <sup>3</sup>J<sub>HH</sub> = 5.6 Hz, CNCiPrH<sub>C</sub>Me<sub>2</sub>O), 2.84 (s, 6 H, NMe<sub>2</sub>), 2.76 (s, 6 H, NMe<sub>2</sub>), 1.74 (m, 1 H, CNC(CHMe<sub>2</sub>)H<sub>C</sub>Me<sub>2</sub>O), 1.35 (s, 3 H, CNCiPrH<sub>C</sub>Me<sub>2</sub>O), 1.24 (s, 3 H, CNCiPrH<sub>C</sub>Me<sub>2</sub>O), 1.16 (d, <sup>3</sup>J<sub>HH</sub> = 6.8 Hz, 3 H, CNC(CHMe<sub>2</sub>)H<sub>C</sub>Me<sub>2</sub>O), 0.99 (d, <sup>3</sup>J<sub>HH</sub> = 6.8 Hz, 3 H, CNC(CHMe<sub>2</sub>)H<sub>C</sub>Me<sub>2</sub>O). <sup>13</sup>C{<sup>1</sup>H} NMR (benzene-*d*<sub>6</sub>, 150 MHz): δ 194.29 (br, CNCiPrHCH<sub>2</sub>O), 152.26 (br, *ipso*-C<sub>6</sub>H<sub>5</sub>), 151.51 (br, *ipso*-C<sub>6</sub>H<sub>5</sub>), 135.14 (*ortho*-C<sub>6</sub>H<sub>5</sub>), 133.11 (*ortho*-C<sub>6</sub>H<sub>5</sub>), 127.51 (*meta*-C<sub>6</sub>H<sub>5</sub>), 126.42 (*meta*-C<sub>6</sub>H<sub>5</sub>), 125.93 (*para*-C<sub>6</sub>H<sub>5</sub>), 125.01 (*para*-C<sub>6</sub>H<sub>5</sub>), 123.51 (C<sub>5</sub>H<sub>4</sub>), 123.33 (C<sub>5</sub>H<sub>4</sub>), 114.41 (C<sub>5</sub>H<sub>4</sub>), 113.64 (C<sub>5</sub>H<sub>4</sub>), 84.61 (CNCiPrH<sub>C</sub>Me<sub>2</sub>O), 78.03 (CNCiPrH<sub>C</sub>Me<sub>2</sub>O), 44.51 (NMe<sub>2</sub>), 41.99 (NMe<sub>2</sub>), 30.44 (CNC(CHMe<sub>2</sub>)H<sub>C</sub>Me<sub>2</sub>O), 30.02 (CNCiPrH<sub>C</sub>Me<sub>2</sub>O), 21.96 (CNCiPrH<sub>C</sub>Me<sub>2</sub>O), 20.68 (CNC(CHMe<sub>2</sub>)H<sub>C</sub>Me<sub>2</sub>O), 20.21 (CNC(CHMe<sub>2</sub>)H<sub>C</sub>Me<sub>2</sub>O). <sup>11</sup>B NMR (benzene-*d*<sub>6</sub>, 128 MHz): δ -11.7. <sup>15</sup>N{<sup>1</sup>H} NMR (benzene-*d*<sub>6</sub>, 71 MHz): δ -155.2 (CNCiPrH<sub>C</sub>Me<sub>2</sub>O). IR (KBr, cm<sup>-1</sup>): 3045 w, 3008 w, 2967 s, 2931 s, 2772 w, 1562 m (CN), 1489 w, 1467 s, 1431 w, 1388 m, 1260 s, 1194 s, 1093 s, 1054 s, 947 s, 884 w, 855 w, 804 s, 734 s. Anal. Calcd for C<sub>29</sub>H<sub>40</sub>BN<sub>3</sub>OZr: C, 63.48; H, 7.35; N, 7.66. Found: C, 63.31; H, 7.01; N, 7.19. Mp: 121-124 °C, dec. [α]<sub>D</sub><sup>20</sup> = -82.02° (C<sub>6</sub>H<sub>6</sub>).

**2,2-Diethoxypent-4-enylamine.** 2,2-Diethoxypent-4-enitrile was synthesized according to the published procedure.<sup>55</sup>

A oven dried 2-neck Schlenk flask fitted with reflux condenser was charged with LiAlH<sub>4</sub> (0.350 g, 9.22 mmol). The flask was cooled to 0 °C and diethyl ether (60 mL) was added. To the suspension at 0 °C, 2,2-diethoxypent-4-enitrile (0.630 g, 3.72 mmol) was added drop wise. The resultant solution was stirred overnight at room temperature. Then, the solution was cooled to 0 °C and 3 mL water was added slowly drop wise. The solution stirred 1 h at room

temperature. The ether layer was decanted and the white precipitation was extracted with diethyl ether 3 times. All the organic solutions were combined, dried with  $\text{Na}_2\text{SO}_4$  and filtered. The solvent was removed *in vacuo* to give crude 2,2-diethoxypent-4-enylamine. Vacuum distillation (80 °C, 5 mm Hg) of the crude product afforded the pure 2,2-diethoxypent-4-enylamine as a colorless oil, which was stored in glove box with activated molecular sieve (0.520 g, 3.00 mmol, 80.6% yield).  $^1\text{H}$  NMR (benzene- $d_6$ , 400 MHz):  $\delta$  5.90-5.79 (m, 1H,  $\text{CH}=\text{CH}_2$ ), 5.08-5.01 (m, 2H,  $\text{CH}=\text{CH}_2$ ), 3.40-3.31 (m, 4H,  $\text{OCH}_2\text{CH}_3$ ), 2.79 (s, 2H,  $\text{NH}_2\text{CH}_2$ ), 2.55 (d,  $^3J_{\text{HH}} = 6.8$  Hz, 2H,  $=\text{CHCH}_2$ ), 3.40-3.31 (t,  $^3J_{\text{HH}} = 6.8$  Hz, 6H,  $\text{OCH}_2\text{CH}_3$ ), 0.63 (br s, 2H,  $\text{NH}_2$ ).  $^{13}\text{C}\{1\text{H}\}$  NMR (benzene- $d_6$ , 100.6 MHz):  $\delta$  134.74 ( $\text{CH}=\text{CH}_2$ ), 117.70 ( $\text{CH}=\text{CH}_2$ ), 103.20 ( $\text{C}(\text{OCH}_2\text{CH}_3)_2$ ), 55.98 ( $\text{C}(\text{OCH}_2\text{CH}_3)_2$ ), 44.81 ( $\text{CH}_2\text{NH}_2$ ), 37.97 ( $=\text{CHCH}_2$ ), 15.99 ( $\text{C}(\text{OCH}_2\text{CH}_3)_2$ ).  $^{15}\text{N}$  NMR (benzene- $d_6$ , 61 MHz):  $\delta$  -364.6. IR (KBr,  $\text{cm}^{-1}$ ): 3396 w, 3077 m, 2976 s, 2930 s, 2883 s, 1641 m, 1621 w, 1481 w, 1456 m, 1443 s, 1417 w, 1389 m, 1365 w, 1316 w, 1266 w, 1218 s, 1157 s, 1116 s, 1080 s, 1053 s, 1001 s, 915 s, 879 w, 825 s, 770 w, 677 w. MS (ESI) exact mass Calcd for  $\text{C}_9\text{H}_{19}\text{NNaO}_2$ :  $m/z$  196.1308 ( $[\text{M}^+ + \text{Na}^+]$ ), Found: 196.1303 ( $\Delta$  2.89 ppm).

**2-(4-Pentenyl)-2-phenyl-6-heptenylamine.** A flame-dried Schlenk flask was charged with diisopropylamine (2.00 mL, 14.27 mmol) and 50 mL of THF. The flask was cooled to -78 °C and *n*BuLi (5.71 mL, 14.27 mmol, 2.5 M solution in hexanes) was added in a drop wise fashion. The resulting solution was stirred for 60 min at 0 °C. 29 mL of this solution of lithium diisopropylamide (LDA) was transferred to a dropping funnel, fitted with a dried 3-neck flask with a water condenser containing phenylacetonitrile (0.80 mL, 6.93 mmol) in THF (50 mL). The flask was cooled to -78 °C and the LDA solution was added drop wise over 10 min. The



resultant yellow solution was stirred for 90 min at this temperature and was then treated with 5-bromo-1-pentene (0.8 mL, 6.75 mmol) drop wise. The solution was stirred for another 15 min at  $-78\text{ }^{\circ}\text{C}$  and was then allowed to warm to room temperature. After stirring for 90 min at rt, the solution was cooled back to  $-78\text{ }^{\circ}\text{C}$ , and the second part of LDA was added over 10 min. The solution was allowed to warm to  $0\text{ }^{\circ}\text{C}$  and was stirred for 90 min. After cooling back to  $-78\text{ }^{\circ}\text{C}$ , the solution was treated with 5-bromo-1-pentene (1.0 mL, 8.44 mmol). The resultant yellow reaction mixture was allowed to warm slowly to room temperature and stirred overnight. The reaction was quenched by addition of water (5 mL), and the solvent was removed *in vacuo*. The residue was taken up with  $\text{Et}_2\text{O}$  (100 mL), washed with water ( $2 \times 15\text{ mL}$ ) and brine ( $1 \times 15\text{ mL}$ ), and dried over  $\text{Na}_2\text{SO}_4$ . Concentration *in vacuo* gave a light yellow oil, which was purified by silica gel column chromatography (hexane: $\text{EtOAc}$ : $\text{Et}_3\text{N}$ :: 9:1:1,  $R_f = 0.75$ ) to afford 2-(4-pentenyl)-2-phenyl-6-heptenenitrile (1.50 g, 5.92 mmol, 85.4%).

An oven-dried 2-neck Schlenk flask fitted with a reflux condenser was charged with  $\text{LiAlH}_4$  (1.0 g, 26.35 mmol). The flask was cooled to  $0\text{ }^{\circ}\text{C}$  and diethyl ether (150 mL) was added. 2-(4-pentenyl)-2-phenyl-6-heptenenitrile (1.50 g, 5.92 mmol) was added in a drop wise manner to the suspension. The resulting mixture was stirred overnight at room temperature. Then, the solution was cooled to  $0\text{ }^{\circ}\text{C}$  and water (5 mL) was added in a drop wise fashion. The solution was allowed to stir for 1 h at room temperature. The ether layer was decanted and the white precipitate was extracted with diethyl ether ( $4 \times 50\text{ mL}$ ). All the organic solutions were combined, dried with  $\text{Na}_2\text{SO}_4$ , and filtered. The solvent was removed under reduced pressure to give crude 2-(4-pentenyl)-2-phenyl-6-heptenylamine. The crude product was stirred with  $\text{CaH}_2$  under argon for 3 days and then filtered to afford the pure 2-homoallyl-2-phenyl-hex-5-enylamine as a colorless oil, which was stored in glove box with activated  $4\text{ \AA}$  molecular sieves

(1.36 g, 5.28 mmol, 89.2%).  $^1\text{H}$  NMR (benzene- $d_6$ , 400 MHz):  $\delta$  7.21-7.06 (m, 5 H,  $\text{C}_6\text{H}_5$ ), 5.75-5.65 (m, 2 H,  $\text{CH}=\text{CH}_2$ ), 5.01-4.94 (m, 4 H,  $\text{CH}=\text{CH}_2$ ), 2.74 (s, 2 H,  $\text{CH}_2\text{NH}_2$ ), 1.93 (m, 2 H,  $\text{H}_2\text{C}=\text{CHCH}_2\text{CH}_2\text{CH}_2$ ), 1.60 (m, 2 H,  $\text{H}_2\text{C}=\text{CHCH}_2\text{CH}_2\text{CH}_2$ ), 1.15 (m, 2 H,  $\text{H}_2\text{C}=\text{CHCH}_2\text{CH}_2\text{CH}_2$ ), 0.37 (br s, 2 H,  $\text{CH}_2\text{NH}_2$ ).  $^{13}\text{C}\{^1\text{H}\}$  NMR (100 MHz, benzene- $d_6$ ):  $\delta$  146.79 ( $\text{C}_6\text{H}_5$ ), 139.36 ( $\text{CH}=\text{CH}_2$ ), 128.85 ( $\text{C}_6\text{H}_5$ ), 127.39 ( $\text{C}_6\text{H}_5$ ), 126.25 ( $\text{C}_6\text{H}_5$ ), 115.01 ( $\text{CH}=\text{CH}_2$ ), 48.98 ( $\text{CH}_2\text{NH}_2$ ), 45.67 [ $\text{C}(\text{C}_6\text{H}_5)$ ], 35.30, 35.16 ( $=\text{CHCH}_2\text{CH}_2\text{CH}_2$ ,  $=\text{CHCH}_2\text{CH}_2\text{CH}_2$ ), 23.59 ( $=\text{CHCH}_2\text{CH}_2\text{CH}_2$ ).  $^{15}\text{N}$  NMR (benzene- $d_6$ , 61 MHz):  $\delta$  -369.9. IR (KBr,  $\text{cm}^{-1}$ ): 3388 w, 3321 w, 3075 s, 3062 s, 3023 m, 2996 s, 2976 s, 2935 s, 2865 s, 1945 w, 1869 w, 1824 w, 1640 s, 1601 m, 1580 w, 1498 s, 1463 s, 1443 s, 1415 m, 1372 w, 1327 w, 1260 m, 1192 w, 1157 w, 1077 m, 1032 s, 994 s, 910 s, 804 s, 764 s, 700 s. MS (ESI) exact mass Calculated for  $\text{C}_{18}\text{H}_{27}\text{N}$ :  $m/z$  258.2221 ( $[\text{M}^++\text{H}^+]$ ), Found: 258.2203.

**4,4-Diethoxy-2-methylpyrrolidine.**  $^1\text{H}$  NMR (chloroform- $d$ , 400 MHz):  $\delta$  3.41-3.36 (m, 4 H,  $\text{OCH}_2\text{CH}_3$ ), 3.22-3.17 (m, 1 H,  $\text{CHMeNH}$ ), 3.01 (d,  $^2J_{\text{HH}} = 11.6$  Hz, 1 H,  $\text{CH}_2\text{NH}$ ), 2.81 (d,  $^2J_{\text{HH}} = 11.6$  Hz, 1 H,  $\text{CH}_2\text{NH}$ ), 2.06-2.01 (m, 1 H,  $\text{CH}_2\text{CHMe}$ ), 1.47 (br, 2 H,  $\text{NH}_2$ ), 1.43-1.37 (m,  $\text{CH}_2\text{CHMe}$ ), 1.12 (t,  $^3J_{\text{HH}} = 6.8$  Hz, 6 H,  $\text{OCH}_2\text{CH}_3$ ), 1.09 (d,  $^3J_{\text{HH}} = 6.4$  Hz,  $\text{CHMeNH}$ ).  $^{13}\text{C}\{^1\text{H}\}$  NMR (100.6 MHz, chloroform- $d$ ):  $\delta$  111.99  $\text{C}(\text{OCH}_2\text{CH}_3)_2$ , 57.54 ( $\text{OCH}_2\text{CH}_3$ ), 55.39 ( $\text{CH}_2\text{NH}$ ), 53.58 ( $\text{CHMeNH}$ ), 44.17 ( $\text{CH}_2\text{CHMe}$ ), 21.37 ( $\text{CHCH}_3$ ), 15.61 ( $\text{OCH}_2\text{CH}_3$ ). IR (KBr,  $\text{cm}^{-1}$ ): 2975 s, 2930 s, 2883 s, 1641 w, 1542 w, 1481 w, 1444 m, 1391 s, 1350 m, 1336 m, 1321 m, 1265 m, 1234 m, 1158 s, 1126 s, 1077 s, 1054 s, 1012 m, 949 m, 888 w, 810 m. MS (ESI) exact mass Calcd. for  $\text{C}_9\text{H}_{19}\text{NO}_2$ :  $m/z$  174.1489 ( $[\text{M}^++\text{H}^+]$ ), Found: 174.1488 ( $\Delta$  0.32 ppm).

### General procedure for catalytic hydroamination/cyclization

a) **NMR scale catalysis at rt:** In a typical small-scale hydroamination experiment, a J. Young style NMR tube with a re-sealable Teflon valve was charged with 50  $\mu\text{mol}$  of aminoalkene substrate, 5.0  $\mu\text{mol}$  of catalyst, and 0.5 mL of solvent (benzene- $d_6$ , methylene chloride- $d_2$ , toluene- $d_8$  or tetrahydrofuran- $d_8$ ). The vessel was sealed, and the reaction was monitored by  $^1\text{H}$  NMR spectroscopy at regular intervals.

b) **NMR scale catalysis at 0 °C:** In the glove box, the appropriate aminoalkene (50  $\mu\text{mol}$ ) was dissolved in 0.3 mL of toluene- $d_8$  and transferred to a NMR tube. The NMR tube was sealed with a rubber septum and cooled to 0 °C for 0.5 h outside of the glove box. The appropriate catalyst (5.0  $\mu\text{mol}$ ) was placed in a small test tube and dissolved in 0.2 mL of toluene- $d_8$ . The test tube was capped with a rubber septum and cooled to 0 °C for 0.5 h. Then, the catalyst solution was quickly transferred to the NMR tube at 0 °C by syringe. The NMR tube containing the reaction mixture was allowed to stand at 0 °C for 10 to 12 h continuously and was then checked by  $^1\text{H}$  NMR spectroscopy.

c) **NMR scale catalysis at -30 °C:**

In the glove box, appropriate aminoalkene (50  $\mu\text{mol}$ ) and catalyst (5.0  $\mu\text{mol}$ ) were charged into two separate vials. 0.4 mL toluene- $d_8$  was added to both vials and cooled to -30 °C in the glove box freezer for 30 min. Then, the cold solution of aminoalkene was added to the vial containing catalyst and put back the solution mixture into the freezer of the glove box for couple of days. The cold solution was taken out from the glove box and quench immediately, and was checked by NMR spectroscopy.

d) **Procedure for isolation of optically active pyrrolidines.** A flask was charged with the catalyst [ $\{\text{PhB}(\text{C}_5\text{H}_4)(\text{Ox}^{i\text{Pr,Me}_2})_2\}\text{Zr}(\text{NMe}_2)_2$ ] (0.060 g, 0.103 mmol), benzene (20-30 mL) and

the appropriate aminoalkene (2.58 mmol). The solution was stirred at room temperature for 3 h. Then, the products were purified by fractional distillation in vacuo to afford the cyclic amines as colorless oils.

2-methyl-4,4-diphenylpyrrolidine (**8b**) was purified by Kugelrohr distillation. Yield: 93%, bp: 125 °C,  $10^{-5}$  mBar (dynamic vacuum on a high vacuum line).

2-Methyl-4,4-bis(2-propenyl)pyrrolidine (**11b**). Yield: 95 %, bp: 86-90 °C, 5 mm Hg.

3-methyl-2-aza-spiro[4,5]decane (**12b**); yield: 94%, bp: 100-105 °C, 0.1 mm Hg (dynamic vacuum).

2-methyl-6,6-diphenylazepane (**16b**);

2-methyl-4,4-diethoxypyrrrolidine (**19b**); Yield: 84%, bp: 80 °C, 5 mm Hg.

4-allyl-2-methyl-4-(4-bromophenyl)pyrrolidine (**20b**): Yield: 97%, bp: 120-125 °C, 0.1 mm Hg (dynamic vacuum).

4-allyl-2,4-dimethyl-pyrrolidine (**21b**). Yield: 95%, bp: 47-52 °C, 5 mm Hg.

2-methyl-4-phenylpyrrolidine (**23b**), Yield: 92%, bp: 47-52 °C, 5 mm Hg.

**Procedures for NMR kinetic measurements.** Reaction progress was monitored by single scan acquisition of a series of  $^1\text{H}$  NMR spectra at regular intervals on a Bruker DRX400 spectrometer. The concentrations of *C*-(1-allyl-cyclohexyl)-methylamine and 3-methyl-2-aza-spiro[4,5]decane were determined by integration of resonances corresponding to species of interest and integration of a tetrakis(trimethylsilyl)silane standard of accurately known and constant concentration (4.36 mM in toluene- $d_8$ ). The temperature in the NMR probe was preset for each experiment, and it was kept constant and monitored during each experiment. For reactions heated above 296 K, the probe temperature was calibrated using an 80% ethylene glycol sample in 20% DMSO- $d_6$  using

the equation:  $T = [(4.218 - \Delta)/0.009132]$  K ( $\Delta$  equals the chemical shift difference of the two ethylene glycol resonances). For reactions at performed at 296 K or below, the probe was calibrated using CH<sub>3</sub>OH using the equation  $T = [-23.832 \cdot \Delta^2 - 29.46 \cdot \Delta + 403]$  K ( $\Delta$  = chemical shift difference of two peaks of CH<sub>3</sub>OH).

**Representative example:** Catalytic conversion of *C*-(1-allyl-cyclohexyl)-methylamine into 3-methyl-2-aza-spiro[4,5]decane using 10 mol %  $\{\text{PhB}(\text{C}_5\text{H}_4)(\text{Ox}^{4S-i\text{Pr},\text{Me}_2})_2\}\text{Zr}(\text{NMe}_2)_2$  ( $\{S-2\}\text{Zr}(\text{NMe}_2)_2$ ) as a catalyst is described. A 5 mL stock solution in toluene-*d*<sub>8</sub> containing a known concentration of the internal standard tetrakis(trimethylsilyl)silane (0.0070 g, 0.0218 mmol, 4.36 mM) was prepared using a 5 mL volumetric flask. The stock solution (0.50 mL) was added by a 1 mL glass syringe to a known amount of  $\{S-2\}\text{Zr}(\text{NMe}_2)_2$  (0.0040 g, 6.52  $\mu\text{mol}$ ) in a glass vial. The resulting solution was transferred to a NMR tube, capped with a rubber septum, and a <sup>1</sup>H NMR spectrum was acquired. The concentration of  $\{S-2\}\text{Zr}(\text{NMe}_2)_2$  was determined from this <sup>1</sup>H NMR spectrum by comparison of integration of resonances assigned to  $\{S-2\}\text{Zr}(\text{NMe}_2)_2$  with that from the internal standard. Neat substrate *C*-(1-allyl-cyclohexyl)-methylamine (0.010 g, 65.2  $\mu\text{mol}$ ) was added to the NMR tube by injecting through the rubber septum. Then, the NMR tube was quickly placed in the NMR probe. Single scan spectra were acquired automatically at preset time intervals at 23 °C. The concentration of substrate and product at any given time was determined by integration of substrate and product resonances relative to the integration of the internal standard. A linear least squares analysis of substrate concentrations (M) vs. time correlated to the equation  $\text{Ln}[\text{subs}]_t = \text{Ln}[\text{subs}]_0 - k_{\text{obs}}t$ .

**Measurement of initial rates of cyclization (saturation kinetics).** A 5 mL stock solution in toluene- $d_8$  containing a known concentration of internal standard tetrakis(trimethylsilyl)silane (0.0070 g, 0.0218 mmol, 4.36 mM) and catalyst (5.39 mM) was prepared using a 5 mL volumetric flask. The stock solution (0.50 mL) was added by a 1 mL glass syringe to a NMR tube, capped with rubber septum and was taken a  $^1\text{H}$  NMR spectra.

The initial rates for the hydroamination of C-(1-allyl-cyclohexyl)-methylamine (**12a**) were measured for several substrate concentrations at constant catalyst concentration (5.39 mM). Linear regression fits for versus time for the first 504 s of the reaction provided the initial rate ( $d[\mathbf{12a}]/dt$ ) for a particular initial substrate concentration (calculated as average substrate concentration over 504 s). A non-linear least squares regression analysis of  $d[\mathbf{12a}]/dt$  vs.  $[\mathbf{12a}]_{\text{ini}}$  showed good correlation to the equation:

$$\frac{-d[\mathbf{12a}]}{dt} = \frac{k_2\{[\mathbf{S-2}]\text{Zr}(\text{NMe}_2)_2\} \{[\mathbf{12a}] - \{[\mathbf{S-2}]\text{Zr}(\text{NMe}_2)_2\}\}}{K' + \{[\mathbf{12a}] - \{[\mathbf{S-2}]\text{Zr}(\text{NMe}_2)_2\}\} + K_{\text{SI}}\{[\mathbf{12a}] - \{[\mathbf{S-2}]\text{Zr}(\text{NMe}_2)_2\}\}^2}$$

which is a modified version of the general equation:

$$\frac{-d[\text{substrate}]}{dt} = \frac{k_2[\text{substrate}][\text{catalyst}]}{K' + [\text{substrate}] + \frac{[\text{substrate}]^2}{K_{\text{SI}}}}$$

Particular modifications:

(a) One equiv. of substrate is consumed in a pre-catalyst activation step. Thus, the observed substrate concentration must be modified to include this factor, which does not otherwise appear in the rate law or the reaction mechanism. Thus  $[\text{substrate}] = [\mathbf{12a}] - [\text{catalyst}]$ .

(b)  $K_{SI}$  (equilibrium constant for substrate inhibition) is normally defined as:  $K_{SI} = \frac{[\text{substrate}][\text{catalyst-substrate}]}{[\text{catalyst-substrate}^2]}$  (i.e., a *dissociation* constant). For more straightforward chemical interpretation,  $K_{SI}$  is defined here as the substrate binding constant:  $K_{SI} = \frac{[\text{catalyst-substrate}^2]}{[\text{substrate}][\text{catalyst-substrate}]}$ .

### Measurement of the activation parameters.

**1. Eyring plot from second-order rate constants:** Rate constants  $k$  were measured at the constant catalyst and initial substrate concentrations, over five temperatures ranging from 266 K to 314 K using the method described above. The plot  $\ln(k'/T)$  vs.  $1/T$  provides the values of 11.0 kcal mol<sup>-1</sup> and  $\Delta S^\ddagger = -24.5$  cal·mol<sup>-1</sup>K<sup>-1</sup> using standard Eyring analysis.

**2. Eyring plot from initial rates:** Using the initial rate method described above, the rate constants  $k_2$  were measured at temperatures ranging from 273 K to 322 K, keeping the catalyst and initial substrate concentration constant in each experiment. The plot  $\ln(k_2/T)$  vs.  $1/T$  provides the values of  $\Delta H^\ddagger = 6.7$  kcal·mol<sup>-1</sup> and  $\Delta S^\ddagger = -43.2$  cal·mol<sup>-1</sup>K<sup>-1</sup> are calculated, using standard Eyring analysis.

### Procedure for determination of enantiomeric excess of pyrrolidine products.

**NMR spectroscopy.** The <sup>1</sup>H and <sup>19</sup>F NMR methods were used to evaluate the % ee of the pyrrolidines products of enantioselective hydroamination/cyclization. 2,4,4-Trimethylpyrrolidine, 3-methyl-2-aza-spiro[4,5]decane (b.p. = 100 °C, 0.15 mBar), 3-methyl-2-

aza-spiro[4,4]nonane (b.p. = 45 °C, 2 mBar) were separated from the catalyst by vacuum transfer ( $10^{-5}$  mBar) to a 10 mL flask. 2-Methyl-4,4-diphenylpyrrolidine (b.p. = 150 °C, 0.08 mBar) was purified by silica gel flash chromatography (pipette column) with 95:5 CH<sub>2</sub>Cl<sub>2</sub>:CH<sub>3</sub>OH as an eluent, and then all volatiles were removed by rotary evaporation.

Benzene (2 mL) and triethylamine (5.0 equivalent based on the amount of aminoalkene used during catalysis) were added to the purified pyrrolidine. To this solution, (+)-(*S*)- $\alpha$ -methoxy- $\alpha$ -(trifluoromethyl)phenylacetyl chloride (1.2 equivalent based on the amount of aminoalkene used during catalysis) was added. The solution was mixed and immediately a white suspension appeared ([HNEt<sub>3</sub>][Cl]). The mixture was stirred for 1 h, and all the solvents were removed under vacuum. The white residue was extracted with pentane. Pentane was removed under vacuum to give the corresponding Mosher-amide as a clear colorless oil. No further purification was performed, since crystallization, chromatography, or sublimation could result in biased results by separation of the diastereomers. The enantioselectivities were determined by either integration of <sup>1</sup>H NMR (23 °C, CDCl<sub>3</sub>) or <sup>19</sup>F NMR (60 °C, CDCl<sub>3</sub>) signals; these were referenced to literature values and compared against authentic diastereomers of racemic samples reproduced in our laboratory.

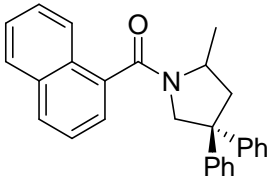
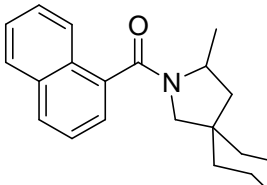
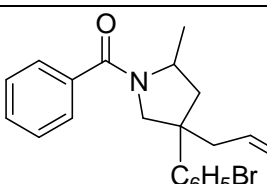
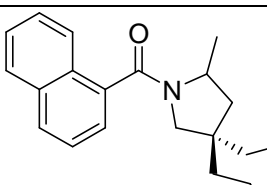
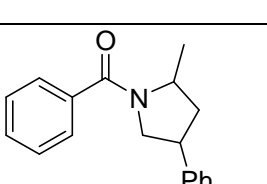
**HPLC analysis.** The enantiomeric excess of chiral pyrrolidines were also determined by HPLC analysis of the naphthoyl derivatized product (flow rate = 1.0 mL/min,  $\lambda$  = 254 nm) using Regis (*S,S*)-Whelk O1 column (Spherical Kromasil® Silica, column dimensions = 25 cm  $\times$  4.6 mm i.d., particle size = 5  $\mu$ m, 100 Å) following literature procedures.

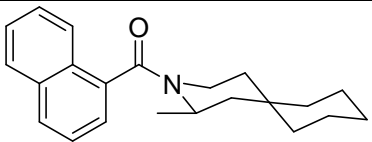
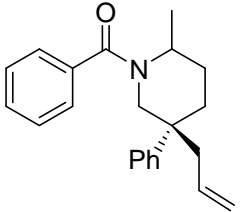
Typical procedure of derivatization: In a glove box, 1-naphthyl chloride (1.05 equiv.) or benzoyl chloride was added to a CH<sub>2</sub>Cl<sub>2</sub> solution of pyrrolidine (1.0 equiv.) and triethylamine



(3.0 equiv.) at room temperature. The resultant mixture was stirred for 2 h, and then the volatile materials were removed by rotary evaporation giving a white solid. The product was extracted with pentane and pentane was removed in vacuo. The crude product was purified by preparative silica gel TLC with appropriate eluent.

### Chiral Stationary Phase HPLC Conditions for Determination of Enantiomeric Excess

Compounds	Eluent of preparative TLC to purify product derivative	Eluent ratio of HPLC	Back pressure during HPLC	Retention time in HPLC
	cyclohexane/EtOAc; 3/1	hexane:EtOH; 75:25	55 bar	22.1 min 66.4 min
	hexane/EtOAc; 2/1	hexane:EtOH; 75:25	55 bar	13.9 min 82.8 min
	hexane/EtOAc; 2/1	hexane:EtOH; 96:4	40 bar	42.7 min 57.8 min 107.7 min 115.2 min
	hexane/EtOAc; 3/2	hexane:EtOH; 75:25	56 bar	11.8 min 74.1 min
	hexane/Et <sub>2</sub> O; 1/7	hexane:EtOH; 95:5	41 bar	38.5 min 58.6 min 62.4 min

				67.3 min
	hexane/EtOAc; 3/2	hexane:EtOH; 75:25	52 bar	11.4 min 59.6 min
	hexane/EtOAc; 2/1	hexane:EtOH; 70:30	56 bar	7.8 min 10.4 min 12.8 min 13.5 min

**Error analysis for enantioselectivity.** % ee values are given based on average % ee determined from multiple (> 3) catalytic experiments run under identical conditions; the standard deviation for the % ee's for a particular set of conditions, calculated from  $^{19}\text{F}$  NMR integration, was determined to be  $\pm 0.5$  (e.g., the % ee for **8b**, cyclized in benzene- $d_6$  at 23 °C is  $93 \pm 0.5\%$ ).  $^1\text{H}$  and  $^{19}\text{F}$  NMR spectra of Mosher amides, obtained by reaction of the pyrrolidine products with Mosher chloride are shown below for both the racemic and representative enantioenriched samples.

## References

- (1) a) Hong, S.; Marks, T. J. *Acc. Chem. Res.* **2004**, *37*, 673-686. b) Müller, T. E.; Hultsch, K. C.; Yus, M.; Foubelo, F.; Tada, M. *Chem. Rev.* **2008**, *108*, 3795-3892.
- (2) a) Gagne, M. R.; Brard, L.; Conticello, V. P.; Giardello, M. A.; Stern, C. L.; Marks, T. J. *Organometallics* **1992**, *11*, 2003-2005. b) Giardello, M. A.; Conticello, V. P.; Brard, L.; Gagne, M. R.; Marks, T. J. *J. Am. Chem. Soc.* **1994**, *116*, 10241-10254. c) Douglass, M. R.; Ogasawara, M.; Hong, S.; Metz, M. V.; Marks, T. J. *Organometallics* **2002**, *21*, 283-292. d) Hong, S.; Tian, S.; Metz Matthew, V.; Marks Tobin, J. *J. Am. Chem. Soc.* **2003**, *125*, 14768-14783. e) Ryu, J.-S.;

Marks, T. J.; McDonald, F. E. *J. Org. Chem.* **2004**, *69*, 1038-1052. f) Yu, X.; Marks, T. J. *Organometallics* **2007**, *26*, 365-376.

(3) a) O'Shaughnessy, P. N.; Scott, P. *Tetrahedron: Asymmetry* **2003**, *14*, 1979-1983. b) O'Shaughnessy, P. N.; Knight, P. D.; Morton, C.; Gillespie, K. M.; Scott, P. *Chem. Commun.* **2003**, 1770-1771. c) O'Shaughnessy, P. N.; Gillespie, K. M.; Knight, P. D.; Munslow, I. J.; Scott, P. *Dalton Trans.* **2004**, 2251-2256.

(4) a) Collin, J.; Daran, J.-C.; Schulz, E.; Trifonov, A. *Chem. Commun.* **2003**, 3048-3049. b) Collin, J.; Daran, J.-C.; Jacquet, O.; Schulz, E.; Trifonov, A. *Chem. Eur. J.* **2005**, *11*, 3455-3462. c) Riegert, D.; Collin, J.; Meddour, A.; Schulz, E.; Trifonov, A. *J. Org. Chem.* **2006**, *71*, 2514-2517. d) Riegert, D.; Collin, J.; Daran, J.-C.; Fillebeen, T.; Schulz, E.; Lyubov, D.; Fukin, G.; Trifonov, A. *Eur. J. Inorg. Chem.* **2007**, *2007*, 1159-1168. d) Riegert, D.; Collin, J.; Daran, J.-C.; Fillebeen, T.; Schulz, E.; Lyubov, D.; Fukin, G.; Trifonov, A. *Eur. J. Inorg. Chem.* **2007**, *2007*, 1159-1168. e) Aillaud, I.; Lyubov, D.; Collin, J.; Guillot, R.; Hannedouche, J.; Schulz, E.; Trifonov, A. *Organometallics* **2008**, *27*, 5929-5936. f) Hannedouche, J.; Aillaud, I.; Collin, J.; Schulz, E.; Trifonov, A. *Chem. Commun.* **2008**, 3552-3554.

g) Chapurina, Y.; Ibrahim, H.; Guillot, R.; Kolodziej, E.; Collin, J.; Trifonov, A.; Schulz, E.; Hannedouche, J. *J. Org. Chem.* **2011**, *76*, 10163-10172. h) Queffelec, C.; Boeda, F.; Pouilhès, A.; Meddour, A.; Kouklovsky, C.; Hannedouche, J.; Collin, J.; Schulz, E. *ChemCatChem* **2011**, *3*, 122-126.

(5) a) Gribkov, D. V.; Hultsch, K. C.; Hampel, F. *Chem. Eur. J.* **2003**, *9*, 4796-4810. b) Gribkov, D. V.; Hampel, F.; Hultsch, K. C. *Eur. J. Inorg. Chem.* **2004**, 4091-4101. c) Gribkov, D. V.; Hultsch, K. C. *Chem. Commun.* **2004**, 730-731. d) Gribkov, D. V.; Hultsch, K. C.; Hampel, F. *J. Am. Chem. Soc.* **2006**, *128*, 3748-3759. e) Reznichenko, A. L.; Hampel, F.;

- Hultsch, K. C. *Chem. Eur. J.* **2009**, *15*, 12819-12827. f) Vitanova, D. V.; Hampel, F.; Hultsch, K. C. *J. Organomet. Chem.* **2007**, *692*, 4690-4701. g) Reznichenko, A. L.; Nguyen, H. N.; Hultsch, K. C. *Angew. Chem., Int. Ed.* **2010**, *49*, 8984-8987.
- (6) Heck, R.; Schulz, E.; Collin, J.; Carpentier, J.-F. *J. Mol. Catal. A: Chem.* **2007**, *268*, 163-168.
- (7) a) Kim, J. Y.; Livinghouse, T. *Org. Lett.* **2005**, *7*, 1737-1739. b) Kim, H.; Kim, Y. K.; Shim, J. H.; Kim, M.; Han, M.; Livinghouse, T.; Lee, P. H. *Adv. Synth. Catal.* **2006**, *348*, 2609-2618.
- (8) a) Meyer, N.; Zulus, A.; Roesky, P. W. *Organometallics* **2006**, *25*, 4179-4182. b) Benndorf, P.; Jenter, J.; Zielke, L.; Roesky, P. W. *Chem. Commun.* **2011**, *47*, 2574-2576.
- (9) a) Xiang, L.; Wang, Q.; Song, H.; Zi, G. *Organometallics* **2007**, *26*, 5323-5329. b) Wang, Q.; Xiang, L.; Song, H.; Zi, G. *Inorg. Chem.* **2008**, *47*, 4319-4328. c) Zi, G.; Xiang, L.; Song, H. *Organometallics* **2008**, *27*, 1242-1246.
- (10) Manna, K.; Kruse, M. L.; Sadow, A. D. *ACS Catalysis* **2011**, *1*, 1637-1642.
- (11) a) Martinez, P. H.; Hultsch, K. C.; Hampel, F. *Chem. Commun.* **2006**, 2221-2223. b) Ogata, T.; Ujihara, A.; Tsuchida, S.; Shimizu, T.; Kaneshige, A.; Tomioka, K. *Tetrahedron Lett.* **2007**, *48*, 6648-6650. c) Deschamp, J.; Collin, J.; Hannedouche, J.; Schulz, E. *Eur. J. Org. Chem.* **2011**, *2011*, 3329-3338.
- (12) a) Buch, F.; Harder, S. *Z. Naturforsch.* **2008**, *63b*, 169-177. b) Horrillo-Martínez, P.; Hultsch, K. C. *Tetrahedron Lett.* **2009**, *50*, 2054-2056. c) Neal, S. R.; Ellern, A.; Sadow, A. D. *J. Organomet. Chem.* **2011**, *696*, 228-234. d) Wixey, J. S.; Ward, B. D. *Chem. Commun.* **2011**, *47*, 5449-5451. e) Wixey, J. S.; Ward, B. D. *Dalton Trans.* **2011**, *40*, 7693-7696. f) Zhang, X.; Emge, T. J.; Hultsch, K. C. *Angew. Chem. Int. Ed.* **2012**, *51*, 394-398.
- (13) Knight, P. D.; Munslow, I.; O'Shaughnessy, P. N.; Scott, P. *Chem. Commun.* **2004**, 894-895.
- (14) Watson, D. A.; Chiu, M.; Bergman, R. G. *Organometallics* **2006**, *25*, 4731-4733.

- (15) a) Wood, M. C.; Leitch, D. C.; Yeung, C. S.; Kozak, J. A.; Schafer, L. L. *Angew. Chem., Int. Ed.* **2007**, *46*, 354-358. b) Ayinla, R. O.; Gibson, T.; Schafer, L. L. *J. Organomet. Chem.* **2011**, *696*, 50-60.
- (16) a) Gott, A. L.; Clarke, A. J.; Clarkson, G. J.; Scott, P. *Organometallics* **2007**, *26*, 1729-1737. b) Zi, G.; Zhang, F.; Xiang, L.; Chen, Y.; Fang, W.; Song, H. *Dalton Trans.* **2010**, *39*, 4048-4061.
- (17) Reznichenko, A. L.; Hultsch, K. C. *Organometallics* **2010**, *29*, 24-27.
- (18) a) Reznichenko, A. L.; Emge, T. J.; Audörsch, S.; Klauber, E. G.; Hultsch, K. C.; Schmidt, B. *Organometallics* **2011**, *30*, 921-924. b) Zhang, F.; Song, H.; Zi, G. *Dalton Trans.* **2011**, *40*, 1547-1566.
- (19) a) Gott, A. L.; Clarke, A. J.; Clarkson, G. J.; Scott, P. *Chem. Commun.* **2008**, 1422-1424. b) Gott, A. L.; Clarkson, G. J.; Deeth, R. J.; Hammond, M. L.; Morton, C.; Scott, P. *Dalton Trans.* **2008**, 2983-2990.
- (20) Shen, X.; Buchwald, S. L. *Angew. Chem. Int. Ed.* **2010**, *49*, 564-567.
- (21) a) Gagne, M. R.; Marks, T. J. *J. Am. Chem. Soc.* **1989**, *111*, 4108-4109. b) Gagne, M. R.; Stern, C. L.; Marks, T. J. *J. Am. Chem. Soc.* **1992**, *114*, 275-294.
- (22) Hangaly, N. K.; Petrov, A. R.; Rufanov, K. A.; Harms, K.; Elfferding, M.; Sundermeyer, J. *Organometallics* **2011**, *30*, 4544-4554.
- (23) Stubbert, B. D.; Marks, T. J. *J. Am. Chem. Soc.* **2007**, *129*, 6149-6167.
- (24) Dunne, J. F.; Fulton, D. B.; Ellern, A.; Sadow, A. D. *J. Am. Chem. Soc.* **2010**, *132*, 17680-17683.
- (25) a) Crimmin, M. R.; Arrowsmith, M.; Barrett, A. G. M.; Casely, I. J.; Hill, M. S.; Procopiou, P. A. *J. Am. Chem. Soc.* **2009**, *131*, 9670-9685. b) Arrowsmith, M.; Crimmin, M. R.; Barrett, A.

- G. M.; Hill, M. S.; Kociok-Köhn, G.; Procopiou, P. A. *Organometallics* **2011**, *30*, 1493-1506. c)
- Brinkmann, C.; Barrett, A. G. M.; Hill, M. S.; Procopiou, P. A. *J. Am. Chem. Soc.* **2011**, *134*, 2193-2207.
- (26) Liu, B.; Roisnel, T.; Carpentier, J.-F.; Sarazin, Y. *Angew. Chem. Int. Ed.* **2012**, *51*, 4943-4946.
- (27) Allan, L. E. N.; Clarkson, G. J.; Fox, D. J.; Gott, A. L.; Scott, P. *J. Am. Chem. Soc.* **2010**, *132*, 15308-15320.
- (28) Leitch, D. C.; Platel, R. H.; Schafer, L. L. *J. Am. Chem. Soc.* **2011**, *133*, 15453-15463.
- (29) Manna, K.; Ellern, A.; Sadow, A. D. *Chem. Commun.* **2010**, *46*, 339-341.
- (30) Gribkov, D. V.; Hultsch, K. C. *Angew. Chem. Int. Ed.* **2004**, *43*, 5542-5546.
- (31) (a) Walsh, P. J.; Baranger, A. M.; Bergman, R. G. *J. Am. Chem. Soc.* **1992**, *114*, 1708-1719.  
(b) Kissounko, D. A.; Epshteyn, A.; Fettingner, J. C.; Sita, L. R. *Organometallics* **2006**, *25*, 1076-1078.
- (32) Leitch, D. C.; Turner, C. S.; Schafer, L. L. *Angew. Chem. Int. Ed.* **2010**, *49*, 6382-6386.
- (33) Katayev, E.; Li, Y.; Odom, A. L. *Chem. Commun.* **2002**, 838-839.
- (34) a) Neukom, J. D.; Perch, N. S.; Wolfe, J. P. *J. Am. Chem. Soc.* **2010**, *132*, 6276-6277. b)  
Neukom, J. D.; Perch, N. S.; Wolfe, J. P. *Organometallics* **2011**, *30*, 1269-1277.
- (35) a) Tye, J. W.; Hartwig, J. F. *J. Am. Chem. Soc.* **2009**, *131*, 14703-14712. b) Hanley, P. S.;  
Markovic, D.; Hartwig, J. F. *J. Am. Chem. Soc.* **2010**, *132*, 6302-6303.
- (36) Manna, K.; Xu, S.; Sadow, A. D. *Angew. Chem. Int. Ed.* **2011**, *50*, 1865-1868.
- (37) Dunne, J. F.; Manna, K.; Wiench, J. W.; Ellern, A.; Pruski, M.; Sadow, A. D. *Dalton Trans.* **2010**, *39*, 641-653.
- (38) Baird, B.; Pawlikowski, A. V.; Su, J.; Wiench, J. W.; Pruski, M.; Sadow, A. D. *Inorg.*

*Chem.* **2008**, *47*, 10208-10210.

(39) Kidd, R. G. *Boron-11*; Academic Press: New York, 1983; Vol. 2.

(40) a) Herberich, G. E.; Fischer, A. *Organometallics* **1996**, *15*, 58-67. b) Roitershtein, D.; Domingos, Â.; Marques, N. *Organometallics* **2004**, *23*, 3483-3487.

(41) Pawlikowski, A. V.; Gray, T. S.; Schoendorff, G.; Baird, B.; Ellern, A.; Windus, T. L.; Sadow, A. D. *Inorg. Chim. Acta* **2009**, *362*, 4517-4525.

(42) a) Vera Ralevic *European Journal of Pharmacology* *472* (2003) 1-21. b) Nicolaou, K. C.; Roecker, A. J.; Pfefferkorn, J. A.; Cao, G.-Q. *J. Am. Chem. Soc.* **2000**, *122*, 2966-2967. c) Hao Sun, Chad Moore, Patrick M. Dansette, Santosh Kumar, James R. Halpert, and Garold S. Yost *Drug Metabolism and Disposition*; Vol. 37, No. 3 page 672-684. d) Gueritte, F.; Fahy, J. *Anticancer Agents from Natural Products*; Cragg, G. M., Kingston, D. G. I., Newman, D. J., Eds.; CRC Press: Boca Raton, FL, 2005; pp 123-135.

(43) For examples of separation of racemates using an (*S,S*)-Whelk-O1 column, see: (a) Pirkle, W. H.; Welch, C. J. *Tetrahedron: Asymmetry* **1994**, *5*, 777-780. (b) Pirkle, W. H.; Welch, C. J.; Lamm, B. *J. Org. Chem.* **1992**, *57*, 3854-3860.

(44) Cornish-Bowden, A. *Fundamentals of enzyme kinetics*; 3rd ed.; Portland Press: London, 2004.

(45) Panda, T. K.; Gamer, M. T.; Roesky, P. W. *Organometallics*, **2003**, *22*, 877-878.

(46) Thomas, J. C.; Peters, J. C. *Inorg. Chem.*, **2003**, *42*, 5055-5073.

(47) Diamond, G. M.; Jordan, R. F.; Petersen, J. L. *J. Am. Chem. Soc.*, **1996**, *118*, 8024.

(48) Diamond, G. M.; Jordan, R. F.; Petersen, J. L. *Organometallics*, **1996**, *15*, 4030.

(49) Bender, C. F.; Widenhofer, R. A. *J. Am. Chem. Soc.*, **2005**, *127*, 1070.

(50) Muñiz, K.; Hövelmann, C. H.; Streuff, J. *J. Am. Chem. Soc.* **2008**, *130*, 763-773.

- (51) Kondo, T.; Okada, T.; Mitsudo, T.; *J. Am. Chem. Soc.* **2002**, *124*, 186.
- (51) Gutekunst, G.; Brook, A. G. *J. Organomet. Chem.*, **1982**, *225*, 1.
- (52) T. H. Applewhite, H. Waite, C. Niemann, *J. Am. Chem. Soc.* **1958**, *80*, 1465-1469.
- (53) S. E. Gibson, N. Mainolfi, S. B. Kalindjian, P. T. Wright, A. J. P. White, *Chem. Eur. J.* **2005**, *11*, 69-80.
- (54) W. R. Leonard, J. L. Romine, A. I. Meyers, *J. Org. Chem.* **1991**, *56*, 1961-1963.
- (55) Mai, D. N.; Wolfe, J. P. *J. Am. Chem. Soc.* **2010**, *132*, 12157-12159.



### Chapter 3. The desymmetrization of non-conjugated aminodienes and aminodiyne through enantioselective and diastereoselective hydroamination

Modified from a paper to be submitted to *Nature Chemistry*

Kuntal Manna,<sup>‡</sup> Aaron D. Sadow<sup>\*</sup>

#### Abstract

The optically active cyclopentadienyl-bis(oxazolanyl)borato zirconium complex  $\{\text{PhB}(\text{C}_5\text{H}_4)(\text{Ox}^{4S-i\text{Pr,Me}2})_2\}\text{Zr}(\text{NMe}_2)_2$  [ $\{S\text{-2}\}\text{Zr}(\text{NMe}_2)_2$ ] catalyzes the cyclization of achiral non-conjugated aminodienes and aminodiyne to generate two stereocenters. One results from N–C bond formation *via* enantioselective hydroamination and other results from selection of one of the two diastereotopic unsaturated moieties. The desymmetrization of olefin moieties during enantioselective cyclohydroamination of aminodienes affords cyclic amines with high diastereomeric ratios and high enantiomeric excesses. Similarly, the desymmetrization of alkyne moieties in  $\{S\text{-2}\}\text{Zr}(\text{NMe}_2)_2$ -catalyzed cyclization of aminodiyne provide corresponding cyclic imines bearing quaternary stereocenters with enantiomeric excesses up to 93%. These stereoselective desymmetrization reactions are significantly affected by concentration of the substrate, temperature, and the presence of a noncyclizable primary amine. In addition, both the diastereomeric ratio and enantiomeric excess of the products are markedly enhanced by *N*-deuteration of the substrates.

<sup>‡</sup> Primary researcher and author

<sup>\*</sup> Author for correspondence

## Introduction

Asymmetric hydroamination of aminoolefins is a powerful approach for the synthesis of optically active nitrogen heterocycles, which are important in chemical and pharmaceutical industries.<sup>1</sup> Despite marked advances of preparing highly enantioenriched 2-alkyl-azacycles,<sup>2,3,4,5,6,7</sup> challenges remain to improve the versatility of hydroamination for the synthesis of complex enantiopure heterocycles. Specifically, current enantioselective hydroamination catalysts are limited to generate a stereocenter at 2-position with respect to nitrogen of the cyclic amine.

Strategies for synthesizing nitrogen heterocycles bearing multiple stereocenters *via* hydroamination/cyclization of racemic aminoalkenes lead to the mixture of diastereomers. The cyclization of racemic  $\alpha$ -alkyl substituted aminopentenes catalyzed by achiral lanthanocenes affords racemic 2,5-disubstituted pyrrolidines with high *trans/cis* diastereomeric ratio.<sup>8</sup> The *trans/cis* ratio of product is sensitive to reaction temperature, substrate concentration, addition of non-cyclizable primary amine, and *N*-deuteration of substrate. Kinetic resolution of the racemic  $\alpha$ -substituted aminopentenes using chiral hydroamination catalysts provide corresponding 2,5-disubstituted pyrrolidines with excellent *trans/cis* ratios and moderate enantiomeric excesses.<sup>4c,4d</sup> The  $\alpha$ -stereocenter in these racemic aminopentenes significantly affects the new stereocenter formed in enantioselective hydroamination due to the close proximity between the two stereocenters. Therefore, diastereomeric ratio of the cyclized products is highly dependent on the position of the existing stereocenter within the racemic aminoalkene;  $\beta$ -substituted racemic aminopentene provides corresponding pyrrolidine with equal amount of *cis*- and *trans*-diastereomers.<sup>7b,8,9</sup> However, enantioselective cyclization of achiral non-conjugated aminodienes generally provide azacycles with poor diastereomeric ratio.

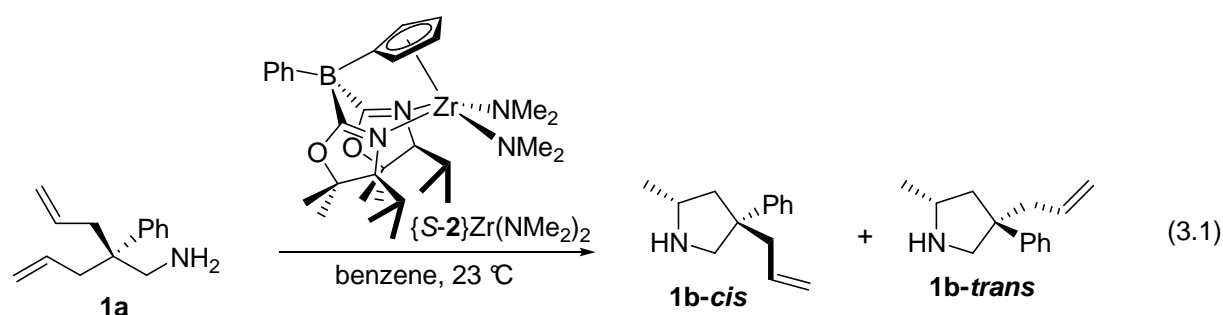
In this context, developing enantioselective catalyst that can desymmetrize olefin moieties of achiral non-conjugated aminodienes during cyclohydroamination might improve the diastereomeric ratio of the products. Recently, a gold-catalyzed enantioselective synthesis of methylene pyrrolidines *via* desymmetrization of achiral 1,4-dynamides was reported.<sup>10</sup> The cyclization of 1,4-dynamides provided methylene pyrrolidines bearing a quaternary stereocenter with enantioselectivities up to 93%. Herein, we disclose an interesting desymmetrization of achiral non-conjugated aminodienes during cyclization by a chiral zirconium catalyst to provide cyclic amines with high enantio- and diastereomeric excesses. The cyclization of achiral non-conjugated aminodienes also affords cyclic imines bearing a quaternary-stereocenter at 4-, 5-, and 6-positions with excellent enantioselectivity.

## Results and Discussion

### *Catalytic hydroamination/cyclization of aminoalkenes and aminoalkynes*

Optically active cyclopentadienyl-bis(4*S*-isopropyl-5,5-dimethyl-2-oxazolanyl)borate-supported zirconium complex  $\text{PhB}(\text{C}_5\text{H}_4)(\text{Ox}^{4*S*-i\text{Pr},\text{Me}^2})_2\text{Zr}(\text{NMe}_2)_2$  [ $\{S-2\}\text{Zr}(\text{NMe}_2)_2$ ]<sup>11</sup> is a precatalyst for cyclization 2-allyl-2-phenyl-pent-4-enylamine (**1a**) at room temperature to provide corresponding 4-allyl-2-methyl-4-phenylpyrrolidine (**2b**) as a mixture of diastereomers with *cis*-**2b** as the major product (eq 3.1). Both diastereomers are formed with high enantiomeric excess favoring *R*-configuration, but the ratio of *cis*- and *trans*-diastereomers is low (3.3:1). The assignment of the major isomer as *cis* is supported by NOE experiments in benzene-*d*<sub>6</sub> in which irradiation of the 2-methyl signal of the major isomer (1.00 ppm) results in decreased intensity of the *ortho*- and *meta*-phenyl resonances at 7.27 ppm and 6.69 ppm. The <sup>19</sup>F NMR spectrum of the (*R*)-Mosher amide of 2- methyl-pyrrolidine **2b** contains two sharp upfield signals for the major

diastereomers and two broad downfield resonances for the minor diastereomers. Because the  $^{19}\text{F}$  NMR signals for *R,R*-Mosher amide of 2*R*-2-methyl-pyrrolidine are systematically upfield and sharp while the *S,R*-Mosher amide of 2*S*-2-methyl-pyrrolidines are downfield and broad, the configuration of the stereocenters resulting from C–N bond formation are equivalent (*i.e.* *R*) in the diastereomeric products. The poor *cis/trans* ratio, however high enantiomeric excess of each diastereomer suggest that the catalyst is not efficient in distinguishing the two olefins, but the N–C bond formation is favored for the *Re* face for both olefins.



Interestingly, the *cis/trans* ratio of the pyrrolidine **1b** improves upon dilution of the reaction medium. As shown in Table 3.1, the *cis/trans* ratio increases on decreasing the substrate concentration using 10 mol % catalyst loading, while the enantioselectivity remains high. The *cis/trans* ratio 3.3:1 (**1a**) = 65.4 mM, [**S-2**]Zr(NMe<sub>2</sub>)<sub>2</sub>] = 6.54 mM) increased to 9:1 upon diluting the reaction mixture by 12 fold. The *cis/trans* ratio could be further improved to 12:1 upon 30 fold dilution, albeit at the expense of an extended reaction time (Table 3.1; entry 5).

**Table 3.1.** Catalytic cyclization of 2-allyl-2-phenyl-pent-4-enylamine (**1a**) with precatalyst **{S-2}Zr(NMe<sub>2</sub>)<sub>2</sub>** at different concentrations.<sup>a</sup>

Entry	[catalyst] mM	[substrate- <b>1a</b> ] mM	Time (h)	Yield (%)	d.r. <sup>b</sup> ( <i>cis:trans</i> )	% ee <sup>c</sup> ( <i>cis, trans</i> )
1	6.54	65.4	0.5	100	3.3:1	96.3, 95.9
2	3.27	32.7	2	100	5:1	96.1, 95.5
3	1.09	10.9	5	100	7.2:1	96.3, 95.3
4	0.55	5.45	6	100	8.9:1	95.5, 95.4
5	0.22	2.20	12	100	12:1	95.1, 94.8

<sup>a</sup> Reaction conditions: 10 mol % catalyst, r.t. <sup>b</sup> Diastereomeric ratios (*cis:trans*) were determined by <sup>1</sup>H and/or <sup>19</sup>F NMR spectra of Mosher amide derivatives. <sup>c</sup> The % ee values were determined by <sup>19</sup>F NMR spectra of Mosher amide derivatives.

The interesting effect of concentration on desymmetrization of **1a** during cyclization catalyzed by  $\{S-2\}Zr(NMe_2)_2$  led us to investigate whether variation of concentration of the substrate, catalyst, or both changes the diastereoselectivity. The *cis/trans* ratio of **1b** is unchanged on varying the concentration of precatalyst  $\{S-2\}Zr(NMe_2)_2$  (13.6 mM to 2.72 mM) keeping the substrate concentration unchanged (52.3 mM) (Figure 3.1). However, *cis/trans* ratio increases upon decreasing the substrate concentration (116 mM to 31 mM) at constant concentration of  $\{S-2\}Zr(NMe_2)_2$  (6.45 mM) (Figure 3.2). The above experiments suggest that the desymmetrization of aminodiene is unaffected by catalyst concentration.

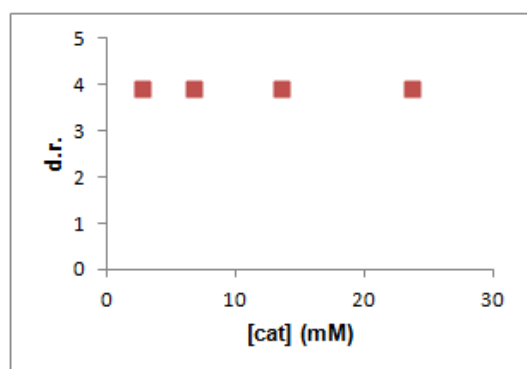


**Figure 3.1.** Plot of d.r. (*cis/trans*) of **1b** vs.  $\{S-2\}Zr(NMe_2)_2$  at constant  $[1a]_{ini}$

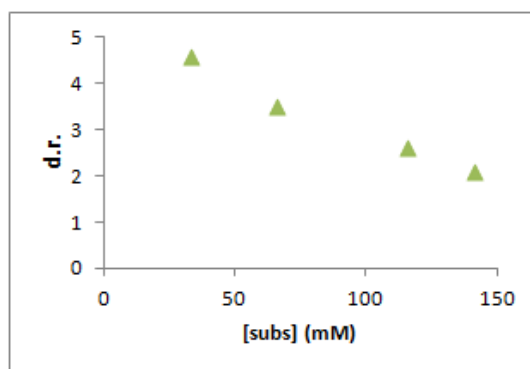
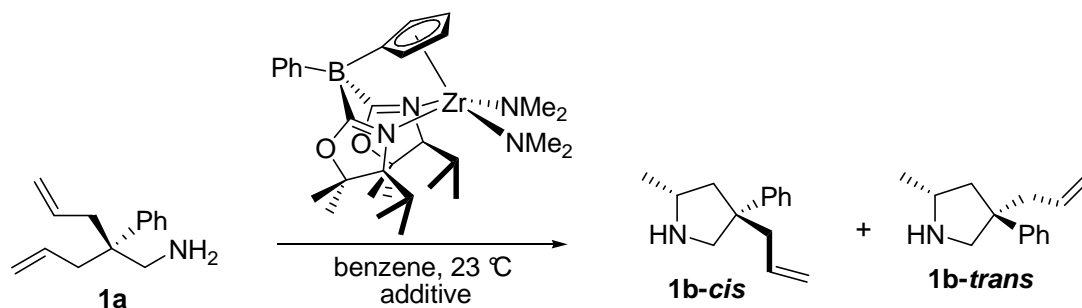


**Figure 3.2.** Plot of d.r. (*cis/trans*) of **1b** vs.  $[1a]$  (mM) at constant  $\{S-2\}Zr(NMe_2)_2$

When the cyclization of **1a** is carried out in presence of amyl amine, the *cis/trans* ratio decreases. The *cis/trans* ratio of **1b** decreases with increasing concentration of amylamine (Table 3.4; entries 2, 3 & 4), which suggests that the coordination of an amine to the metal center favors *trans* product. Interestingly, the *cis/trans* ratio is unaffected by the presence of the product *R-1b* (*cis:trans* = 3.3:1). The ratio of *cis-1b* to *trans-1b* is the same (3.3:1) after cyclization of **1a** in

the presence or absence of **R-1b** (Table 3.4; entry 5). Moreover, the cyclization of **1a** in presence of **S-1b** (*cis:trans* = 3.3:1) don't change *cis/trans* ratio of the product (Table 3.4; entry 6).

**Table 3.4.** Cyclization of 2-allyl-2-phenyl-pent-4-enylamine (**1a**) catalyzed by {**S-2**}Zr(NMe<sub>2</sub>)<sub>2</sub> in presence of amyl amine or **1b**.<sup>a</sup>



Entry	[catalyst] (mM)	[ <b>1a</b> ] (mM)	[additive] (mM)	Time (h)	Yield (%)	d.r. <sup>b</sup> ( <i>cis:trans</i> )	% ee <sup>c</sup> ( <i>cis, trans</i> )
1	6.50	65.0	-	0.5	100	3.3:1	96.3, 95.9
2	6.50	65.0	14.0 (amyl amine)	24	100	2.5:1	96, 96
3	6.50	65.0	29.0 (amyl amine)	48	94	1.96:1	96, 96
4	6.50	65.0	43.0 (amyl amine)	72	90	1.75:1	96, 96
5	6.50	65.0	32.0 ( <b>R-1b</b> )	24	95	3.2:1	n.a.
6	6.50	65.0	32.0 ( <b>S-1b</b> )	24	95	3.3:1	n.a.

<sup>a</sup> Reaction conditions: 10 mol % catalyst, r.t. <sup>b</sup> *cis/trans* ratios were determined by <sup>1</sup>H and/or <sup>19</sup>F NMR spectra of Mosher amide derivatives. <sup>c</sup> The % ee values were determined by <sup>19</sup>F NMR spectra of Mosher amide derivatives.

A significant effect of temperature on both diastereomeric d.r. and enantiomeric excesses of **1b** was observed. The *cis:trans* increases on increasing temperature ranging from 0 °C to 40 °C at constant concentration of **1a** and {**S-2**}Zr(NMe<sub>2</sub>)<sub>2</sub>, and *cis-1b* is always the major diastereomer at any substrate concentration in this temperature range (Figure 3.3). However, the enantioselectivity decreases as temperature increases from -30 °C to 40 °C, and at 40 °C both diastereomers are obtained in poorer % ee than at -30 °C. The *cis/trans* ratio increases upon dilution of the reaction mixture at any temperature as shown in Figure 3.3.

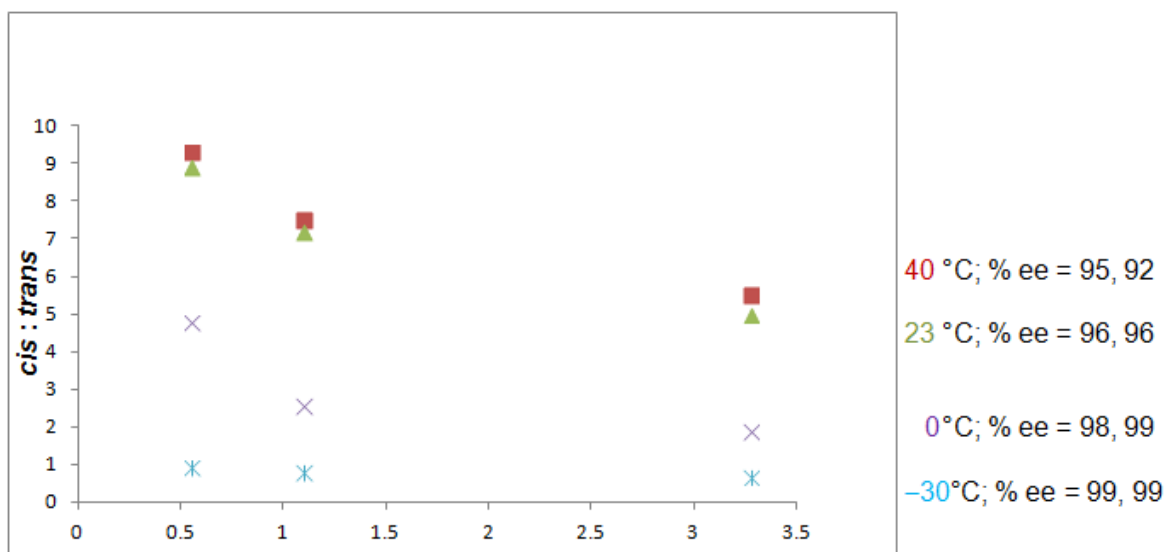


**Figure 3.3.** Plots of d.r. (**1b-cis:1b-trans**) vs. [**1a**] at  $-30\text{ }^{\circ}\text{C}$ ,  $0\text{ }^{\circ}\text{C}$ ,  $23\text{ }^{\circ}\text{C}$ , and  $40\text{ }^{\circ}\text{C}$ .

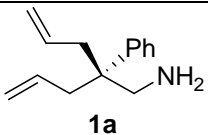
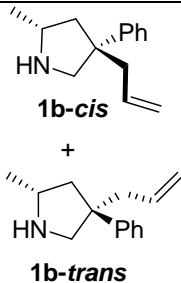
Interestingly, cyclizations of **1a** catalyzed by  $\{S-2\}\text{Zr}(\text{NMe}_2)_2$  at  $-30\text{ }^{\circ}\text{C}$  gives *trans-1b* as the major product. Impressively, both diastereomers are obtained in 99% ee (Figure 3.3; Table 3.2, entry 4). On increasing concentration of the substrate from 32.7 M to 327 mM, the *trans/cis* ratio increases from 1.1:1 to 4.5:1 respectively (Table 3.2, entries 3 & 4). Hence, the formation of the *trans* product favors on increasing the substrate concentration and lowering the reaction temperature, whereas the *cis* product becomes favorable on decreasing substrate concentration and increasing temperature. Therefore, the ratio of the two diastereomers can be systematically tuned by controlling the substrate concentration, temperature of the reaction medium, and also by the addition of primary amine.

The interesting desymmetrization of **1a** during cyclization motivated further study of the cyclization of other achiral non-conjugated aminodienes in order to obtain cyclic amines with high diastereomeric ratio and enantiomeric excesses. The precatalyst  $\{S-2\}\text{Zr}(\text{NMe}_2)_2$  cyclizes 2-allyl-2-methyl-pent-4-enylamine (**2a**) to provide optically active 2,4,4-trimethylpyrrolidine (**2b**) in 92% yield with 93% (*cis-2b*) and 92% (*trans-2b*) ee. The *cis/trans* ratio is achieved up to

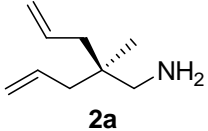
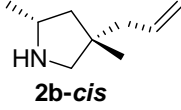
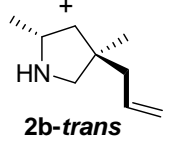
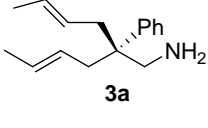
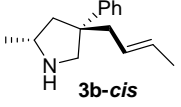
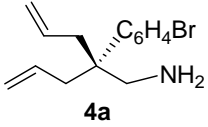
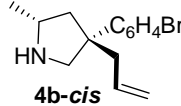
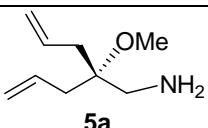
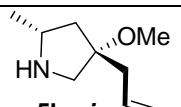
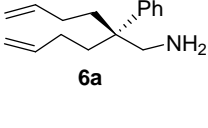
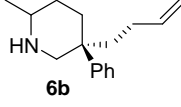
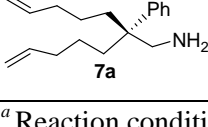
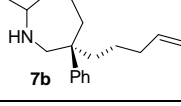
4.2:1 in diluted reaction medium ( $[2a] = 5.45 \text{ mM}$ ) at room temperature (Table 3.2, entry 7). Interestingly, the cyclization of **2a** ( $[2a] = 327 \text{ mM}$ ) at  $-30 \text{ }^\circ\text{C}$  in presence of propylamine (100 mM) affords **2b** with 1:6.5 *cis/trans* ratio, and the *trans*-**2b** is the major product (Table 3.2, entry 8).

The desymmetrization of olefin moieties is also observed for halogen- and oxo-functionalized aminodienes. 2-Allyl-2-(4-bromophenyl)pent-4-enylamine (**4a**) ( $[4a] = 65.4 \text{ mM}$ ) is cyclized within 0.5 h at room temperature to a 2:1 diastereomeric mixture of *cis* and *trans* 4-allyl-2-methyl-4-(4-bromophenyl)pyrrolidine in 97% and 95% ee respectively (Table 3.2, entry 11). Upon 12 fold dilution, the d.r. is increased to 9:1 with 95% ee of *cis* product (Table 3.2, entry 12). Similarly, *cis* isomer of 2-methyl-4-allyl-4-methoxypyrrolidine (**5b**) is obtained as a single enantiomer by hydroamination/cyclization of **5a** (Table 3.2, entry 14). The assignment of the major isomer as *cis*-**5b** is supported by NOE experiments in benzene- $d_6$  in which irradiation of the 2-H signal of the major isomer (3.26 ppm) results in decreased intensity of the olefin resonances at 5.86 and 5.04 ppm.

**Table 3.2.** Hydroamination/cyclization of aminoalkenes catalyzed by  $\{S-2\}\text{Zr}(\text{NMe}_2)_2$ .<sup>a</sup>

Substrate	Product	Entry	[substrate] mM	Time	Yield % <sup>b</sup>	d.r. ( <i>cis:trans</i> ) <sup>c</sup>	% ee <sup>d</sup> (major, minor)
 <b>1a</b>	 <b>1b-cis</b> + <b>1b-trans</b>	1	65.4	0.5 h	100	3.3:1 (96)	96, 96
		2	5.45	6 h	100	8.9:1	96, 95
		3	5.45	4 d	95 <sup>e</sup>	1:1.1	99, 99 <sup>f</sup>
		4	327	4 d	95 <sup>e</sup>	1:4.5	99, 99
		5	327 <sup>g</sup>	6 d	100	1:6	99, 99



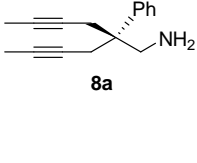
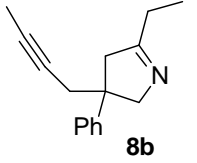
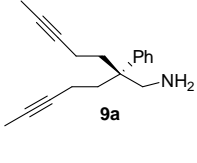
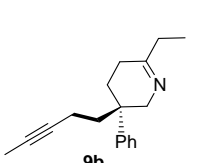
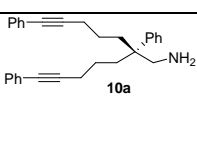
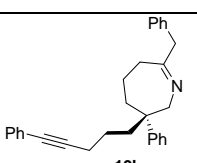
 <b>2a</b>	 <b>2b-cis</b>	6	65.4	0.5 h	100	1.1:1 (92)	93, 92
	+	7	5.45	2 d	100	4.2:1	93, 92
	 <b>2b-trans</b>	8	327 <sup>g</sup>	6 d	100 <sup>e</sup>	1:6.5	96, 95
 <b>3a</b>	 <b>3b-cis</b>	9	65.4	4 d	87	2:1	93, 95
	+	10	10.9	8 d	81	8:1	92, 93
 <b>4a</b>	 <b>4b-cis</b>	11	65.4	0.5 h	100	4:1 (94)	97, 95
	+	12	5.45	3 h	100	8.9:1	95 ( <i>cis</i> )
 <b>5a</b>	 <b>5b-cis</b>	13	327	48 h	90	10:1	97 ( <i>cis</i> )
	+	14	65.4	48 h	90	55:1	97 ( <i>cis</i> )
 <b>6a</b>	 <b>6b</b>	15	65.4	3 d	90	2.9:12	33, 12 <sup>f</sup>
		16	5.45	4 d	85	6.6:1	32, 12 <sup>f</sup>
 <b>7a</b>	 <b>7b</b>	17	65.4	4 d	90	2.8:1	89, 92
		18	16.4	6 d	86	7.1:1	89, 91

<sup>a</sup> Reaction conditions: 10 mol % catalyst, r.t. <sup>b</sup> Yield of isolated product is given in parentheses. <sup>c</sup> *cis/trans* ratios were determined by <sup>1</sup>H and/or <sup>19</sup>F NMR spectra of Mosher amide derivatives. <sup>d</sup> % ee ( $\pm 0.5\%$ ) was determined by <sup>19</sup>F NMR spectra of Mosher amide derivatives. <sup>e</sup>  $-30\text{ }^{\circ}\text{C}$ . <sup>f</sup> The % ee values were verified by HPLC. <sup>g</sup> Cyclization was done in presence of propyl amine (100 mM).

The effect of concentration on diastereomeric ratio is also observed in the cyclization of aminohexenes and aminoheptenes. The rate of cyclization of aminohexene **6a** is significantly slower than for the aminopentenes. Additionally, the enantiomeric excesses of both *cis* and *trans* diastereomers of the product 5-(homoallyl)-5-phenyl-2-methyl-piperidine (**6b**) are marked lower compared to that for the pyrrolidines. The ratio of *cis*-**6b** to *trans*-**6b** is obtained up to 6.6:1 at room temperature (Table 3.2, entries 15 & 16). In contrast to 2-methylpiperidine (**6b**), 2-methylazepane **7b** is obtained with 7.1:1 *cis/trans* ratio and higher enantiomeric excesses (89% (*cis*) and 92% (*trans*) ee; Table 3.2, entry 18) at room temperature ([**6a**] = 16.4 mM).

The desymmetrization of non-conjugated aminodienes catalyzed by precatalyst {*S*-**2**}Zr(NMe<sub>2</sub>)<sub>2</sub> inspired us to prepare enantioenriched cyclic imines from non-conjugated aminodiyne. The fact is, the alkynes desymmetrization is suggested by the observation that C–N stereocenter and desymmetrization stereocenter are inequivalently affected by the reaction conditions. The hydroamination/cyclization of 2-(but-2-ynyl)-2-phenylhex-4-yn-1-amine (**8a**) ([**8a**] = 6.54 mM) generates the corresponding cyclic imine **8b** bearing a quaternary stereogenic center at the 4-position in 95% yield with 87% ee (Table 3.3, entry 1). **8b** with 91% ee is achieved upon performing the catalysis in 12 fold diluted reaction mixture (Table 3.3, entry 2). The cyclization of aminodiyne **9a** requires longer reaction time than **8a**. The 6-membered cyclic imine **9b** is obtained with 93% yield and 71% ee at room temperature ([**9a**] = 65.4 mM). Enantioselectivity increases to 77% after performing the reaction with 5.45 mM of **9a** (Table 3.3, entry 4). The enantioenriched nitrogen heterocycles bearing quaternary stereocenters are difficult to prepare in enantioenriched form by other methods and are found in many natural products and drug molecules such as (+)-Vincamine, Quadrigemine C, and Capnellene.<sup>13,14</sup>

**Table 3.3.** Hydroamination/cyclization of aminoalkynes catalyzed by {*S*-2}Zr(NMe<sub>2</sub>)<sub>2</sub>.<sup>a</sup>

Substrate	Product	Entry	[substrate] mM	Time	% conversion <sup>b</sup>	% ee <sup>c</sup>
 8a	 8b	1	65.4	40 min	100 (95)	87
		2	5.45	2 h	100	91
 9a	 9b	3	65.4	20 h	100 (93)	71
		4	5.45	48 h	100	77
 10a	 10b	5	5.45	72 h	100	84

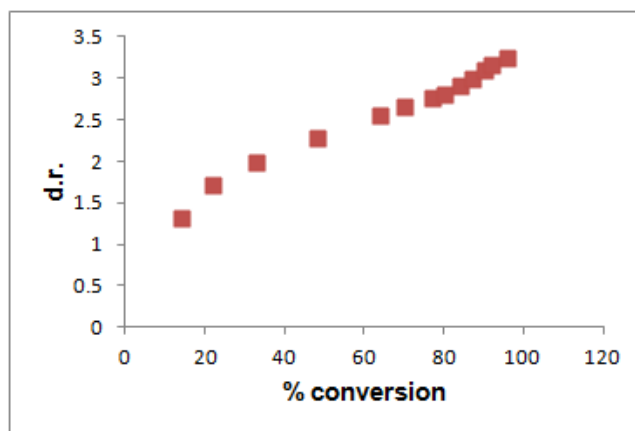
<sup>a</sup> Reaction conditions: 10 mol % catalyst, r.t. <sup>b</sup> Yield of isolated product is given in parentheses. <sup>c</sup> The % ee values were determined by HPLC using a chiral stationary phase column.

### Catalytic reaction mechanism

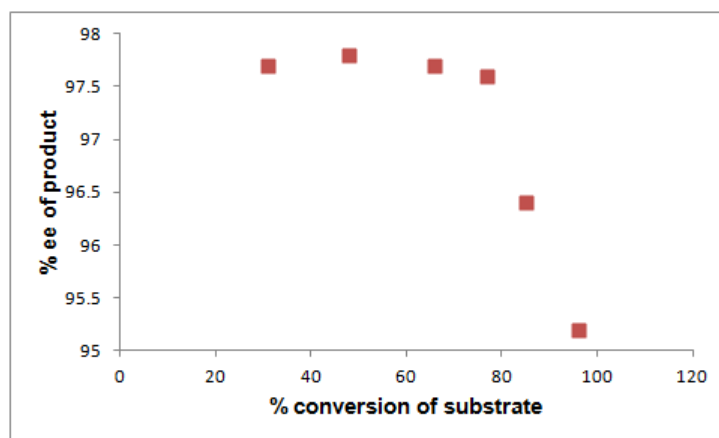
We then turned our attention to the mechanistic features to gain insight of the desymmetrization processes. HNMe<sub>2</sub> and pyrrolidine **1b** was observed within 30 s of addition of **1a** to the toluene solution of precatalyst {*S*-2}Zr(NMe<sub>2</sub>)<sub>2</sub>. Although the active catalyst is not directly observed at room temperature by in situ <sup>1</sup>H NMR spectroscopy of the reaction mixture, any correlation between desymmetrization pathway and change of catalyst structure can be eliminated by our previous observation of independency of d.r. on precatalyst concentration as discussed before.

The *cis/trans* ratio of **1b** was monitored as a function of % conversion during the course of the reaction and is plotted in Figure 3.4. The plot shows that the *cis/trans* ratio increases on increasing % conversion of substrate **1a**. At low conversion (14-25% *i.e.* at higher substrate concentration), the *cis/trans* ratio of **1b** is low. This plot suggests that the speciation of the

catalyst changes with substrate concentration. Interestingly, the % ee of **1b** remain unchanged from 30-77% conversion, and then the enantioselectivity begins to drop as shown in Figure 3.5. These experiments suggest that the stereocenter formed from desymmetrization and the stereocenter adjacent to nitrogen formed by hydroamination are not controlled by the same step.



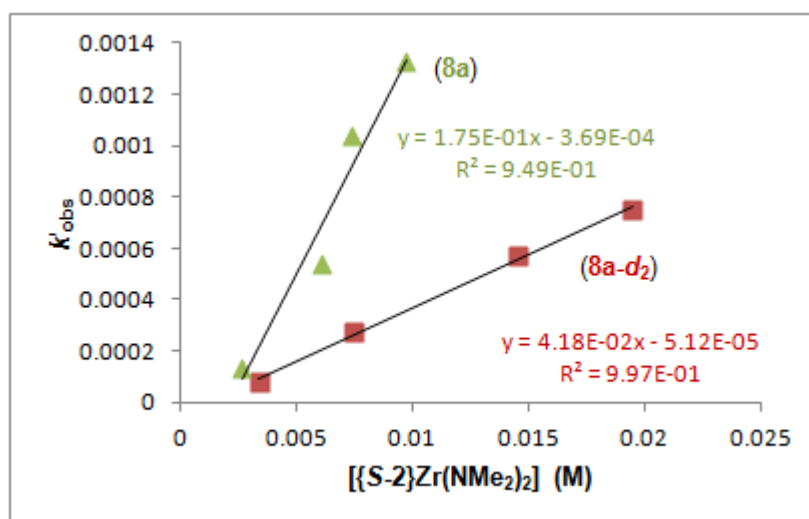
**Figure 3.4.** Plot showing the correlation of d.r. (*cis:trans*) of pyrrolidine product **1b** with catalytic conversion of substrate **1a**.



**Figure 3.5.** Plot showing the correlation of enantiomeric excess of pyrrolidine product **1b** with catalytic conversion of substrate **1a**.

The Figure 3.4 provides a hint at coordination of additional substrates to the metal center might have a profound role for desymmetrizing olefin moieties.

The desymmetrization pathway was further characterized by kinetic studies. Ln[**1a**] varies linearly with time for two half-lives to provide  $k_{\text{obs}}$ . The rate law of the catalytic conversion of **1a**  $-d[\mathbf{1a}]/dt = k[\mathbf{1a}]^1[\{\text{S-2}\}\text{Zr}(\text{NMe}_2)_2]^1$  ( $k = 0.125 \text{ M}^{-1} \text{ s}^{-1}$ ) is established by linear plot of  $k_{\text{obs}}$  vs.  $[\{\text{S-2}\}\text{Zr}(\text{NMe}_2)_2]$ . In case of cyclization of aminodiyne **8a** by  $\{\text{S-2}\}\text{Zr}(\text{NMe}_2)_2$ , a similar second order rate law  $-d[\mathbf{1a}]/dt = k'[\mathbf{1a}]^1[\{\text{S-2}\}\text{Zr}(\text{NMe}_2)_2]^1$  ( $k' = 0.175(8) \text{ M}^{-1} \text{ s}^{-1}$ ) is established for two half-lives. Conversion of 2-(but-2-ynyl)-2-phenylhex-4-yn-1-amine-ND<sub>2</sub> (**8a-d<sub>2</sub>**), catalyzed by  $\{\text{S-2}\}\text{Zr}(\text{NMe}_2)_2$ , is much slower than conversion of **8a** itself. Linear least squares best fits of plots of  $k'_{\text{obs}}^{(\text{D})}$  versus catalyst concentration provide the second-order rate constant  $k'^{(\text{D})}$  ( $0.042(2) \text{ M}^{-1} \text{ s}^{-1}$ ). The large  $k'_{\text{obs}}^{(\text{H})}/k'_{\text{obs}}^{(\text{D})}$  value (4.18 (4)) that is consistent with a primary isotope effect, suggests an N–H or N–D bond is broken in the turnover-limiting step (Figure 3.6).

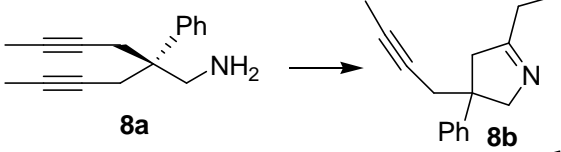
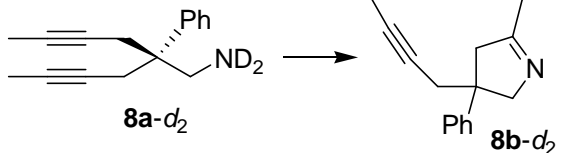
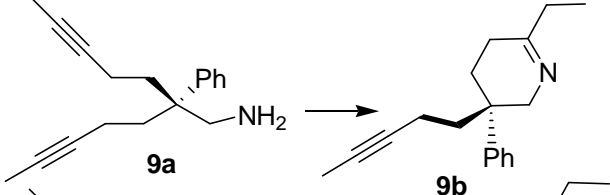
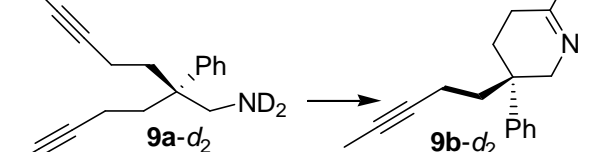


**Figure 3.6.** Plots of pseudo first order rate constants ( $k'_{\text{obs}}$ ) vs. catalyst concentration for proteo- and deuterio-substrate. Reactions were performed at 23 °C in toluene-*d*<sub>8</sub>.

Notable, the desymmetrization of aminodienes and aminodiyne is significantly affected by *N*-deuteration of substrates. The cyclization of *N*-deuterated aminodienes provides deuterioazacycles with *cis/trans* ratio and ee values that are systematically and significantly higher than those values of the corresponding proteo-analogs (Table 3.5). In the most dramatic example, the *cis/trans* ratio of **1b** increases from 8:1 to 31:1, and the ee of major *cis*-**1b** is also improved from 95% to 99% upon *N*-deuteration of the substrate **1a** under identical reaction conditions (Table 3.5; entry 1 & 2). Interesting, both *N*-deuteration and dilution of substrate favor the *cis*-diastereomer. The *N*-deuteration of aminodiyne also drastically increases the % ee of 5- and 6-membered cyclic imines (Table 3.5; entry 5 & 6; entry 7 & 8).

**Table 3.5.** The d.r. and % ee values for proteo- and deuterio-pyrrolidines obtained by hydroamination/cyclization of aminoalkenes and aminoalkynes catalyzed by  $\{S-2\}\text{Zr}(\text{NMe}_2)_2$ .<sup>a</sup>

	Entry	d.r. <sup>b</sup>	% ee <sup>c</sup>
<p>Reaction of <b>1a</b> (with Ph group) yields <b>1b-cis</b> and <b>1b-trans</b>.</p>	1	8:1	95.5, 95.4 ( <i>cis</i> , <i>trans</i> )
<p>Reaction of <b>1a-d<sub>2</sub></b> (with ND<sub>2</sub> group) yields <b>1b-d<sub>2</sub> (cis)</b> and <b>1b-d<sub>2</sub> (trans)</b>.</p>	2	31:1	99.6 (major- <i>cis</i> ) <sup>d</sup>
<p>Reaction of <b>2a</b> yields <b>2b-cis</b> and <b>2b-trans</b>.</p>	3	2.7:1	93, 92 ( <i>cis</i> , <i>trans</i> )
<p>Reaction of <b>2a-d<sub>2</sub></b> yields <b>2b-d<sub>2</sub> (cis)</b> and <b>2b-d<sub>2</sub> (trans)</b>.</p>	4	5.3:1	98, 95 ( <i>cis</i> , <i>trans</i> )

 <p><b>8a</b> → <b>8b</b></p>	5	n.a.	91 <sup>d</sup>
 <p><b>8a-d<sub>2</sub></b> → <b>8b-d<sub>2</sub></b></p>	6	n.a.	93 <sup>d</sup>
 <p><b>9a</b> → <b>9b</b></p>	7	n.a.	77 <sup>d</sup>
 <p><b>9a-d<sub>2</sub></b> → <b>9b-d<sub>2</sub></b></p>	8	n.a.	81 <sup>d</sup>

<sup>a</sup> Reaction conditions: 10 mol % catalyst, r.t. <sup>b</sup> *cis/trans* ratios were determined by <sup>19</sup>F NMR spectra of Mosher amide derivatives. <sup>c</sup> The % ee values were determined by <sup>19</sup>F NMR spectra of Mosher amide derivatives. <sup>d</sup> % ee was verified by HPLC.

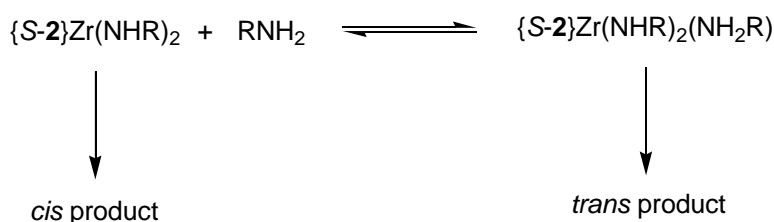
The H (or D) atom from the amine is central to the step that determine stereochemistry, which rule out the intramolecular [2π+2π] cycloaddition of a Zr-imidoolefin species in the catalytic cycle, because of the lack of NH (or ND) group in the imido moiety.

To test the valence require of zirconium center for catalysis, the complex PhB(Ox)<sup>4S-</sup><sub>*iPr,Me*2</sub>CpZrCl(NMe<sub>2</sub>) (*{S-2}ZrCl(NMe<sub>2</sub>)*) having one available valency was added to 10 equiv of aminodiene **1a** or aminodiyne **8a**. HNMe<sub>2</sub> was formed immediately after addition of substrate to a toluene solution of *{S-2}ZrCl(NMe<sub>2</sub>)*. However, no cyclization of aminoolefin was observed at room temperature, even at higher temperature up to 150 °C. This result is therefore inconsistent with the insertive pathways involving the insertion of olefin into a Zr-amido bond as the C–N bond forming step.

Taken together, all the accumulated data including rate law, the KIE, isotopic perturbation on enantioselectivity, and the inactivity of  $\{S-2\}ZrCl(NMe_2)$  complex in cyclization of aminodiene and aminodiyne eliminate olefin insertion and  $[2\pi+2\pi]$  cycloaddition as possible mechanisms for  $\{S-2\}Zr(NMe_2)_2$ -catalyzed enantioselective C–N bond formation. Our kinetic and spectroscopic data rather suggest C–N and C–H bond formation and cleavage of the N–H bond of  $\{S-2\}Zr(\text{amidoolefin})_2$  ( $\{S-2\}Zr(NHR)_2$ ) species occurring in a concerted fashion in the turnover-limiting step.

However, our experimental data suggest that the desymmetrization of olefin moieties and enantioselective C–N bond formation are not controlled by the same step. The speciation of the catalyst changes on increasing primary amine concentration. The formation of *trans* diastereomer is more favorable on increasing substrate concentration and also in presence of primary amine additive. Our working rationalization of the *cis/trans* selectivity is that the reversible associate of catalyst  $\{S-2\}Zr(NHR)_2$  with primary amine generates catalytically active  $\{S-2\}Zr(NHR)_2(NH_2R)$  intermediate, which favor *trans*-diastereomeric product.

### Scheme 1



### Conclusions

In conclusion, the desymmetrization of achiral aminodienes in hydroamination/cyclization catalyzed by precatalyst  $\{S-2\}Zr(NMe_2)_2$  affords cyclic amines with excellent diastereomeric ratio and enantiomeric excesses. The *cis/trans* ratio of cyclic amines can



be systematically tuned by controlling substrate concentration, reaction temperature, and *N*-deuteration of substrate. The two stereocenters, one results from desymmetrization of alkene moieties and other forms from enantioselective hydroamination, are not controlled by the same step. We have extended the synthetic utility of {*S*-**2**}Zr(NMe<sub>2</sub>)<sub>2</sub>-catalyzed desymmetrization reaction to aminodiyne, which provide cyclic imines with excellent optical purities. Furthermore, the cyclization of aminodiyne affords enantioenriched 5-, 6-, and 7-membered cyclic imines bearing a quaternary stereogenic center. Therefore, the mixed cyclopentadienyl-bis(oxazolonyl)borate ligand with zirconium highlights the potential for this class of ligands in asymmetric catalysis.

### Experiment details.

**General Procedures.** All reactions were performed under a dry argon atmosphere using standard Schlenk techniques or under a nitrogen atmosphere in a glove box unless otherwise indicated. Dry, oxygen-free solvents were used throughout. Benzene, toluene, pentane and tetrahydrofuran were degassed by sparging with nitrogen, filtered through activated alumina columns, and stored under N<sub>2</sub>. Benzene-*d*<sub>6</sub>, toluene-*d*<sub>8</sub> and tetrahydrofuran-*d*<sub>8</sub> were vacuum transferred from Na/K alloy and stored under N<sub>2</sub> in a glove box. PhB(C<sub>5</sub>H<sub>5</sub>)(Ox<sup>4*S*</sup>-*i*Pr,Me<sub>2</sub>)<sub>2</sub>Zr(NMe<sub>2</sub>)<sub>2</sub>,<sup>11</sup> 2-allyl-2-phenylpent-4-enylamine (**1a**),<sup>17</sup> 2-allyl-2-methylpent-4-enylamine (**2a**),<sup>11a,18</sup> 2-allyl-2-(4-bromophenyl)pent-4-enylamine (**4a**),<sup>6</sup> and 2-(but-2-ynyl)-2-phenylhex-4-yn-1-amine (**8a**)<sup>19</sup> were prepared by published procedures. All aminoalkenes and alkynes were distilled from CaH<sub>2</sub>, degassed and stored with freshly activated 4 Å molecular sieves in a glove box prior to use. All other chemicals used here are commercially available. (+)-(*S*)- $\alpha$ -methoxy- $\alpha$ -(trifluoromethyl)phenylacetyl chloride (*S*-Mosher's chloride) was obtained from Alfa-Aesar

(>98%, (+)-137.3).  $^1\text{H}$ ,  $^{13}\text{C}\{^1\text{H}\}$  NMR spectra were collected either on a Bruker DRX-400 spectrometer, Bruker Avance III 700 spectrometer or an Agilent MR 400 spectrometer.  $^{15}\text{N}$  chemical shifts were determined by  $^1\text{H}$ - $^{15}\text{N}$  HMBC experiments either on a Bruker Avance III 700 spectrometer or on a Bruker Avance III 600 spectrometer.  $^{15}\text{N}$  chemical shifts were originally referenced to liquid  $\text{NH}_3$  and recalculated to the  $\text{CH}_3\text{NO}_2$  chemical shift scale by adding  $-381.9$  ppm.  $^{11}\text{B}$  NMR spectra were referenced to an external sample of  $\text{BF}_3\cdot\text{Et}_2\text{O}$ . Accurate mass ESI mass spectrometry was performed using an Agilent QTOF 6530 equipped with the Jet Stream ESI source. An Agilent ESI test mix was used for tuning and calibration. Accurate mass data was obtained in the positive ion mode using a reference standard with ions at 121.05087 and 922.00979. The mass resolution (FWHM) was maintained at 18,000. Elemental analysis was performed using a Perkin-Elmer 2400 Series II CHN/S by the Iowa State Chemical Instrumentation Facility.  $[\alpha]_D$  values were measured on a ATAGO AP-300 polarimeter at  $23\text{ }^\circ\text{C}$ .

**2-Allyl-2-methoxypent-4-enylamine.** A flame dried Schlenk flask was charged with diisopropylamine (11.7 mL, 83.1 mmol) and dissolved in 50.0 mL THF. The flask was cooled to  $-78\text{ }^\circ\text{C}$  and *n*BuLi (33.2 mL, 83.1 mmol, 2.50 M solution in hexanes) was added drop wise. The resulting solution was stirred for 90 min at  $0\text{ }^\circ\text{C}$ . 47.4 mL of this solution of lithium diisopropylamide (LDA) was transferred to a dropping funnel, fitted with a dried 2-neck flask containing methoxyacetonitrile (3.0 mL, 40.3 mmol) in THF (40.0 mL). The flask was cooled to  $-78\text{ }^\circ\text{C}$  and the LDA solution was added drop wise over 20 min. The resultant yellow slurry was stirred for 90 min at this temperature and then was treated with allyl bromide (3.41 mL, 39.4 mmol) drop wise and the solution became clear yellow. The solution was stirred for another 15 min at  $-78\text{ }^\circ\text{C}$  and was then allowed to warm to room temperature. After stirring for 90 min at rt,

the solution was cooled back to  $-78\text{ }^{\circ}\text{C}$ , and the second part of LDA was added over 20 min. The solution was allowed to warm to  $0\text{ }^{\circ}\text{C}$  and was stirred for 70 min. After cooling back to  $-78\text{ }^{\circ}\text{C}$  the solution was treated with allyl bromide (4.20 mL, 48.5 mmol). The reaction mixture was allowed to warm slowly to room temperature and stirred overnight. The reaction was quenched by addition of water (10 mL), and the solvent was removed *in vacuo* ( $40\text{ }^{\circ}\text{C}$ , 130 mbar). The residue was taken up with  $\text{Et}_2\text{O}$  (200 mL), washed with water (2 x 30 mL) and brine (50 mL), dried over  $\text{Na}_2\text{SO}_4$ . Concentration *in vacuo* ( $40\text{ }^{\circ}\text{C}$ , 200 mbar) gave a red oil, which was distilled ( $88\text{-}90\text{ }^{\circ}\text{C}$ , 30 mm Hg) to give 2-allyl-2-methoxypent-4-enitrile as a colorless oil (1.20 g, 8.75 mmol, 21.7%).  $^1\text{H}$  NMR (chloroform-*d*, 400 MHz):  $\delta$  5.86-5.75 (m, 2 H,  $\text{CH}=\text{CH}_2$ ), 5.27-5.21 (m, 4 H,  $\text{CH}=\text{CH}_2$ ), 3.48 (s, 3 H,  $\text{OCH}_3$ ), 2.55 (d,  $^3J_{\text{H-H}} = 7.2\text{ Hz}$ , 4 H,  $\text{H}_2\text{C}=\text{CHCH}_2$ ).

An oven dried two-neck Schlenk flask fitted with reflux condenser was charged with  $\text{LiAlH}_4$  (0.500 g, 13.2 mmol). The flask was cooled to  $0\text{ }^{\circ}\text{C}$  and diethyl ether (100 mL) was added. To the suspension at  $0\text{ }^{\circ}\text{C}$ , 2-Allyl-2-methoxypent-4-enitrile (0.600 g, 4.37 mmol) was added drop wise. The resultant solution was stirred overnight at room temperature. Then, the solution was cooled to  $0\text{ }^{\circ}\text{C}$  and 2 mL water was added slowly drop wise. The solution was stirred 1 h at room temperature. The ether solution was decanted and the white precipitation was extracted with diethyl ether (3 x 50 mL). All the organic solutions were combined, dried with  $\text{Na}_2\text{SO}_4$  and filtered. The solvent was removed under *vacuo* to give crude 2-allyl-2-methoxypent-4-enylamine. Vacuum distillation ( $65\text{-}67\text{ }^{\circ}\text{C}$ , 9 mm Hg) of the crude product afforded the pure 2,2-diethoxypent-4-enylamine as a colorless oil (0.610 g, 3.93 mmol, 89.9%), which was stored in glove box with activated molecular sieve.  $^1\text{H}$  NMR (benzene-*d*<sub>6</sub>, 400 MHz):  $\delta$  5.86-5.76 (m, 2 H,  $\text{CH}=\text{CH}_2$ ), 5.04-5.00 (m, 4 H,  $\text{CH}=\text{CH}_2$ ), 2.94 (s, 3 H,  $\text{OCH}_3$ ), 2.52 (s, 2 H,  $\text{NH}_2\text{CH}_2$ ), 2.18 (d,  $^3J_{\text{H-H}} = 7.2\text{ Hz}$ , 4 H,  $=\text{CHCH}_2$ ), 0.62 (br s, 2 H,  $\text{NH}_2$ ).  $^{13}\text{C}\{^1\text{H}\}$  NMR (benzene-*d*<sub>6</sub>, 100.6 MHz):

$\delta$  134.93 (CH=CH<sub>2</sub>), 117.67 (CH=CH<sub>2</sub>), 79.06 (C(OCH<sub>3</sub>)), 48.94 (OCH<sub>3</sub>), 45.79 (CH<sub>2</sub>NH<sub>2</sub>), 38.10 (=CHCH<sub>2</sub>). <sup>15</sup>N NMR (benzene-*d*<sub>6</sub>, 61 MHz):  $\delta$  -366.1. IR (KBr, cm<sup>-1</sup>): 3389 m, 3319 w, 3075 s, 3007 m, 2977 s, 2937 s, 2827 s, 1832 w, 1638 s, 1618 m, 1459 s, 1433 s, 1415 m, 1318 w, 1293 w, 1262 w, 1211 m, 1183 m, 1153 w, 1079 s, 997 s, 914 s, 864 s, 821 w, 768 s, 703 w, 670 w. MS (ESI) exact mass Calcd for C<sub>9</sub>H<sub>17</sub>NO: m/z 156.1383 ([M<sup>+</sup>+H<sup>+</sup>]), Found: 156.1381 ( $\Delta$  1.23 ppm).

**2-Homoallyl-2-phenyl-hex-5-enylamine.** A flame-dried Schlenk flask was charged with diisopropylamine (5.30 mL, 37.8 mmol) and 50.0 mL of THF. The flask was cooled to -78 °C and *n*BuLi (15.2 mL, 38.0 mmol, 2.50 M solution in hexanes) was added in a drop wise fashion. The resulting solution was stirred for 60 min at 0 °C. 36.0 mL of this solution of lithium diisopropylamide (LDA) was transferred to a dropping funnel, fitted with a dried 3-neck flask with a water condenser containing phenylacetonitrile (2.10 mL, 18.2 mmol) in THF (50 mL). The flask was cooled to -78 °C and the LDA solution was added drop wise over 10 min. The resultant yellow solution was stirred for 90 min at this temperature and was then treated with 4-bromo-1-butene (1.80 mL, 17.7 mmol) drop wise. The solution was stirred for another 15 min at -78 °C and was then allowed to warm to room temperature. After stirring for 90 min at rt, the solution was cooled back to -78 °C, and the second part of LDA was added over 10 min. The solution was allowed to warm to 0 °C and was stirred for 90 min. After cooling back to -78 °C, the solution was treated with 4-bromo-1-butene (2.20 mL, 21.7 mmol). The resultant yellow reaction mixture was allowed to warm slowly to room temperature and stirred overnight. The reaction was quenched by addition of water (5 mL), and the solvent was removed *in vacuo*. The residue was taken up with Et<sub>2</sub>O (150 mL), washed with water (2 × 25 mL) and brine (1 × 25

mL), and dried over  $\text{Na}_2\text{SO}_4$ . Concentration *in vacuo* gave 2-homoallyl-2-phenyl-hex-5-enenitrile (4.00 g, 17.8 mmol, 97.8%) as a light yellow oil, which was sufficiently pure for the next step and was used without any purification.

An oven-dried 2-neck Schlenk flask fitted with a reflux condenser was charged with  $\text{LiAlH}_4$  (3.00 g, 79.1 mmol). The flask was cooled to 0 °C and diethyl ether (150 mL) was added. 2-homoallyl-2-phenyl-hex-5-enenitrile (4.00 g, 17.8 mmol) was added in a drop wise manner to the suspension. The resulting mixture was stirred overnight at room temperature. Then, the solution was cooled to 0 °C and water (5 mL) was added in a drop wise fashion. The solution was allowed to stir for 1 h at room temperature. The ether layer was decanted and the white precipitate was extracted with diethyl ether (4 × 70 mL). All the organic solutions were combined, dried with  $\text{Na}_2\text{SO}_4$ , and filtered. The solvent was removed under reduced pressure to give crude 2-homoallyl-2-phenyl-pent-4-enylamine. The crude product was stirred with  $\text{CaH}_2$  under argon for 3 days and then vacuum distilled (115-120 °C, 0.5 mm Hg) to afford the pure 2-homoallyl-2-phenyl-pent-4-enylamine as a colorless oil (4.10 g, 15.3 mmol, 86.0%), which was stored in glove box with activated 4 Å molecular sieves.  $^1\text{H}$  NMR (chloroform-*d*, 400 MHz):  $\delta$  7.35-7.17 (m, 5 H,  $\text{C}_6\text{H}_5$ ), 5.84-5.74 (m, 2 H,  $\text{CH}=\text{CH}_2$ ), 5.01-4.91 (m, 4 H,  $\text{CH}=\text{CH}_2$ ), 2.91 (s, 2 H,  $\text{CH}_2\text{NH}_2$ ), 1.93-1.75 (m, 8 H,  $\text{H}_2\text{C}=\text{CHCH}_2\text{CH}_2$ ), 0.76 (br s, 2 H,  $\text{CH}_2\text{NH}_2$ ).  $^{13}\text{C}\{^1\text{H}\}$  NMR (100 MHz, chloroform-*d*):  $\delta$  145.22 ( $\text{C}_6\text{H}_5$ ), 139.05 ( $\text{CH}=\text{CH}_2$ ), 128.50 ( $\text{C}_6\text{H}_5$ ), 126.81 ( $\text{C}_6\text{H}_5$ ), 126.02 ( $\text{C}_6\text{H}_5$ ), 114.41 ( $\text{CH}=\text{CH}_2$ ), 48.82 ( $\text{CH}_2\text{NH}_2$ ), 45.34 [ $\text{C}(\text{C}_6\text{H}_5)$ ], 34.15 ( $=\text{CHCH}_2\text{CH}_2$ ), 28.05 ( $=\text{CHCH}_2\text{CH}_2$ ).  $^{15}\text{N}$  NMR (chloroform-*d*, 61 MHz):  $\delta$  -369.6. IR (KBr,  $\text{cm}^{-1}$ ): 3388 w, 3322 w, 3076, 3030 s, 2997 s, 2975 s, 2934 s, 2867 s, 1824 w, 1640 s, 1601 m, 1580 s, 1541 w, 1498 s, 1461 s, 1445 s, 1415 m, 1363 w, 1310 w, 1195 w, 1157 w, 1076 m, 1034 m, 995 s, 910 s,

815 s, 758 s, 700 s. MS (ESI) exact mass Calculated for  $C_{16}H_{23}N$ :  $m/z$  230.1903 ( $[M^+ + H^+]$ ), Found: 230.1897 ( $\Delta$  2.73 ppm).

**2-(2-Butenyl)-2-phenyl-hex-4-enylamine.** A flame-dried Schlenk flask was charged with diisopropylamine (2.50 mL, 17.8 mmol) and 50.0 mL of THF. The flask was cooled to  $-78$  °C and *n*BuLi (7.10 mL, 17.9 mmol, 2.50 M solution in hexanes) was added in a drop wise fashion. The resulting solution was stirred for 60 min at 0 °C. 30.0 mL of this solution of lithium diisopropylamide (LDA) was transferred to a dropping funnel, fitted with a dried 3-neck flask with a water condenser containing phenylacetonitrile (1.0 mL, 8.66 mmol) in THF (50 mL). The flask was cooled to  $-78$  °C and the LDA solution was added drop wise over 10 min. The resultant yellow solution was stirred for 90 min at this temperature and was then treated with crotyl bromide (1.10 mL, 8.50 mmol, 85% purity from Aldrich) drop wise. The solution was stirred for another 15 min at  $-78$  °C and was then allowed to warm to room temperature. After stirring for 90 min at rt, the solution was cooled back to  $-78$  °C, and the second part of LDA was added over 10 min. The solution was allowed to warm to 0 °C and was stirred for 90 min. After cooling back to  $-78$  °C, the solution was treated with crotyl bromide (1.30 mL, 10.4 mmol). The resultant yellow reaction mixture was allowed to warm slowly to room temperature and stirred overnight. The reaction was quenched by addition of water (2 mL), and the solvent was removed *in vacuo*. The residue was taken up with Et<sub>2</sub>O (100 mL), washed with water (2 × 15 mL) and brine (1 × 20 mL), and dried over Na<sub>2</sub>SO<sub>4</sub>. Concentration of the solution *in vacuo* gave a light yellow, which was purified by silica gel column chromatography (hexane : Et<sub>2</sub>O = 10:1;  $R_f$  = 0.75) to yield 2-(2-butenyl)-2-phenyl-hex-4-enenitrile as colorless oil (1.42 g, 6.30 mmol, 72.8%).

An oven-dried 2-neck Schlenk flask fitted with a reflux condenser was charged with  $\text{LiAlH}_4$  (0.620 g, 16.3 mmol). The flask was cooled to 0 °C and diethyl ether (100 mL) was added. 2-homoallyl-2-phenyl-hex-5-enenitrile (1.22 g, 5.41 mmol) was added in a drop wise manner to the suspension. The resulting mixture was stirred overnight at room temperature. Then, the solution was cooled to 0 °C and water (2.5 mL) was added in a drop wise fashion. The solution was allowed to stir for 1 h at room temperature. The ether layer was decanted and the white precipitate was extracted with diethyl ether (4 × 70 mL). All the organic solutions were combined, dried with  $\text{Na}_2\text{SO}_4$ , and filtered. The solvent was removed under reduced pressure to give crude 2-(2-Butenyl)-2-phenyl-hex-4-enylamine. The crude product was stirred with  $\text{CaH}_2$  under argon for 2 days and then vacuum distilled (116-120 °C, 0.01 mm Hg) to afford the pure 2-(2-butenyl)-2-phenyl-hex-4-enylamine as a colorless oil, which was stored in glove box with activated 4 Å molecular sieves (0.950 g, 4.15 mmol, 76.6%).  $^1\text{H}$  NMR (chloroform-*d*, 400 MHz):  $\delta$  7.36-7.29 (m, 4 H,  $\text{C}_6\text{H}_5$ ), 7.18 (m, 1 H,  $\text{C}_6\text{H}_5$ ), 5.50-5.42 (m, 2 H,  $\text{MeHC}=\text{CHCH}_2$ ), 5.28-5.18 (m, 2 H,  $\text{MeHC}=\text{CHCH}_2$ ), 2.86 (s, 2 H,  $\text{CH}_2\text{NH}_2$ ), 2.36 (d,  $^2J_{\text{HH}} = 7.2$  Hz, 4 H,  $\text{MeHC}=\text{CHCH}_2$ ), 1.61 (d,  $^2J_{\text{HH}} = 6.0$  Hz, 6 H,  $\text{MeHC}=\text{CHCH}_2$ ), 0.79 (br s, 2 H,  $\text{CH}_2\text{NH}_2$ ).  $^{13}\text{C}\{^1\text{H}\}$  NMR (100 MHz, chloroform-*d*):  $\delta$  145.07 ( $\text{C}_6\text{H}_5$ ), 128.44 ( $\text{C}_6\text{H}_5$ ), 128.06 ( $\text{CH}=\text{CH}_2$ ), 127.16 ( $\text{CH}=\text{CH}_2$ ), 126.99 ( $\text{C}_6\text{H}_5$ ), 125.98 ( $\text{C}_6\text{H}_5$ ), 49.25 ( $\text{CH}_2\text{NH}_2$ ), 46.17 [ $\text{C}(\text{C}_6\text{H}_5)$ ], 38.68 ( $\text{MeHC}=\text{CHCH}_2$ ), 18.29 ( $\text{MeHC}=\text{CHCH}_2$ ).  $^{15}\text{N}$  NMR (chloroform-*d*, 61 MHz):  $\delta$  -369.3. IR (KBr,  $\text{cm}^{-1}$ ): 3391 w, 3323 w, 3089 m, 3058 s, 3023 s, 2917 s, 2855 s, 2732 s, 1945 w, 1871 w, 1802 w, 1744 w, 1668 w, 1601 s, 1582 m, 1498 s, 1445 s, 1377 s, 1342 w, 1310 w, 1247 w, 1076 m, 1036 m, 1003 m, 970 s, 915 m, 865 s, 809 s, 758 s.

**4-Allyl-2-methoxy-2-methyl-pyrrolidine.**  $^1\text{H}$  NMR (chloroform-*d*, 400 MHz):  $\delta$  5.85-5.71 (m,  $\text{CH}=\text{CH}_2$ ), 5.09-5.03 (m,  $\text{CH}=\text{CH}_2$ ), 3.29-3.21 (m,  $\text{CHMeNH}$ ), 3.07 (s,  $\text{OCH}_3$ ), 3.06 (s,  $\text{OCH}_3$ ), 3.03-2.98 (m,  $\text{CHMeNH}$ ), 2.89 (d,  $^2J_{\text{HH}} = 12$  Hz,  $\text{CH}_2\text{NH}$ ), 2.75 (d,  $^2J_{\text{HH}} = 12$  Hz,  $\text{CH}_2\text{NH}$ ), 2.27 (d,  $^3J_{\text{HH}} = 7.2$  Hz,  $\text{CH}_2\text{CH}=\text{CH}_2$ ), 2.18 (d,  $^3J_{\text{HH}} = 7.2$  Hz,  $\text{CH}_2\text{CH}=\text{CH}_2$ ), 2.01-1.96 (m,  $\text{CH}_2\text{CHMe}$ ), 1.72-1.67 (m,  $\text{CH}_2\text{CHMe}$ ), 1.41-1.36 (m,  $\text{CH}_2\text{CHMe}$ ), 1.31 (br, NH), 1.12 (d,  $^3J_{\text{HH}} = 6.0$  Hz,  $\text{CHMeNH}$ ), 1.05 (d,  $^3J_{\text{HH}} = 6.0$  Hz,  $\text{CHMeNH}$ ).  $^{13}\text{C}\{^1\text{H}\}$  NMR (benzene-*d*<sub>6</sub>, 100.6 MHz):  $\delta$  134.84 ( $\text{CH}=\text{CH}_2$ ), 134.33 ( $\text{CH}=\text{CH}_2$ ), 118.17 ( $\text{CH}=\text{CH}_2$ ), 117.89 ( $\text{CH}=\text{CH}_2$ ), 87.59 [ $\text{C}(\text{OCH}_2\text{CH}_3)_2$ ], 87.17 [ $\text{C}(\text{OCH}_2\text{CH}_3)_2$ ], 57.08 ( $\text{CH}_2\text{NH}$ ), 56.34 ( $\text{CH}_2\text{NH}$ ), 55.22 ( $\text{CHMeNH}$ ), 53.92 ( $\text{CHMeNH}$ ), 50.27 ( $\text{OCH}_3$ ), 44.84 ( $\text{CH}_2\text{CH}=\text{CH}_2$ ), 44.59 ( $\text{CH}_2\text{CH}=\text{CH}_2$ ), 40.22 ( $\text{CH}_2\text{CHMe}$ ), 39.69 ( $\text{CH}_2\text{CHMe}$ ), 21.97 ( $\text{CHMe}$ ), 21.77 ( $\text{CHMe}$ ). IR (KBr,  $\text{cm}^{-1}$ ): 3075 m, 2962 s, 2030 s, 2826 m, 1640 s, 1542 w, 1457 s, 1432 s, 1378 m, 1350 w, 1321 s, 1263 m, 1225 w, 1161 w, 1079 s, 997 m, 914 m, 810 m, 764 w. MS (ESI) exact mass Calcd for  $\text{C}_9\text{H}_{17}\text{NO}$ :  $m/z$  156.1383 ( $[\text{M}^+ + \text{H}^+]$ ), Found: 156.1380 ( $\Delta$  1.87 ppm).

**5-(Homoallyl)-5-phenyl-2-methyl-piperidine.**  $^1\text{H}$  NMR (chloroform-*d*, 400 MHz):  $\delta$  7.32-7.05 (m,  $\text{C}_6\text{H}_5$ ), 5.66-5.57 (m,  $\text{CH}=\text{CH}_2$ ), 4.91-4.87 (m,  $\text{CH}=\text{CH}_2$ ), 3.50 (m,  $\text{CHMeNH}$ ), 3.08 (m,  $\text{CHMeNH}$ ), 2.63-2.60 (m,  $\text{CH}_2\text{NH}$ ), 2.52-2.47 (m,  $\text{CH}_2\text{NH}$ ), 2.17 (m,  $\text{CH}_2\text{CH}_2\text{CH}=\text{CH}_2$ ), 1.78-1.23 (m,  $\text{CH}_2\text{CH}_2\text{CH}=\text{CH}_2$ ,  $\text{CH}_2\text{CH}_2\text{CHMe}$ ), 0.95 (d,  $^3J_{\text{H,H}} = 6.0$  Hz,  $\text{CHMeNH}$ ), 0.81 (d,  $^3J_{\text{H,H}} = 6.0$  Hz,  $\text{CHMeNH}$ ).  $^{13}\text{C}\{^1\text{H}\}$  NMR (100 MHz, chloroform-*d*):  $\delta$  143.98 ( $\text{C}_6\text{H}_5$ ), 139.23 ( $\text{CH}=\text{CH}_2$ ), 128.69 ( $\text{C}_6\text{H}_5$ ), 127.64 ( $\text{C}_6\text{H}_5$ ), 125.78 ( $\text{C}_6\text{H}_5$ ), 114.10 ( $\text{CH}=\text{CH}_2$ ), 53.09 ( $\text{CH}_2\text{NH}$ ), 43.85 ( $\text{CH}_2\text{CH}_2\text{CH}=\text{CH}_2$ ), 40.81 ( $\text{CHMeNH}$ ), 39.14 ( $\text{C}(\text{C}_6\text{H}_5)$ ), 35.17 ( $\text{CH}_2\text{CH}_2\text{CH}=\text{CH}_2$ ), 31.57 ( $\text{CH}_2\text{CH}_2\text{CHMe}$ ), 27.94 ( $\text{CH}_2\text{CH}_2\text{CHMe}$ ), 22.72 ( $\text{CHMe}$ ).  $^{15}\text{N}$  NMR (chloroform-*d*, 61 MHz):  $\delta$  -333.5, -334.9. IR (KBr,  $\text{cm}^{-1}$ ): 3060 m, 3023 m, 2928 s, 2856 s, 2796 m, 2737 m, 1945 w,



1871 w, 1817 w, 1640 s, 1601 m, 1580 w, 1497 s, 1447 s, 1415 w, 1376 s, 1319 w, 1191 w, 1157 w, 1131 m, 1114 m, 1078 w, 995 m, 909 s, 851 m, 805 w, 759 s, 737 s, 700 s. MS (ESI) exact mass calculated for  $C_{16}H_{23}N$ :  $m/z$  230.1903 ( $[M^+ + H^+]$ ), Found: 230.1861.

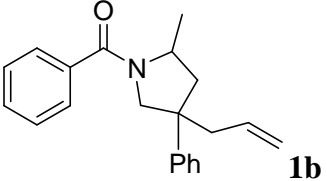
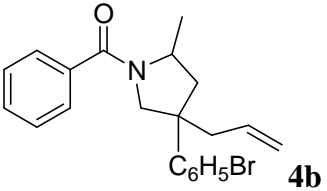
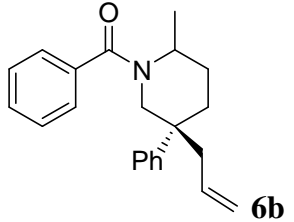
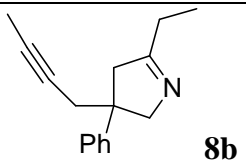
#### **Procedure for determination of enantiomeric excess of pyrrolidine products.**

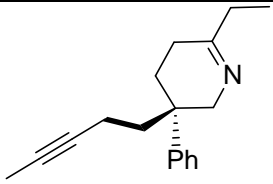
**NMR spectroscopy.** Benzene (3 mL) and triethylamine (5.0 equivalent based on the amount of aminoalkene used during catalysis) were added to the purified pyrrolidine. To this solution, (+)-(*S*)- $\alpha$ -methoxy- $\alpha$ -(trifluoromethyl)phenylacetyl chloride (1.2 equivalent based on the amount of aminoalkene used during catalysis) was added. The solution was mixed and immediately a white suspension appeared ( $[HNEt_3][Cl]$ ). The mixture was stirred for 1 h, and all the solvents were removed under vacuum. The white residue was extracted with pentane. Pentane was removed under vacuum to give the corresponding Mosher-amide as a clear colorless oil. No further purification was performed, since crystallization, chromatography, or sublimation could result in biased results by separation of the diastereomers. The enantioselectivities were determined by either integration of  $^1H$  NMR (23 °C,  $CDCl_3$ ) or  $^{19}F$  NMR (60 °C,  $CDCl_3$ ) signals; these were referenced to literature values and compared against authentic diastereomers of racemic samples reproduced in our laboratory.

**HPLC analysis.** The enantiomeric excess of chiral pyrrolidines, piperidines, and cyclic imines were determined by HPLC analysis (flow rate = 1.0 mL/min,  $\lambda$  = 254 nm) using Regis (*S,S*)-Whelk O1 column (Spherical Kromasil® Silica, column dimensions = 25 cm  $\times$  4.6 mm i.d., particle size = 5  $\mu$ m, 100 Å). The chiral pyrrolidines and piperidines were converted to their benzoyl-derivative prior to HPLC analysis. Pure sample of cyclic imines were used to determine their enantiomeric excesses by HPLC.

Typical procedure of derivatization of pyrrolidines and piperidines: In a glove box, benzoyl chloride (1.05 equiv.) was added to a  $\text{CH}_2\text{Cl}_2$  solution of pyrrolidine (1.0 equiv.) and triethylamine (3.0 equiv.) at room temperature. The resultant mixture was stirred for 2 h, and then the volatile materials were removed by rotary evaporation giving a white solid. The product was extracted with pentane and pentane was removed in vacuo. The crude product was purified by preparative silica gel TLC with appropriate eluent.

### Chiral Stationary Phase HPLC Conditions for Determination of Enantiomeric Excess

Compounds	Eluent of preparative TLC to purify product derivative	Eluent ratio of HPLC	Back pressure during HPLC	Retention time in HPLC
 <b>1b</b>	hexane/EtOAc; 3/2	hexane:EtOH; 90:10	44 bar	16.9 min 23.3 min 33.1 min 37.4 min
 <b>4b</b>	hexane/EtOAc; 2/1	hexane:EtOH; 96:4	40 bar	42.7 min 57.8 min 107.7 min 115.2 min
 <b>6b</b>	hexane/EtOAc; 2/1	hexane:EtOH; 70:30	56 bar	7.8 min 10.4 min 12.8 min 13.5 min
 <b>8b</b>	-	hexane:EtOH; 99:1	55 bar	19.9 min 56.5 min

 <p style="text-align: right;"><b>9b</b></p>	-	hexane:EtOH; 99:1	55 bar	34.3 min 108.5 min
---	---	----------------------	--------	-----------------------

## References

- (1) Müller, T. E.; Hultsch, K. C.; Yus, M.; Foubelo, F.; Tada, M. *Chem. Rev.* **2008**, *108*, 3795-3892.
- (2) a) Gagne, M. R.; Brard, L.; Conticello, V. P.; Giardello, M. A.; Stern, C. L.; Marks, T. J. *Organometallics* **1992**, *11*, 2003-2005. b) Giardello, M. A.; Conticello, V. P.; Brard, L.; Gagne, M. R.; Marks, T. J. *J. Am. Chem. Soc.* **1994**, *116*, 10241-10254. c) Douglass, M. R.; Ogasawara, M.; Hong, S.; Metz, M. V.; Marks, T. J. *Organometallics* **2002**, *21*, 283-292. d) Hong, S.; Tian, S.; Metz Matthew, V.; Marks Tobin, J. *J. Am. Chem. Soc.* **2003**, *125*, 14768-14783. e) Ryu, J.-S.; Marks, T. J.; McDonald, F. E. *J. Org. Chem.* **2004**, *69*, 1038-1052. f) Yu, X.; Marks, T. J. *Organometallics* **2007**, *26*, 365-376.
- (3) a) Collin, J.; Daran, J.-C.; Schulz, E.; Trifonov, A. *Chem. Commun.* **2003**, 3048-3049. b) Collin, J.; Daran, J.-C.; Jacquet, O.; Schulz, E.; Trifonov, A. *Chem. Eur. J.* **2005**, *11*, 3455-3462. c) Riegert, D.; Collin, J.; Meddour, A.; Schulz, E.; Trifonov, A. *J. Org. Chem.* **2006**, *71*, 2514-2517. d) Riegert, D.; Collin, J.; Daran, J.-C.; Fillebeen, T.; Schulz, E.; Lyubov, D.; Fukin, G.; Trifonov, A. *Eur. J. Inorg. Chem.* **2007**, 1159-1168. e) Aillaud, I.; Lyubov, D.; Collin, J.; Guillot, R.; Hannedouche, J.; Schulz, E.; Trifonov, A. *Organometallics* **2008**, *27*, 5929-5936. f) Hannedouche, J.; Aillaud, I.; Collin, J.; Schulz, E.; Trifonov, A. *Chem. Commun.* **2008**, 3552-3554. g) Chapurina, Y.; Ibrahim, H.; Guillot, R.; Kolodziej, E.; Collin, J.; Trifonov, A.; Schulz,

E.; Hannedouche, J. *J. Org. Chem.* **2011**, *76*, 10163-10172. h) Queffelec, C.; Boeda, F.; Pouilhès, A.; Meddour, A.; Kouklovsky, C.; Hannedouche, J.; Collin, J.; Schulz, E. *ChemCatChem* **2011**, *3*, 122-126.

(4) a) Gribkov, D. V.; Hultsch, K. C.; Hampel, F. *Chem. Eur. J.* **2003**, *9*, 4796-4810. b) Gribkov, D. V.; Hampel, F.; Hultsch, K. C. *Eur. J. Inorg. Chem.* **2004**, 4091-4101. c) Gribkov, D. V.; Hultsch, K. C. *Chem. Commun.* **2004**, 730-731. d) Gribkov, D. V.; Hultsch, K. C.; Hampel, F. *J. Am. Chem. Soc.* **2006**, *128*, 3748-3759. e) Reznichenko, A. L.; Hampel, F.; Hultsch, K. C. *Chem. Eur. J.* **2009**, *15*, 12819-12827. f) Vitanova, D. V.; Hampel, F.; Hultsch, K. C. *J. Organomet. Chem.* **2007**, *692*, 4690-4701. g) Reznichenko, A. L.; Nguyen, H. N.; Hultsch, K. C. *Angew. Chem., Int. Ed.* **2010**, *49*, 8984-8987.

(5) a) Kim, J. Y.; Livinghouse, T. *Org. Lett.* **2005**, *7*, 1737-1739. b) Kim, H.; Kim, Y. K.; Shim, J. H.; Kim, M.; Han, M.; Livinghouse, T.; Lee, P. H. *Adv. Synth. Catal.* **2006**, *348*, 2609-2618. c) Meyer, N.; Zulus, A.; Roesky, P. W. *Organometallics* **2006**, *25*, 4179-4182. d) Benndorf, P.; Jenter, J.; Zielke, L.; Roesky, P. W. *Chem. Commun.* **2011**, *47*, 2574-2576. e) Xiang, L.; Wang, Q.; Song, H.; Zi, G. *Organometallics* **2007**, *26*, 5323-5329. f) Wang, Q.; Xiang, L.; Song, H.; Zi, G. *Inorg. Chem.* **2008**, *47*, 4319-4328. g) Zi, G.; Xiang, L.; Song, H. *Organometallics* **2008**, *27*, 1242-1246.

(6) Manna, K.; Kruse, M. L.; Sadow, A. D. *ACS Catalysis* **2011**, *1*, 1637-1642.

(7) a) Watson, D. A.; Chiu, M.; Bergman, R. G. *Organometallics* **2006**, *25*, 4731-4733. b) Wood, M. C.; Leitch, D. C.; Yeung, C. S.; Kozak, J. A.; Schafer, L. L. *Angew. Chem., Int. Ed.* **2007**, *46*, 354-358. c) Gott, A. L.; Clarke, A. J.; Clarkson, G. J.; Scott, P. *Chem. Commun.* **2008**, 1422-1424. d) Reznichenko, A. L.; Hultsch, K. C. *Organometallics* **2010**, *29*, 24-27. e) Shen, X.; Buchwald, S. L. *Angew. Chem. Int. Ed.* **2010**, *49*, 564-567. f) Reznichenko, A. L.; Emge, T. J.;

- Audörsch, S.; Klauber, E. G.; Hultsch, K. C.; Schmidt, B. *Organometallics* **2011**, *30*, 921-924.
- g) Zhang, X.; Emge, T. J.; Hultsch, K. C. *Angew. Chem. Int. Ed.* **2012**, *51*, 394-398.
- (8) Gagne, M. R.; Stern, C. L.; Marks, T. J. *J. Am. Chem. Soc.* **1992**, *114*, 275-294.
- (9) a) Lauterwasser, F.; Hayes, P. G.; Piers, W. E.; Schafer, L. L.; Brase, S. *Adv. Synth. Catal.* **2011**, *353*, 1384-1390. b) Ayinla, R. O.; Gibson, T.; Schafer, L. L. *J. Organomet. Chem.* **2011**, *696*, 50-60.
- (10) Mourad, A. K.; Leutzow, J.; Czekelius, C. *Angew. Chem. Int. Ed.* **2012**, *51*, 11149-11152.
- (11) Manna, K.; Xu, S.; Sadow, A. D. *Angew. Chem. Int. Ed.* **2011**, *50*, 1865-1868.
- (12) Rho, H. S.; Oh, S. H.; Lee, J. W.; Lee, J. Y.; Chin, J.; Song, C. E. *Chem. Commun.*, **2008**, 1208-1210.
- (13) For reviews, see a) Fuji, K. *Chem. Rev.* **1993**, *93*, 2037. b) Christoffers, J.; Baro, A. *Adv. Synth. Catal.* **2005**, *347*, 1473. c) Trost, B. M.; Jiang, C. *Synthesis* **2006**, 369. d) Hawner, C.; Alexakis, C. A. *Chem. Commun.* **2010**, *46*, 7295. e) Ward, R. S. *Chem. Soc. Rev.* **1990**, *19*, 1.
- (14) a) Lebsack, A. D.; Link, J. T.; Overman, L. E.; Stearns, B. A. *J. Am. Chem. Soc.* **2002**, *124*, 9008. b) Willis, M. C.; Powell, L. H. W.; Claverie, C. K.; Watson, S. J. *Angew. Chem.* **2004**, *116*, 1269; *Angew. Chem. Int. Ed.* **2004**, *43*, 1249. c) Lee, J. Y.; You, Y. S.; Kang, S. H. *J. Am. Chem. Soc.* **2011**, *133*, 1772.
- (15) Stubbert, B. D.; Marks, T. J. *J. Am. Chem. Soc.* **2007**, *129*, 6149-6167.
- (16) Leitch, D. C.; Platel, R. H.; Schafer, L. L. *J. Am. Chem. Soc.* **2011**, *133*, 15453-15463.
- (17) a) Ciganek, E. *J. Org. Chem.* **1995**, *60*, 5803-5807. (b) Majumder, S.; Odom, A. L. *Organometallics* **2008**, *27*, 1174-1177.
- (18) Bender, C. F.; Widenhofer, R. A. *J. Am. Chem. Soc.*, **2005**, *127*, 1070-1071.
- (19) Sperger, C. A.; Fiksdahl, A. *J. Org. Chem.* **2010**, *75*, 4542-4553.

**Chapter 4. Concerted C–N and C–H bond formation in highly enantioselective  
yttrium(III)-catalyzed hydroamination: Comparison of stereoinduction with zirconium  
analogs**

Modified from a paper to be submitted to *Organometallics*

Kuntal Manna,<sup>‡</sup> Marissa L. Kruse, Arkady Ellern, Aaron D. Sadow<sup>\*</sup>

**Abstract**

$C_s$ - and  $C_1$ -symmetric cyclopentadienyl-bis(oxazolanyl)borato yttrium alkyl complexes  $\text{PhB}(\text{C}_5\text{H}_4)(\text{Ox}^{\text{R}})_2\text{YCH}_2\text{SiMe}_3$  [**1**] $\text{YCH}_2\text{SiMe}_3$ ,  $\text{Ox}^{\text{R}} = 4,4$ -dimethyl-2-oxazoline; **S-2**] $\text{YCH}_2\text{SiMe}_3$ ,  $\text{Ox}^{\text{R}} = 4S$ -isopropyl-5,5-dimethyl-2-oxazoline; **S-3**] $\text{YCH}_2\text{SiMe}_3$ ,  $\text{Ox}^{\text{R}} = 4S$ -tert-butyl-2-oxazoline) are highly active precatalysts in hydroamination/cyclization of aminoolefins to corresponding cyclic amines. These yttrium complexes are synthesized by reaction of proligand  $\text{H}[\text{PhB}(\text{Ox}^{\text{R}})_2(\text{C}_5\text{H}_5)]$  with one equiv of  $\text{Y}(\text{CH}_2\text{SiMe}_3)_3(\text{THF})_2$  at room temperature. The optically active yttrium complex **S-3**] $\text{YCH}_2\text{SiMe}_3$  is highly enantioselective in the cyclization of aminoalkenes at room temperature, affording *S*-configured pyrrolidine, piperidine, and azepane with enantiomeric excesses up to 96%. Interestingly, the configuration of pyrrolidines obtained by using these optically active yttrium precatalysts are opposite compared to the ones prepared by the corresponding zirconium precatalysts, even though the identical chiral ancillary ligand is present. A cationic zirconium monoamide complex [**S-2**] $\text{Zr}(\text{NMe}_2)[\text{B}(\text{C}_6\text{F}_5)_4]$  is also synthesized *via* amide abstraction of **S-2**] $\text{Zr}(\text{NMe}_2)_2$  using  $[\text{Ph}_3\text{C}][\text{B}(\text{C}_6\text{F}_5)_4]$ . This cationic zirconium complex cyclizes primary aminopentenes to afford

<sup>‡</sup> Primary researcher and author

<sup>\*</sup> Author for correspondence

pyrrolidines with *S*-configuration similar to those obtained using yttrium catalysts. The kinetic studies of  $\{S\text{-}3\}\text{YCH}_2\text{SiMe}_3$  catalyzed intramolecular hydroamination reveal significant isotope effects on reaction rate, which is first order dependence on substrate concentration. Additionally, substrate saturation on initial reaction rates is observed that indicates the existence of reversible substrate-catalyst association preceding the turn-over limiting step in the catalytic cycle. The nonzero x-intercept in the initial rate plot that coincides with concentration of the precatalyst indicates that 1.0 equiv. of substrate is required to activate the precatalyst. Based on the rate law for conversion, substrate saturation under initial rates conditions, kinetic isotope effects and isotopic perturbation of enantioselectivity, a noninsertive mechanism involving a six-membered transition state by a concerted C–N bond formation and N–H bond cleavage is proposed for  $\{S\text{-}3\}\text{YCH}_2\text{SiMe}_3$ -catalyzed cyclization. These features are conserved between neutral cyclopentadienyl-bis(oxazolinyl)borate yttrium and zirconium-mediated aminoalkene cyclizations, suggesting related transition states for these systems. However, inversion of the products' absolute configuration between yttrium and zirconium catalysts highlights dissimilar mechanisms of stereoinduction.

## Introduction

Stereochemistry is an extremely powerful tool for mechanistic investigations applicable to a wide range of reactions such as nucleophilic substitutions reactions,  $\alpha$ -olefin hydrogenation, and polymerization.<sup>1-4</sup> Early transition-metal and rare earth catalyzed enantioselective hydroamination of olefins have been shown to be related to the latter two reactions, as proposed mechanisms involving insertion of an olefin into a M–N bond could play a significant role in determining the absolute configuration of valuable chiral amine products.<sup>5-7</sup> Thus, the products'

stereochemistry, as well as the factors that influence products' stereochemistry, can provide important informations for understanding reaction mechanism.

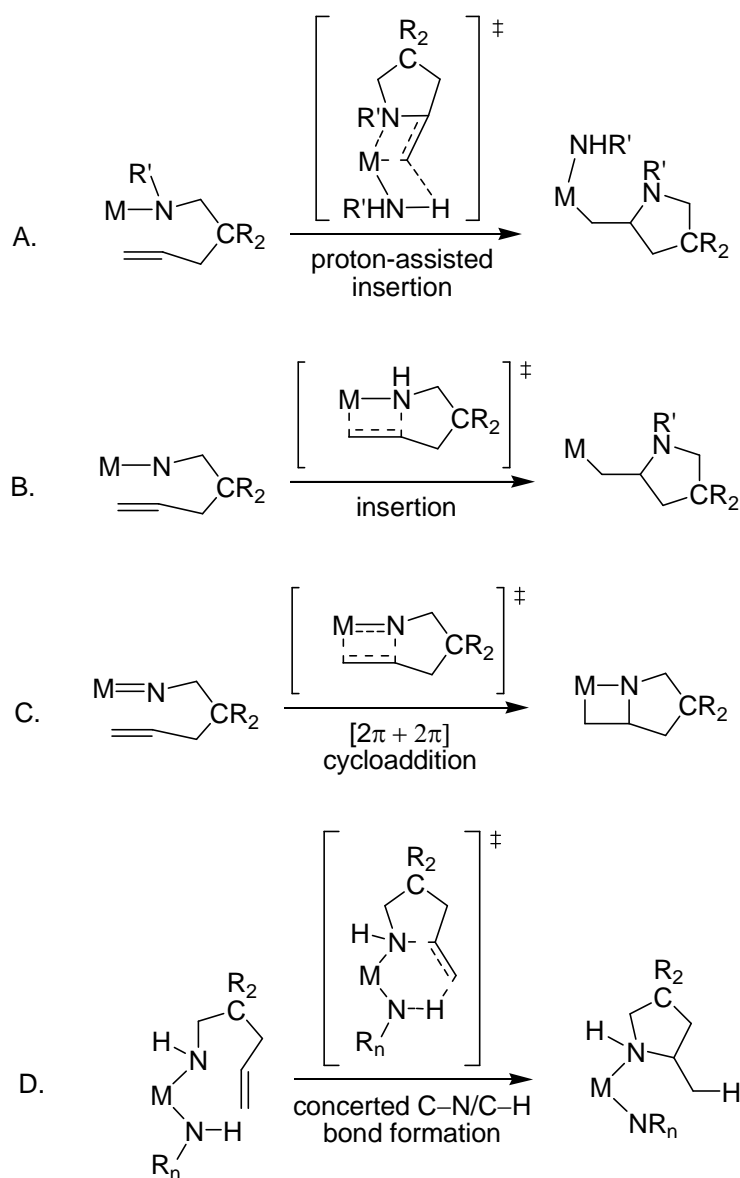
Among catalytic systems, rare earth complexes stand out for their very high turnover rates, particularly for intramolecular cyclization reactions of aminoalkenes,<sup>8-11</sup> in addition to their high activity in insertion-based catalyses such as hydrogenation, hydrosilylation, and polymerization.<sup>12-16</sup> Despite generally well-understood stereochemical effects for olefin insertion into M–H and M–C bonds, stereochemical studies of alkene insertion into M–N bonds are poorly developed. In this context, some features of rare earth-catalyzed hydroamination/cyclization are dissimilar from the characteristics associated with olefin insertions into M–C and M–H bonds, including large kinetic isotope effects on cyclization rates and significant isotope effects on the diastereoselectivity of cyclization of racemic aminoalkenes.<sup>9</sup> On the basis of these observation, a proton-assisted insertion mechanism has been proposed (Scheme 4.1; A).<sup>9,17,18</sup> However, rare earth-mediated proton-assisted insertion is disfavored to simple olefin insertion without proton-assistance as suggested by computational studies.<sup>19-22</sup>

Interestingly, the cationic zirconocene system  $\text{Cp}_2\text{ZrMe}_2/\text{B}(\text{C}_6\text{F}_5)_3$  also follows insertive mechanism in hydroamination/cyclization of aminoolefins (Scheme 4.1; B). This cation catalyst system is only active for cyclization of secondary aminoolefins, as primary aminoolefins form catalytically inactive  $\text{Zr}=\text{N}$  species.<sup>23</sup> Several other zirconium cationic catalysts shown similar features in olefin hydroamination.<sup>24</sup> In contrast, neutral Zr-catalysts typically cyclize only primary aminoalkenes *via* formation of  $\text{Zr}=\text{N}$  imido, followed by  $[2\pi+2\pi]$  cycloaddition (Scheme 4.1; C).<sup>25,28</sup> However, neutral dipyrrolylmethane group 4 complexes cyclize both primary and secondary aminoolefins<sup>26</sup>. Thus, investigation of structure-activity relationship of catalysts and understanding of the mechanism help designing catalysts for solving many synthetic problems in



hydroamination, such as general substrate applicability, enantioselectivity, diastereoselectivity, and enantioselective intermolecular hydroamination.

**Scheme 4.1. Proposed pathways for C–N bond formation in  $d^0$  and  $f^nd^0$  metal catalyzed aminopentene cyclizations.**



Previously, we reported highly enantioselective neutral cyclopentadienyl-bis(oxazolinyl)borato zirconium(IV) hydroamination catalysts, which are proposed to cyclize

aminoolefins *via* non-insertive concerted C–N/C–H bond formation in the turnover-limiting step.<sup>27</sup> Key evidences of this non-insertive six-center mechanism is the significant isotopic perturbation on enantioselectivity, the requirement of two valencies of zirconium, the requirement of substrate/precatalyst >2 for catalytic turnover, and the cyclization of secondary aminoalkenes requires a primary amine additive.

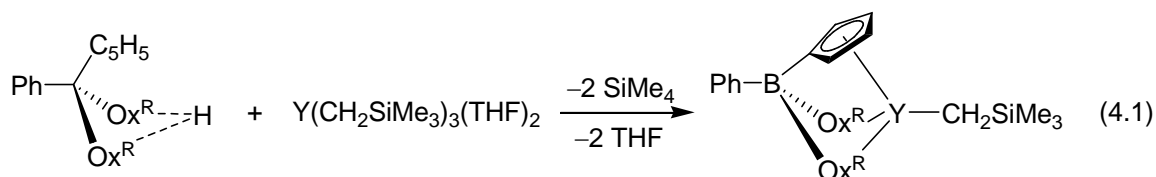
A similar six-center proton-transfer pathway was suggested in a related zirconium catalyst, but ultimately ruled out in favor of  $[2\pi + 2\pi]$  cycloaddition mechanism.<sup>28</sup> The two-substrate pathways have been recently proposed for magnesium and calcium,<sup>29</sup> rare earth,<sup>30</sup> and other zirconium-based<sup>31</sup> hydroamination catalysts. However, these studies have not included the stereochemical effects that are an important mechanistic tool.

Therefore, the excellent enantioselectivity as well as several unusual mechanistic features of our neutral cyclopentadienyl-bis(oxazolanyl)borato zirconium(IV) hydroamination catalysts<sup>27,32</sup> motivated us to investigate optically active cyclopentadienyl-bis(oxazolanyl)borate supported cationic zirconium and its isoelectronic yttrium catalyzed aminoalkene cyclization. Our current studies on these systems have addressed the substrates scope in enantioselective hydroamination, stereochemical and kinetic properties, and also the effect of the oxazoline groups on catalysts' stability, activity, and stereoselectivity. Additionally, the stereochemical and other mechanistic features of these Y- and cationic Zr-catalysts are compared to other optically active oxazolanylborato systems to rationalize the mechanism of stereinduction.

## Results and discussion

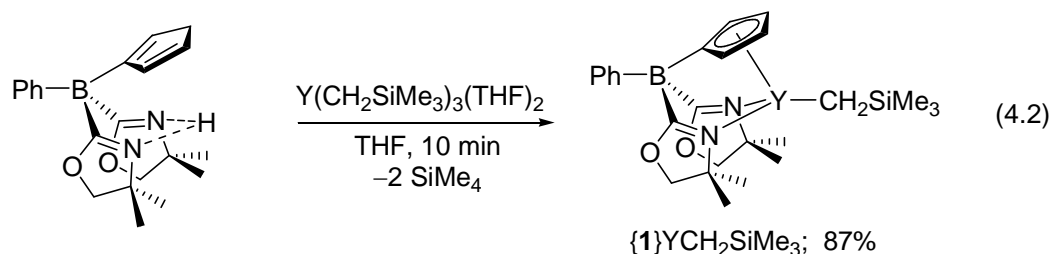
### *Synthesis and characterization of mixed cyclopentadienyl-bis(oxazolinyl)borate supported yttrium and zirconium cation compounds.*

The general scheme for synthesizing cyclopentadienyl-bis(oxazolinyl)borato yttrium complexes involves the reaction of  $Y(CH_2SiMe_3)_3(THF)_2$  with protonated proligands  $H[PhB(C_5H_5)(Ox^{Me_2})_2]$  [ $H_2\{\mathbf{1}\}$ ],  $H[PhB(C_5H_5)(Ox^{4S-iPr,Me_2})_2]$  [ $H_2\{S-2\}$ ],  $H[PhB(C_5H_5)(Ox^{4S-tBu})_2]$  [ $H_2\{S-3\}$ ] via alkane elimination (eq 4.1).<sup>33</sup>  $^{11}B$  and  $^{15}N$  NMR chemical shifts, and infrared C=N stretching frequencies for all the achiral and optically active yttrium complexes are reported in Table 4.1.



The treatment of isomeric mixture of achiral proligand  $H_2\{\mathbf{1}\}$  with one equiv of  $Y(CH_2SiMe_3)_3(THF)_2$  in THF at room temperature affords  $\{PhB(C_5H_4)(Ox^{Me_2})_2\}YCH_2SiMe_3$  ( $\{\mathbf{1}\}YCH_2SiMe_3$ ) with the elimination of 2.0 equiv of  $SiMe_4$ . This yttrium alkyl complex decomposes fast at room temperature by  $SiMe_4$  elimination ( $t_{1/2} = 40$  min, THF), however analytically pure, THF-free material is obtained by vapor diffusion of pentane into THF solution at  $-30$  °C in 87% yield. The  $^1H$  NMR spectrum in tetrahydrofuran- $d_8$  showed one set of oxazoline resonances as two singles (1.29 and 1.21 ppm) for inequivalent methyl groups and two doublets for inequivalent methylene groups (3.87 and 3.82 ppm). The  $^1H$  NMR multiplets associated with the three  $C_5H_5B$  isomers are replaced with two resonances (6.38 and 6.18 ppm) assigned to  $C_5H_4B$ . The pattern of this  $^1H$  NMR suggests that  $\{\mathbf{1}\}YCH_2SiMe_3$  is  $C_s$ -symmetric. The  $^{11}B$  NMR spectrum in tetrahydrofuran- $d_8$  showed one resonance at  $-15.2$  ppm. Only one  $\nu_{CN}$

band ( $1549\text{ cm}^{-1}$ , KBr) was observed in the IR spectrum of  $\{1\}\text{YCH}_2\text{SiMe}_3$  at lower energy than that for non-coordinated 4,4-dimethyl-2-oxazoline ( $\nu_{\text{CN}} = 1630\text{ cm}^{-1}$ ). The single  $\nu_{\text{CN}}$  infrared band of  $\{S-2\}\text{YCH}_2\text{SiMe}_3$  suggests that both oxazolines are coordinated to yttrium in the solid state.



An enantiopure yttrium complex  $\{S-2\}\text{YCH}_2\text{SiMe}_3$  is synthesized following a similar route using chiral proligand  $\text{H}[\text{PhB}(\text{C}_5\text{H}_5)(\text{Ox}^{4S-i\text{Pr},\text{Me}2})_2]$  ( $\text{H}_2\{S-2\}$ ).  $\text{H}_2\{S-2\}$  and  $\text{Y}(\text{CH}_2\text{SiMe}_3)_3(\text{THF})_2$  react rapidly in benzene at room temperature affording  $\{\text{PhB}(\text{C}_5\text{H}_4)(\text{Ox}^{4S-i\text{Pr},\text{Me}2})_2\}\text{YCH}_2\text{SiMe}_3$  ( $\{S-2\}\text{YCH}_2\text{SiMe}_3$ ) in 78% yield (eq 4.3). Two sets of oxazoline resonances (*e.g.*, two septets and four doublets assigned to the isopropyl groups and four singlets for the 5-methyl groups) and four downfield multiplets ranging from 6.92 to 6.61 ppm for the cyclopentadienyl group in the  $^1\text{H}$  NMR spectrum suggested  $C_1$ -symmetric species for  $\{S-2\}\text{YCH}_2\text{SiMe}_3$ . Two multiplets were observed for the two diastereotopic methylene protons of  $\text{CH}_2\text{SiMe}_3$ . Additionally, the broad  $^{11}\text{B}$  NMR resonance at  $-15.7$  ppm resulting from overlapping signals from isomers of  $\text{H}_2\{S-2\}$  is replaced with a sharper signal at  $-15.9$  ppm (76 Hz at half-height).  $^1\text{H}$ - $^{15}\text{N}$  HMBC experiment provided the  $^{15}\text{N}$  NMR chemical shift and displayed two signals at  $-154.4$  and  $-156.8$  ppm for  $C_1$ -symmetric  $\{S-2\}\text{YCH}_2\text{SiMe}_3$ . These  $^{15}\text{N}$  chemical shifts are upfield of free  $2\text{H-Ox}^{4S-i\text{Pr},\text{Me}2}$  ( $-143.0$  ppm).<sup>27</sup> Additionally, the solid state IR spectrum revealed one  $\nu_{\text{CN}}$  stretching frequency of oxazolines ( $1558\text{ cm}^{-1}$ ) in lower energy than that of  $2\text{H-}$

Ox<sup>4*S*-*i*Pr,Me<sub>2</sub></sup> (1632 cm<sup>-1</sup>). The <sup>15</sup>N NMR and infrared data of {*S*-2}YCH<sub>2</sub>SiMe<sub>3</sub> suggest that both oxazolines are coordinated to yttrium in solid state and also in benzene.

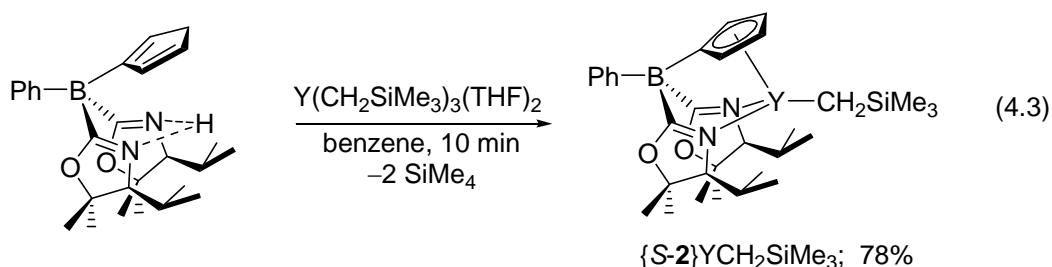
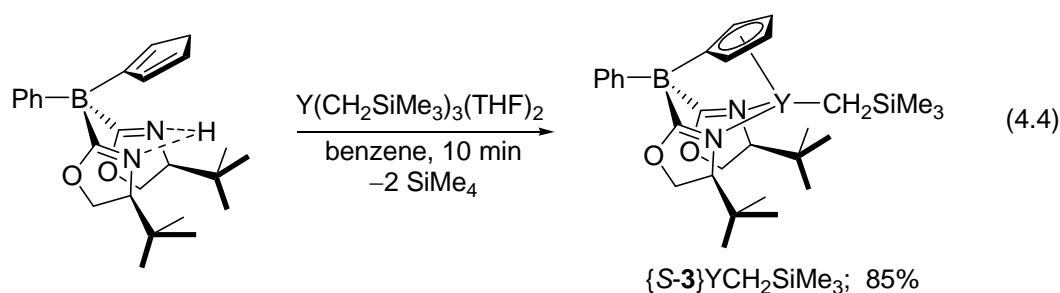


**Table 4.1.** <sup>11</sup>B, <sup>15</sup>N NMR chemical shifts and  $\nu_{\text{CN}}$  values for cyclopentadienyl-bis(oxazolonyl)borate zirconium and yttrium complexes.

Compound	<sup>11</sup> B NMR ( $\delta$ ) benzene- <i>d</i> <sub>6</sub>	<sup>15</sup> N NMR ( $\delta$ ) benzene- <i>d</i> <sub>6</sub>	$\nu_{\text{CN}}$ (KBr, cm <sup>-1</sup> )
{PhB(C <sub>5</sub> H <sub>4</sub> )(Ox <sup>4<i>S</i>-<i>i</i>Pr,Me<sub>2</sub></sup> ) <sub>2</sub> }Zr(NMe <sub>2</sub> ) <sub>2</sub> { <i>S</i> -2}Zr(NMe <sub>2</sub> ) <sub>2</sub>	-14.5	-152.6, -155.0	1565
[{PhB(C <sub>5</sub> H <sub>4</sub> )(Ox <sup>4<i>S</i>-<i>i</i>Pr,Me<sub>2</sub></sup> ) <sub>2</sub> }Zr(NMe <sub>2</sub> )] [B(C <sub>6</sub> F <sub>5</sub> ) <sub>4</sub> ] [ <i>S</i> -2}Zr(NMe <sub>2</sub> )] [B(C <sub>6</sub> F <sub>5</sub> ) <sub>4</sub> ]	-15.1, -15.9	-159.1, -164.4	1554
{PhB(C <sub>5</sub> H <sub>4</sub> )(Ox <sup>Me<sub>2</sub></sup> ) <sub>2</sub> }YCH <sub>2</sub> SiMe <sub>3</sub> { <b>1</b> }YCH <sub>2</sub> SiMe <sub>3</sub>	-15.2	n.a.	1549
{PhB(C <sub>5</sub> H <sub>4</sub> )(Ox <sup>4<i>S</i>-<i>i</i>Pr,Me<sub>2</sub></sup> ) <sub>2</sub> }YCH <sub>2</sub> SiMe <sub>3</sub> { <i>S</i> -2}YCH <sub>2</sub> SiMe <sub>3</sub>	-15.9	-154.4, -156.8	1558
{PhB(C <sub>5</sub> H <sub>4</sub> )(Ox <sup><i>S</i>-<i>t</i>Bu</sup> ) <sub>2</sub> }YCH <sub>2</sub> SiMe <sub>3</sub> { <i>S</i> -3}YCH <sub>2</sub> SiMe <sub>3</sub>	-15.7	-148.5, -150.2	1586
Tl <sub>2</sub> [PhB(C <sub>5</sub> H <sub>4</sub> )(Ox <sup>Me<sub>2</sub></sup> ) <sub>2</sub> ] Tl <sub>2</sub> { <b>1</b> }	-17.0	-99.8	1578, 1567
{PhB(C <sub>5</sub> H <sub>4</sub> )(Ox <sup>Me<sub>2</sub></sup> ) <sub>2</sub> }YNH <sup><i>t</i></sup> Bu { <b>1</b> }YNH <sup><i>t</i></sup> Bu	-15.8	-146.6	1577
Tl <sub>2</sub> [PhB(C <sub>5</sub> H <sub>4</sub> )(Ox <sup><i>S</i>-<i>t</i>Bu</sup> ) <sub>2</sub> ] Tl <sub>2</sub> { <i>S</i> -3}	-16.0	-125.2	1559

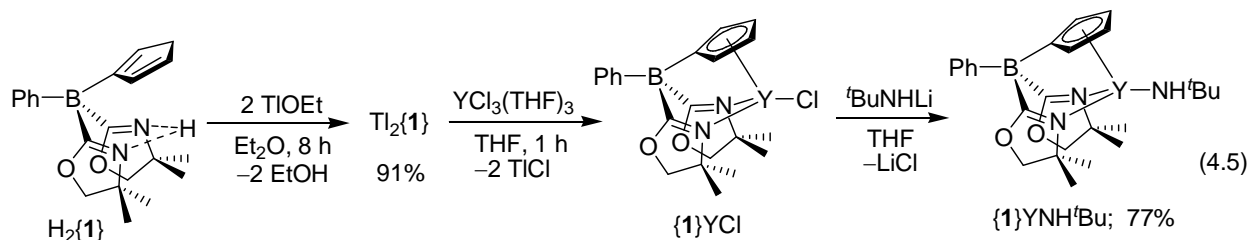
$\{\text{PhB}(\text{C}_5\text{H}_4)(\text{Ox}^{S\text{-}t\text{Bu}})_2\}\text{YCl}$	-15.9	-148.5, -150.2.	1552
$\{S\text{-}3\}\text{YCl}$			

Another optically active yttrium complex  $\{\text{PhB}(\text{C}_5\text{H}_4)(\text{Ox}^{S\text{-}t\text{Bu}})_2\}\text{YCH}_2\text{SiMe}_3$  ( $\{S\text{-}3\}\text{YCH}_2\text{SiMe}_3$ ) is prepared by reaction of  $\text{Y}(\text{CH}_2\text{SiMe}_3)_3(\text{THF})_2$  and chiral proligand  $\text{H}[\text{PhB}(\text{C}_5\text{H}_5)(\text{Ox}^{S\text{-}t\text{Bu}})_2]$  [ $\text{H}_2\{S\text{-}3\}$ ] in benzene at room temperature (eq 4.4).  $\{S\text{-}3\}\text{YCH}_2\text{SiMe}_3$  is  $C_1$ -symmetric as shown by two sets of oxazoline resonances and four downfield cyclopentadienyl resonances (6.82, 6.77, 6.64 and 6.53 ppm) in its  $^1\text{H}$  NMR spectrum. Symmetry cannot establish the coordination geometry, however the  $^{15}\text{N}$  NMR chemical shifts (-148.5 and -150.2 ppm) are upfield of  $4S\text{-}2\text{H-Ox}^{t\text{Bu}}$  (-148.0 ppm).<sup>33</sup> A single strong  $\nu_{\text{CN}}$  band at  $1586\text{ cm}^{-1}$  (KBr) in the IR spectrum, which is also lower in energy than free  $4S\text{-}2\text{H-Ox}^{t\text{Bu}}$  ( $1635\text{ cm}^{-1}$ ) suggests that both oxazolines are coordinated to yttrium. A sharp resonance at -15.7 ppm in the  $^{11}\text{B}$  spectrum indicates that a single product is formed.  $\{S\text{-}3\}\text{YCH}_2\text{SiMe}_3$  is stable in benzene for about 2 h at room temperature followed by slow decomposition by elimination of  $\text{SiMe}_4$ .



An achiral yttrium amido complex  $\{\mathbf{1}\}\text{YNH}^t\text{Bu}$  and its optically active analog  $\{S\text{-}3\}\text{YNH}^t\text{Bu}$  are synthesized *via* salt metathesis route. The reaction of  $\text{H}_2\{\mathbf{1}\}$  with two equiv of TIOEt in  $\text{Et}_2\text{O}$  for 8 h provides the thallium salt of achiral cyclopentadienyl-bis(oxazoliny)borate ligand  $[\text{Tl}_2\{\mathbf{1}\}]$  in 91% yield (eq 4.5). The  $^1\text{H}$  NMR multiplets of three

$C_5H_5B$  isomers of  $H_2\{1\}$  are replaced with two resonances (6.18 and 5.84 ppm). One  $^{11}B$  NMR resonance was observed at  $-17.0$  ppm.



X-ray quality single crystals are obtained from concentrated solution of  $Et_2O$  cooled to  $-30$  °C, and the ORTEP view of the crystal structure is presented in Figure 4.1.  $Tl_2[PhB(Ox^{Me_2})_2Cp]$  is monomeric in the solid state. Two thallium atoms are in opposite face of  $C_5H_4$  ring. One of the thallium atoms (Tl1) is dicoordinated by nitrogen atom (N1) of an oxazoline and a carbon atom of  $C_5H_4$  ring. Second thallium atom (Tl2) is  $\eta^5$ -coordinated to the  $C_5H_4$  ring and to the nitrogen atom (N2) of the second oxazoline. The  $C_5H_4$  is unsymmetrically bonded to Tl2 with Tl–C bond lengths ranging from 2.687(16) to 2.881(18) Å. The two Tl–N<sub>oxazoline</sub> distances are within 0.01 Å [Tl1–N1, 2.705(15); Tl2–N2, 2.695(14) Å].

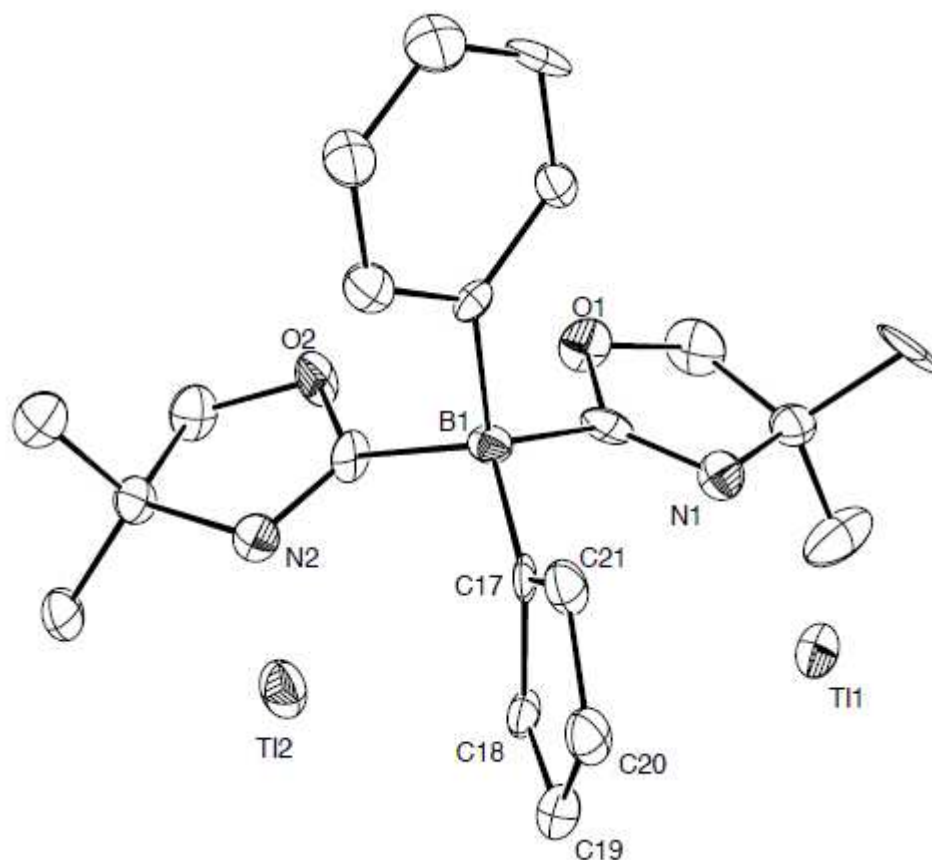


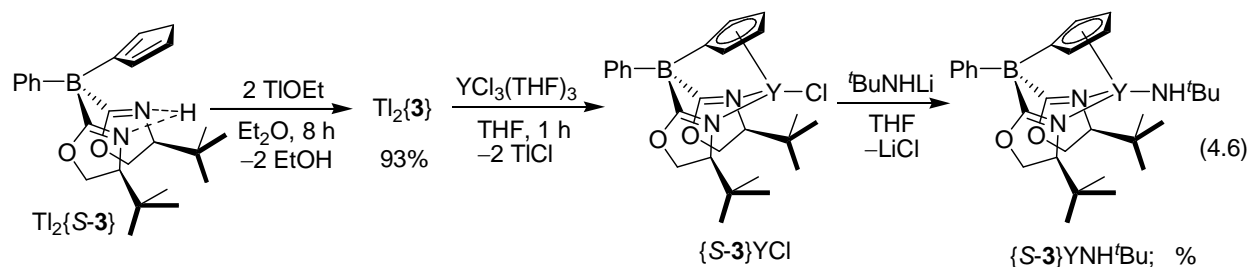
**Figure 4.1.** ORTEP diagram of  $\text{Tl}_2[\text{PhB}(\text{Ox}^{\text{Me}_2})_2\text{Cp}]$  [ $\text{Tl}_2\{\mathbf{1}\}$ ]. Ellipsoids are plotted at 50% probability, and hydrogen atoms are not illustrated for clarity. Selected bond distances ( $\text{\AA}$ ):  $\text{Tl1-N1}$ , 2.705(15);  $\text{Tl1-C21}$ , 2.896(18);  $\text{Tl2-N2}$ , 2.695(14);  $\text{Tl2-C17}$ , 2.687(16);  $\text{Tl2-C18}$ , 2.721(16);  $\text{Tl2-C19}$ , 2.881(18);  $\text{Tl2-C21}$ , 2.848(17).

$\text{Tl}_2\{\mathbf{1}\}$  reacts with  $\text{YCl}_3(\text{THF})_3$  in THF at room temperature to afford  $\{\text{PhB}(\text{C}_5\text{H}_4)(\text{Ox}^{\text{Me}_2})_2\}\text{YCl}$  ( $\{\mathbf{1}\}\text{YCl}$ ). The  $^1\text{H}$  NMR spectrum in tetrahydrofuran- $d_8$  contained one set of oxazoline resonances (*e.g.*, two singlets for methyl groups at 1.18 and 1.17 ppm, two doublets at 3.84 and 3.77 ppm for methylene groups) and two multiplets for  $\text{C}_5\text{H}_4\text{B}$  group (6.26 and 6.05 ppm) suggesting a  $\text{C}_s$ -symmetric species. One  $^{11}\text{B}$  resonance at  $-16.0$  ppm suggested the formation of a single product. Unfortunately,  $\{\mathbf{1}\}\text{YCl}$  decomposes upon evaporation of THF, and is unable to isolate. Therefore,  $\{\mathbf{1}\}\text{YCl}$  is prepared *in situ* for the synthesis of the desire

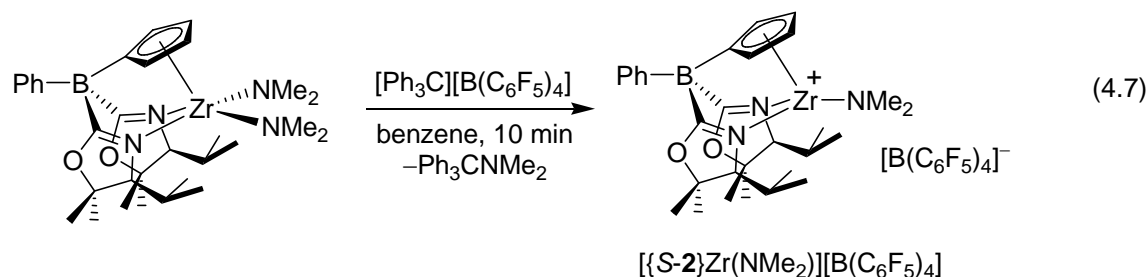


compound  $\{\mathbf{1}\}\text{YNH}^t\text{Bu}$ .  $\{\mathbf{1}\}\text{YNH}^t\text{Bu}$  is prepared by treatment of one equiv of  $^t\text{BuNHLi}$  to THF solution of  $\{\mathbf{1}\}\text{YCl}$  prepared *in situ*. After removal of LiCl and volatiles,  $\{\mathbf{1}\}\text{YNH}^t\text{Bu}$  is obtained as a white solid in 77% yield (eq 4.5). Unlike  $\{\mathbf{1}\}\text{YCH}_2\text{SiMe}_3$ ,  $\{\mathbf{1}\}\text{YNH}^t\text{Bu}$  is unchanged in THF even after 7 days at room temperature. The  $^1\text{H}$  NMR of  $\{\mathbf{1}\}\text{YNH}^t\text{Bu}$  in tetrahydrofuran- $d_8$  showed broad resonances of oxazolines and cyclopentadienyl protons. One single  $^{11}\text{B}$  peak was observed at  $-15.8$  ppm. Upon cooling to 220 K, the proton resonances became sharp and revealed a  $C_1$ -symmetric species. Four singlets in a 1:1:1:1 for four methyl groups and a pair of doublets for methylene protons of oxazolines, and four multiplets of  $\text{C}_5\text{H}_4\text{B}$  were observed for  $\{\mathbf{1}\}\text{YNH}^t\text{Bu}$ . The variable temperature NMR experiments suggest that  $\{\mathbf{1}\}\text{YNH}^t\text{Bu}$  is fluxional in solution due to dissociation and coordination of oxazolines to yttrium. At 220 K, this dynamic process is slower than NMR time scale, and thus  $C_1$ -symmetric species is observed.

The optically active yttrium amide complex  $\{\text{PhB}(\text{C}_5\text{H}_4)(\text{Ox}^{S-t\text{Bu}})_2\}\text{YNH}^t\text{Bu}$  [ $\{S\text{-}\mathbf{3}\}\text{NH}^t\text{Bu}$ ] is synthesized using  $\text{H}_2\{S\text{-}\mathbf{3}\}$  (eq 4.6).  $\text{Ti}_2\{S\text{-}\mathbf{3}\}$  is first prepared by reaction of  $\text{H}_2\{S\text{-}\mathbf{3}\}$  and  $\text{TiOEt}$  in 93% yield. The treatment of  $\text{Ti}_2\{S\text{-}\mathbf{3}\}$  with  $\text{YCl}_3(\text{THF})_3$  affords  $\{\text{PhB}(\text{C}_5\text{H}_4)(\text{Ox}^{S-t\text{Bu}})_2\}\text{YCl}$  ( $\{S\text{-}\mathbf{3}\}\text{YCl}$ ) as a white solid in 89% isolated yield. The  $^1\text{H}$  NMR resonances associated with the ancillary ligand indicated  $\{S\text{-}\mathbf{3}\}\text{YCl}$  as  $C_1$ -symmetric as expected. In the next step,  $\{S\text{-}\mathbf{3}\}\text{YCl}$  reacts with one equiv of  $^t\text{BuNHLi}$  in THF at room temperature to provide  $\{S\text{-}\mathbf{3}\}\text{NH}^t\text{Bu}$  in 83% yield (eq 4.6). In the  $^1\text{H}$  NMR spectrum of  $\{S\text{-}\mathbf{3}\}\text{NH}^t\text{Bu}$ , two singlet resonances at 0.97 and 0.91 ppm were assigned to *tert*-butyl substituents on two inequivalent oxazoline groups, and four downfield multiplets ranging from 6.55 to 5.96 ppm were assigned to the cyclopentadienyl group.



Additionally, an optically active cationic zirconium complex is synthesized to compare the catalytic activity in hydroamination and also the configuration of amine products with analogous yttrium and neutral tetravalent zirconium catalysts. The treatment of  $\{S-2\}Zr(NMe_2)_2$  with one equiv of  $[Ph_3C][B(C_6F_5)_4]$  in benzene at room temperature affording  $[\{S-2\}Zr(NMe_2)][B(C_6F_5)_4]$  as a light yellow solid in 73.4% yield (eq 4.7). The  $^1H$  NMR in bromobenzene- $d_5$  showed two septets, four doublets and four singlets assigned to oxazoline isopropyl and methyl groups for  $C_1$ -symmetric  $[\{S-2\}Zr(NMe_2)][B(C_6F_5)_4]$ . One strong  $\nu_{CN}$  band at  $1554\text{ cm}^{-1}$  (KBr) was observed in the IR spectrum.

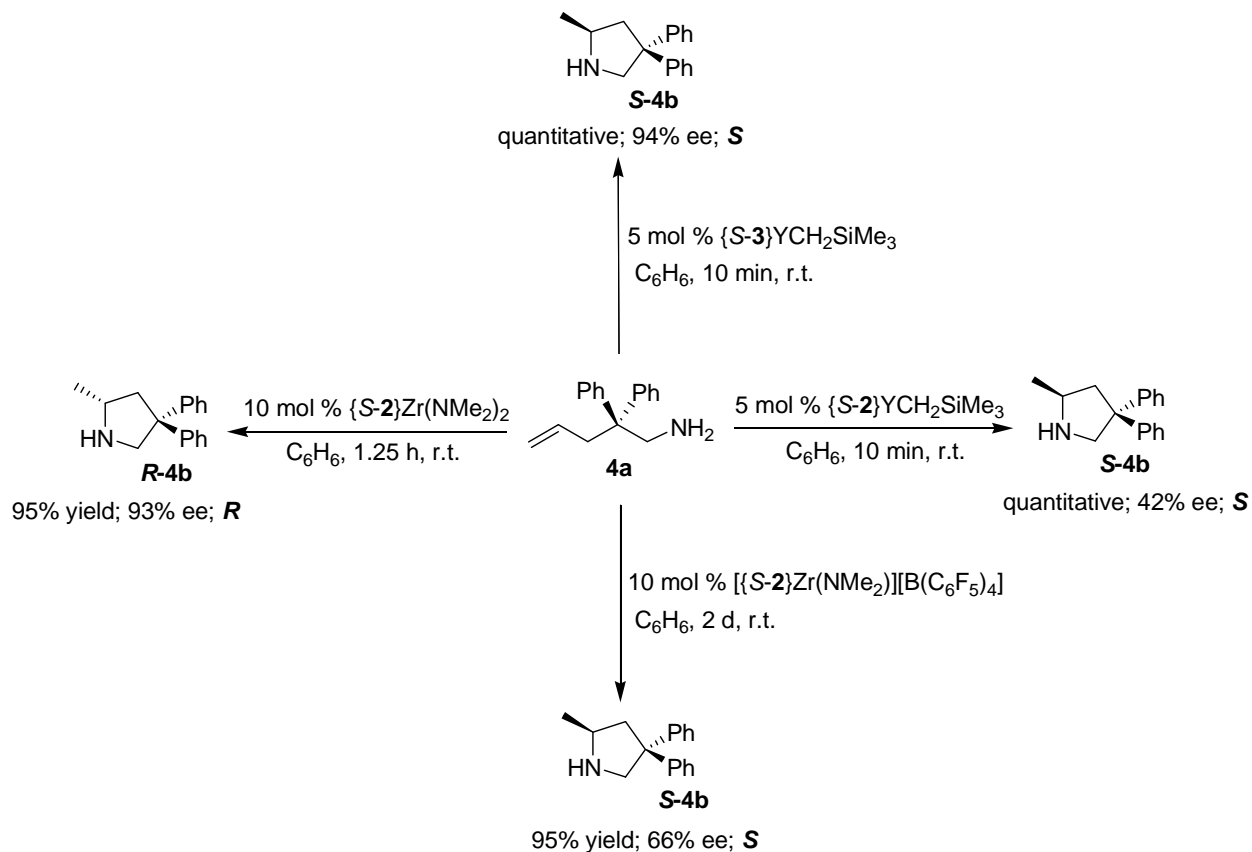


### ***Catalytic Hydroamination/Cyclization of Aminoalkenes.***

The cyclopentadienyl-bis(oxazolonyl)borate coordinated neutral yttrium alkyl and cationic zirconium monoamide complexes are tested as precatalysts for the cyclization of aminoolefins to cyclic amines at room temperature. The enantioselectivities were determined by integration of  $^{19}F$  NMR spectra of Mosher-amide derivatives and by HPLC analysis using chiral stationary phase column.

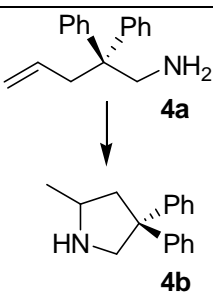
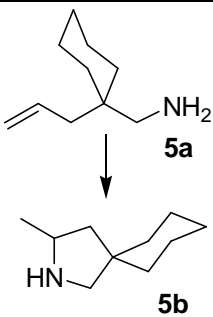
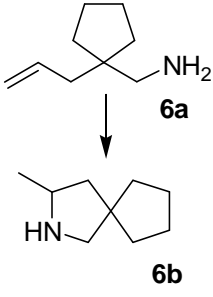
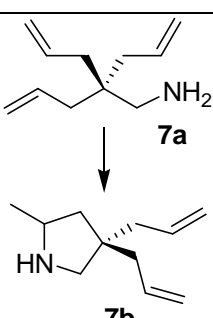
The achiral  $\{1\}YCH_2SiMe_3$  is a precatalyst for cyclization of primary and secondary aminoalkenes at room temperature, providing racemic cyclic amines in excellent yields (Table 4.2; entries 1, 6, 11, 16, 21, 26). The optically active yttrium alkyl complexes  $\{S-2\}YCH_2SiMe_3$  and  $\{S-3\}YCH_2SiMe_3$  are also precatalysts in cyclohydroamination of aminoolefins at room temperature. However, the ancillary ligands in these precatalysts affect the enantioselectivity significantly, following the trend  $\{S-3\}YCH_2SiMe_3 > \{S-2\}YCH_2SiMe_3$ . This trend is opposite for neutral zirconium catalysts, where  $\{S-2\}Zr(NMe_2)_2$  is more enantioselective than  $\{S-3\}Zr(NMe_2)_2$ .<sup>27,33</sup> Interestingly, the absolute configuration of the product depends on the nature of the metal center as shown in Scheme 4.2.  $\{S-2\}YCH_2SiMe_3$  provides *S*-pyrrolidine (**S-4b**) from 2,2-diphenyl-4-penten-1-amine (**4a**), whereas *R*-pyrrolidine (**R-4b**) is obtained from  $\{S-2\}Zr(NMe_2)_2$  even though both catalysts contain identical  $\{S-2\}$ -chiral ancillary ligand. The change of stereoinduction during cyclization is also observed between  $\{S-3\}$ -coordinated neutral yttrium and zirconium catalysts.  $\{S-3\}YCH_2SiMe_3$  and  $\{S-3\}Zr(NMe_2)_2$  catalyze cyclization of **4a** to provide *S-4b* and *R-4b* respectively (Scheme 4.2 and Table 4.2). Additionally, the configurational flip of products is observed between cationic zirconium monoamide complex  $[\{S-2\}Zr(NMe_2)][B(C_6F_5)_4]$  and neutral zirconium bisamide complex  $\{S-2\}Zr(NMe_2)_2$ .  $[\{S-2\}Zr(NMe_2)][B(C_6F_5)_4]$  is less active and enantioselective than  $\{S-2\}Zr(NMe_2)_2$  in cyclization of aminopentenes providing *S*-pyrrolidines as the major enantiomer.

**Scheme 4.2.** Cyclization of 2,2-diphenylaminopentene **4a** and absolute configuration of products **4b** for optically active Y- and Zr-catalyzed hydroamination



In general, the chiral yttrium precatalysts cyclize several aminoalkenes to give optically active pyrrolidines, piperidines, and azepanes at room temperature, and these results are summarized in Table 4.2-4.3. These tables are organized by substrate type: Table 4.2 shows conditions and products in cyclization of aminopentenes **4a-9a** that have aliphatic or aromatic 2,2-disubstitution; Table 4.3 contains cyclizations of functionalized substrates **10a-11a** that give halogenated and acetal, and also contains 6- and 7-membered rings from substrates **13a-14a**.

**Table 4.2.** Cyclization of aminoalkenes and absolute configurations of products for Y- and Zr-catalyzed hydroamination<sup>a</sup>

Substrate	Entry	Precatalyst <sup>b</sup>	Time	Yield (%) <sup>c</sup>	ee (%) <sup>d</sup>
 <p>4a</p> <p>4b</p>	1	{ <b>1</b> }YCH <sub>2</sub> SiMe <sub>3</sub>	10 min	100	racemic
	2	{ <i>S</i> - <b>2</b> }YCH <sub>2</sub> SiMe <sub>3</sub>	10 min	100	42 ( <i>S</i> )
	3	{ <i>S</i> - <b>3</b> }YCH <sub>2</sub> SiMe <sub>3</sub>	10 min	100 (93)	94 ( <i>S</i> )
	4	[{ <i>S</i> - <b>2</b> }Zr(NMe <sub>2</sub> )][B(C <sub>6</sub> F <sub>5</sub> ) <sub>4</sub> ]	2 d	95	66 ( <i>S</i> )
	5	{ <i>S</i> - <b>2</b> }Zr(NMe <sub>2</sub> ) <sub>2</sub>	1.25 h	95	93 ( <i>R</i> )
 <p>5a</p> <p>5b</p>	6	{ <b>1</b> }YCH <sub>2</sub> SiMe <sub>3</sub>	10 min	100	racemic
	7	{ <i>S</i> - <b>2</b> }YCH <sub>2</sub> SiMe <sub>3</sub>	10 min	100	34 ( <i>S</i> )
	8	{ <i>S</i> - <b>3</b> }YCH <sub>2</sub> SiMe <sub>3</sub>	10 min	100 (95)	93 ( <i>S</i> )
	9	[{ <i>S</i> - <b>2</b> }Zr(NMe <sub>2</sub> )][B(C <sub>6</sub> F <sub>5</sub> ) <sub>4</sub> ]	3 d	90	79 ( <i>S</i> )
	10	{ <i>S</i> - <b>2</b> }Zr(NMe <sub>2</sub> ) <sub>2</sub>	1.25 h	95	90 ( <i>R</i> )
 <p>6a</p> <p>6b</p>	11	{ <b>1</b> }YCH <sub>2</sub> SiMe <sub>3</sub>	10 min	100	racemic
	12	{ <i>S</i> - <b>2</b> }YCH <sub>2</sub> SiMe <sub>3</sub>	10 min	100	34 ( <i>S</i> )
	13	{ <i>S</i> - <b>3</b> }YCH <sub>2</sub> SiMe <sub>3</sub>	3 h	95	89 ( <i>S</i> )
	14	[{ <i>S</i> - <b>2</b> }Zr(NMe <sub>2</sub> )][B(C <sub>6</sub> F <sub>5</sub> ) <sub>4</sub> ]	3 d	92	81 ( <i>S</i> )
	15	{ <i>S</i> - <b>2</b> }Zr(NMe <sub>2</sub> ) <sub>2</sub>	4 h	88	92 ( <i>R</i> )
 <p>7a</p> <p>7b</p>	16	{ <b>1</b> }YCH <sub>2</sub> SiMe <sub>3</sub>	10 min	100	racemic
	17	{ <i>S</i> - <b>2</b> }YCH <sub>2</sub> SiMe <sub>3</sub>	10 min	100	51 ( <i>S</i> )
	18	{ <i>S</i> - <b>3</b> }YCH <sub>2</sub> SiMe <sub>3</sub>	10 min	100 (97)	96 ( <i>S</i> )
	19	[{ <i>S</i> - <b>2</b> }Zr(NMe <sub>2</sub> )][B(C <sub>6</sub> F <sub>5</sub> ) <sub>4</sub> ]	2 d	92	69 ( <i>S</i> )
	20	{ <i>S</i> - <b>2</b> }Zr(NMe <sub>2</sub> ) <sub>2</sub>	0.75 h	98	93 ( <i>R</i> )

<p><b>8a</b></p> <p><b>8b</b></p>	21	{ <b>1</b> }YCH <sub>2</sub> SiMe <sub>3</sub>	25 min	100 d.r. = 1.2:1	racemic
	22	{ <i>S</i> - <b>2</b> }YCH <sub>2</sub> SiMe <sub>3</sub>	10 min	100 d.r. = 1.2:1	43, 40
	23	{ <i>S</i> - <b>3</b> }YCH <sub>2</sub> SiMe <sub>3</sub>	15 min	100 (95) d.r. = 1.2:1	95, 95
	24	[[ <i>S</i> - <b>2</b> ]Zr(NMe <sub>2</sub> )][B(C <sub>6</sub> F <sub>5</sub> ) <sub>4</sub> ]	2 d	94 d.r. = 1.4:1	72, 67
	25	{ <i>S</i> - <b>2</b> }Zr(NMe <sub>2</sub> ) <sub>2</sub>	30 min	95 d.r. = 1.1:1	93, 92
<p><b>9a</b></p> <p><b>9b</b></p>	26	{ <b>1</b> }YCH <sub>2</sub> SiMe <sub>3</sub>	15 min	100 d.r. = 1.1:1	racemic
	27	{ <i>S</i> - <b>2</b> }YCH <sub>2</sub> SiMe <sub>3</sub>	10 min	100 d.r. = 1.2:1	46, 42
	28	{ <i>S</i> - <b>3</b> }YCH <sub>2</sub> SiMe <sub>3</sub>	15 min	100 (96) d.r. = 1.2:1	95, 96
	29	[[ <i>S</i> - <b>2</b> ]Zr(NMe <sub>2</sub> )][B(C <sub>6</sub> F <sub>5</sub> ) <sub>4</sub> ]	2 d	100 d.r. = 1.5:1	84, 83
	30	{ <i>S</i> - <b>2</b> }Zr(NMe <sub>2</sub> ) <sub>2</sub>	30 min	95 d.r. = 3.3:1	96, 96

<sup>a</sup> Reaction conditions: C<sub>6</sub>H<sub>6</sub>, r.t. <sup>b</sup> Catalyst loading Zr: 10 mol %; Y: 5 mol %. <sup>c</sup> Yield of isolated product is given in parentheses. <sup>d</sup> % ee ( $\pm 0.5\%$ ) was determined by <sup>19</sup>F NMR spectra of Mosher amide derivatives. Absolute configuration assignments based on literature reports.<sup>17</sup>

The enantioselectivities of reactions catalyzed by {*S*-**3**}YCH<sub>2</sub>SiMe<sub>3</sub> are high for a range of aminopentene and aminoheptene substrates. A series of pyrrolidines such as diphenylpyrrolidine (**4b**; 94% ee), spiro-cyclohexyl-pyrrolidine (**5b**; 93%), cyclopentyl-pyrrolidine (**6b**; 89%), and diallyl-pyrrolidine (**7b**; 96%) are afforded at room temperature with excellent optical purities (Table 4.2). {*S*-**3**}YCH<sub>2</sub>SiMe<sub>3</sub> also catalyzes cyclization of 2-allyl-2-methyl-pent-4-enylamine (**8a**) and 2-allyl-2-phenyl-pent-4-enylamine (**9a**) at room temperature to provide diastereomeric mixture of *cis* and *trans* pyrrolidines (Table 4.2; entries 23 and 28). Although the distereoselectivity (*cis:trans*) is poor, however impressively, the enantiomeric excesses of **8b** (*cis*: 95% ee; *trans*: 95% ee; d.r.; *cis:trans* = 1:1.2) and **9b** (*cis*: 95% ee; *trans*: 96% ee; d.r.; *cis:trans* = 1.2:1) are very high for both diastereomers. No significant effects of temperature and concentration on enantioselectivity and *cis/trans* ratio were observed.

In contrast to  $\{S-3\}YCH_2SiMe_3$ ,  $\{S-2\}YCH_2SiMe_3$  is much less enantioselective regardless of the substrate.  $\{S-2\}YCH_2SiMe_3$  provides *S*-pyrrolidines (**4b-9b**) at room temperature with 34-51% ee (Table 4.2; entries 2, 7, 12, 17, 22, and 27). Changing the reaction conditions such as temperature, concentration and catalysts loading don't improve the enantioselectivity.

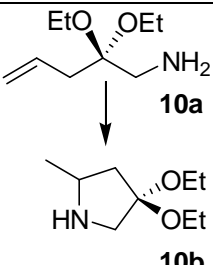
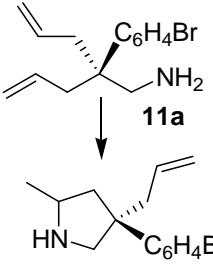
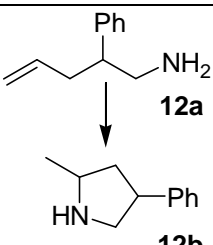
The cationic zirconium  $[\{S-2\}Zr(NMe_2)][B(C_6F_5)_4]$  is relatively lower active and enantioselective in cyclohydroamination compared to  $\{S-3\}YCH_2SiMe_3$  and  $\{S-2\}Zr(NMe_2)_2$ , and therefore longer reaction time is required. For example, 2,2-diphenyl-4-penten-1-amine (**4a**) is cyclized by  $[\{S-2\}Zr(NMe_2)][B(C_6F_5)_4]$  at room temperature over 2 days to afford *S*-diphenylpyrrolidine (**S-4b**) in 66% ee (Table 4.2; entry 4), whereas  $\{S-2\}Zr(NMe_2)_2$  affords **R-4b** at room temperature in 93% ee within 1.25 h (Table 4.2; entry 5). Relatively lower optical purities are also observed for other azacycles mediated by  $[\{S-2\}Zr(NMe_2)][B(C_6F_5)_4]$  (**S-5b**: 79%; **S-7b**: 69%) in comparison to  $\{S-2\}Zr(NMe_2)_2$  (**S-5b**: 90%; **S-7b**: 93%).

The high enantioselectivity of  $\{S-3\}YCH_2SiMe_3$  in aminopentene cyclization motivated further study of the formation of other five-membered rings containing oxo- or halogen-functional groups. 2,2-Diethoxypent-4-enenylamine (**10a**) is cyclized by  $\{S-3\}YCH_2SiMe_3$  affording diethoxy-pyrrolidine (**10b**) in 4 h at room temperature with 94% ee (Table 4.3; entry 3). The  $\{S-2\}YCH_2SiMe_3$  and achiral  $\{1\}YCH_2SiMe_3$  also catalyze the cyclization at approximately the same rate as  $\{S-3\}YCH_2SiMe_3$ , however,  $[\{S-2\}Zr(NMe_2)][B(C_6F_5)_4]$  is inactive even at elevated temperature with prolonged reaction time.

2-Allyl-2-(4-bromophenyl)pent-4-enylamine (**11a**) is cyclized quantitatively by achiral  $\{1\}YCH_2SiMe_3$  to a 2.7:1 diastereomeric mixture of *cis* and *trans* pyrrolidines within 10 min at room temperature (Table 4.3; entry 5). The optically active  $\{S-2\}YCH_2SiMe_3$  precatalyst is also

efficient in cyclization of **11a**, however it provides **11b** with low diastereomeric ratio (*cis:trans* = 2:1) and low optical purity (*cis*: 38% ee; *trans*: 33% ee) (Table 4.3; entry 6). Not surprisingly,  $\{S-3\}YCH_2SiMe_3$  again displays high enantioselectivity for cyclization of **11a**. Although the distereoselectivity (*cis:trans* = 2:1) is low, 95% ee for *cis*-**11b** and 92% ee of *trans*-**11b** are obtained at room temperature (Table 4.3; entry 7).

**Table 4.3.** Catalytic hydroamination/cyclization of aminoalkenes. <sup>a</sup>

Substrate	Entry	Precatalyst <sup>b</sup>	Time	Yield (%) <sup>c</sup>	ee (%) <sup>d</sup>
 <b>10a</b> <b>10b</b>	1	$\{1\}YCH_2SiMe_3$	4 h	90	racemic
	2	$\{S-2\}YCH_2SiMe_3$	4 h	95	23 ( <i>S</i> )
	3	$\{S-3\}YCH_2SiMe_3$	4 h	90	94 ( <i>S</i> )
	4	$[\{S-2\}Zr(NMe_2)][B(C_6F_5)_4]$	2 d	0	n.a.
 <b>11a</b> <b>11b</b>	5	$\{1\}YCH_2SiMe_3$	10 min	100	racemic
	6	$\{S-2\}YCH_2SiMe_3$	15 min	100	d.r. = 2.7:1 38, 33
	7	$\{S-3\}YCH_2SiMe_3$	15 min	100 (94)	d.r. = 2:1 95, 92
	8	$[\{S-2\}Zr(NMe_2)][B(C_6F_5)_4]$	1.5 d	100	d.r. = 1.9:1 73, 65
 <b>12a</b> <b>12b</b>	9	$\{1\}YCH_2SiMe_3$	3 h	100	racemic
	10	$\{S-2\}YCH_2SiMe_3$	2.5 h	100	63, 56
	11	$\{S-3\}YCH_2SiMe_3$	2.5 h	100 (93)	21, 20
	12	$[\{S-2\}Zr(NMe_2)][B(C_6F_5)_4]$	3 d	20	n.a.



	13	{ <b>1</b> }YCH <sub>2</sub> SiMe <sub>3</sub>	6 h	100	racemic
	14	{ <i>S</i> - <b>2</b> }YCH <sub>2</sub> SiMe <sub>3</sub>	50 min	100	22 ( <i>S</i> )
	15	{ <i>S</i> - <b>3</b> }YCH <sub>2</sub> SiMe <sub>3</sub>	20 h	87	58 ( <i>S</i> )
	16	[{ <i>S</i> - <b>2</b> }Zr(NMe <sub>2</sub> )][B(C <sub>6</sub> F <sub>5</sub> ) <sub>4</sub> ]	2 d	85	41 ( <i>S</i> )
	17	{ <b>1</b> }YCH <sub>2</sub> SiMe <sub>3</sub>	2 d	84	racemic
	18	{ <i>S</i> - <b>2</b> }YCH <sub>2</sub> SiMe <sub>3</sub>	3 d	92	14 ( <i>S</i> )
	19	{ <i>S</i> - <b>3</b> }YCH <sub>2</sub> SiMe <sub>3</sub>	3 d	89	84 ( <i>S</i> )
	20	[{ <i>S</i> - <b>2</b> }Zr(NMe <sub>2</sub> )][B(C <sub>6</sub> F <sub>5</sub> ) <sub>4</sub> ]	4 d	0	n.a.
	21	{ <b>1</b> }YCH <sub>2</sub> SiMe <sub>3</sub>	12 h	100	racemic
	22	{ <i>S</i> - <b>2</b> }YCH <sub>2</sub> SiMe <sub>3</sub>	20 h	100	9
	23	{ <i>S</i> - <b>3</b> }YCH <sub>2</sub> SiMe <sub>3</sub>	24 h	95	44
	24	[{ <i>S</i> - <b>2</b> }Zr(NMe <sub>2</sub> )][B(C <sub>6</sub> F <sub>5</sub> ) <sub>4</sub> ]	3 d	0	n.a.
	25	{ <i>S</i> - <b>2</b> }Zr(NMe <sub>2</sub> ) <sub>2</sub>	3 d	0	n.a.
	26	{ <b>1</b> }YCH <sub>2</sub> SiMe <sub>3</sub>	4 d	40	racemic
	27	{ <i>S</i> - <b>2</b> }YCH <sub>2</sub> SiMe <sub>3</sub>	3 d	88 ( <b>16b</b> + <b>16c</b> )	21 ( <b>16b</b> )
	28	{ <i>S</i> - <b>3</b> }YCH <sub>2</sub> SiMe <sub>3</sub>	3 d	85 ( <b>16b</b> )	70
	29	[{ <i>S</i> - <b>2</b> }Zr(NMe <sub>2</sub> )][B(C <sub>6</sub> F <sub>5</sub> ) <sub>4</sub> ]	3 d	0	n.a.
	30	{ <i>S</i> - <b>2</b> }Zr(NMe <sub>2</sub> ) <sub>2</sub>	3 d	0	n.a.

<sup>a</sup> Reaction conditions: C<sub>6</sub>H<sub>6</sub>, r.t. <sup>b</sup> Catalyst loading Zr: 10 mol %; Y: 5 mol %. <sup>c</sup> Yield of isolated product is given in parentheses. <sup>d</sup> % ee (±0.5%) was determined by <sup>19</sup>F NMR spectra of Mosher amide derivatives.

The high catalytic activity and enantioselectivity of {*S*-**3**}YCH<sub>2</sub>SiMe<sub>3</sub> in cyclization of aminopentenes motivated to prepared enantioenriched larger heterocycles. The rate of cyclization of 2,2-diphenyl-5-hexen-1-amine (**13a**) catalyzed by {*S*-**2**}YCH<sub>2</sub>SiMe<sub>3</sub> is marked decreased compared to 2,2-diphenyl-4-penten-1-amine (**4a**). In addition, the % ee of the 2-

methyl-5,5-diphenyl piperidine **13b** (58% ee; Table 4.3; entry 15) is significantly lower than the 2-methyl-4,4-diphenyl pyrrolidines (**4b**; 94% ee). Interestingly, piperidines obtained by {*S*-2} and {*S*-3}-based yttrium catalysts have *S*-configuration, whereas *R*-configured piperidines are obtained by all neutral {*S*-2} and {*S*-3}-containing group 4 catalysts.

The cyclization of aminoheptene **14a** is also slower than aminopentenes. Azepane **14b** is obtained using {*S*-2}YCH<sub>2</sub>SiMe<sub>3</sub> and {*S*-3}YCH<sub>2</sub>SiMe<sub>3</sub> at room temperature with 14% and 84% ee respectively (Table 4.3; entries 18 and 19). However, [{*S*-2}Zr(NMe<sub>2</sub>)][B(C<sub>6</sub>F<sub>5</sub>)<sub>4</sub>] is inactive to cyclize **14a** at room or elevated temperatures.

Finally, all Y- and Zr-precatalysts are tested for cyclization of secondary aminopentenes. Both {*S*-2}YCH<sub>2</sub>SiMe<sub>3</sub> and {*S*-3}YCH<sub>2</sub>SiMe<sub>3</sub> precatalysts are poor enantioselective in cyclization of *N*-methyl-2,2-diphenyl-4-penten-1-amine (**15a**) to corresponding *N*-methyl-pyrrolidine (**15b**) (Table 4.3, entries 22 and 23). *N*-Allyl-2,2-diphenylpent-4-enylamine (**16a**) is cyclized by {*S*-2}YCH<sub>2</sub>SiMe<sub>3</sub> at room temperature in benzene to give a mixture of *N*-allyl-2,2-phenyl-2-methyl-pyrrolidine (**16b**) via monocyclization and 2,2-diphenyl-6-methyl-pyrrolizine (**16c**) (mixture of *cis* and *trans*) via hydroamination/bicyclization with low enantiomeric excesses (Table 4.3, entry 27). Interestingly, {*S*-3}YCH<sub>2</sub>SiMe<sub>3</sub> provides only the monocyclized product **16b** at room temperature with 70% ee (Table 4.3, entry 28). No pyrrolizine is formed by {*S*-3}YCH<sub>2</sub>SiMe<sub>3</sub> even after 7 days at room temperature. Unfortunately, [{*S*-2}Zr(NMe<sub>2</sub>)][B(C<sub>6</sub>F<sub>5</sub>)<sub>4</sub>] is inactive to cyclize secondary amines (Table 4.3, entries 24 and 29).

### ***Spectroscopic and mechanistic features of catalytic reaction***

The high enantioselectivity in {*S*-3}YCH<sub>2</sub>SiMe<sub>3</sub> catalyzed cyclization of aminoolefins inspired us to investigate the possible catalytic mechanism. We have collected kinetic and

spectroscopic data of  $\{S\text{-}3\}\text{YCH}_2\text{SiMe}_3$  system, and compared to other reported rare earth catalysts to identify the possible catalytic pathways. Additionally, the kinetic, spectroscopic and stereochemical features of trivalent  $\{S\text{-}3\}\text{YCH}_2\text{SiMe}_3$  are compared to tetravalent  $\{S\text{-}2\}\text{Zr}(\text{NMe}_2)_2$  system to understand the change of stereoinduction during cyclization between these two systems, and obtain a model that rationalizes the stereochemical outcomes.

$\text{SiMe}_4$  and pyrrolidine are observed within 30 s of addition of *C*-(1-allyl-cyclohexyl)-methylamine (**5a**) to  $\{S\text{-}3\}\text{YCH}_2\text{SiMe}_3$  at room temperature. Although the active catalyst is not directly observed, it is formed quickly at room temperature after addition of **5a**, based on the appearance of pyrrolidine product **5b** in the  $^1\text{H}$  NMR spectrum of the reaction mixture.

For three half-lives,  $\ln[\mathbf{5a}]$  varies linearly with time to provide  $k_{\text{obs}}$ , and this is consistent with first-order dependence on substrate concentration (Figure 4.1). First-order dependence on aminoalkene concentration is uncommon for rare earth catalysts, that typically gives rate laws for aminoolefin cyclization:  $\text{rate} = k[\text{catalyst}]^1[\text{substrate}]^{0.9,17}$ . First-order substrate dependence has been reported for zirconium-,<sup>27,32</sup> yttrium-,<sup>30</sup> and alkaline-earth<sup>29a,20b</sup> metal-catalyzed aminoolefin cyclizations. A linear relationship between  $k_{\text{obs}}$  and  $[\{S\text{-}3\}\text{YCH}_2\text{SiMe}_3]$  provides the empirical rate law  $-d[\mathbf{5a}]/dt = k'[\{S\text{-}3\}\text{YCH}_2\text{SiMe}_3]^1[\mathbf{5a}]^1$  ( $k' = 0.105(5) \text{ M}^{-1} \text{ s}^{-1}$ ) (Figure 4.2)

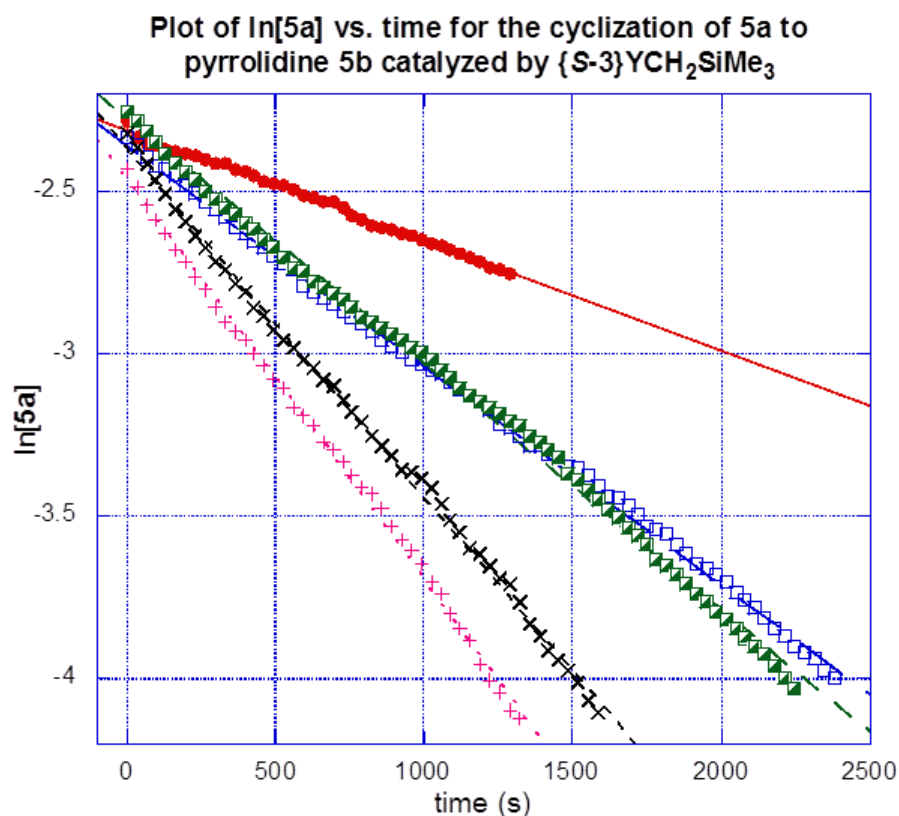


**Figure 4.1.** Plots of ln[5a] vs. time for the cyclization of *C*-(1-allyl-cyclohexyl)-methylamine catalyzed by {*S*-3}YCH<sub>2</sub>SiMe<sub>3</sub> showing first-order dependence on substrate in the cyclization at 296 K.

To measure the effect of *N*-deuteration on reactions with {*S*-3}YCH<sub>2</sub>SiMe<sub>3</sub> as precatalyst, the conversion of substrate *C*-(1-allyl-cyclohexyl)-methylamine-ND<sub>2</sub> (**5a-d<sub>2</sub>**) was investigated. Conversion of *C*-(1-allyl-cyclohexyl)-methylamine-ND<sub>2</sub> (**5a-d<sub>2</sub>**), catalyzed by [*S*-2]Zr(NMe<sub>2</sub>)<sub>2</sub>, is much slower than conversion **5a** itself. Linear least squares best fits of plots of  $k_{\text{obs}}^{(\text{D})}$  vs. catalyst concentration provide the second-order rate constant  $k'^{(\text{D})}$  [0.040(5) M<sup>-1</sup> s<sup>-1</sup>], giving a large  $k'_{\text{obs}}^{(\text{H})}/k'_{\text{obs}}^{(\text{D})}$  value equal to 2.6(4) (Figure 4.3). This primary isotope effect indicates that N–H or N–D bond is broken in the turnover-limiting step.

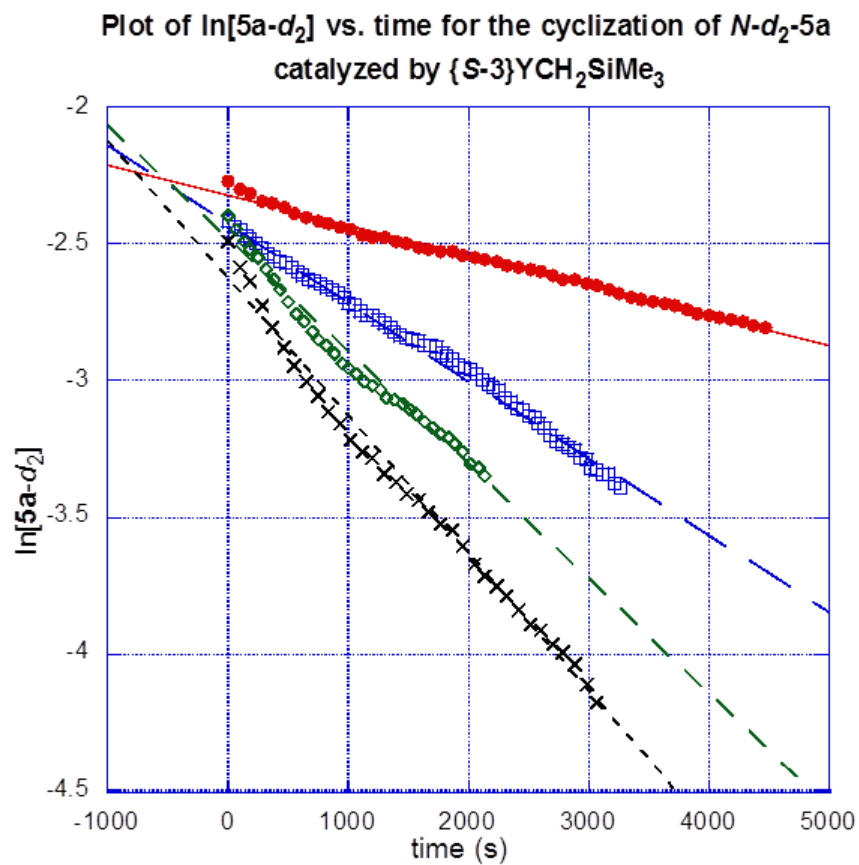


**Figure 4.2.** Plots of  $\ln[5a-d_2]$  vs. time for the conversion of  $N-d_2$  aminoalkene substrate into the corresponding pyrrolidine catalyzed by  $\{S-3\}YCH_2SiMe_3$  at 296 K.

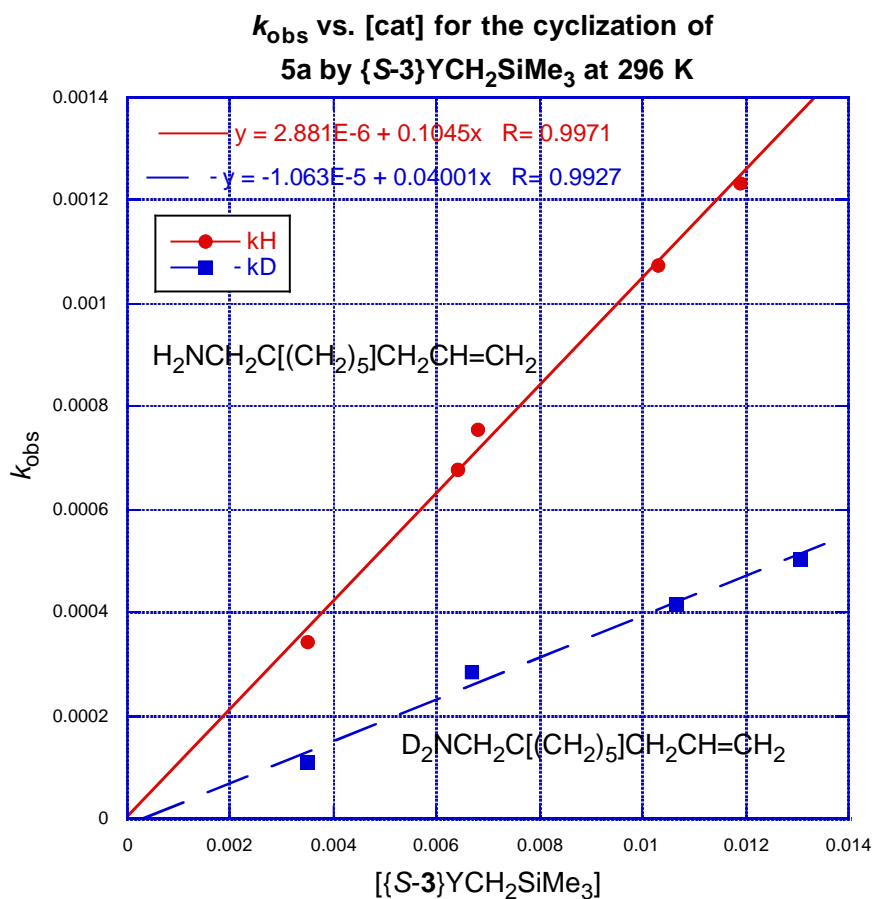


**Figure 4.3.** Plot of  $k_{\text{obs}}$  vs. catalyst concentration for the cyclization of **5a** to **5b** and **5a-d<sub>2</sub>** to **5b-d<sub>2</sub>** by {S-3}YCH<sub>2</sub>SiMe<sub>3</sub>;  $k_{\text{obs}}$  values are taken from slopes of linear regression analysis obtaining in Figures 4.1 and 4.2. The rate law for the cyclization is:  $-d[\mathbf{5a}]/dt = k'[\{\text{S-3}\}\text{YCH}_2\text{SiMe}_3]^1[\mathbf{5a}]^1$   $k' = 0.105(5) \text{ M}^{-1} \text{ s}^{-1}$  ( $k'_{\text{D}} = 0.040(5) \text{ M}^{-1} \text{ s}^{-1}$ ). The error was estimated from the standard deviation of values of  $k'$  obtained from  $k_{\text{obs}}/[\text{cat}]$ . From the slopes of the two curves,  $k_{\text{H}}/k_{\text{D}} = 2.6(4)$ .

To investigate the nature of the turnover-limiting step, the temperature dependence of the cyclization rate of **5a** was measured by determining the second order rate constant  $k'$  at different temperature ranging from 271 K to 315 K (Figure 4.4). The standard Eyring plot  $\ln(k'/T)$  vs.  $1/T$  generated from these data provides the values of activation parameters:  $\Delta H^{\ddagger} = 7.5(3) \text{ kcal}\cdot\text{mol}^{-1}$  and  $\Delta S^{\ddagger} = -38(1) \text{ cal}\cdot\text{mol}^{-1}\text{K}^{-1}$ .

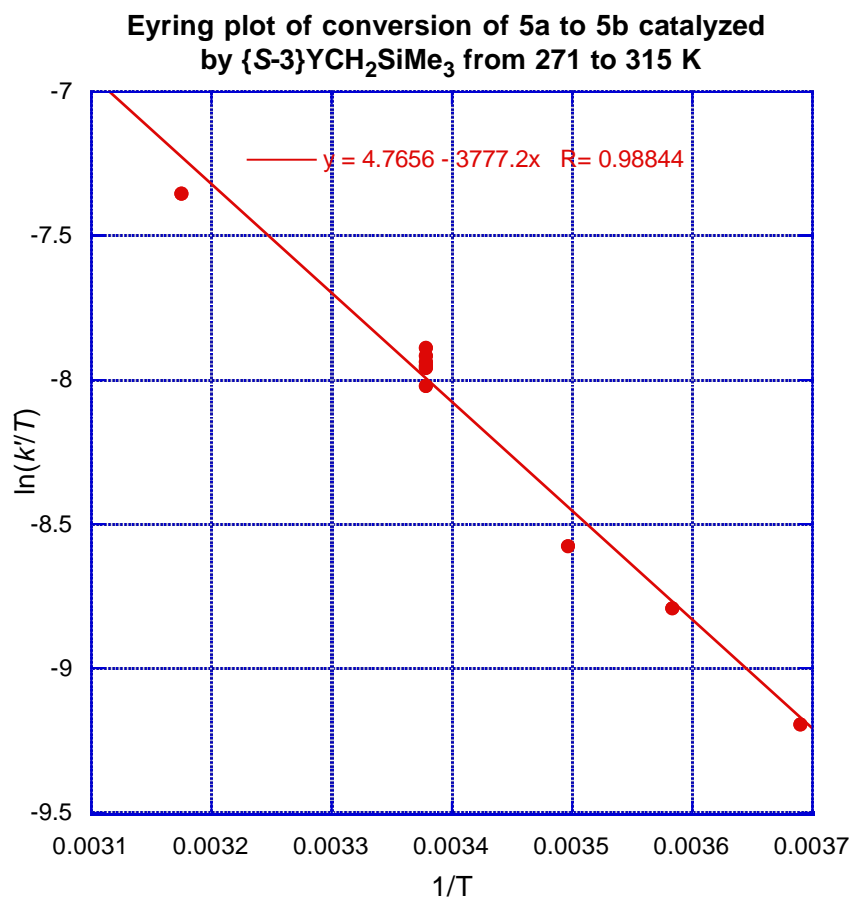
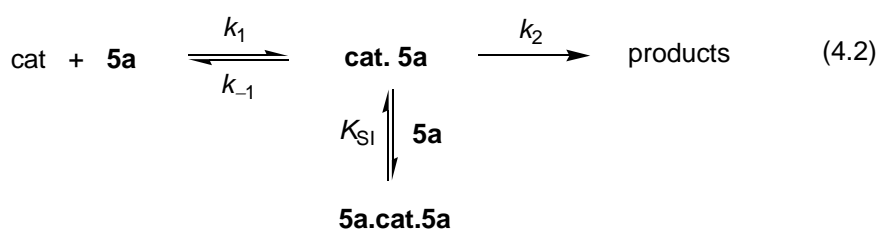


**Figure 4.4.** Plot of  $\ln(k'/T)$  vs.  $1/T$  for cyclization of **5a**. From this plot,  $\Delta H^\ddagger = 7.5(3)$  kcal mol<sup>-1</sup> and  $\Delta S^\ddagger = -38(1)$  cal mol<sup>-1</sup> K<sup>-1</sup>.

Substrate saturation on initial rate is observed in {S-3}YCH<sub>2</sub>SiMe<sub>3</sub> catalyzed hydroamination. The initial cyclization rates were measured over 8.97–118 mM [**5a**] range at constant {S-3}YCH<sub>2</sub>SiMe<sub>3</sub> concentration (5.23 mM, 296 K). The initial cyclization rate increases on increasing [**5a**] until saturation is observed at around 84 mM. At higher [**5a**] (>85 mM), the initial rates decrease slightly due to inhibitory association of another equivalent of substrate. The plot also contains a non-zero x-intercept that coincides with precatalyst concentration [{S-3}YCH<sub>2</sub>SiMe<sub>3</sub>]. A non-linear least squares regression analysis of the data provides good correlation with eq 4.1, corresponding to the reaction mechanism shown in eq 4.2

that describes the initial portion of the reaction.<sup>34</sup> At 296 °C, saturation is observed at  $[5a] = 0.045$  M ( $[cat] = 0.00523$  M). For comparison  $[5a] = 0.07$  M ( $[S-2]Zr(NMe_2)_2 = 0.0054$  M) at saturation for the  $\{S-2\}Zr(NMe_2)_2$ , *i.e.* saturation of initial rates with  $\{S-3\}YCH_2SiMe_3$  occurs as at lower substrate concentration than with  $\{S-2\}Zr(NMe_2)_2$ .

$$\frac{-d[5a]}{dt} = \frac{k_2[\{S-3\}YCH_2SiMe_3]^1 \{[5a] - [\{S-3\}YR]\}^1}{\{[5a] - [\{S-3\}YR]\} + K' + K_{SI}\{[5a] - [\{S-3\}YR]\}^2} \quad (4.1)$$



The three parameters obtained from the fit are  $k_2$  ( $2.4 \pm 0.3 \times 10^{-2} \text{ M}^{-1} \text{ s}^{-1}$ ),  $K'$  ( $1.64 \pm 0.7 \times 10^{-2} \text{ M}$ ;  $(k_{-1} + k_2)/k_1$ ), and  $K_{SI}$  ( $3.9 \pm 1 \text{ M}^{-1}$ ;  $[\text{catalyst} \cdot \text{subs}^2]/[\text{subs}][\text{catalyst} \cdot \text{subs}]$ ; substrate inhibition). The curve does not pass through the origin because one equiv of substrate is required to form the active catalyst giving the terms  $([\text{subs}] - [\text{cat}])$ ; *i.e.*, corrected substrate concentration). This analysis separates the turnover-limiting step ( $k_2$ ) from the substrate binding constant ( $K'$ ), allowing the measurement of the isotope effect ( $k_H/k_D$ ) for  $k_2$ . A non-linear least squares fit ( $R = 0.99$ ) of  $-d[5a-d_2]/dt)_{ini}$  vs.  $[5a-d_2]_{ini}$  provides a curve with the values:  $k_2^{(D)} = 7.1 \pm 0.5 \times 10^{-3} \text{ M}^{-1} \text{ s}^{-1}$ ,  $K'^{(D)} = 1.1 \pm 0.2 \times 10^{-2} \text{ M}$ , and  $K_{SI}^{(D)} = 5.6 \pm 1.3 \text{ M}^{-1}$ . The kinetic isotope effect (KIE) from initial rate plots  $k_2^{(H)}/k_2^{(D)}$  (3.5) and from second-order rate constants,  $k'_{obs}{}^{(H)}/k'_{obs}{}^{(D)} = 2.6$  indicate that N–H (or N–D) bond is broken in the turnover-limiting step.



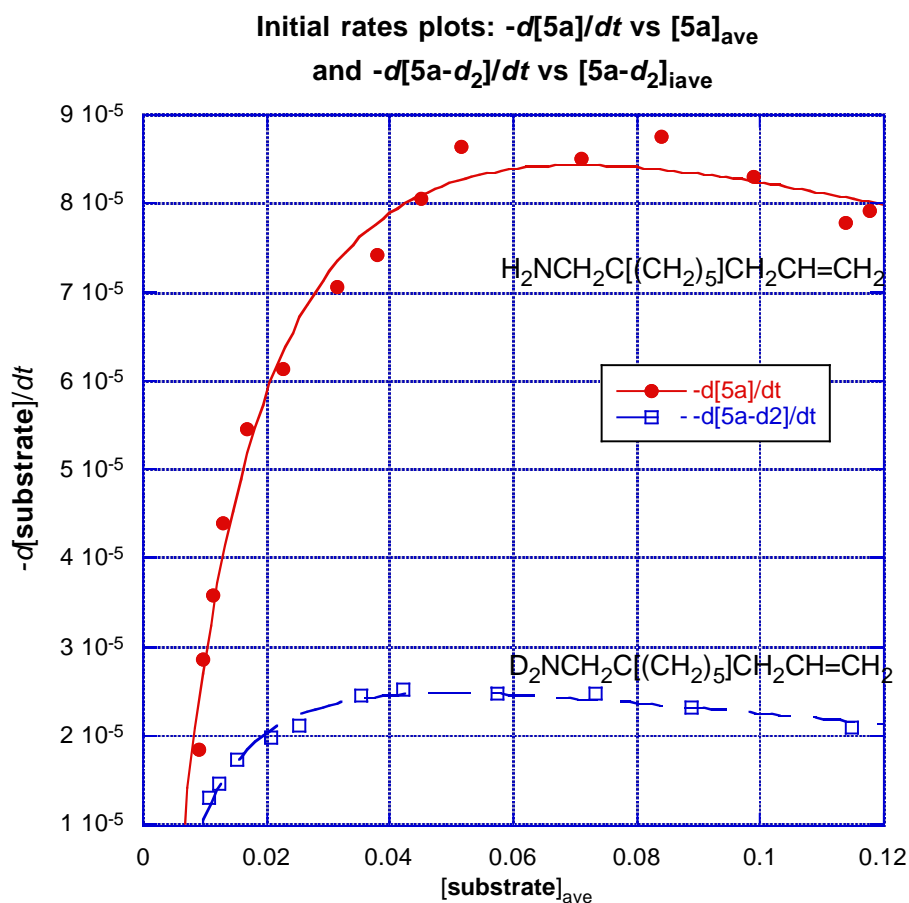


**Figure 4.5.** Plots of initial rates of cyclization  $-d[5a]/dt$  vs.  $[5a]_{ave}$  (and  $-d[5a-d_2]/dt$  vs.  $[5a-d_2]_{ave}$ ) for cyclization of **5a** and **5a-d<sub>2</sub>** by {*S*-**3**}YCH<sub>2</sub>SiMe<sub>3</sub> (0.00523 M). The curves represent non-linear least-squares regression analysis of the data to the equation:  $-d[\text{substrate}]/dt = k_2[\text{catalyst}][\text{substrate}]/\{K' + [\text{substrate}] + K_{SI}[\text{substrate}]^2\}$ .

To gain an insight of the nature of the transition state, activation parameters were measured by the saturation kinetics at different temperatures. The initial rate plots at constant catalyst concentration (5.23 mM) for temperatures at 273, 285, 296 and 312 K provided the rate constant  $k_2$  for the corresponding temperature. The linear Eyring plot using the  $k_2$  values gives the activation parameters  $\Delta H^\ddagger = 7.4 \text{ kcal}\cdot\text{mol}^{-1}$ ,  $\Delta S^\ddagger = -40.8 \text{ cal}\cdot\text{mol}^{-1}\text{K}^{-1}$ . The temperature

dependence of the overall cyclization based on the second order rate constant  $k'$  is also measured, that provide  $\Delta H^\ddagger = 7.3 \text{ kcal}\cdot\text{mol}^{-1}$  and  $\Delta S^\ddagger = -38.6 \text{ cal}\cdot\text{mol}^{-1}\text{K}^{-1}$ .

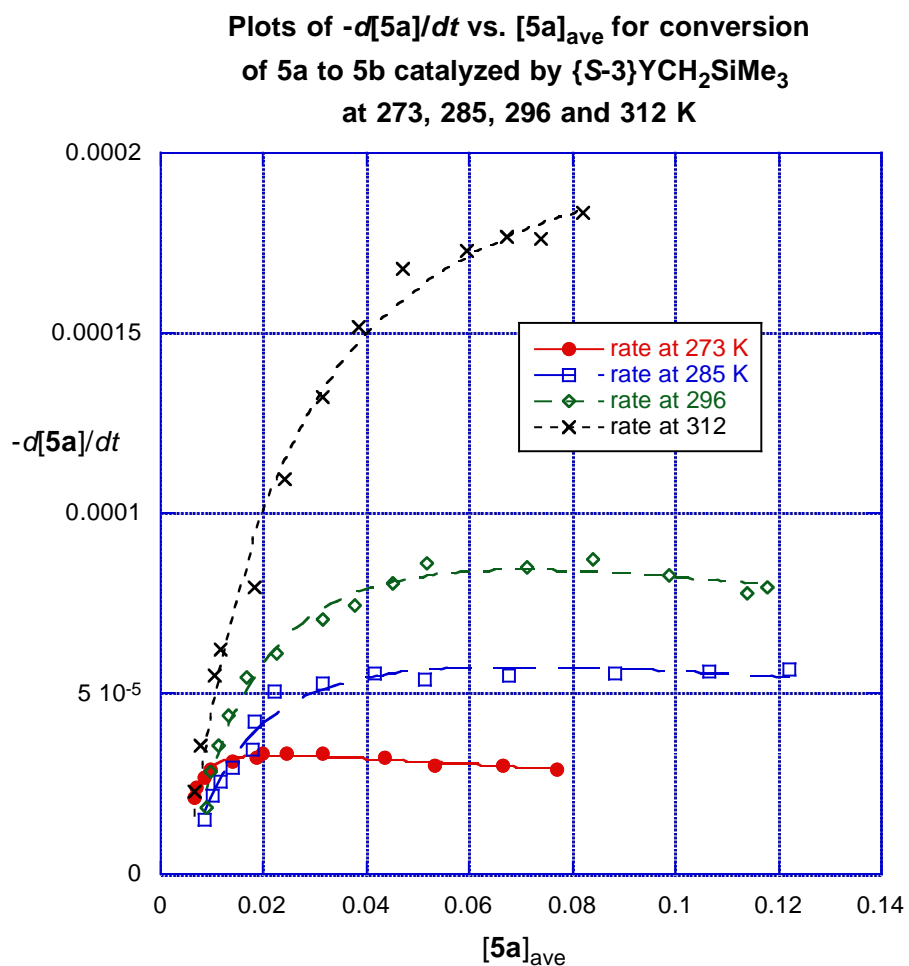


**Figure 4.6.** Plots of initial rates of cyclization  $-d[5a]/dt$  vs.  $[5a]_{\text{ave}}$  for cyclization of **5a** by  $\{S-3\}YCH_2SiMe_3$  (0.00523 M) at 273, 285, 296 and 312 K. The curves represent non-linear least-squares regression analysis of the data to the equation:  $-d[\text{substrate}]/dt = k_2[\text{catalyst}][\text{substrate}]/\{K' + [\text{substrate}] + K_{S1}[\text{substrate}]^2\}$ .

Importantly, the % ee's for deuterio-pyrrolidines are systematically and significantly lower than the values for the corresponding proteo pyrrolidines using  $\{S-3\}YCH_2SiMe_3$ . This effect contrasts all the bisoxazolinyborato zirconium catalyzed hydroamination, where

enantioselectivity increases upon *N*-deuteration of substrate (Table 4.4). For example, the % ee values for deuterio-heterocycles (**4b-d<sub>2</sub>**, 83%; **5b-d<sub>2</sub>**, 87%) are lower compared to the corresponding proteo-heterocycles (**4b**, 94%; **5b**, 92%) for {*S*-3}YCH<sub>2</sub>SiMe<sub>3</sub>. In contrast, the ee values for deuterio-heterocycles (**4b-d<sub>2</sub>**, 96%; **5b-d<sub>2</sub>**, 91%) are higher than corresponding proteo-heterocycles (**4b**, 93%; **5b**, 86%) for precatalyst {*S*-3}Zr(NMe<sub>2</sub>)<sub>2</sub>.

**Table 4.4. Effect of *N*-d<sub>2</sub> substitution on % ee in {*S*-3}YCH<sub>2</sub>SiMe<sub>3</sub>, {*S*-3}Zr(NMe<sub>2</sub>)<sub>2</sub>, and [{*S*-2}Zr(NMe<sub>2</sub>)] [B(C<sub>6</sub>F<sub>5</sub>)<sub>4</sub>]-catalyzed enantioselective hydroamination**

Substrate → Product	Entry	{ <i>S</i> -3} YCH <sub>2</sub> SiMe <sub>3</sub>	{ <i>S</i> -3} Zr(NMe <sub>2</sub> ) <sub>2</sub>	[{ <i>S</i> -2} Zr(NMe <sub>2</sub> )] [B(C <sub>6</sub> F <sub>5</sub> ) <sub>4</sub> ]
<p><b>4a</b> → <b>4b</b></p>	1	94 ( <i>S</i> )	93 ( <i>R</i> )	66 ( <i>S</i> )
<p><b>4a-d<sub>2</sub></b> → <b>4b-d<sub>2</sub></b></p>	2	83 ( <i>S</i> )	96 ( <i>R</i> )	61 ( <i>S</i> )
<p><b>5a</b> → <b>5b</b></p>	3	92 ( <i>S</i> )	86 ( <i>R</i> )	79 ( <i>S</i> )
<p><b>5a-d<sub>2</sub></b> → <b>5b-d<sub>2</sub></b></p>	4	87 ( <i>S</i> )	91 ( <i>R</i> )	76 ( <i>S</i> )

### *Mechanism of enantioselective C–N bond formation*

{*S*-3}YCH<sub>2</sub>SiMe<sub>3</sub> catalyze cyclization of aminoolefin at room temperature affording *S*-configured cyclic amines with high enantiomeric excesses. The observed substrate saturation on the initial rates suggests the presence of a reversible step followed by turnover-limiting step in the catalytic cycle. The primary kinetic isotope effect {2.4(4)} obtained from second order rate

law, and also from initial rate plots {3.8(2)} indicate the cleavage of an N–H or N–D bond in the turnover-limiting step. The similarity of activation parameters determined using  $k_2^{(H)}$  (from initial rates measurements) and  $k^{(H)}$  (for overall conversion) indicates that the reaction mechanism remains consistent from the initial portion through at least two half-lives. Two plausible mechanistic scenarios are consistent with these observed distinct features in {*S*-3}YCH<sub>2</sub>SiMe<sub>3</sub> catalyzed cyclization. First, a concerted C–N and C–H bond formation through N–C ring closure concurrent with amino proton delivery at the terminal methylene unit. Another pathway involves a stepwise  $\sigma$ -insertive pathway that involves a reversible migratory olefin insertion into the Y–N amido  $\sigma$ -bond followed by turn-over limiting Y–C bond protonolysis.

In this context, concerted C–N/C–H bond forming mechanism is established in neutral tetravalent {*S*-2}Zr(NMe<sub>2</sub>)<sub>2</sub> catalyzed cyclization of aminoolefins, which is supported by the second order rate law, the primary KIE, isotopic perturbation of enantioselectivity, the KIE for the two enantiotopic pathway, and inability of complex {*S*-2}ZrCl(NMe<sub>2</sub>) to cyclize aminoalkene.<sup>27</sup> The {*S*-3}YCH<sub>2</sub>SiMe<sub>3</sub>-catalyzed cyclizations have also similar kinetic and spectroscopic features. However, the configurational flip between Y- and neutral Zr- catalysts indicate different mechanisms of stereoinduction.

The significant isotope effects on enantioselectivity in {*S*-2} and {*S*-3}-supported yttrium and zirconium catalyzed hydroamination suggest that N–H or N–D bond is involved in the stereochemistry-determining step for all systems. For {*S*-3}YCH<sub>2</sub>SiMe<sub>3</sub>, the isotope effect for the favored diastereomeric pathway ( $k_H^S/k_D^S$ ) is 2.7(4) and for the unfavored diastereomers ( $k_H^R/k_D^R$ ) is 1.6(3) (from  $k_H^S/k_D^S$ ). The zirconium catalyst {*S*-2}Zr(NMe<sub>2</sub>)<sub>2</sub> is characterized by  $k_H^R/k_D^R = 3.5$ ,  $k_H^S/k_D^S = 7.7(1)$  and  $k_H^R/k_D^R = 2.2(5)$ .<sup>27</sup> Interestingly, *N*-deuteration slows the *S*-diastereomeric pathway by a greater extent than the *R*-pathway for both yttrium- and zirconium-

catalyzed reactions. This similarity provides a powerful argument that the *S* transition-states for Zr and Y catalysts are similar, as are the *R* transition-states, even though the energetically favored diastereomeric pathways are opposite.

Interestingly, the cationic zirconium [ $\{S-2\}Zr(NMe_2)] [B(C_6F_5)_4]$  also catalyze cyclization of primary aminopentenes. The catalytic activity of [ $\{S-2\}Zr(NMe_2)] [B(C_6F_5)_4]$  contrasts to other reported cationic group 4 catalysts that cyclize only secondary aminoalkenes.<sup>23</sup> The observed isotopic perturbation on stereoselectivity in [ $\{S-2\}Zr(NMe_2)] [B(C_6F_5)_4]$  catalyzed hydroamination rule out the involvement of  $[2\pi+2\pi]$  cycloaddition in a zirconium imidoalkene species, as an NH group is absent in the imido species. Additionally, the formation of *S*-configured products mediated by [ $\{S-2\}Zr(NMe_2)] [B(C_6F_5)_4]$  and  $\{S-3\}YCH_2SiMe_3$  suggests that the nature of stereochemistry determining turnover-limiting steps are similar for both trivalent catalysts.

Our kinetic and spectroscopic data show that cyclopentadienyl-bis(oxazolinyl)borate containing trivalent yttrium, tetravalent neutral zirconium, and trivalent cationic zirconium catalysts have similar catalytic pathways. Two substrates are required for cyclization in all these systems and also the catalytic cycle contains a reversible catalyst-substrate association followed by the turnover-limiting step. In all these systems, the turnover-limiting step involves N–H bond cleavage. In addition, N–H bond cleavage also significantly affects the configuration of the new stereocenter (*i.e.*, it is associated with C–N bond formation) in the chiral Zr and Y systems. All these observations disfavor the olefin insertion mechanism for the  $\{S-3\}YCH_2SiMe_3$ -system; a concerted C–H and C–N bond formation *via* a six-center cyclic transition state is proposed as the C–N bond forming step (Figure 4.7).

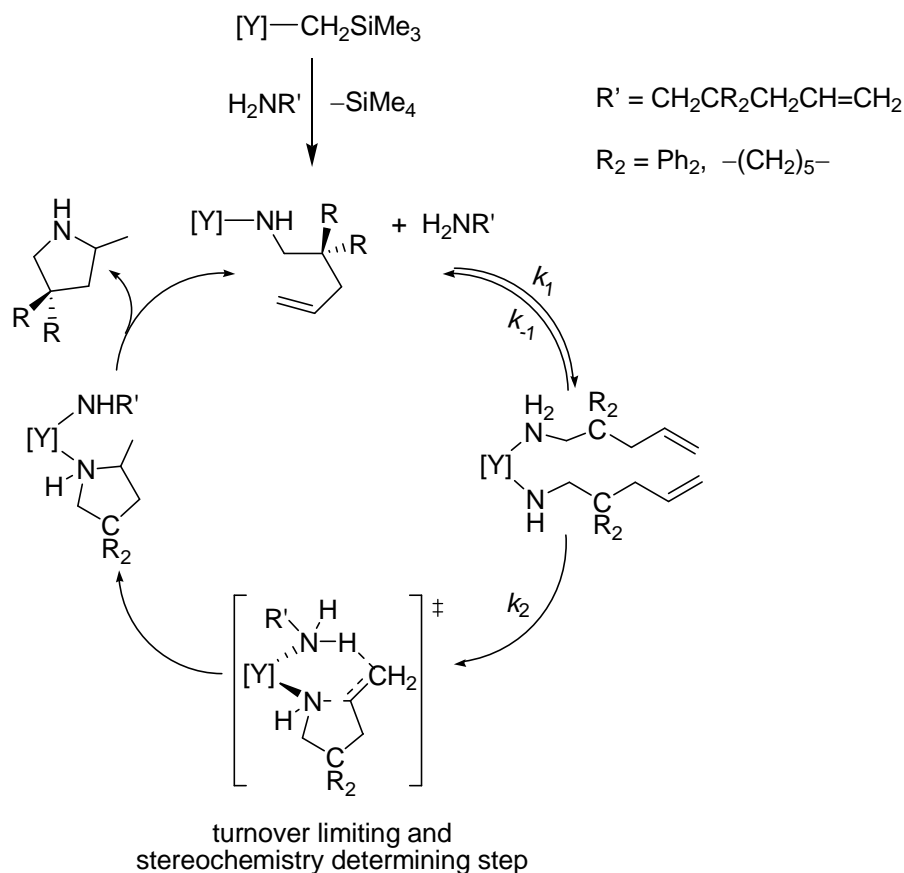


**Figure 4.7.** Proposed catalytic cycle for  $\{S\text{-}3\}\text{YCH}_2\text{SiMe}_3$  catalyzed hydroamination of aminoalkenes

Although the general mechanistic features of the C–N bond forming step (and even the two diastereomeric transition-states) appear to be related for Zr and Y catalysts, the oppositely configured stereocenters in the catalytic products reveal that mechanisms for stereoinduction are not equivalent for Y and Zr. Our working rationalization of the stereochemistry is that the  $C_1$ -symmetric ancillary differentiates the two amidoalkenes in the transition-state in the zirconium system (Figure 4.8, i), whereas the configuration of the two diastereomeric intermediates  $\{S\text{-}3\}\text{YNHR}(\text{NH}_2\text{R})$  significantly influences the favored diastereomeric pathway in the trivalent system (Figure 4.8, ii).

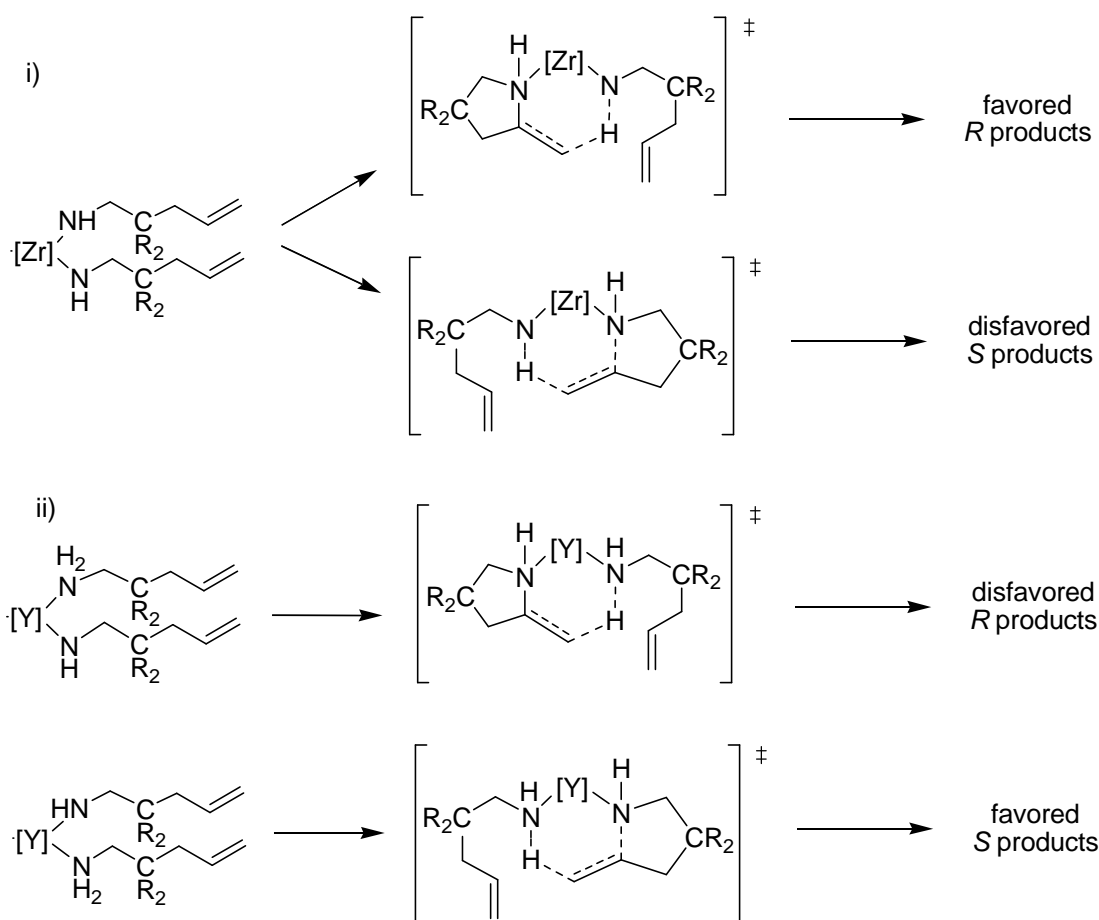


**Figure 4.8.** Proposed stereomechanism for Zr- and Y-catalyzed hydroamination.

## Conclusions

Cyclopentadienyl-bis(oxazolinyl)borato yttrium complex  $\{\text{PhB}(\text{C}_5\text{H}_4)(\text{Ox}^{\text{S-}}\text{t}^{\text{Bu}})_2\}\text{YCH}_2\text{SiMe}_3$  is a highly enantioselective precatalyst for hydroamination/cyclization of aminoolefins. The precatalyst provides nitrogen heterocycles with high enantiomeric excesses up to 96%. Enantioselectivities are remained high with substrate substitution patterns and also in the presence of oxo- and halogen-functional groups. A non-insertive mechanism involving concerted C–N/C–H bond formation was proposed based on the kinetics, primary isotope effects, isotopic perturbation of enantioselectivity, the non-linear effect of concentration on cyclization rate, and

the requirement of substrate/precatalyst  $>2$  for catalytic turnover. Similar stereochemical and kinetic features of optically active cyclopentadienyl-bis(oxazolinyl)borate containing yttrium as well as cationic and neutral zirconium catalyzed hydroamination suggest similar transition states in all these systems.

### Experiment details.

**General Procedures.** All reactions were performed under a dry argon atmosphere using standard Schlenk techniques or under a nitrogen atmosphere in a glove box unless otherwise indicated. Dry, oxygen-free solvents were used throughout. Benzene, toluene, pentane and tetrahydrofuran were degassed by sparging with nitrogen, filtered through activated alumina columns, and stored under  $N_2$ . Benzene- $d_6$ , toluene- $d_8$  and tetrahydrofuran- $d_8$  were vacuum transferred from Na/K alloy and stored under  $N_2$  in a glove box. Bromobenzene- $d_5$  was degassed with three freeze-pump-thaw cycles and dried over activated molecular sieves in the glove box.  $Y(CH_2SiMe_3)_3(THF)_2$ ,<sup>35</sup> sodium cyclopentadienide,<sup>36</sup>  $H[PhB(C_5H_5)(Ox^{Me_2})_2]$ ,<sup>32</sup>  $H[PhB(C_5H_5)(Ox^{4S-iPr,Me_2})_2]$ ,<sup>27</sup> 2,2-diphenyl-4-penten-1-amine (**4a**),<sup>37</sup> C-(1-allyl-cyclohexyl)-methylamine (**5a**),<sup>38</sup> 2-allyl-2-methylpent-4-enylamine (**6a**),<sup>39</sup> 2,2-diphenyl-5-hexen-1-amine (**7a**),<sup>40</sup> N-methyl-2,2-diphenyl-4-penten-1-amine (**8a**),<sup>41</sup> 2-allyl-2-phenyl-pent-4-enylamine (**10a**),<sup>42,26</sup> 2,2-bis(2-propenyl)-4-pentenylamine (**12a**)<sup>43</sup> and tetrakis(trimethylsilyl)silane<sup>44</sup> were prepared by published procedures. All aminoalkenes were distilled from  $CaH_2$ , degassed and stored with freshly activated 4 Å molecular sieves in a glove box prior to use. All other chemicals used here are commercially available. (+)-(S)- $\alpha$ -methoxy- $\alpha$ -(trifluoromethyl)phenylacetyl chloride (S-Mosher's chloride) was obtained from Alfa-Aesar (>98%, (+)-137.3).  $^1H$ ,  $^{13}C\{^1H\}$ ,  $^{11}B$ ,  $^{19}F$  and  $^{29}Si\{^1H\}$  NMR spectra were collected either on a



Bruker DRX-400 spectrometer or an Agilent MR400 spectrometer.  $^{15}\text{N}$  chemical shifts were determined either by  $^1\text{H}$ - $^{15}\text{N}$  CIGARAD experiments on an Agilent MR400 spectrometer or by  $^1\text{H}$ - $^{15}\text{N}$  HMBC experiments on a Bruker Avance II 700 spectrometer with a Bruker Z-gradient inverse TXI  $^1\text{H}/^{13}\text{C}/^{15}\text{N}$  5 mm cryoprobe.  $^{15}\text{N}$  chemical shifts were originally referenced to liquid  $\text{NH}_3$  and recalculated to the  $\text{CH}_3\text{NO}_2$  chemical shift scale by adding  $-381.9$  ppm.  $^{11}\text{B}$  NMR spectra were referenced to an external sample of  $\text{BF}_3\cdot\text{Et}_2\text{O}$ . Accurate mass ESI mass spectrometry was performed using an Agilent QTOF 6530 equipped with the Jet Stream ESI source. An Agilent ESI test mix was used for tuning and calibration. Accurate mass data was obtained in the positive ion mode using a reference standard with ions at 121.05087 and 922.00979. The mass resolution (FWHM) was maintained at 18,000. Elemental analysis was performed using a Perkin-Elmer 2400 Series II CHN/S by the Iowa State Chemical Instrumentation Facility.  $[\alpha]_{\text{D}}$  values were measured on a ATAGO AP-300 polarimeter at  $23\text{ }^\circ\text{C}$ .

$\{\text{PhB}(\text{C}_5\text{H}_4)(\text{Ox}^{\text{Me}_2})_2\}\text{YCH}_2\text{SiMe}_3$ .  $\text{H}[\text{PhB}(\text{C}_5\text{H}_5)(\text{Ox}^{\text{Me}_2})_2]$  (0.200 g, 0.571 mmol) was dissolved in a mixture of tetrahydrofuran (4 mL), and this solution was cooled to  $-30\text{ }^\circ\text{C}$ .  $\text{Y}(\text{CH}_2\text{SiMe}_3)_3(\text{THF})_2$  (0.282 g, 0.571 mmol) was placed in a separate flask, and the solid was cooled to  $-30\text{ }^\circ\text{C}$ . The cooled solution was quickly added to  $\text{Y}(\text{CH}_2\text{SiMe}_3)_3(\text{THF})_2$ , and the resulting solution was gently agitated for 5 min. Cold pentane (5 mL) was added, and a yellow solid precipitated. The mixture was cooled to  $-30\text{ }^\circ\text{C}$  and filtered. The solid was dried in vacuo for 10 min affording  $\{\text{PhB}(\text{C}_5\text{H}_4)(\text{Ox}^{\text{Me}_2})_2\}\text{YCH}_2\text{SiMe}_3$  as a light yellow solid (0.260 g, 49.6 mmol, 87.0% yield). This material was stored at  $-30\text{ }^\circ\text{C}$  in the dark.  $^1\text{H}$  NMR (tetrahydrofuran- $d_8$ , 400 MHz):  $\delta$  7.55 (d,  $^3J_{\text{HH}} = 6.8$  Hz, 2 H, *ortho*- $\text{C}_6\text{H}_5$ ), 6.97 (t,  $^3J_{\text{HH}} = 6.8$  Hz, 2 H, *meta*- $\text{C}_6\text{H}_5$ ), 6.88 (t,  $^3J_{\text{HH}} = 7.2$  Hz, 1 H, *para*- $\text{C}_6\text{H}_5$ ), 6.38 (m, 2 H,  $\text{C}_5\text{H}_4$ ), 6.18 (m, 2 H,  $\text{C}_5\text{H}_4$ ), 3.87

(d, 2 H,  $^2J_{\text{HH}} = 8.4$  Hz,  $\text{CNCMe}_2\text{CH}_2\text{O}$ ), 3.82 (d, 2 H,  $^2J_{\text{HH}} = 8.4$  Hz,  $\text{CNCMe}_2\text{CH}_2\text{O}$ ), 1.29 (s, 6 H,  $\text{CNCMe}_2\text{CH}_2\text{O}$ ), 1.21 (s, 6 H,  $\text{CNCMe}_2\text{CH}_2\text{O}$ ), 0.01 (s, 9 H,  $\text{CH}_2\text{SiMe}_3$ ),  $-0.35$  (d,  $^2J_{\text{YH}} = 7.2$  Hz, 2 H,  $\text{YCH}_2\text{SiMe}_3$ ).  $^{13}\text{C}\{^1\text{H}\}$  NMR (tetrahydrofuran- $d_8$ , 100 MHz):  $\delta$  192.51 ( $\text{CNCMe}_2\text{CH}_2\text{O}$ ), 136.54 (*ortho*- $\text{C}_6\text{H}_5$ ), 126.22 (*meta*- $\text{C}_6\text{H}_5$ ), 124.37 (*para*- $\text{C}_6\text{H}_5$ ), 121.45 ( $\text{C}_5\text{H}_4$ ), 112.82 ( $\text{C}_5\text{H}_4$ ), 80.42 ( $\text{CNCMe}_2\text{CH}_2\text{O}$ ), 70.77 ( $\text{CNCMe}_2\text{CH}_2\text{O}$ ), 35.61 (d,  $^1J_{\text{YC}} = 35$  Hz,  $\text{YCH}_2\text{SiMe}_3$ ), 30.80 ( $\text{CNCMe}_2\text{CH}_2\text{O}$ ), 28.87 ( $\text{CNCMe}_2\text{CH}_2\text{O}$ ), 5.16 ( $\text{CH}_2\text{SiMe}_3$ ).  $^{11}\text{B}$  NMR (tetrahydrofuran- $d_8$ , 128 MHz):  $\delta$   $-15.2$ . IR (KBr,  $\text{cm}^{-1}$ ): 3068 w, 3045 w, 2958 s, 2891 s, 1549 (s,  $\nu_{\text{CN}}$ ), 1490 w, 1462 m, 1431 w, 1387 w, 1368 m, 1352 w, 1272 m, 1264 m, 1249 s, 1237 s, 1195 s, 1176 s, 1155 s, 1104 w, 1066 w, 1051 m, 1034 w, 1022 w, 993 w, 971 m, 917 w, 860 s, 813 s, 776 s, 732 s, 704 s, 668 m. Anal. Calcd for  $\text{C}_{25}\text{H}_{36}\text{BN}_2\text{O}_2\text{SiY}$ : C, 57.26; H, 6.92; N, 5.34. Found: C, 57.13; H, 6.88; N, 4.97. Mp: 90-95 °C, dec.

**{PhB(C<sub>5</sub>H<sub>4</sub>)(Ox<sup>4*S*-iPr,Me<sup>2</sup>)<sub>2</sub>YCH<sub>2</sub>SiMe<sub>3</sub>}. H[PhB(C<sub>5</sub>H<sub>5</sub>)(Ox<sup>4*S*-iPr,Me<sup>2</sup>)<sub>2</sub>]</sup></sup>** (0.060 g, 0.138 mmol) and **Y(CH<sub>2</sub>SiMe<sub>3</sub>)<sub>3</sub>(THF)<sub>2</sub>** (0.065 g, 0.131 mmol) were dissolved in benzene (5 mL) at room temperature. The resulting solution was stirred for 10 min and then was filtered. Evaporation of the filtrate provided light yellow gel. The gel was triturated with pentane, giving **{PhB(C<sub>5</sub>H<sub>4</sub>)(Ox<sup>4*S*-iPr,Me<sup>2</sup>)<sub>2</sub>YCH<sub>2</sub>SiMe<sub>3</sub>}</sup>** as a light yellow solid (0.065 g, 0.107 mmol, 77.5% yield). This material was stored at  $-30$  °C.  $^1\text{H}$  NMR (benzene- $d_6$ , 400 MHz):  $\delta$  7.74 (d,  $^3J_{\text{HH}} = 7.2$  Hz, 2 H, *ortho*- $\text{C}_6\text{H}_5$ ), 7.38 (m, 2 H, *meta*- $\text{C}_6\text{H}_5$ ), 7.21 (m, 1 H, *para*- $\text{C}_6\text{H}_5$ ), 6.92 (m, 1 H,  $\text{C}_5\text{H}_4$ ), 6.80 (m, 1 H,  $\text{C}_5\text{H}_4$ ), 6.72 (m, 1 H,  $\text{C}_5\text{H}_4$ ), 6.61 (m, 1 H,  $\text{C}_5\text{H}_4$ ), 3.26 (d, 2 H,  $^3J_{\text{HH}} = 6.0$  Hz,  $\text{CNCi-PrHcMe}_2\text{O}$ ), 3.14 (d, 2 H,  $^3J_{\text{HH}} = 6.0$  Hz,  $\text{CNCi-PrHcMe}_2\text{O}$ ), 1.88 (m, 2 H,  $\text{CNC(CHMe}_2\text{)HcMe}_2\text{O}$ ), 1.27-0.90 (24 H,  $\text{CNC(CHMe}_2\text{)HcMe}_2\text{O}$ ), 0.32 (s, 9 H,  $\text{CH}_2\text{SiMe}_3$ ),  $-0.42$  (m, 1 H,  $\text{CH}_2\text{SiMe}_3$ ),  $-0.60$  (m, 1 H,  $\text{CH}_2\text{SiMe}_3$ ).  $^{13}\text{C}\{^1\text{H}\}$  NMR (benzene- $d_6$ , 100 MHz):  $\delta$

193.41 (br, CNCi-PrHCH<sub>2</sub>O), 141.50 (br, *ipso*-C<sub>6</sub>H<sub>5</sub>), 135.10 (*ortho*-C<sub>6</sub>H<sub>5</sub>), 127.51 (*meta*-C<sub>6</sub>H<sub>5</sub>), 125.26 (*para*-C<sub>6</sub>H<sub>5</sub>), 122.36 (C<sub>5</sub>H<sub>4</sub>), 120.49 (C<sub>5</sub>H<sub>4</sub>), 118.30 (C<sub>5</sub>H<sub>4</sub>), 116.79 (C<sub>5</sub>H<sub>4</sub>), 87.75 (CNCi-PrHCHMe<sub>2</sub>O), 86.99 (CNCi-PrHCHMe<sub>2</sub>O), 78.22 (CNCi-PrHCHMe<sub>2</sub>O), 76.61 (CNCi-PrHCHMe<sub>2</sub>O), 36.74 (d, <sup>1</sup>J<sub>YC</sub> = 35 Hz, YCH<sub>2</sub>SiMe<sub>3</sub>), 30.44 (CNC(CHMe<sub>2</sub>)HCHMe<sub>2</sub>O), 30.27 (CNC(CHMe<sub>2</sub>)HCHMe<sub>2</sub>O), 30.94 (CNCi-PrHCHMe<sub>2</sub>O), 30.09 (CNCi-PrHCHMe<sub>2</sub>O), 29.26 (CNCi-PrHCHMe<sub>2</sub>O), 28.89 (CNCi-PrHCHMe<sub>2</sub>O), 22.28 (CNC(CHMe<sub>2</sub>)HCHMe<sub>2</sub>O), 21.55 (CNC(CHMe<sub>2</sub>)HCHMe<sub>2</sub>O), 21.28 (CNC(CHMe<sub>2</sub>)HCHMe<sub>2</sub>O), 20.82 (CNC(CHMe<sub>2</sub>)HCHMe<sub>2</sub>O), 4.93 (CH<sub>2</sub>SiMe<sub>3</sub>). <sup>15</sup>N NMR (benzene-*d*<sub>6</sub>, 71 MHz): δ -154.4, -156.8. <sup>29</sup>Si{<sup>1</sup>H} NMR (79.5 MHz, benzene-*d*<sub>6</sub>): δ -2.79. <sup>11</sup>B NMR (benzene-*d*<sub>6</sub>, 128 MHz): δ -15.9. IR (KBr, cm<sup>-1</sup>): 3071 w, 3041 w, 2962 s, 2891 s, 2770 m, 1558 s (CN), 1482 m, 1464 m, 1425 w, 1397 m, 1365 m, 1344 w, 1272 m, 1262 w, 1248 s, 1234 m, 1192 s, 1169 s, 1155 s, 1114 w, 1060 w, 1052 m, 1032 w, 1019 m, 995 w, 917 w, 860 s, 805 s, 786 s, 743 s, 711 m. Anal. Calcd for C<sub>32</sub>H<sub>48</sub>BN<sub>2</sub>O<sub>2</sub>SiY: C, 61.19; H, 7.95; N, 4.60. Found: C, 60.74; H, 7.73; N, 4.26. [α]<sub>D</sub> = -39.23° (C<sub>6</sub>H<sub>6</sub>). Mp: 155-160 °C, dec.

**4S-2H-Ox<sup>tBu</sup>**. **Error! Bookmark not defined.** **Error! Bookmark not defined.** <sup>15</sup>N NMR (acetonitrile-*d*<sub>3</sub>, 71 MHz): δ -148.0.

{PhB(C<sub>5</sub>H<sub>4</sub>)(Ox<sup>4S-tBu</sup>)<sub>2</sub>}YCH<sub>2</sub>SiMe<sub>3</sub>. H[PhB(C<sub>5</sub>H<sub>5</sub>)(Ox<sup>4S-tBu</sup>)<sub>2</sub>] (0.048 g, 0.119 mmol) was dissolved in benzene (2 mL) and added to Y(CH<sub>2</sub>SiMe<sub>3</sub>)<sub>3</sub>(THF)<sub>2</sub> (0.056 g, 0.113 mmol) to give a light yellow solution. This solution was allowed to stir for 3 min at room temperature. The solution was quickly filtered, and the filtrate was concentrated under vacuum to give a yellow gel. The gel was triturated with pentane to provide {PhB(C<sub>5</sub>H<sub>4</sub>)(Ox<sup>4S-tBu</sup>)<sub>2</sub>}YCH<sub>2</sub>SiMe<sub>3</sub> as a light

yellow solid (0.055 g, 0.095 mmol, 84.6% yield), which was stored at  $-30\text{ }^{\circ}\text{C}$ .  $^1\text{H}$  NMR (benzene- $d_6$ , 400 MHz):  $\delta$  7.67 (d,  $^3J_{\text{HH}} = 7.6\text{ Hz}$ , 2 H, *ortho*- $\text{C}_6\text{H}_5$ ), 7.34 (m, 2 H, *meta*- $\text{C}_6\text{H}_5$ ), 7.18 (m, 1 H, *para*- $\text{C}_6\text{H}_5$ ), 6.82 (m, 1 H,  $\text{C}_5\text{H}_4$ ), 6.77 (m, 1 H,  $\text{C}_5\text{H}_4$ ), 6.64 (m, 1 H,  $\text{C}_5\text{H}_4$ ), 6.53 (m, 1 H,  $\text{C}_5\text{H}_4$ ), 3.68-3.56 (m, 4 H,  $\text{CNC}t\text{-BuHCH}_2\text{O}$ ), 3.16-3.03 (m, 2 H,  $\text{CNC}t\text{-BuHCH}_2\text{O}$ ), 0.67 (s, 9 H,  $\text{CNC}t\text{-BuHCH}_2\text{O}$ ), 0.64 (s, 9 H,  $\text{CNC}t\text{-BuHCH}_2\text{O}$ ), 0.01 (s, 9 H,  $\text{CH}_2\text{SiMe}_3$ ), -0.34 (m, 1 H,  $\text{CH}_2\text{SiMe}_3$ ), -0.51 (m, 1 H,  $\text{CH}_2\text{SiMe}_3$ ).  $^{13}\text{C}\{^1\text{H}\}$  NMR (benzene- $d_6$ , 100 MHz):  $\delta$  195.31 (br,  $\text{CNC}t\text{-BuHCH}_2\text{O}$ ), 150.38 (*ipso*- $\text{C}_6\text{H}_5$ ), 134.90 (*ortho*- $\text{C}_6\text{H}_5$ ), 127.97 (*meta*- $\text{C}_6\text{H}_5$ ), 125.95 (*para*- $\text{C}_6\text{H}_5$ ), 123.73 ( $\text{C}_5\text{H}_4$ ), 123.64 ( $\text{C}_5\text{H}_4$ ), 115.46 ( $\text{C}_5\text{H}_4$ ), 115.25 ( $\text{C}_5\text{H}_4$ ), 74.24 ( $\text{CNC}t\text{-BuHCH}_2\text{O}$ ), 72.62 ( $\text{CNC}t\text{-BuHCH}_2\text{O}$ ), 68.31 ( $\text{CNC}t\text{-BuHCH}_2\text{O}$ ), 67.25 ( $\text{CNC}t\text{-BuHCH}_2\text{O}$ ), 38.25 (d,  $^1J_{\text{YC}} = 35\text{ Hz}$ ,  $\text{YCH}_2\text{SiMe}_3$ ), 32.37 ( $\text{CNC}(\text{CMe}_3)\text{HCH}_2\text{O}$ ), 27.52 ( $\text{CNC}(\text{CMe}_3)\text{HCH}_2\text{O}$ ), 25.41 ( $\text{CNC}(\text{CMe}_3)\text{HCH}_2\text{O}$ ), 25.20 ( $\text{CNC}(\text{CMe}_3)\text{HCH}_2\text{O}$ ), 5.24 ( $\text{CH}_2\text{SiMe}_3$ ).  $^{15}\text{N}$  NMR (benzene- $d_6$ , 41 MHz):  $\delta$  -148.5, -150.2.  $^{11}\text{B}$  NMR (benzene- $d_6$ , 128 MHz):  $\delta$  -15.7.  $^{29}\text{Si}\{^1\text{H}\}$  NMR (79.5 MHz, benzene- $d_6$ ):  $\delta$  -3.28. IR (KBr,  $\text{cm}^{-1}$ ): 3068 w, 3044 w, 2955 s, 2902 s, 2870 s, 1586 (s,  $\nu_{\text{CN}}$ ), 1540 w, 1479 s, 1431 w, 1419 w, 1397 w, 1369 m, 1320 w, 1287 m, 1249 s, 1238 s, 1207 s, 1184 s, 1108 w, 1065 w, 1048 w, 1026 w, 1001 w, 969 s, 860 s, 814 m, 793 w, 726 s, 703 s, 677 w. Anal. Calcd for  $\text{C}_{29}\text{H}_{44}\text{BN}_2\text{O}_2\text{SiY}$ : C, 60.00; H, 7.64; N, 4.83. Found: C, 59.62; H, 7.32; N, 5.06.  $[\alpha]_{\text{D}} = -46.74^{\circ}$  ( $\text{C}_6\text{H}_6$ ). Mp: 120-125  $^{\circ}\text{C}$ , dec.

**$\text{Tl}_2[\text{PhB}(\text{C}_5\text{H}_4)(\text{Ox}^{\text{Me}_2})_2]$** . In a glove box, a vial was charged with  $\text{H}[\text{PhB}(\text{C}_5\text{H}_5)(\text{Ox}^{\text{Me}_2})_2]$  (0.214 g, 0.611 mmol) and dissolved in  $\text{Et}_2\text{O}$  (7 mL). To the solution, thallium(1) ethoxide (86.5  $\mu\text{L}$ , 1.22 mmol) was added by a microliter syringe. The resulting solution was stirred at room temperature for 8 h. During stirring, a yellow solid crushed out from the solution. The solution was decanted to get the yellow solid precipitation in the glove box. The solid was washed with

Et<sub>2</sub>O and dried *in vacuo* to give  $\text{Ti}_2[\text{PhB}(\text{C}_5\text{H}_4)(\text{Ox}^{\text{Me}_2})_2]$  as a yellow solid (0.420 g, 0.555 mmol, 90.8%), which was stored in glove box. <sup>1</sup>H NMR (tetrahydrofuran-*d*<sub>8</sub>, 400 MHz):  $\delta$  7.34 (d, <sup>3</sup>J<sub>HH</sub> = 6.8 Hz, 2 H, *ortho*-C<sub>6</sub>H<sub>5</sub>), 7.05 (t, <sup>3</sup>J<sub>HH</sub> = 7.2 Hz, 2 H, *meta*-C<sub>6</sub>H<sub>5</sub>), 6.96 (t, <sup>3</sup>J<sub>HH</sub> = 7.2 Hz, 1 H, *para*-C<sub>6</sub>H<sub>5</sub>), 6.18 (m, 2 H, C<sub>5</sub>H<sub>4</sub>), 5.84 (m, 2 H, C<sub>5</sub>H<sub>4</sub>), 3.74 (4 H,  $\overline{\text{CNCMe}_2\text{CH}_2\text{O}}$ ), 1.30 (s, 6 H,  $\overline{\text{CNCMe}_2\text{CH}_2\text{O}}$ ), 1.28 (s, 6 H,  $\overline{\text{CNCMe}_2\text{CH}_2\text{O}}$ ). <sup>13</sup>C{<sup>1</sup>H} NMR (tetrahydrofuran-*d*<sub>8</sub>, 100 MHz):  $\delta$  198.62 (br,  $\overline{\text{CNCMe}_2\text{CH}_2\text{O}}$ ), 155.95 (br, *ipso*-C<sub>6</sub>H<sub>5</sub>), 137.58 (*ipso*-C<sub>5</sub>H<sub>4</sub>), 133.61 (*ortho*-C<sub>6</sub>H<sub>5</sub>), 127.35 (*meta*-C<sub>6</sub>H<sub>5</sub>), 124.47 (*para*-C<sub>6</sub>H<sub>5</sub>), 116.90 (C<sub>5</sub>H<sub>4</sub>), 111.29 (C<sub>5</sub>H<sub>4</sub>), 80.08 ( $\overline{\text{CNCMe}_2\text{CH}_2\text{O}}$ ), 67.82 ( $\overline{\text{CNCMe}_2\text{CH}_2\text{O}}$ ), 29.67 ( $\overline{\text{CNCMe}_2\text{CH}_2\text{O}}$ ), 29.51 ( $\overline{\text{CNCMe}_2\text{CH}_2\text{O}}$ ). <sup>11</sup>B NMR (tetrahydrofuran-*d*<sub>8</sub>, 128 MHz):  $\delta$  -17.0. <sup>15</sup>N NMR (tetrahydrofuran-*d*<sub>8</sub>, 71 MHz):  $\delta$  -99.8. IR (KBr, cm<sup>-1</sup>): 3059 w, 2958 s, 2924 m, 2878 m, 1578 s, 1567 s, 1484 w, 1459 m, 1428 w, 1380 w, 1361 m, 1342 w, 1290 m, 1250 m, 1190 m, 1120 s, 1056 w, 1037 m, 1017 w, 966 s, 936 w, 876m, 824 s, 792 w, 777 m, 747 s, 731 s, 704 m, 661 w. Anal. Calcd for C<sub>21</sub>H<sub>25</sub>BO<sub>2</sub>N<sub>2</sub>Ti<sub>2</sub>: C, 33.32; H, 3.33; N, 3.70. Found: C, 32.61; H, 2.94; N, 3.72. Mp: 195-200 °C, dec.

**{PhB(C<sub>5</sub>H<sub>4</sub>)(Ox<sup>Me<sub>2</sub>)<sub>2</sub>)}YNH<sup>t</sup>Bu.</sup>** In a glove box, a vial was charged with  $\text{Ti}_2[\text{PhB}(\text{C}_5\text{H}_4)(\text{Ox}^{\text{Me}_2})_2]$  (0.276 g, 0.364 mmol) and  $\text{YCl}_3(\text{THF})_3$  (0.150 g, 0.364 mmol). THF (5 mL) was added and immediately a white slurry was formed. The mixture was stirred at room temperature for 1 h. The solution was filtered to obtain the THF solution of  $\{\text{PhB}(\text{C}_5\text{H}_4)(\text{Ox}^{\text{Me}_2})_2\}\text{YCl}$ . Unfortunately, the complex couldn't be isolated in pure form.

<sup>1</sup>H NMR (tetrahydrofuran-*d*<sub>8</sub>, 400 MHz):  $\delta$  7.55 (d, <sup>3</sup>J<sub>HH</sub> = 6.8 Hz, 2 H, *ortho*-C<sub>6</sub>H<sub>5</sub>), 6.99 (t, <sup>3</sup>J<sub>HH</sub> = 7.2 Hz, 2 H, *meta*-C<sub>6</sub>H<sub>5</sub>), 6.90 (t, <sup>3</sup>J<sub>HH</sub> = 6.4 Hz, 1 H, *para*-C<sub>6</sub>H<sub>5</sub>), 6.26 (m, 2 H, C<sub>5</sub>H<sub>4</sub>),

6.05 (m, 2 H, C<sub>5</sub>H<sub>4</sub>), 3.84 (d, <sup>3</sup>J<sub>HH</sub> = 7.6 Hz, 2 H,  $\overline{\text{CNCMe}_2\text{CH}_2\text{O}}$ ), 3.76 (d, <sup>3</sup>J<sub>HH</sub> = 7.6 Hz, 2 H,  $\overline{\text{CNCMe}_2\text{CH}_2\text{O}}$ ), 1.37 (s, 6 H,  $\overline{\text{CNCMe}_2\text{CH}_2\text{O}}$ ), 1.34 (s, 6 H,  $\overline{\text{CNCMe}_2\text{CH}_2\text{O}}$ ). <sup>11</sup>B NMR (tetrahydrofuran-*d*<sub>8</sub>, 128 MHz): δ -16.0.

{PhB(C<sub>5</sub>H<sub>4</sub>)(Ox<sup>Me<sub>2</sub></sup>)<sub>2</sub>}YNH<sup>t</sup>Bu was synthesized using the THF solution of {PhB(C<sub>5</sub>H<sub>4</sub>)(Ox<sup>Me<sub>2</sub></sup>)<sub>2</sub>}YCl prepared *in situ*. <sup>t</sup>BuNHLi (0.029 g, 0.365 mmol) was added to the THF solution of {PhB(C<sub>5</sub>H<sub>4</sub>)(Ox<sup>Me<sub>2</sub></sup>)<sub>2</sub>}YCl and then stirred for 2 h at room temperature. The solution was filtered to remove LiCl. Removal of solvent *in vacuo* provided {PhB(C<sub>5</sub>H<sub>4</sub>)(Ox<sup>Me<sub>2</sub></sup>)<sub>2</sub>}YNH<sup>t</sup>Bu as a white solid (0.143 g, 0.281 mmol, 77.2%). <sup>1</sup>H NMR (tetrahydrofuran-*d*<sub>8</sub>, 400 MHz): δ 7.39 (d, <sup>3</sup>J<sub>HH</sub> = 6.8 Hz, 2 H, *ortho*-C<sub>6</sub>H<sub>5</sub>), 7.05 (t, <sup>3</sup>J<sub>HH</sub> = 6.8 Hz, 2 H, *meta*-C<sub>6</sub>H<sub>5</sub>), 6.96 (t, <sup>3</sup>J<sub>HH</sub> = 7.2 Hz, 1 H, *para*-C<sub>6</sub>H<sub>5</sub>), 5.85 (m, 1 H, C<sub>5</sub>H<sub>4</sub>), 5.57 (m, 1 H, C<sub>5</sub>H<sub>4</sub>), 5.47 (m, 1 H, C<sub>5</sub>H<sub>4</sub>), 4.95 (m, 1 H, C<sub>5</sub>H<sub>4</sub>), 4.72 (d, <sup>2</sup>J<sub>YH</sub> = 7.2 Hz, 1 H, NH<sup>t</sup>Bu), 3.70 (d, <sup>3</sup>J<sub>HH</sub> = 7.2 Hz, 2 H,  $\overline{\text{CNCMe}_2\text{CH}_2\text{O}}$ ), 3.43 (d, <sup>3</sup>J<sub>HH</sub> = 7.6 Hz, 2 H,  $\overline{\text{CNCMe}_2\text{CH}_2\text{O}}$ ), 1.37 (s, 9 H, <sup>t</sup>Bu), 1.27 (s, 3 H,  $\overline{\text{CNCMe}_2\text{CH}_2\text{O}}$ ), 1.11 (s, 3 H,  $\overline{\text{CNCMe}_2\text{CH}_2\text{O}}$ ), 1.06 (s, 3 H,  $\overline{\text{CNCMe}_2\text{CH}_2\text{O}}$ ), 1.00 (s, 3 H,  $\overline{\text{CNCMe}_2\text{CH}_2\text{O}}$ ). <sup>13</sup>C{<sup>1</sup>H} NMR (tetrahydrofuran-*d*<sub>8</sub>, 100 MHz): δ 198.62 (br,  $\overline{\text{CNCMe}_2\text{CH}_2\text{O}}$ ), 154.91 (br, *ipso*-C<sub>6</sub>H<sub>5</sub>), 132.98 (*ortho*-C<sub>6</sub>H<sub>5</sub>), 127.42 (*meta*-C<sub>6</sub>H<sub>5</sub>), 122.07 (*para*-C<sub>6</sub>H<sub>5</sub>), 115.87 (C<sub>5</sub>H<sub>4</sub>), 110.38 (C<sub>5</sub>H<sub>4</sub>), 80.67 ( $\overline{\text{CNCMe}_2\text{CH}_2\text{O}}$ ), 66.82 ( $\overline{\text{CNCMe}_2\text{CH}_2\text{O}}$ ), 30.59 ( $\overline{\text{CNCMe}_2\text{CH}_2\text{O}}$ ), 29.73 ( $\overline{\text{CNCMe}_2\text{CH}_2\text{O}}$ ), 28.98 (NHCMe<sub>3</sub>), 26.40 (NHCMe<sub>3</sub>). <sup>11</sup>B NMR (tetrahydrofuran-*d*<sub>8</sub>, 128 MHz): δ -15.8. <sup>15</sup>N NMR (tetrahydrofuran-*d*<sub>8</sub>, 71 MHz): δ -146.6 ( $\overline{\text{CNCMe}_2\text{CH}_2\text{O}}$ ). IR (KBr, cm<sup>-1</sup>): 2965 s, 2927 m, 2877 m, 1576 s, 1460 s, 1430 m, 1367 s, 1303 w, 1260 m, 1192 s, 1149 w, 994 m, 970 s, 897 m, 779 m, 730 s, 703 s, 684 w. Anal. Calcd for C<sub>25</sub>H<sub>35</sub>BN<sub>3</sub>O<sub>2</sub>Y: C, 58.96; H, 6.93; N, 8.25. Found: C, 58.61; H, 6.49; N, 6.82. Mp: above 200°C.

**Tl<sub>2</sub>[PhB(C<sub>5</sub>H<sub>4</sub>)(Ox<sup>4*S-t*Bu</sup>)<sub>2</sub>]**. In a glove box, a vial was charged with H[PhB(C<sub>5</sub>H<sub>5</sub>)(Ox<sup>4*S-t*Bu</sup>)<sub>2</sub>] (0.300 g, 0.738 mmol) and dissolved in Et<sub>2</sub>O (7 mL). To the solution, thallium(1) ethoxide (104 μL, 1.476 mmol) was added by a microliter syringe. The resulting solution was stirred at room temperature for 12 h. During stirring, an off white solid crushed out from the solution. The solution was decanted to obtain the solid precipitation. The solid was washed with Et<sub>2</sub>O twice and dried *in vacuo* to give Tl<sub>2</sub>[PhB(C<sub>5</sub>H<sub>4</sub>)(Ox<sup>4*S-t*Bu</sup>)<sub>2</sub>] as a yellow solid (0.560 g, 0.689 mmol, 93%), which was stored in glove box. <sup>1</sup>H NMR (tetrahydrofuran-*d*<sub>8</sub>, 400 MHz): δ 7.86 (d, <sup>3</sup>J<sub>HH</sub> = 7.2 Hz, 2 H, *ortho*-C<sub>6</sub>H<sub>5</sub>), 7.47 (t, <sup>3</sup>J<sub>HH</sub> = 7.6 Hz, 2 H, *meta*-C<sub>6</sub>H<sub>5</sub>), 7.28 (t, <sup>3</sup>J<sub>HH</sub> = 7.6 Hz, 1 H, *para*-C<sub>6</sub>H<sub>5</sub>), 6.36 (m, 2 H, C<sub>5</sub>H<sub>4</sub>), 6.21 (m, 2 H, C<sub>5</sub>H<sub>4</sub>), 3.95-3.90 (m, 3 H, CNC*t*-BuHCH<sub>2</sub>O, CNC*t*-BuHCH<sub>2</sub>O, overlapped), 3.74 (t, <sup>3</sup>J<sub>HH</sub> = 8.8 Hz, 1 H, CNC*t*-BuHCH<sub>2</sub>O), 3.47-3.42 (m, 2 H, CNC*t*-BuHCH<sub>2</sub>O), 0.78 (s, 9 H, CNC*t*-BuHCH<sub>2</sub>O), 0.76 (s, 9 H, CNC*t*-BuHCH<sub>2</sub>O). <sup>13</sup>C{<sup>1</sup>H} NMR (benzene-*d*<sub>6</sub>, 150 MHz): δ 199.81 (br, CNC*t*-BuHCH<sub>2</sub>O), 157.28 (*ipso*-C<sub>6</sub>H<sub>5</sub>), 138.67 (*ipso*-C<sub>5</sub>H<sub>4</sub>), 134.12 (*ortho*-C<sub>6</sub>H<sub>5</sub>), 128.68 (*meta*-C<sub>6</sub>H<sub>5</sub>), 127.82 (*para*-C<sub>6</sub>H<sub>5</sub>), 125.06 (C<sub>5</sub>H<sub>4</sub>), 117.07 (C<sub>5</sub>H<sub>4</sub>), 76.42 (CNC*t*-BuHCH<sub>2</sub>O), 75.60 (CNC*t*-BuHCH<sub>2</sub>O), 69.92 (CNC*t*-BuHCH<sub>2</sub>O), 68.99 (CNC*t*-BuHCH<sub>2</sub>O), 33.88 (CNC(CMe<sub>3</sub>)HCH<sub>2</sub>O), 33.82 (CNC(CMe<sub>3</sub>)HCH<sub>2</sub>O), 27.28 (CNC(CMe<sub>3</sub>)HCH<sub>2</sub>O), 26.92 (CNC(CMe<sub>3</sub>)HCH<sub>2</sub>O). <sup>15</sup>N NMR (tetrahydrofuran-*d*<sub>8</sub>, 71 MHz): δ -125.2. <sup>11</sup>B NMR (tetrahydrofuran-*d*<sub>8</sub>, 128 MHz): δ -16.0. IR (KBr, cm<sup>-1</sup>): 3061 m, 2955 s, 2889 m, 2866 m, 1559 s, 1479 m, 1426 w, 1390 w, 1361 m, 1349 w, 1327 w, 1279 w, 1206 w, 1182 m, 1170 m, 1144 s, 1061 m, 1036 m, 1025 m, 995 w, 962 s, 930 w, 901 w, 868 w, 847 m, 779 w, 735 s, 711 m, 698 m, 659 s. Anal. Calcd for C<sub>25</sub>H<sub>33</sub>BO<sub>2</sub>N<sub>2</sub>Tl<sub>2</sub>: C, 36.93; H, 4.09; N, 3.45. Found: C, 36.55; H, 4.01; N 2.98. Mp: 186-190 °C.

**{PhB(C<sub>5</sub>H<sub>4</sub>)(Ox<sup>S-tBu</sup>)<sub>2</sub>}YCl**. In a glove box, YCl<sub>3</sub>(THF)<sub>3</sub> (0.101 g, 0.245 mmol) was dissolved in THF (5 mL) and the solution was transferred to a vial containing Ti<sub>2</sub>[PhB(C<sub>5</sub>H<sub>4</sub>)(Ox<sup>S-tBu</sup>)<sub>2</sub>] (0.200 g, 0.245 mmol). The resultant white slurry was stirred for 1 h at room temperature, and then filtered to remove TiCl byproduct. Removal of volatiles of the filtrate *in vacuo* provided {PhB(C<sub>5</sub>H<sub>4</sub>)(Ox<sup>S-tBu</sup>)<sub>2</sub>}YCl as a white solid (0.115 g, 0.218 mmol, 89.0%). <sup>1</sup>H NMR (tetrahydrofuran-*d*<sub>8</sub>, 400 MHz): δ 7.59 (d, <sup>3</sup>J<sub>HH</sub> = 7.2 Hz, 2 H, *ortho*-C<sub>6</sub>H<sub>5</sub>), 7.06 (t, <sup>3</sup>J<sub>HH</sub> = 6.8 Hz, 2 H, *meta*-C<sub>6</sub>H<sub>5</sub>), 6.95 (t, <sup>3</sup>J<sub>HH</sub> = 6.8 Hz, 1 H, *para*-C<sub>6</sub>H<sub>5</sub>), 6.44 (m, 1 H, C<sub>5</sub>H<sub>4</sub>), 6.31 (m, 1 H, C<sub>5</sub>H<sub>4</sub>), 6.27 (m, 1 H, C<sub>5</sub>H<sub>4</sub>), 5.95 (m, 1 H, C<sub>5</sub>H<sub>4</sub>), 4.30-3.97 (m, 6 H, CNC*t*-BuHCH<sub>2</sub>O, CNC*t*-BuHCH<sub>2</sub>O; overlapped), 0.93 (s, 9 H, CNC*t*-BuHCH<sub>2</sub>O), 0.87 (s, 9 H, CNC*t*-BuHCH<sub>2</sub>O). <sup>13</sup>C{<sup>1</sup>H} NMR (benzene-*d*<sub>6</sub>, 100 MHz): δ 193.01 (br, CNC*t*-BuHCH<sub>2</sub>O), 134.81 (*ortho*-C<sub>6</sub>H<sub>5</sub>), 128.69 (*meta*-C<sub>6</sub>H<sub>5</sub>), 125.11 (*para*-C<sub>6</sub>H<sub>5</sub>), 123.91 (C<sub>5</sub>H<sub>4</sub>), 122.62 (C<sub>5</sub>H<sub>4</sub>), 116.66 (C<sub>5</sub>H<sub>4</sub>), 115.19 (C<sub>5</sub>H<sub>4</sub>), 73.04 (CNC*t*-BuHCH<sub>2</sub>O), 72.38 (CNC*t*-BuHCH<sub>2</sub>O), 68.56 (CNC*t*-BuHCH<sub>2</sub>O), 67.11 (CNC*t*-BuHCH<sub>2</sub>O), 33.21 (CNC(CMe<sub>3</sub>)HCH<sub>2</sub>O), 28.17 (CNC(CMe<sub>3</sub>)HCH<sub>2</sub>O), 25.82 (CNC(CMe<sub>3</sub>)HCH<sub>2</sub>O), 25.01 (CNC(CMe<sub>3</sub>)HCH<sub>2</sub>O). <sup>15</sup>N NMR (benzene-*d*<sub>6</sub>, 41 MHz): δ -148.5, -150.2. <sup>11</sup>B NMR (tetrahydrofuran-*d*<sub>8</sub>, 128 MHz): δ -15.9. IR (KBr, cm<sup>-1</sup>): 3069 w, 3045 w, 2958 s, 2906 m, 2870 m, 1552 s, 1478 s, 1429 w, 1396 w, 1367 m, 1349 w, 1286 w, 1263 w, 1184 s, 1053 m, 1039 m, 960 s, 850 m, 785 s, 725 s, 659 m. Anal. Calcd for C<sub>25</sub>H<sub>33</sub>BClN<sub>2</sub>O<sub>2</sub>Y: C, 56.79; H, 6.29; N, 5.30. Found: C, 56.03; H, 6.11; N, 4.86. Mp: above 200 °C.

**[PhB(C<sub>5</sub>H<sub>4</sub>)(Ox<sup>4R-iPr,Me2</sup>)<sub>2</sub>Zr(NMe<sub>2</sub>)] [B(C<sub>6</sub>F<sub>5</sub>)<sub>4</sub>]**. In a glove box, {PhB(C<sub>5</sub>H<sub>4</sub>)(Ox<sup>4R-iPr,Me2</sup>)<sub>2</sub>}Zr(NMe<sub>2</sub>)<sub>2</sub> (0.150 g, 0.245 mmol) was dissolved in 5 mL benzene and the solution was transferred to a vial containing [Ph<sub>3</sub>C][B(C<sub>6</sub>F<sub>5</sub>)<sub>4</sub>] (0.226 g, 0.245 mmol). The mixture was stirred for 5 min, and a light yellow precipitate formed. The solution was decanted, and the precipitate



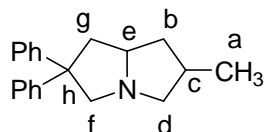
was washed with pentane. The solid was dried in vacuum to afford  $[\text{PhB}(\text{C}_5\text{H}_4)(\text{Ox})^{4R-}{}^{i\text{Pr,Me}_2}{}_{2}\text{Zr}(\text{NMe}_2)][\text{B}(\text{C}_6\text{F}_5)_4]$  as a light yellow solid (0.226 g, 0.181 mmol, 73.9%), which was stored at  $-30\text{ }^\circ\text{C}$  in glove box.  $^1\text{H}$  NMR (bromobenzene- $d_5$ , 400 MHz):  $\delta$  7.97 (d,  $^3J_{\text{HH}} = 7.2$  Hz, 2 H, *ortho*- $\text{C}_6\text{H}_5$ ), 7.46 (m, 2 H, *meta*- $\text{C}_6\text{H}_5$ ), 7.37 (m, 1 H, *para*- $\text{C}_6\text{H}_5$ ), 6.67 (m, 1 H,  $\text{C}_5\text{H}_4$ ), 6.50 (m, 1 H,  $\text{C}_5\text{H}_4$ ), 6.23 (m, 1 H,  $\text{C}_5\text{H}_4$ ), 6.12 (m, 1 H,  $\text{C}_5\text{H}_4$ ), 3.31 (d, 2 H,  $^3J_{\text{HH}} = 6.6$  Hz,  $\text{CNCiPrHMe}_2\text{O}$ ), 3.24 (d, 2 H,  $^3J_{\text{HH}} = 6.6$  Hz,  $\text{CNCiPrHMe}_2\text{O}$ ), 2.76 (s, 6 H,  $\text{NMe}_2$ ), 1.67 (m, 2 H,  $\text{CNC}(\text{CHMe}_2)\text{HMe}_2\text{O}$ ), 1.31-0.93 (24 H,  $\text{CNC}(\text{CHMe}_2)\text{HMe}_2\text{O}$ ).  $^{13}\text{C}\{^1\text{H}\}$  NMR (bromobenzene- $d_5$ , 150 MHz):  $\delta$  153.42 (br, *ipso*- $\text{C}_6\text{H}_5$ ), 148.01 (br,  $\text{C}_6\text{F}_5$ ), 145.96 (br,  $\text{C}_6\text{F}_5$ ), 138.25 (br,  $\text{C}_6\text{F}_5$ ), 135.99 (br,  $\text{C}_6\text{F}_5$ ), 134.74 (br,  $\text{C}_6\text{F}_5$ ), 133.71 (*ortho*- $\text{C}_6\text{H}_5$ ), 128.90 (*meta*- $\text{C}_6\text{H}_5$ ), 124.02 (*para*- $\text{C}_6\text{H}_5$ ), 123.57 ( $\text{C}_5\text{H}_4$ ), 119.62 ( $\text{C}_5\text{H}_4$ ), 113.37 ( $\text{C}_5\text{H}_4$ ), 112.82 ( $\text{C}_5\text{H}_4$ ), 87.21 ( $\text{CNCiPrHMe}_2\text{O}$ ), 85.63 ( $\text{CNCiPrHMe}_2\text{O}$ ), 79.85 ( $\text{CNCiPrHMe}_2\text{O}$ ), 78.49 ( $\text{CNCiPrHMe}_2\text{O}$ ), 45.40 ( $\text{NMe}_2$ ), 31.04 ( $\text{CNC}(\text{CHMe}_2)\text{HMe}_2\text{O}$ ), 31.57 ( $\text{CNC}(\text{CHMe}_2)\text{HMe}_2\text{O}$ ), 30.84 ( $\text{CNCiPrHMe}_2\text{O}$ ), 30.44 ( $\text{CNCiPrHMe}_2\text{O}$ ), 21.96 ( $\text{CNCiPrHMe}_2\text{O}$ ), 21.81 ( $\text{CNCiPrHMe}_2\text{O}$ ), 20.75 ( $\text{CNC}(\text{CHMe}_2)\text{HMe}_2\text{O}$ ), 20.52 ( $\text{CNC}(\text{CHMe}_2)\text{HMe}_2\text{O}$ ), 20.41 ( $\text{CNC}(\text{CHMe}_2)\text{HMe}_2\text{O}$ ), 20.25 ( $\text{CNC}(\text{CHMe}_2)\text{HMe}_2\text{O}$ ).  $^{19}\text{F}$  NMR (bromobenzene- $d_5$ , 376 MHz,  $25\text{ }^\circ\text{C}$ ):  $\delta$  -132.1 (s br, *ortho*-F), -161.8 (t,  $^3J_{\text{FF}} = 21.1$  Hz, *para*-F), -165.7 (t,  $^3J_{\text{FF}} = 16.8$  Hz, *meta*-F).  $^{11}\text{B}$  NMR (bromobenzene- $d_5$ , 128 MHz):  $\delta$  -15.1, -15.9.  $^{15}\text{N}\{^1\text{H}\}$  NMR (benzene- $d_6$ , 71 MHz):  $\delta$  -159.1, -164.4 ( $\text{CNCiPrHMe}_2\text{O}$ ). IR (KBr,  $\text{cm}^{-1}$ ): 2972 m, 2966 w, 1554 s, 1464 s, 1375 w, 1275 m, 1088 m, 980 s, 887 w, 821 w, 775 m, 756 m, 684 m, 662 m. Anal. Calcd for  $\text{C}_{53}\text{H}_{43}\text{B}_2\text{F}_{20}\text{N}_3\text{O}_2\text{Zr}$ : C, 51.06; H, 3.48; N, 3.37. Found: C, 50.41; H, 3.04; N, 2.97. Mp:  $133\text{-}137\text{ }^\circ\text{C}$ , dec.

**N-Allyl-2,2-diphenylpent-4-enylamine (16a).** 2,2-diphenylpent-4-enal was prepared according to the literature procedure.<sup>44</sup> A flame dried flask was charged with MgSO<sub>4</sub> (1.00 g) and a solution of 2,2-diphenylpent-4-enal (0.639 g, 2.70 mmol) in 7 mL methylene chloride. The flask was cooled to 0 °C and then excess allylamine (3.0 mL, 40.0 mmol) was added by a syringe. The solution mixture was stirred at room temperature overnight. The solution was filtered and extracted with methylene chloride. All the volatiles were removed under vacuo to give the imine as a light yellow gel (0.720 g, 2.61 mmol, 96.6%). <sup>1</sup>H NMR (chloroform-*d*, 400 MHz): δ 8.01 (s, 1 H, CH=N), 7.32-7.18 (m, 10 H, C<sub>6</sub>H<sub>5</sub>), 6.04-5.94 (m, 1 H, H<sub>2</sub>C=CHCH=N), 5.73-5.63 (m, 1 H, H<sub>2</sub>C=CHCH<sub>2</sub>C), 5.16-5.08 (m, 2 H, H<sub>2</sub>C=CHCH=N), 4.91-4.85 (m, 2 H, H<sub>2</sub>C=CHCH<sub>2</sub>C), 4.09 (d, <sup>3</sup>J<sub>HH</sub> = 8.0 Hz, 2 H, H<sub>2</sub>C=CHCH=N), 3.19 (d, <sup>3</sup>J<sub>HH</sub> = 8.0 Hz, 2 H, H<sub>2</sub>C=CHCH<sub>2</sub>C). <sup>13</sup>C{<sup>1</sup>H} NMR (100 MHz, chloroform-*d*): δ 168.73 (CH=N), 143.93 (C<sub>6</sub>H<sub>5</sub>), 136.12 (CH=CH<sub>2</sub>), 135.19 (CH=CH<sub>2</sub>), 129.07 (C<sub>6</sub>H<sub>5</sub>), 128.36 (C<sub>6</sub>H<sub>5</sub>), 126.75 (C<sub>6</sub>H<sub>5</sub>), 117.60 (CH=CH<sub>2</sub>), 115.91 (CH=CH<sub>2</sub>), 63.34 (H<sub>2</sub>C=CHCH=N), 56.65 [C(C<sub>6</sub>H<sub>5</sub>)<sub>2</sub>], 41.55 (H<sub>2</sub>C=CHCH<sub>2</sub>C).

A flame dried flask was charged with solution of imine (0.720 g, 2.61 mmol) in 5 mL dry methanol. The flask was cooled to 0 °C and then NaBH<sub>4</sub> (0.090 g, 2.38 mmol) was added in small portions under argon flow. The reaction mixture was stirred at room temperature overnight. Aqueous NaOH (25%, 2.5 mL) was added at 0 °C and then stir at room temperature for 1 h. The organic layer was separated and the aqueous layer was extracted with diethyl ether (3 x 20 mL). The combined organic layers were dried with Na<sub>2</sub>SO<sub>4</sub>. After removal of the solvent, a light yellow gel was obtained that was purified by short silica gel column chromatography (hexane:EtOAc = 3:1, R<sub>f</sub> = 0.68) to yield N-allyl-2,2-diphenylpent-4-enylamine as a colorless gel (0.544 g, 1.96 mmol, 75.1%). The amine was dissolved in dry pentane in glove box, stir with CaH<sub>2</sub> for 3 days and then filter. Removal of solvent provided dry N-allyl-2,2-diphenylpent-4-

enylamine, and was used in catalysis.  $^1\text{H}$  NMR (chloroform-*d*, 400 MHz):  $\delta$  7.28-7.16 (m, 10 H,  $\text{C}_6\text{H}_5$ ), 5.82-5.73 (m, 1 H,  $\text{H}_2\text{C}=\text{CHCH}_2\text{N}$ ), 5.42-5.32 (m, 1 H,  $\text{H}_2\text{C}=\text{CHCH}_2\text{C}$ ), 5.09-4.91 (m, 4 H,  $\text{H}_2\text{C}=\text{CHCH}_2\text{N}$ ), 3.18 (s, 2 H,  $\text{CH}_2\text{NH}$ ), 3.16 (d,  $^3J_{\text{HH}} = 6.0$  Hz, 2 H,  $\text{H}_2\text{C}=\text{CHCH}_2\text{N}$ ), 3.00 (d,  $^3J_{\text{HH}} = 6.8$  Hz, 2 H,  $\text{H}_2\text{C}=\text{CHCH}_2\text{C}$ ), 0.56 (1 H, *NH*).  $^{13}\text{C}\{^1\text{H}\}$  NMR (100 MHz, chloroform-*d*):  $\delta$  147.05 ( $\text{C}_6\text{H}_5$ ), 137.60 ( $\text{CH}=\text{CH}_2$ ), 135.10 ( $\text{CH}=\text{CH}_2$ ), 128.27 ( $\text{C}_6\text{H}_5$ ), 128.16 ( $\text{C}_6\text{H}_5$ ), 126.17 ( $\text{C}_6\text{H}_5$ ), 117.81 ( $\text{CH}=\text{CH}_2$ ), 115.73 ( $\text{CH}=\text{CH}_2$ ), 55.48 ( $\text{CH}_2\text{NH}$ ), 53.02 ( $\text{CH}_2\text{NH}$ ), 50.26 [ $\text{C}(\text{C}_6\text{H}_5)_2$ ], 41.84 ( $\text{H}_2\text{C}=\text{CHCH}_2\text{C}$ ). IR (KBr,  $\text{cm}^{-1}$ ): 3059 s, 3024 s, 2977 s, 2912 s, 2817 s, 1947 w, 1875 w, 1806 w, 1751 w, 1639 s, 1598 m, 1580 w, 1495 s, 1445 s, 1414 s, 1333 m, 1315 m, 1292 m, 1259 m, 1186 w, 1147 m, 1114 m, 1032 m, 996 s, 915 s, 785 m, 757 s, 729 m, 699 s, 657 w. MS (ESI) exact mass Calcd. for  $\text{C}_{20}\text{H}_{23}\text{N}$ :  $m/z$  278.1903 ( $[\text{M}^+ + \text{H}^+]$ ), Found: 278.1909 ( $\Delta -2.07$  ppm).

**N-Allyl-2,2-phenyl-2-methyl-pyrrolidine (16b).**  $^1\text{H}$  NMR (chloroform-*d*, 400 MHz):  $\delta$  7.27-7.01 (m, 10 H,  $\text{C}_6\text{H}_5$ ), 5.92-5.82 (m, 1 H,  $\text{H}_2\text{C}=\text{CHCH}_2\text{N}$ ), 5.14-4.99 (m, 2 H,  $\text{H}_2\text{C}=\text{CHCH}_2\text{C}$ ), 3.75 (d,  $^3J_{\text{HH}} = 10.0$  Hz, 1 H,  $\text{Ph}_2\text{CCH}_2\text{N}$ ), 3.42 (m, 1 H,  $\text{H}_2\text{C}=\text{CHCH}_2\text{C}$ ), 2.78 (m, 1 H,  $\text{Ph}_2\text{CCH}_2\text{N}$ ), 2.72 (d,  $^3J_{\text{HH}} = 10.0$  Hz, 1 H,  $\text{H}_2\text{C}=\text{CHCH}_2\text{C}$ ), 2.67 (m, 1 H,  $\text{CH}_2\text{CHMe}$ ), 2.60 (m, 1 H,  $\text{CH}_2\text{CHMe}$ ), 2.07 (m, 1 H,  $\text{CH}_2\text{CHMe}$ ), 1.02 (d,  $^3J_{\text{HH}} = 6.0$  Hz, 3 H,  $\text{CHMeNH}$ ).  $^{13}\text{C}\{^1\text{H}\}$  NMR (100 MHz, chloroform-*d*):  $\delta$  150.69 ( $\text{C}_6\text{H}_5$ ), 149.10 ( $\text{C}_6\text{H}_5$ ), 136.80 ( $\text{CH}=\text{CH}_2$ ), 128.43 ( $\text{C}_6\text{H}_5$ ), 128.23 ( $\text{C}_6\text{H}_5$ ), 127.63 ( $\text{C}_6\text{H}_5$ ), 127.42 ( $\text{C}_6\text{H}_5$ ), 126.06 ( $\text{C}_6\text{H}_5$ ), 125.73 ( $\text{C}_6\text{H}_5$ ), 116.86 ( $\text{CH}=\text{CH}_2$ ), 66.80 ( $\text{Ph}_2\text{CCH}_2\text{N}$ ), 59.93 ( $\text{CHMe}$ ), 57.18 ( $\text{H}_2\text{C}=\text{CHCH}_2\text{C}$ ), 52.74 [ $\text{C}(\text{C}_6\text{H}_5)_2$ ], 48.21 ( $\text{CH}_2\text{CHMe}$ ), 19.59 ( $\text{CHMe}$ ). MS (ESI) exact mass Calcd. for  $\text{C}_{20}\text{H}_{23}\text{N}$ :  $m/z$  278.1903 ( $[\text{M}^+ + \text{H}^+]$ ), Found: 278.1909 ( $\Delta -2.07$  ppm).

**2,2-Diphenyl-6-methyl-pyrrolizine (diastereomeric mixture of *cis* and *trans*) (16c)**

$^1\text{H}$  NMR (chloroform-*d*, 400 MHz):  $\delta$  7.43-7.12 (m, 10 H, C<sub>6</sub>H<sub>5</sub>), 4.08-4.05 (d,  $^2J_{\text{HH}} = 9.2$  Hz, 1 H, **f**), 3.62-3.54 (m, 1 H, **e**), 3.32-3.28 (m, 1 H, **d**), 2.91-2.89 (d,  $^2J_{\text{HH}} = 9.6$  Hz, 1 H, **f**), 2.67-2.59 (m, 1 H, **g**), 2.50-2.42 (m, 1 H, **c**), 2.21-2.17 (m, 2 H, **d** and **g** overlapped), 2.09-2.01 (m, 1 H, **b**), 1.20-1.12 (m, 1 H, **b**), 1.06-1.04 (d,  $^2J_{\text{HH}} = 6.8$  Hz, 3 H, **a**), 1.02-1.00 (d,  $^2J_{\text{HH}} = 6.8$  Hz, 3 H, **a**).

$^{13}\text{C}\{^1\text{H}\}$  NMR (100 MHz, chloroform-*d*):  $\delta$  128.66 (C<sub>6</sub>H<sub>5</sub>), 128.51 (C<sub>6</sub>H<sub>5</sub>), 127.14 (C<sub>6</sub>H<sub>5</sub>), 127.05 (C<sub>6</sub>H<sub>5</sub>), 126.22 (C<sub>6</sub>H<sub>5</sub>), 126.17 (C<sub>6</sub>H<sub>5</sub>), 66.93 (**f**), 66.84 (**f**), 65.36 (**d**), 65.20 (**d**), 59.80 (**e**), 59.74 (**e**), 52.20 (**h**), 52.16 (**h**), 48.41 (**g**), 48.55 (**g**), 35.09 (**b**), 35.04 (**b**), 34.29 (**c**), 34.21 (**c**), 17.75 (**a**), 17.60 (**a**). MS (ESI) exact mass Calcd. for C<sub>20</sub>H<sub>23</sub>N:  $m/z$  278.1903 ([M<sup>+</sup>+H<sup>+</sup>]), Found: 278.1907 ( $\Delta -1.35$  ppm).

**General procedure for catalytic hydroamination/cyclization.**

Procedures for micro-molar scale catalysis, kinetics, and determination of % ee for optically active pyrrolidines are described here specifically for the yttrium chemistry.

**Micromolar-scale catalysis.** In a typical small-scale hydroamination experiment, a J. Young style NMR tube with a re-sealable Teflon valve was charged with 0.120 mmol of an aminoalkene substrate, 6  $\mu\text{mol}$  of catalyst {PhB(C<sub>5</sub>H<sub>4</sub>)(Ox<sup>*S-t*Bu</sup>)<sub>2</sub>}YCH<sub>2</sub>SiMe<sub>3</sub>, and 0.5 mL of solvent (benzene-*d*<sub>6</sub> or toluene-*d*<sub>8</sub>). The tube was sealed, and the reaction was monitored by  $^1\text{H}$  NMR spectroscopy at regular intervals.

**Procedure for isolation of optically active pyrrolidines.** A flask was charged with the catalyst {PhB(C<sub>5</sub>H<sub>4</sub>)(Ox<sup>*S-t*Bu</sup>)<sub>2</sub>}YCH<sub>2</sub>SiMe<sub>3</sub> (0.060 g, 0.103 mmol), benzene (20-30 mL) and the

appropriate aminoalkene (2.58 mmol). The solution was stirred at room temperature for 3 h. Then, the products were purified by fractional distillation *in vacuo* to afford the pyrrolidine products as colorless oils.

2-methyl-4,4-diphenylpyrrolidine (**4b**) was purified by Kugelrohr distillation. Yield: 93%, bp: 125 °C,  $10^{-5}$  mBar (dynamic vacuum on a high vacuum line).

3-methyl-2-aza-spiro[4,5]decane (**5b**); yield: 95%, bp: 100-105 °C, 0.1 mm Hg (dynamic vacuum).

2-Methyl-4,4-bis(2-propenyl)pyrrolidine (**7b**). Yield: 97%, bp: 86-90 °C, 5 mm Hg.

4-allyl-2,4-dimethyl-pyrrolidine (**8b**). Yield: 95%, bp: 47-52 °C, 5 mm Hg.

4-allyl-2-methyl-4-phenyl-pyrrolidine (**10b**). Yield: 96%, bp: 148-153 °C, 2 mm Hg.

4-allyl-2-methyl-4-(4-bromophenyl)pyrrolidine (**11b**): Yield: 94%, bp: 120-125 °C, 0.1 mm Hg (dynamic vacuum).

**Procedures for NMR kinetic measurements.** Reaction progress was monitored by single scan acquisition of a series of  $^1\text{H}$  NMR spectra at regular intervals on a Bruker DRX400 spectrometer. The concentrations of C-(1-allyl-cyclohexyl)-methylamine and 3-methyl-2-aza-spiro[4,5]decane were determined by integration of resonances corresponding to species of interest and integration of a tetrakis(trimethylsilyl)silane standard of accurately known and constant concentration (4.36 mM in toluene- $d_8$ ). The temperature in the NMR probe was preset for each experiment, and it was kept constant and monitored during each experiment. For reactions heated above 296 K, the probe temperature was calibrated using an 80% ethylene glycol sample in 20% DMSO- $d_6$  using the equation:  $T = [(4.218 - \Delta)/0.009132]$  K ( $\Delta$  equals the chemical shift difference of the two ethylene glycol resonances). For reactions at performed at 296 K or below, the probe was

calibrated using CH<sub>3</sub>OH using the equation  $T = [-23.832 \cdot \Delta^2 - 29.46 \cdot \Delta + 403]$  K ( $\Delta$  = chemical shift difference of two peaks of CH<sub>3</sub>OH).<sup>46</sup>

**Method for measuring kinetics of conversion of aminoalkene to pyrrolidine.** Catalytic conversion of *C*-(1-allyl-cyclohexyl)-methylamine into 3-methyl-2-aza-spiro[4,5]decane using {PhB(C<sub>5</sub>H<sub>4</sub>)(Ox<sup>*S-t*Bu</sup>)<sub>2</sub>}YCH<sub>2</sub>SiMe<sub>3</sub> as a catalyst is described. The stock solution of Si(SiMe<sub>3</sub>)<sub>4</sub> in toluene-*d*<sub>8</sub> (0.50 mL) was added by a 1 mL glass syringe to a known amount of {PhB(C<sub>5</sub>H<sub>4</sub>)(Ox<sup>*S-t*Bu</sup>)<sub>2</sub>}YCH<sub>2</sub>SiMe<sub>3</sub> (0.0040 g, 6.89 μmol) in a glass vial. The resulting solution was transferred to a NMR tube, capped with a rubber septum, and a <sup>1</sup>H NMR spectrum was acquired. The concentration of catalyst was determined from this <sup>1</sup>H NMR spectrum by comparison of integration of resonances assigned to catalyst with that from the internal standard. Neat substrate *C*-(1-allyl-cyclohexyl)-methylamine (0.021 g, 137.8 μmol) was added to the NMR tube by injecting through the rubber septum. Then, the NMR tube was quickly placed in the spectrometer. Single scan spectra were acquired automatically at preset time intervals at a constant temperature. The concentrations of substrate and product at any given time were determined by integration of substrate and product resonances relative to the integration of the internal standard. A linear least squares regression analysis of substrate concentrations (M) vs. time correlated to the equation  $\ln[\text{subs}]_t = \ln[\text{subs}]_0 - k_{\text{obs}}t$ .

**Procedure for measuring initial rates of cyclization.** A 5 mL stock solution in toluene-*d*<sub>8</sub> containing a known concentration of internal standard tetrakis(trimethylsilyl)silane (0.0070 g, 0.0218 mmol, 4.36 mM) and catalyst (5.89 mM) was prepared using a 5 mL volumetric flask. The stock solution (0.50 mL) was added to a NMR tube, which was capped with rubber septum.

The substrate *C*-(1-allyl-cyclohexyl)-methylamine (0.021 g, 137.8  $\mu\text{mol}$ ) was added to the NMR tube by injecting through the rubber septum. Then, the NMR tube was quickly placed in the NMR spectrometer. Single scan spectra were acquired automatically at preset time intervals at a constant temperature.

The initial rates for the cyclization of *C*-(1-allyl-cyclohexyl)-methylamine were measured for concentrations of the substrate ranging from 0.10 – 0.123 M at constant catalyst concentration (5.89 mM). Linear regression fits for [substrate] vs. time for the first 126 s of the reaction provided the initial rate ( $d[\text{subs}]/dt$ ) for a particular initial substrate concentration (calculated as average substrate concentration over 126 s). A non-linear least squares regression analysis of  $d[\text{subs}]/dt$  vs.  $[\text{subs}]_{\text{ini}}$  showed good correlation to the equation:

$$\frac{-d[\text{subs}]}{dt} = \frac{k_2[\text{cat}]\{[\text{subs}] - [\text{cat}]\}}{K' + \{[\text{subs}] - [\text{cat}]\} + K_{\text{SI}}\{[\text{subs}] - [\text{cat}]\}^2} \quad (1)$$

Equation 1 is contains modifications from the standard enzymatic equation for inhibition by excess substrate shown in equation 2.<sup>47</sup>

$$v = \frac{k_2 e_0 a}{K'_m + a + \frac{a^2}{K_{\text{SI}}}} \quad (2)$$

$e_0$  is the total enzyme concentration,  $a$  is the substrate concentration,  $k_2$  is the rate constant turnover-limiting step,  $K'_m$  is a modified Michaelis constant ( $K'_m = (k_{-1} + k_2)/k_1$ ). Equation 2 describes the general enzymatic mechanism of equation 3:





**2. Eyring plot from initial rates:** Using the initial rate method described above, the rate constants  $k_2$  were measured at temperatures ranging from 273 K to 312 K, keeping the catalyst and initial substrate concentration constant in each experiment. The plot  $\ln(k_2/T)$  vs.  $1/T$  provides the values of  $\Delta H^\ddagger = 7(1) \text{ kcal}\cdot\text{mol}^{-1}$  and  $\Delta S^\ddagger = -40(4) \text{ cal}\cdot\text{mol}^{-1}\text{K}^{-1}$  are calculated, using standard Eyring analysis.

### Procedure for determination of enantiomeric excess of pyrrolidine products.

**NMR spectroscopy.** The  $^1\text{H}$  and  $^{19}\text{F}$  NMR spectroscopic methods were used to evaluate the % ee of the pyrrolidines products of enantioselective hydroamination/cyclization. 3-methyl-2-aza-spiro[4,5]decane (**5b**), 4-allyl-2,4-dimethyl-pyrrolidine (**8b**), 3-methyl-2-aza-spiro[4,4]nonane (**6b**), 4-allyl-2-methyl-4-phenyl-pyrrolidine (**9b**), and 2-Methyl-4,4-bis(2-propenyl)pyrrolidine (**7b**) were separated from the catalyst by vacuum transfer ( $10^{-5}$  mBar) to a 10 mL flask. 2-Methyl-4,4-diphenylpyrrolidine (**4b**) and 4-allyl-2-methyl-4-(4-bromophenyl)pyrrolidine (**11b**), 2-methyl-5,5-diphenylpiperidine (**13b**) were purified by silica gel flash chromatography (pipette column) with 95:5  $\text{CH}_2\text{Cl}_2:\text{CH}_3\text{OH}$  as an eluent, and then all volatiles were removed by rotary evaporation.

Benzene (2 mL) and triethylamine (5.0 equivalent based on the amount of aminoalkene used during catalysis) were added to the purified pyrrolidine. To this solution, (+)-(*S*)- $\alpha$ -methoxy- $\alpha$ -(trifluoromethyl)phenylacetyl chloride (1.2 equivalent based on the amount of aminoalkene used during catalysis) was added. The solution was mixed and immediately a white suspension appeared ( $[\text{HNEt}_3][\text{Cl}]$ ). The mixture was stirred for 1 h, and all the solvents were removed under vacuum. The residue was extracted with pentane. Pentane was removed under vacuum to give the corresponding Mosher-amide as a colorless oil. No further purification was

performed, since crystallization, chromatography, or sublimation could result in biased results by separation of the diastereomers. The enantioselectivities were determined by either integration of  $^{19}\text{F}$  NMR (60 °C or 83 °C in  $\text{CDCl}_3$ , or 125 °C in  $\text{C}_6\text{D}_5\text{Br}$ ).

## References

- (1) Clayden, J.; Greeves N.; Warren, S.; Wothers, P. *Organic Chemistry*; Oxford University Press, 2000.
- (2) Halpern, J. *Science* **1982**, *217*, 401.
- (3) Clawson, L.; Soto, J.; Buchwald, S. L.; Steigerwald, M. L.; Grubbs, R. H. *J. Am. Chem. Soc.* **1985**, *107*, 3377-3378.
- (4) Piers, W. E.; Bercaw, J. E. *J. Am. Chem. Soc.* **1990**, *112*, 9406-9407.
- (5) Brunet, J. J.; Neibecker, D. In *Catalytic Heterofunctionalization: From Hydroamination to Hydrozirconation*; Togni, A., Grutzmacher, H., Eds.; Wiley-VCH: Weinheim, Germany, 2001; pp 91-142.
- (6) Hong, S.; Marks, T. J. *Acc. Chem. Res.* **2004**, *37*, 673-686.
- (7) Muller, T. E.; Hultsch, K. C.; Yus, M.; Foubelo, F.; Tada, M. *Chem. Rev.* **2008**, *108*, 3795-3892.
- (8) Gagne, M. R.; Marks, T. J. *J. Am. Chem. Soc.* **1989**, *111*, 4108-4109.
- (9) Gagne, M. R.; Stern, C. L.; Marks, T. J. *J. Am. Chem. Soc.* **1992**, *114*, 275-294.
- (10) Giardello, M. A.; Conticello, V. P.; Brard, L.; Gagne, M. R.; Marks, T. J. *J. Am. Chem. Soc.* **1994**, *116*, 10241-10254.
- (11) Tian, S.; Arredondo, V. M.; Stern, C. L.; Marks, T. J. *Organometallics* **1999**, *18*, 2568-2570.

- (12) Jeske, G.; Lauke, H.; Mauermann, H.; Schumann, H.; Marks, T. J. *J. Am. Chem. Soc.* **1985**, *107*, 8111-8118.
- (13) Fu, P.-F.; Brard, L.; Li, Y.; Marks, T. J. *J. Am. Chem. Soc.* **1995**, *117*, 7157-7168.
- (14) Gountchev, T. I.; Tilley, T. D. *Organometallics* **1999**, *18*, 5661-5667.
- (15) Watson, P. L.; Parshall, G. W. *Acc. Chem. Res.* **1985**, *18*, 51-56.
- (16) Shapiro, P. J.; Cotter, W. D.; Schaefer, W. P.; Labinger, J. A.; Bercaw, J. E. *J. Am. Chem. Soc.* **1994**, *116*, 4623-4640.
- (17) Gribkov, D. V.; Hultsch, K. C.; Hampel, F. *J. Am. Chem. Soc.* **2006**, *128*, 3748-3759.
- (18) Stubbert, B. D.; Marks, T. J. *J. Am. Chem. Soc.* **2007**, *129*, 6149-6167.
- (19) Motta, A.; Lanza, G.; Fragala, I. L.; Marks, T. J. *Organometallics* **2004**, *23*, 4097-4104.
- (20) Motta, A.; Fragala, I. L.; Marks, T. J. *Organometallics* **2006**, *25*, 5533-5539.
- (21) Tobisch, S. *Chem.—Eur. J.* **2010**, *16*, 13814-13824.
- (22) Tobisch, S. *Dalton Trans.* **2011**, *40*, 249-261.
- (23) Gribkov, D. V.; Hultsch, K. C. *Angew. Chem. Int. Ed.* **2004**, *43*, 5542-5546.
- (24) Knight, P. D.; Munslow, I.; O'Shaughnessy, P. N.; Scott, P. *Chem. Commun.* **2004**, 894-895.
- (25) a) Kim, H.; Lee, P. H.; Livinghouse, T. *Chem. Commun.*, **2005**, 5205-5207. b) Thomson, R. K.; Bexrud, J. A.; Schafer, L. L. *Organometallics* **2006**, *25*, 4069-4071.
- (26) Majumder, S.; Odom, A. L. *Organometallics* **2008**, *27*, 1174-1177.
- (27) Manna, K.; Xu, S.; Sadow, A. D. *Angew. Chem. Int. Ed.* **2011**, *50*, 1865-1868.
- (28) Allan, L. E. N.; Clarkson, G. J.; Fox, D. J.; Gott, A. L.; Scott, P. *J. Am. Chem. Soc.* **2010**, *132*, 15308-15320.
- (29) a) Dunne, J. F.; Fulton, D. B.; Ellern, A.; Sadow, A. D. *J. Am. Chem. Soc.* **2010**, *132*, 17680-17683. b) Arrowsmith, M.; Crimmin, M. R.; Barrett, A. G. M.; Hill, M. S.; Kociok-Köhn,

- G.; Procopiou, P. A. *Organometallics* **2011**, *30*, 1493-1506. c) Brinkmann, C.; Barrett, A. G. M.; Hill, M. S.; Procopiou, P. A. *J. Am. Chem. Soc.* **2011**, *134*, 2193-2207. d) Liu, B.; Roisnel, T.; Carpentier, J.-F.; Sarazin, Y. *Angew. Chem. Int. Ed.* **2012**, *51*, 4943-4946.
- (30) Hangaly, N. K.; Petrov, A. R.; Rufanov, K. A.; Harms, K.; Elfferding, M.; Sundermeyer, J. *Organometallics* **2011**, *30*, 4544-4554.
- (31) Leitch, D. C.; Platel, R. H.; Schafer, L. L. *J. Am. Chem. Soc.* **2011**, *133*, 15453-15463.
- (32) Manna, K.; Ellern, A.; Sadow, A. D. *Chem. Commun.* **2010**, *46*, 339-341.
- (33) Manna, K.; Kruse, M. L.; Sadow, A. D. *ACS Catalysis* **2011**, *1*, 1637-1642.
- (34) Cornish-Bowden, A. *Fundamentals of enzyme kinetics*; 3rd ed.; Portland Press: London, 2004.
- (35) Lappert, M. F.; Pearce, R. J. *Chem. Soc., Chem. Commun.* **1973**, 126. (b) Hultsch, K. C.; Voth, P.; Beckerle, K.; Spaniol, T. P.; Okuda, J. *Organometallics* **2000**, *19*, 228-243.
- (36) Panda, T. K.; Gamer, M. T.; Roesky, P. W. *Organometallics*, **2003**, *22*, 877-878.
- (37) Hong, S.; Tian, S.; Metz, M. V.; Marks, T. J. *J. Am. Chem. Soc.*, **2003**, *125*, 14768.
- (38) Riegert, D.; Collin, J.; Meddour, A.; Schulz, E.; Trifonov, A. *J. Org. Chem.* **2006**, *71*, 2514-2517.
- (39) a) Martínez, P. H.; Hultsch, K. C.; Hampel, F. *Chem. Commun.* **2006**, 2221-2223. b) Bender, C. F.; Widenhofer, R. A. *J. Am. Chem. Soc.*, **2005**, *127*, 1070-1071.
- (40) Crimmin, M. R. Arrowsmith, M.; Barrett, A. G. M.; Casely, I. J.; Hill, M. S.; Procopiou, P. A. *J. Am. Chem. Soc.*, **2009**, *131*, 9670-9685.
- (41) Stubbert, B. D.; Marks, T. J. *J. Am. Chem. Soc.*, **2007**, *129*, 4253-4271.
- (42) Ciganek, E. *J. Org. Chem.* **1995**, *60*, 5803-5807.

- (43) Wood, M. C.; Leitch, D. C.; Yeung, C. S.; Kozak, J. A.; Schafer, L. L. *Angew. Chem.* **2007**, *119*, 358-362; *Angew. Chem. Int. Ed.* **2007**, *46*, 354-358.
- (44) Gutekunst, G.; Brook, A. G. *J. Organomet. Chem.*, **1982**, *225*, 1.
- (45) Brendan D. Kelly, Julia M. Allen, Rachel E. Tundel, and Tristan H. Lambert, *Org. Lett.* **2009**, *11*, 1381-1383.
- (46) Van Geet, A. L. *Anal. Chem.* **1970**, *6*, 679-670.
- (47) Cornish-Bowden, A. *Fundamentals of enzyme kinetics*; 3rd ed.; Portland Press: London, 2004.
- (48) (a) Espenson, J. H. *Chemical kinetics and reaction mechanisms*; 2nd ed.; McGraw-Hill: New York, 1995. (b) Morse, P. M.; Spencer, M. D.; Wilson, S. R.; Girolami, G. S. *Organometallics* **1994**, *13*, 1646-1655.

## Chapter 5. Acceptorless thermal decarbonylation of alcohols catalyzed by oxazolinyborato iridium complexes

Modified from a paper to be submitted to *J. Am. Chem. Soc.*

Kuntal Manna,<sup>‡</sup> Naresh Eedugurala, Hung-An Ho, Arkady Ellern, Aaron D. Sadow\*

### Abstract

A series of bis- and tris(oxazoliny)borato iridium and rhodium complexes are synthesized with bis(4,4-dimethyl-2-oxazoliny)phenylborane  $[\text{PhB}(\text{Ox}^{\text{Me}_2})_2]_n$ , tris(4,4-dimethyl-2-oxazoliny)borane  $[\text{B}(\text{Ox}^{\text{Me}_2})_3]_n$ , and tris(4,4-dimethyl-2-oxazoliny)phenylborate  $[\text{To}^{\text{M}}]^-$  as proligands.  $[\text{PhB}(\text{Ox}^{\text{Me}_2})_2]_n$  reacts with  $[\text{M}(\mu\text{-Cl})(\eta^4\text{-C}_8\text{H}_{12})]_2$  in methylene chloride at room temperature providing the corresponding complexes  $\text{PhClB}(\text{Ox}^{\text{Me}_2})_2\text{M}(\eta^4\text{-C}_8\text{H}_{12})$  ( $\text{M} = \text{Ir}, \text{Rh}$ ) *via* halide abstraction. The B-Cl moiety of  $\text{PhClB}(\text{Ox}^{\text{Me}_2})_2\text{M}(\eta^4\text{-C}_8\text{H}_{12})$  can be substituted by treatment with nucleophiles to afford  $\text{R}(\text{Ph})\text{B}(\text{Ox}^{\text{Me}_2})_2\text{M}(\eta^4\text{-C}_8\text{H}_{12})$  ( $\text{R} = \text{Ph}, \text{Ph}_3\text{SiO}$ ). Likewise, the reaction of  $[\text{B}(\text{Ox}^{\text{Me}_2})_3]_n$  and  $[\text{Rh}(\mu\text{-Cl})(\text{CO})_2]_2$  in THF affords  $\text{ClB}(\text{Ox}^{\text{Me}_2})_2\text{Rh}(\text{CO})_2$  *via* chloride abstraction. Tris(4,4-dimethyl-2-oxazoliny)phenylborato iridium and rhodium complexes  $\text{To}^{\text{M}}\text{M}(\eta^4\text{-C}_8\text{H}_{12})$  ( $\text{M} = \text{Ir}, \text{Rh}$ ) are also prepared by treatment of  $\text{TITo}^{\text{M}}$  (thallium tris(4,4-dimethyl-2-oxazoliny)phenylborate) and  $[\text{M}(\mu\text{-Cl})(\eta^4\text{-C}_8\text{H}_{12})]_2$  in benzene. All these newly synthesized rhodium and iridium complexes were examined in acceptorless dehydrogenative decarbonylation of primary alcohols. The catalysts survey shows that the compound  $\text{To}^{\text{M}}\text{Ir}(\eta^4\text{-C}_8\text{H}_{12})$  is the most active for the conversion of primary alcohols into alkane,  $\text{H}_2$ , and  $\text{CO}$  at 180 °C in toluene. Several aliphatic and aromatic primary alcohols are

<sup>‡</sup> Primary researcher and author

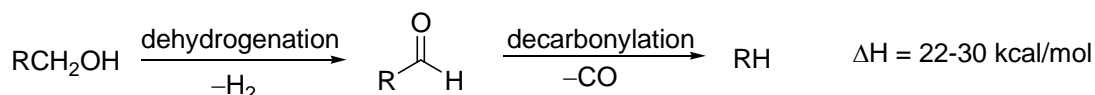
\* Author for correspondence

decarbonylated in the catalytic conditions. Furthermore,  $\text{To}^{\text{M}}\text{Ir}(\eta^4\text{-C}_8\text{H}_{12})$  is also able to decarbonylate polyols such as ethylene glycol and glycerol to syngas ( $\text{H}_2$  and  $\text{CO}$ ) at  $180\text{ }^\circ\text{C}$ .

## Introduction

Biofuels are increasingly important, driven by high oil price, depletion of petroleum resources, and political concerns about fossil fuels. The industrial production of biofuels from biomass feedstocks is primarily based on fermentation and gasification processes.<sup>1</sup> The catalytic defunctionalization such as decarbonylation, deoxygenation, or denitrogenation of highly-functionalized biorenewable materials to hydrocarbons is an alternative approach to produce biofuels. The removal of oxygen- and nitrogen-containing functional groups however requires hydrogen as the stoichiometric reductant.<sup>2</sup> Therefore, the development of catalytic reactions for selective defunctionalization without using any stoichiometric reductant or sacrificial reagents is very crucial to improve hydrogen and carbon efficiency in biofuel production.<sup>3</sup>

In this context, the catalytic alcohol deoxygenation *via* tandem dehydrogenation/decarbonylation is particularly interesting because of its potential application for transforming highly oxygenated biomass-derived materials such as polyols and cellulose into hydrocarbon fuels.<sup>4</sup> Furthermore, the enthalpy content of the products is higher than reactants ( $\Delta H_{\text{rxn}} > 0$ ), and the byproduct is syngas *i.e.*  $\text{H}_2$  and  $\text{CO}$  (Scheme 5.1).<sup>5</sup>



**Scheme 5.1.** Catalytic hydrocarbon formation from alcohol *via* tandem dehydrogenation and decarbonylation processes.

Numerous examples of stoichiometric alcohol decarbonylation have been demonstrated.<sup>6</sup> Several iridium,<sup>6a,6h,6g,6m</sup> rhodium,<sup>6i</sup> and ruthenium<sup>6e,6b,6f,6j,6l</sup> complexes can decarbonylate primary alcohols stoichiometrically under thermal or photochemical conditions to give carbonyl-incorporated complex as the product. Catalytic acceptorless dehydrogenation of alcohols<sup>7</sup> and the decarbonylation of aldehydes<sup>8</sup> are also well documented. However, these two steps are rarely coupled in catalytic processes because dehydrogenation catalysts are often inhibited by CO product of decarbonylation. Therefore, the catalytic decarbonylation of alcohol typically requires a CO trap. In the pioneering studies of acceptorless alcohol decarbonylation, the conversions of ethanol into CO/CO<sub>2</sub>, H<sub>2</sub>, and CH<sub>4</sub> were accomplished by rhodium(I) phosphine catalysts under basic conditions at 150 °C.<sup>9</sup> Similarly, the decarbonylation of alcohol was employed as a CO source in intramolecular Pauson–Khand reactions catalyzed by [(dppp)RhCl(CO)]<sub>2</sub> [dppp = bis(diphenylphosphino)propane].<sup>10</sup> Recently, sunlight-driven dehydrogenation and hydrogenolysis of benzyl alcohol have been achieved by semiconductor-metal photocatalysts.<sup>11</sup>

Our group recently reported an acceptorless decarbonylation of several aliphatic and aromatic primary alcohols to hydrocarbons, CO, and H<sub>2</sub> catalyzed by To<sup>M</sup>Rh(CO)<sub>2</sub> [To<sup>M</sup> = tris(4,4-dimethyl-2-oxazoliny)phenylborate].<sup>12</sup> The decarbonylation reactions were performed under UV irradiation at room temperature in neutral solution. However, the low quantum yields and the inability to decarbonylate polyols limit this photocatalysis for conversion of oxygenates. These limitations motivated us to search for catalysts for acceptorless alcohol decarbonylation under thermal conditions. Herein, we report acceptorless thermal decarbonylation of primary alcohols catalyzed by an oxazolinyborato iridium complex. Furthermore, the iridium catalyst has been applied for conversions of polyols to syngas.

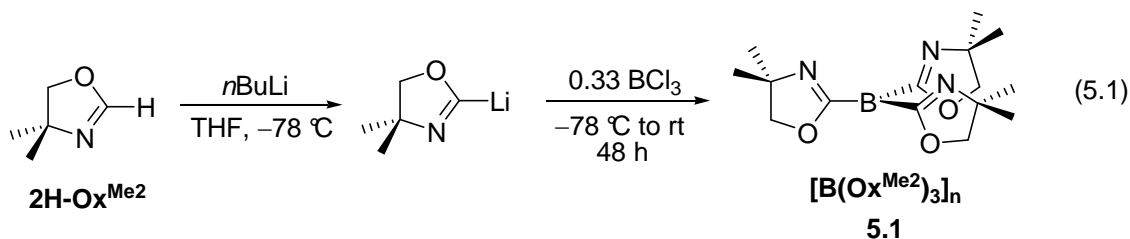


## Results and discussion

### *Synthesis and characterization of proligands*

A series of iridium and rhodium compounds containing bis(oxazolonyl)borate and tris(oxazolonyl)borate ligands are synthesized. We used both borane and borate precursors for metallation. The precursors for bis(oxazolonyl)borate compounds were bis(4,4-dimethyl-2-oxazolonyl)phenylborane  $[\text{PhB}(\text{Ox}^{\text{Me}_2})_2]_n$  and bis(4,4-dimethyl-2-oxazolonyl)diphenylborate  $[\text{Ph}_2\text{B}(\text{Ox}^{\text{Me}_2})_2]^-$ . Additionally, tris(4,4-dimethyl-2-oxazolonyl)borane  $[\text{B}(\text{Ox}^{\text{Me}_2})_3]_n$  and tris(4,4-dimethyl-2-oxazolonyl)phenylborate  $[\text{To}^{\text{M}}]^-$  were used as precursors for synthesizing tris(oxazolonyl)borate complexes.

The synthesis and characterization of oligomeric  $[\text{PhB}(\text{Ox}^{\text{Me}_2})_2]_n$  was described in the chapter 2.<sup>13</sup>  $[\text{B}(\text{Ox}^{\text{Me}_2})_3]_n$  is synthesized through a similar method as  $[\text{PhB}(\text{Ox}^{\text{Me}_2})_2]_n$  from 4,4-dimethyl-2-H-oxazoline ( $2\text{H-Ox}^{\text{Me}_2}$ ) by two steps (eq 5.1).



Deprotonation of  $2\text{H-Ox}^{\text{Me}_2}$  with  $n\text{BuLi}$  in THF at  $-78\text{ }^\circ\text{C}$  occurs selectively at the 2-position to give the 4,4-dimethyl-2-lithio-2-oxazoline ( $2\text{Li-Ox}^{\text{Me}_2}$ ). Addition of 0.33 equiv of  $\text{BCl}_3$  in hexane to the THF solution of  $2\text{Li-Ox}^{\text{Me}_2}$  followed by stirring at room temperature for 36 h generates a white precipitate, which is isolated as  $[\text{B}(\text{Ox}^{\text{Me}_2})_3]_n$  (**5.1**) in 72% yield. **5.1** is insoluble in hydrocarbon solvents including benzene, toluene, THF, and acetonitrile, however it is soluble in methanol. The poor solubility of  $[\text{B}(\text{Ox}^{\text{Me}_2})_3]_n$  suggests that it is an oligomeric species resulting from coordination of one oxazoline to the boron center of another  $\text{B}(\text{Ox}^{\text{Me}_2})_3$  monomer. The similar oligomeric nature of  $[\text{PhB}(\text{Ox}^{\text{Me}_2})_2]_n$  was characterized by solid state  $^{11}\text{B}$  NMR, which

was discussed in chapter 2.<sup>13</sup> The  $^1\text{H}$  NMR of **5.1** in methanol- $d_4$  showed one set of oxazoline resonances as one singlet at 1.23 ppm for inequivalent methyl groups and another singlet at 3.78 ppm for inequivalent methylene protons of the three oxazolines. The pattern of the  $^1\text{H}$  NMR suggests that **5.1** is  $C_{3v}$  symmetric in methanol- $d_4$ . The  $^{11}\text{B}$  NMR spectrum of  $[\text{B}(\text{Ox}^{\text{Me}2})_3]_n$  in methanol- $d_4$  contains one broad singlet at  $-8.1$  ppm (width at half-height,  $\Delta\nu_{1/2} = 190$  Hz). Comparison of  $^{11}\text{B}$  NMR chemical shifts and linewidths with  $[\text{PhB}(\text{Ox}^{\text{Me}2})_2]_n$  ( $-4.1$  ppm in methanol- $d_4$ ,  $\Delta\nu_{1/2} = 82$  Hz) and the lithium salt of tris(4,4-dimethyl-2-oxazoliny)phenylborate<sup>14</sup> ( $\text{Li}[\text{To}^{\text{M}}]$ ,  $-17.0$  ppm in acetonitrile- $d_3$ ,  $\Delta\nu_{1/2} = 12.5$  Hz) suggests that  $[\text{B}(\text{Ox}^{\text{Me}2})_3]_n$  contains a neutral four-coordinated boron center, and it is assigned to the solvent adduct  $\text{B}(\text{Ox}^{\text{Me}2})_3(\text{OHMe})$ . In the solid state IR spectrum of **5.1**, a single oxazoline-based band ( $\nu_{\text{CN}} = 1608$   $\text{cm}^{-1}$ , KBr) was observed at lower energy than that of 4,4-dimethyl-2-H-oxazoline ( $\nu_{\text{CN}} = 1630$   $\text{cm}^{-1}$ ). This IR data is consistent with boron-oxazoline interactions through the imidine nitrogen of **5.1** in the solid state.

A monoanionic ligand thallium bis(4,4-dimethyl-2-oxazoliny)diphenylborate (**5.3**) is synthesized by two steps from  $[\text{PhB}(\text{Ox}^{\text{Me}2})_2]_n$  (eq 5.2). The treatment of PhLi with  $[\text{PhB}(\text{Ox}^{\text{Me}2})_2]_n$  in THF followed by silica gel column chromatography provide bis(oxazoliny)diphenyl borate (**5.2**) as protonated species in 38% yield. The single and sharp  $^{11}\text{B}$  NMR resonance of **5.2** at  $-14.5$  ppm ( $\Delta\nu_{1/2} = 50.5$  Hz) indicates **5.2** as a four coordinated borate. In the next step, the reaction of **5.2** and TlOEt in  $\text{Et}_2\text{O}$  at room temperature yields the thallium salt of bis(4,4-dimethyl-2-oxazoliny)diphenylborate  $\text{Tl}[\text{Ph}_2\text{B}(\text{Ox}^{\text{Me}2})_2]$  (**5.3**) as a white solid in 91% yield. One set of oxazoline resonances in the  $^1\text{H}$  NMR spectrum, and one sharp singlet at  $-13.1$  ppm ( $\Delta\nu_{1/2} = 31.0$  Hz) in  $^{11}\text{B}$  NMR spectrum were observed in benzene- $d_6$ . A single  $^{15}\text{N}$  NMR signal of  $-107.1$  ppm references to nitromethane suggests that both oxazolines in **5.3** are

coordinated to thallium metal. For comparison, the  $^{15}\text{N}$  NMR chemical shift of thallium salt of tris(4,4-dimethyl-2-oxazoliny)phenylborate ligand (TITo<sup>M</sup>) is  $-117.3$  ppm.<sup>15</sup>

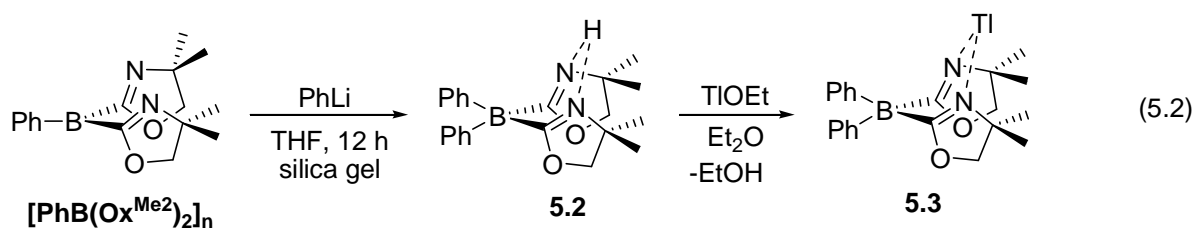


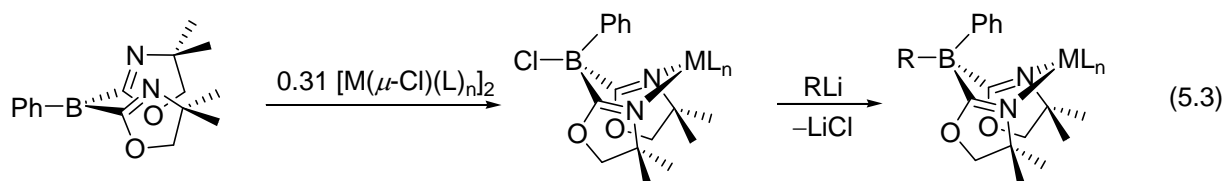
**Table 5.1.**  $^{11}\text{B}$ ,  $^{15}\text{N}$  NMR chemical shifts, and  $\nu_{\text{CN}}$  values for oxazolinyboranes, oxazolinyborates, and their iridium and rhodium complexes.<sup>a</sup>

Compound	$^{11}\text{B}$ NMR ( $\delta$ ) <sup>a</sup>	$^{15}\text{N}$ NMR ( $\delta$ ) <sup>a</sup>	$\nu_{\text{CN}}$ (KBr, $\text{cm}^{-1}$ )
$\text{PhB}(\text{Ox}^{\text{Me}2})_2$ ( <b>4</b> ) in acetonitrile- $d_3$	-8.1	-147.0	1551
$\text{B}(\text{Ox}^{\text{Me}2})_3$ ( <b>5.1</b> ) in methanol- $d_4$	-8.6	n.a.	1608
$\text{H}[\text{Ph}_2\text{B}(\text{Ox}^{\text{Me}2})_2]$ ( <b>5.2</b> )	-14.5	-170.5	1580
$\text{Tl}[\text{Ph}_2\text{B}(\text{Ox}^{\text{Me}2})_2]$ ( <b>5.3</b> )	-13.1	-107.1	1593, 1581
$\text{PhClB}(\text{Ox}^{\text{Me}2})_2\text{Ir}(\eta^4\text{-C}_8\text{H}_{12})$ ( <b>5.4</b> )	-7.6	-182.5	1564
$\text{PhClB}(\text{Ox}^{\text{Me}2})_2\text{Rh}(\eta^4\text{-C}_8\text{H}_{12})$ ( <b>5.5</b> )	-6.8	-180.5	1578
$\text{PhClB}(\text{Ox}^{\text{Me}2})_2\text{Rh}(\text{CO})_2$ ( <b>5.6</b> )	-8.3	-199.0	1580, 1551
$\text{Ph}(\text{Ph}_3\text{SiO})\text{B}(\text{Ox}^{\text{Me}2})_2\text{Rh}(\eta^4\text{-C}_8\text{H}_{12})$ ( <b>5.7</b> )	-4.5	-185.5	1575
$\text{Ph}(\text{Ph}_3\text{SiO})\text{B}(\text{Ox}^{\text{Me}2})_2\text{Li}(\text{THF})_2$ ( <b>5.8</b> )	-6.1	-151.1	1601, 1586
$\text{Ph}_2\text{B}(\text{Ox}^{\text{Me}2})_2\text{Ir}(\eta^4\text{-C}_8\text{H}_{12})$ ( <b>5.9</b> )	-12.8	-152.2	1588, 1555
$\text{ClB}(\text{Ox}^{\text{Me}2})_3\text{Rh}(\text{CO})_2$ ( <b>5.10</b> )	-9.3	n.a.	1599
$\text{To}^{\text{M}}\text{Ir}(\eta^4\text{-C}_8\text{H}_{12})$ ( <b>5.11</b> )	-16.4	-154.9, -192.9	1607, 1558
$\text{To}^{\text{M}}\text{Rh}(\eta^4\text{-C}_8\text{H}_{12})$ ( <b>5.12</b> )	-16.3	-161.1, -169.2	1611, 1567

<sup>a</sup>  $^{11}\text{B}$  and  $^{15}\text{N}$  NMR was taken in benzene- $d_6$ , otherwise noted.

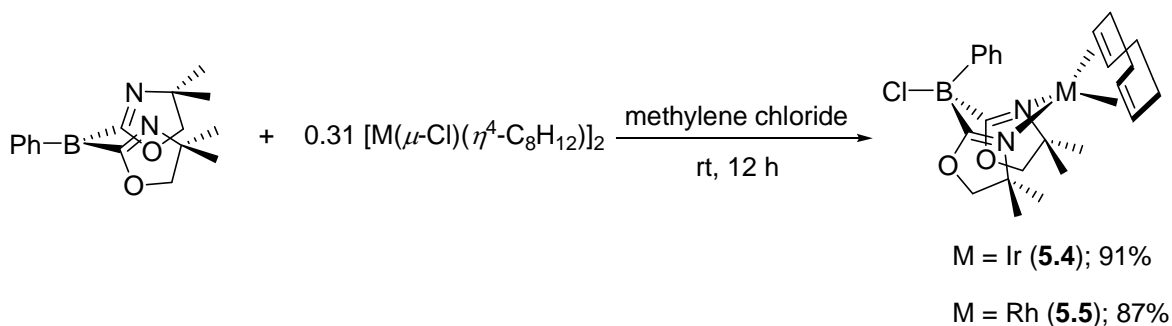
### *Synthesis and characterization of bis- and tris(oxazoliny)borato iridium and rhodium compounds*

Two general routes provide oxazolinyborato iridium and rhodium complexes. The first route involves reaction of oxazolinyboranes and metal chlorides, followed by substitution of chlorine with a nucleophile (*e.g.*, RLi; eq 5.3). A second approach involves salt metathesis of thallium oxazolinyborate salts and metal chlorides. We will first describe the synthesis and structural characterization of bis(oxazoliny)borato iridium and iridium complexes. Then, the synthesis and properties of tris(oxazoliny)borate complexes will be discussed.



$[\text{PhB}(\text{Ox}^{\text{Me}_2})_2]_n$  contains variable amount of LiCl, and therefore excess  $[\text{PhB}(\text{Ox}^{\text{Me}_2})_2]_n$  is needed to prepare bis(oxazoliny)borato metal complexes.  $[\text{PhB}(\text{Ox}^{\text{Me}_2})_2]_n$  reacts with 0.31 equiv of  $[\text{M}(\mu\text{-Cl})(\eta^4\text{-C}_8\text{H}_{12})_2]$  ( $\text{M} = \text{Ir}, \text{Rh}$ ) in methylene chloride at room temperature over 12 h to provide  $\text{PhClB}(\text{Ox}^{\text{Me}_2})_2\text{Ir}(\eta^4\text{-C}_8\text{H}_{12})$  (**5.4**) and  $\text{PhClB}(\text{Ox}^{\text{Me}_2})_2\text{Rh}(\eta^4\text{-C}_8\text{H}_{12})$  (**5.5**) (Scheme 5.2). Analytically pure materials **5.4** and **5.5** are obtained as orange and deep yellow solids respectively after recrystallization at  $-30\text{ }^\circ\text{C}$ . These air-sensitive complexes are unchanged in benzene for 6 h at  $60\text{ }^\circ\text{C}$ , however they decomposes slowly at  $80\text{ }^\circ\text{C}$ . In the  $^1\text{H}$  NMR spectrum, one set of oxazoline resonances (*e.g.*, two singlets assigned to diastereotopic methyl groups at 1.01 and 0.80 ppm, and two doublets at 3.57 and 3.39 ppm for methylene groups) suggest  $C_s$ -symmetric species for **5.4**. Additionally, the  $^{11}\text{B}$  NMR spectrum of **5.4** exhibited a single resonance at  $-7.6$  ppm in benzene- $d_6$ . One  $^{15}\text{N}$  NMR signal was observed at  $-182.5$  ppm, which was 54.6 ppm upfield in comparison to that for  $2\text{H-Ox}^{\text{Me}_2}$  ( $-127.9$  ppm). Furthermore, only one

signal assigned to a CN stretching frequency of oxazolines was observed in the IR spectrum at  $1565\text{ cm}^{-1}$ , which is again lower in energy compared to that for non-coordinated oxazoline ( $\nu_{\text{CN}} = 1630\text{ cm}^{-1}$ ). These  $^{15}\text{N}$  NMR and IR data suggest that both oxazolines coordinate to the iridium center in **5.4**. Similar spectroscopic patterns in the NMR and infrared spectra were observed for  $\text{PhCIB}(\text{Ox}^{\text{Me}_2})_2\text{Rh}(\eta^4\text{-C}_8\text{H}_{12})$  (**5.5**).



**Scheme 5.2.** Synthesis of bis(oxazoliny)borato iridium and rhodium complexes from  $[\text{PhB}(\text{Ox}^{\text{Me}_2})_2]_n$  via chloride abstraction.

X-ray quality crystals of  $\text{PhCIB}(\text{Ox}^{\text{Me}_2})_2\text{Ir}(\eta^4\text{-C}_8\text{H}_{12})$  (**5.4**) and  $\text{PhCIB}(\text{Ox}^{\text{Me}_2})_2\text{Rh}(\eta^4\text{-C}_8\text{H}_{12})$  (**5.5**) are obtained from concentrated solution mixture of toluene and pentane cooled to  $-30\text{ }^\circ\text{C}$ . Single crystal diffraction studies confirmed the structures and the formation of a B–Cl bond in both **5.4** (Figure 5.1) and **5.5** (Figure 5.2). Both structures have a crystallographic mirror plane. The crystal structure of **5.4** shows both oxazolines coordinate to iridium, and the two nitrogen-iridium distances are equivalent ( $\text{Ir1-N1}$ ,  $2.110(2)\text{ \AA}$ ). Chelation forms a six-membered ring, and  $\text{B1-C10-N1-Ir1-N1}^i\text{-C10}^i$  atoms in the ring adopt a boat conformation. The phenyl group is pseudoaxial, and the chlorine is pseudoequatorial. The phenyl group is closer to the iridium than chlorine atom. The B–Cl distance in **5.4** is  $1.894(3)\text{ \AA}$ . The rhodium complex **5.5** has similar crystal structure of **5.4**. The two nitrogen-rhodium distances are also equivalent [ $\text{Rh1-N1}$ ,  $2.110(2)\text{ \AA}$ ], and the B–Cl distance in **5.5** is  $1.900(4)\text{ \AA}$ .

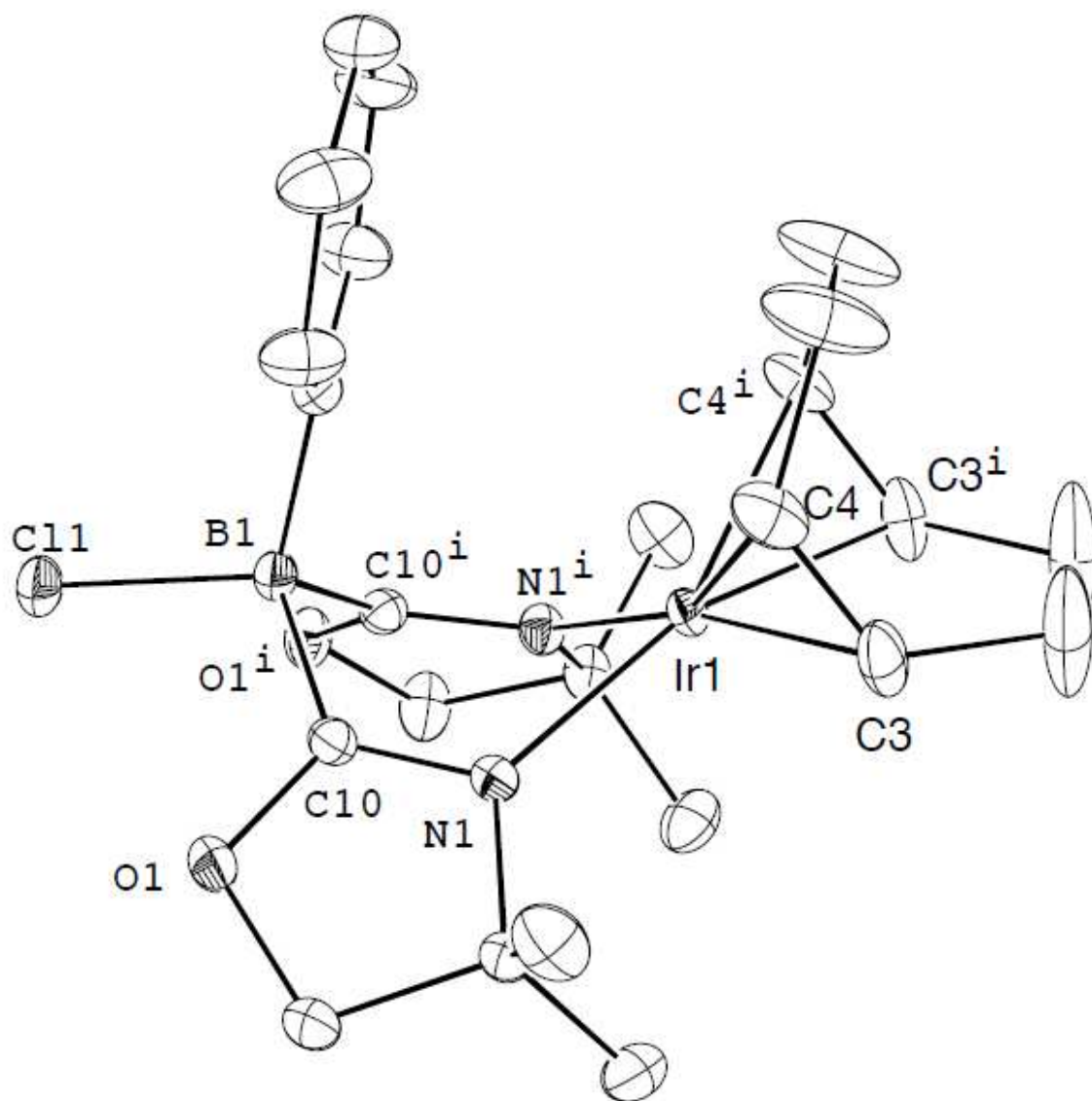


**Figure 5.1.** ORTEP diagram of  $\text{PhClB}(\text{Ox}^{\text{Me}_2})_2\text{Ir}(\eta^4\text{-C}_8\text{H}_{12})$  (**5.4**). Ellipsoids are plotted at 50% probability, and hydrogen atoms are not illustrated for clarity. Bond distances ( $\text{\AA}$ ): Ir1–N1, 2.110(2); Ir1–C4, 2.112(2); Ir1–C3, 2.123(2); B1–Cl1, 1.894(3).

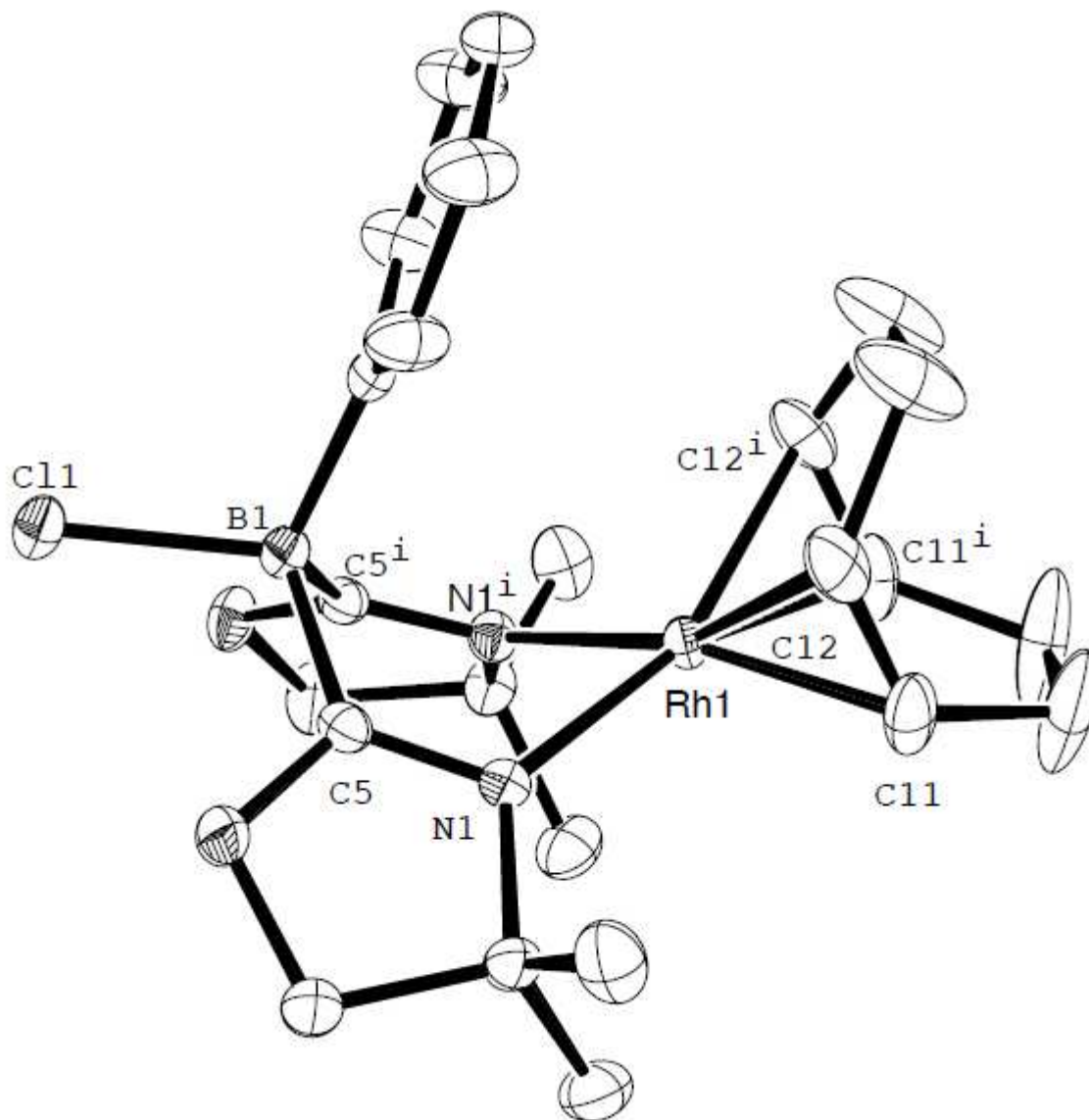
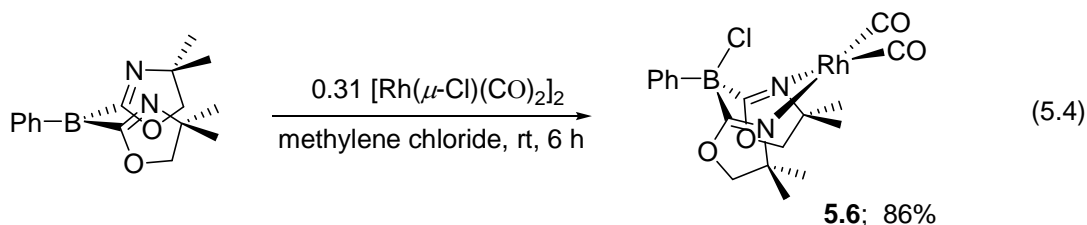


**Figure 5.2.** ORTEP diagram of  $\text{PhClB}(\text{Ox}^{\text{Me}2})_2\text{Rh}(\eta^4\text{-C}_8\text{H}_{12})$  (**5.5**). Ellipsoids are plotted at 50% probability, and hydrogen atoms are not illustrated for clarity. Bond distances (Å): Rh1–C12, 1.852(3); Rh(1)–C(11), 2.127(3); Rh(1)–N(1), 2.123(2); B1–Cl1, 1.900(4).

The abstraction of hydride, alkyl, and amido group from metal center by Lewis acids such as  $\text{B}(\text{C}_6\text{F}_5)_3$ ,  $\text{PhB}(\text{C}_6\text{F}_5)_3$ ,  $\text{BPh}_3$ ,  $[\text{Ph}_3\text{C}][\text{B}(\text{C}_6\text{F}_5)_3]$ , and others are well documented in literature.<sup>16</sup> However, the chloride abstractions from  $[\text{M}(\mu\text{-Cl})(\eta^4\text{-C}_8\text{H}_{12})]_2$  ( $\text{M} = \text{Ir}, \text{Rh}$ ) by phenyl-bis(oxazolinyl)borane  $[\text{PhB}(\text{Ox}^{\text{Me}2})_2]_n$  are rare examples of halide abstraction from a

metal-halogen bond by a Lewis acid. Presumably, the strong Lewis acidity of the boron center in  $[\text{PhB}(\text{Ox}^{\text{Me}_2})_2]_n$ <sup>13</sup> and the coordination of oxazolines facilitate the cleavage of metal-chlorine bond and simultaneous formation of B–Cl bond.

The synthesis of bis(oxazoliny)borato metal complexes using  $[\text{PhB}(\text{Ox}^{\text{Me}_2})_2]_n$  via chlorine abstraction motivated us to synthesize analogous bis- and tris(oxazoliny)borato rhodium dicarbonyl complexes.  $[\text{PhB}(\text{Ox}^{\text{Me}_2})_2]_n$  reacts with 0.31 equiv of  $[\text{Rh}(\mu\text{-Cl})(\text{CO})_2]_2$  affording  $\text{PhClB}(\text{Ox}^{\text{Me}_2})_2\text{Rh}(\text{CO})_2$  (**5.6**) as a dark brown solid in 86% yield after recrystallization (eq 5.4). One set of oxazoliny resonances in <sup>1</sup>H NMR spectrum and a single <sup>15</sup>N chemical shift (–199.0 ppm) in benzene-*d*<sub>6</sub> suggest **5.6** as a *C*<sub>s</sub>-symmetric species, in which both oxazolines coordinate to rhodium.



Crystallization in methylene chloride at –30 °C affords X-ray quality single crystals of **5.6** (an ORTEP diagram is shown in Figure 5.3). The crystallized structure contains a square-planar rhodium center ( $\sum_{\text{L-Rh-L}'} = 359.93^\circ$ ). The chlorine blocks one face of the square-planar complex. The nitrogens of both oxazolines have the same distances to rhodium [2.089(2) Å]. B1-C5-N1-Rh1-N1<sup>i</sup>-C5<sup>i</sup> atoms form a six-membered ring adopting a boat conformation, in which the phenyl group is pseudoequatorial and the chlorine is pseudoaxial. Interestingly, the position of phenyl group and chlorine is reversed in the similar boat conforming six-membered ring of  $\text{PhClB}(\text{Ox}^{\text{Me}_2})_2\text{Rh}(\eta^4\text{-C}_8\text{H}_{12})$  (**5.5**) as shown in Figure 5.2.



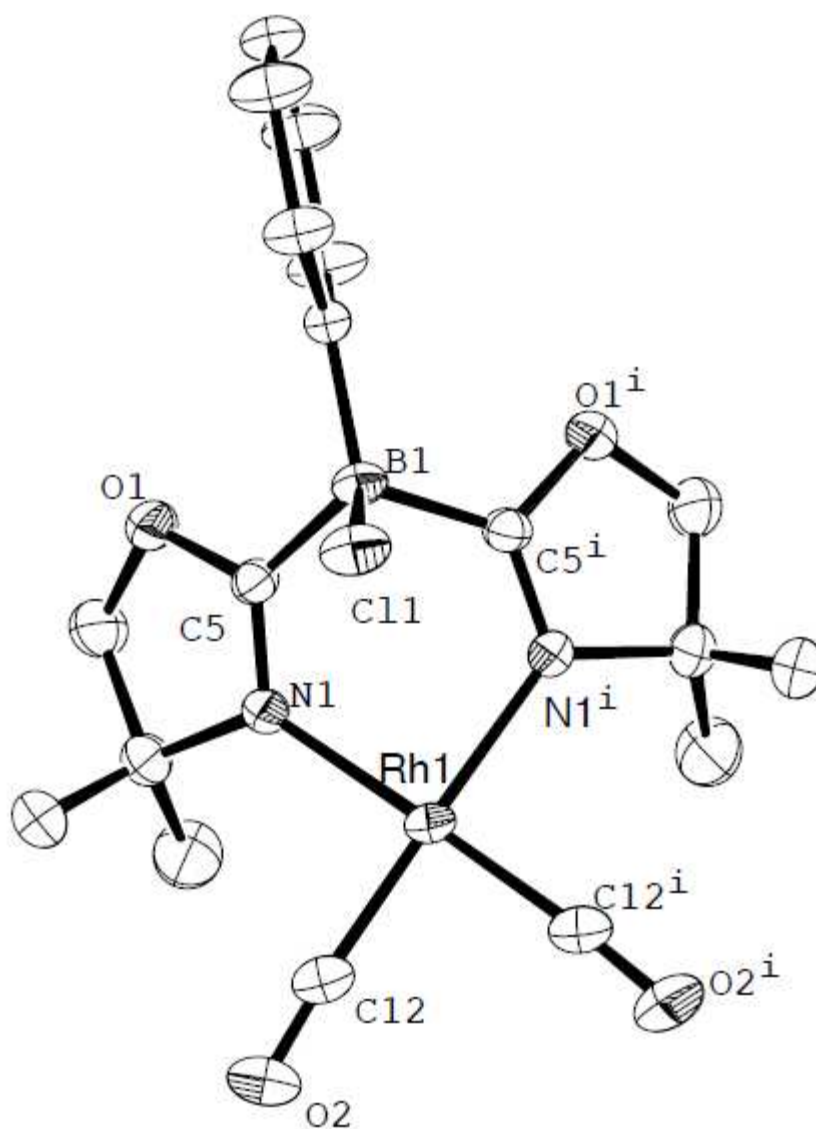
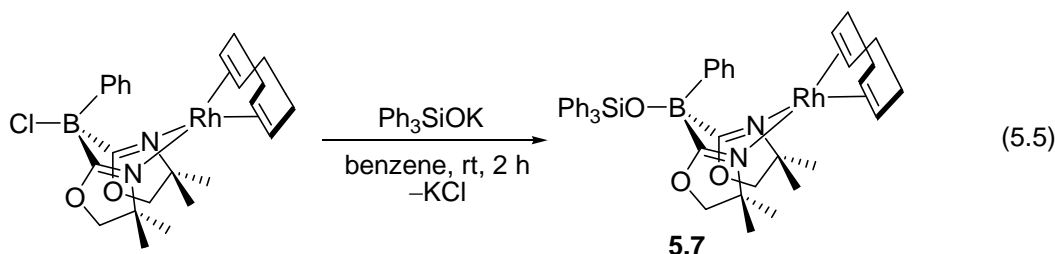


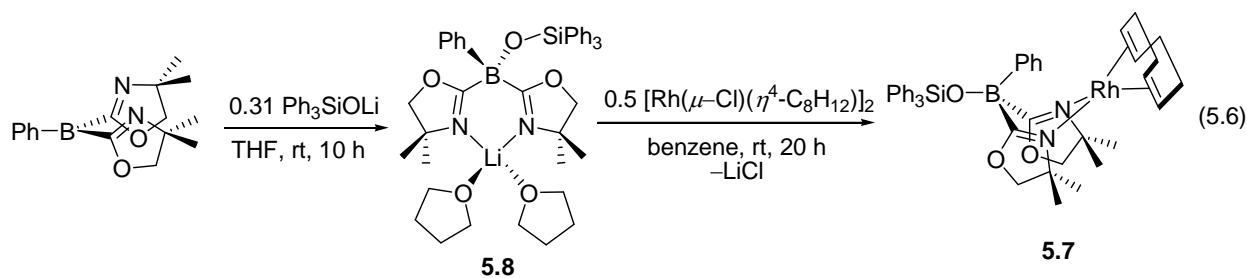
**Figure 5.3.** ORTEP diagram of  $\text{PhClB}(\text{Ox}^{\text{Me}_2})_2\text{Rh}(\text{CO})_2$  (**5.6**). Ellipsoids are plotted at 50% probability, and hydrogen atoms are not illustrated for clarity. Selected bond distances (Å): Rh1–N1, 2.089(2); Ir1–C4, 2.112(2); Ir1–C3, 2.123(2); B1–Cl1, 1.894(3).

Interestingly, all the above metal complexes **5.2-5.6** can be easily derivatized by substituting chlorine atom of B–Cl moiety with nucleophiles. The presence of a B–Cl bond in these ligand-metal pairs therefore provide an excellent opportunity to modify the ligand structures in order to tune the electronic properties of the metal centers and also the stability of

the metal complexes. The treatment of  $\text{Ph}_3\text{SiOK}$  with  $\text{PhClB}(\text{Ox}^{\text{Me}_2})_2\text{Rh}(\eta^4\text{-C}_8\text{H}_{12})$  (**5.5**) in benzene at room temperature affords  $\text{Ph}(\text{Ph}_3\text{SiO})\text{B}(\text{Ox}^{\text{Me}_2})_2\text{Rh}(\eta^4\text{-C}_8\text{H}_{12})$  (**5.7**), which is isolated as a yellow solid in 94% yield (eq 5.5).



Complex **5.7** is  $C_s$ -symmetric similar to **5.5**, according to the  $^1\text{H}$  NMR spectroscopy. A downfield  $^{11}\text{B}$  resonance of **5.7** at  $-4.5$  ppm in benzene- $d_6$  compared to that for **5.5** at  $-6.8$  ppm suggests that the chlorine is replaced by more electron withdrawing oxygen at the boron center. **5.7** is also synthesized by an alternative route as shown in eq 5.6. The reaction of  $[\text{PhB}(\text{Ox}^{\text{Me}_2})_2]_n$  and  $\text{Ph}_3\text{SiOLi}$  in THF at room temperature affords  $\text{Ph}(\text{Ph}_3\text{SiO})\text{B}(\text{Ox}^{\text{Me}_2})_2\text{Li}(\text{THF})_2$  (**5.8**) in 83% yield.



**5.8** crystallized from a concentrated solution in toluene at  $-30$  °C. The X-ray crystal structure of **5.8** in Figure 5.4 shows the ‘B–O–Si’ moiety in the molecule. B1–O1–Si1 bond angle is  $150.57(19)^\circ$ . The Si1–O1 distance is  $1.580(2)$  Å and B1–O1 distance is  $1.457(4)$  Å. The nitrogens of two oxazolines are coordinated to a lithium atom. Two lithium–nitrogen bond distances are not equivalent [Li1–N1,  $1.965(6)$  Å; Li1–N2,  $1.997(6)$  Å].

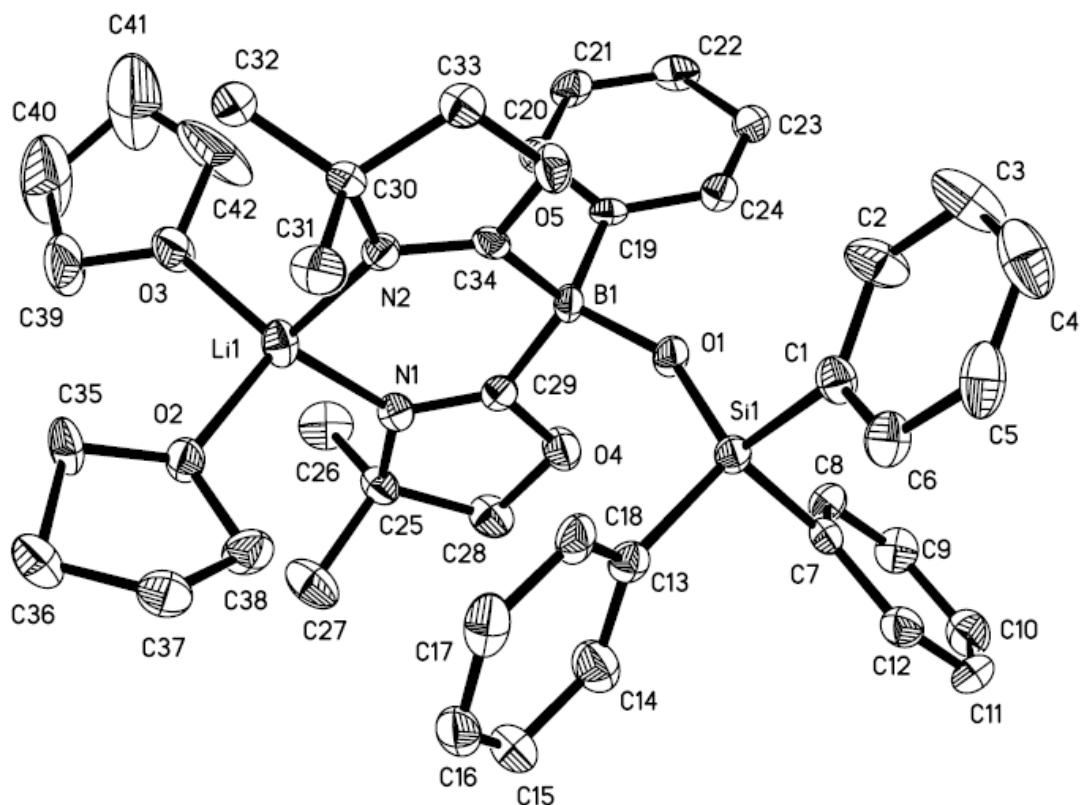
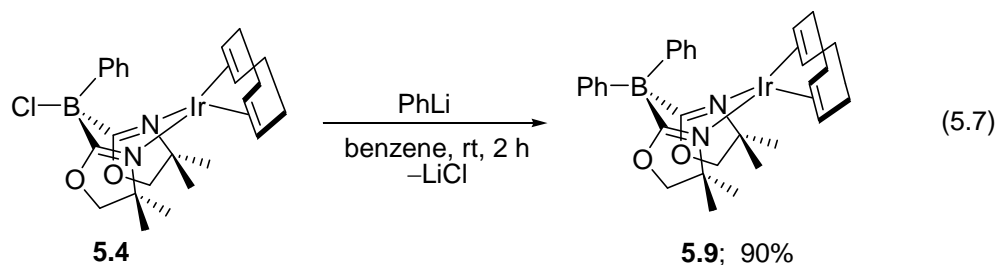


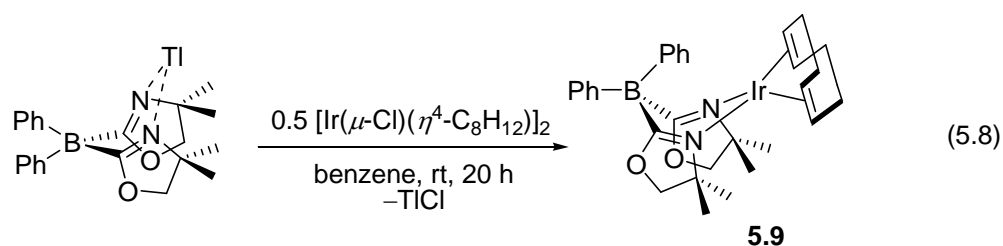
**Figure 5.4.** ORTEP diagram of  $\text{Ph}(\text{Ph}_3\text{SiO})\text{B}(\text{Ox}^{\text{Me}_2})_2\text{Li}(\text{THF})_2$  (**5.8**). Ellipsoids are plotted at 50% probability, and hydrogen atoms are not illustrated for clarity. Selected bond distances (Å): Si1–O1, 1.580(2); B1–O1, 1.457(4); Li1–N1, 1.965(6); Li1–N2, 1.997(6). Selected bond angles (°): B1–O1–Si1, 150.57(19).

In the next step, addition of 0.5 equiv of  $[\text{Rh}(\mu\text{-Cl})(\eta^4\text{-C}_8\text{H}_{12})]_2$  to the benzene solution of **5.8** provided the desired rhodium complex **5.7** at room temperature.

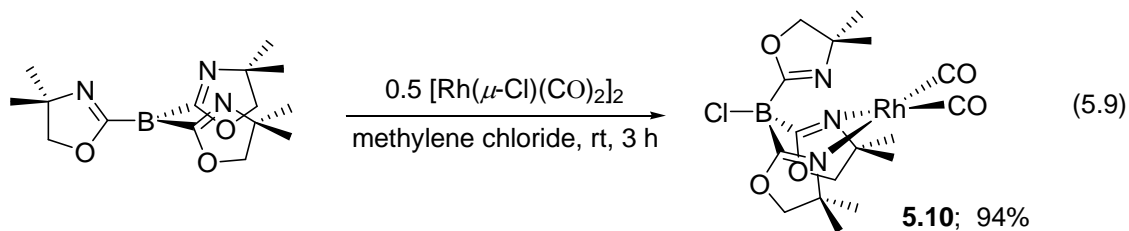
Bis(4,4-dimethyl-2-oxazolinyl)diphenylborato iridium complex  $\text{Ph}_2\text{B}(\text{Ox}^{\text{Me}_2})_2\text{Ir}(\eta^4\text{-C}_8\text{H}_{12})$  (**5.9**) is prepared by substituting the chlorine of  $\text{PhClB}(\text{Ox}^{\text{Me}_2})_2\text{Ir}(\eta^4\text{-C}_8\text{H}_{12})$  with a phenyl group (eq 5.7).  $\text{PhClB}(\text{Ox}^{\text{Me}_2})_2\text{Ir}(\eta^4\text{-C}_8\text{H}_{12})$  (**5.4**) and  $\text{PhLi}$  react rapidly in benzene at room temperature to afford **5.10** in 90% yield. The chemical shift of  $^{11}\text{B}$  NMR at  $-12.8$  ppm ( $\Delta\nu_{1/2} = 63.0$  Hz) indicates the replacement of chlorine by phenyl group at the boron center.



An alternative preparation of **5.10** is also performed by reaction of  $\text{Ti}[\text{Ph}_2\text{B}(\text{Ox}^{\text{Me}_2})_2]$  (**5.3**) and 0.5 equiv of  $[\text{Ir}(\mu\text{-Cl})(\eta^4\text{-C}_8\text{H}_{12})_2]$  in benzene at room temperature (eq 5.8). The complex **5.9** is unchanged in benzene at 80 °C for 20 h, however it decomposes slowly at 120 °C.

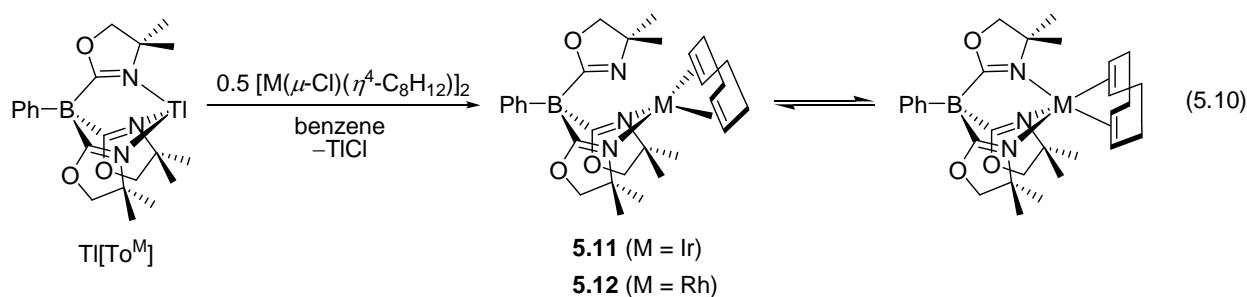


In the related synthesis, addition of 0.5 equiv of  $[\text{Rh}(\mu\text{-Cl})(\text{CO})_2]_2$  to a slurry of tris(oxazolinyl)borane  $[\text{B}(\text{Ox}^{\text{Me}_2})_3]_n$  in THF results a clear yellow solution after stirring for 1 h at room temperature. Removal of the volatiles affords  $\text{ClB}(\text{Ox}^{\text{Me}_2})_3\text{Rh}(\text{CO})_2$  (**5.7**) as a yellow solid in 94% yield (eq 5.5). One singlet at 3.75 ppm for inequivalent methyl groups and another singlet at 1.79 ppm for methylene groups of oxazolines in  $^1\text{H}$  NMR spectrum in tetrahydrofuran- $d_8$  suggest that **5.7** is  $C_{3v}$ -symmetric.



Tris(oxazolinyl)borato iridium and rhodium complexes  $\text{To}^{\text{M}}\text{M}(\eta^4\text{-C}_8\text{H}_{12})$  are prepared by the reaction of  $\text{TiTo}^{\text{M}}$  with 0.5 equiv of  $[\text{M}(\mu\text{-Cl})(\eta^4\text{-C}_8\text{H}_{12})_2]$  in benzene [eq 5.10; **5.11** ( $\text{M} = \text{Ir}$ ):

60 °C, 4 h, 93%; **5.12** (M = Rh): 23 °C, 1 h, 90%]. In contrast to the reaction with  $\text{TiTo}^{\text{M}}$ , the reaction of 2 equiv of  $\text{Li[ToM]}$  with  $[\text{Ir}(\mu\text{-Cl})(\eta^4\text{-C}_8\text{H}_{12})_2]_2$  in benzene or THF provides a dimeric  $\text{LiCl}$  adduct,  $(\text{LiCl})_2[(\kappa^2\text{-ToM}(\eta^4\text{-C}_8\text{H}_{12}))_2]$ .<sup>17</sup>  $\text{To}^{\text{M}}\text{Rh}(\eta^4\text{-C}_8\text{H}_{12})$  (**5.12**) is stable in air for 12 h at room temperature in solid form and also in benzene. In contrast, the analogous iridium complex **5.11** is air sensitive; however, no decomposition of **5.11** was observed even after heating in dry toluene at 60 °C for 3 days and at 180 °C for 10 h.



$^1\text{H}$  NMR spectra of  $\text{To}^{\text{M}}\text{Ir}(\eta^4\text{-C}_8\text{H}_{12})$  (**5.11**) and  $\text{To}^{\text{M}}\text{Rh}(\eta^4\text{-C}_8\text{H}_{12})$  (**5.12**) complexes in benzene- $d_6$  at room temperature contained three singlets for methyl and three singlets for methylene groups of three oxazolines. These spectra are consistent with  $C_s$ -symmetric structures, and also suggest bidentate coordination mode of  $\text{To}^{\text{M}}$ -ligand in the metal complexes. However, two observed  $^{15}\text{N}$  chemical shifts of oxazoline nitrogens (**5.11**:  $-154.9$ ,  $-192.9$  ppm; **5.12**:  $-161.1$ ,  $-169.2$  ppm) are significantly upfield compared to that of non-coordinated 4,4-dimethyl-2-H-oxazoline ( $-127.0$  ppm). These NMR data doesn't confirm the presence of a pendant non-coordinated oxazoline; rather suggest a dynamic exchange process between the pendent oxazoline and the two coordinated oxazolines in solution. Fluxional behaviors of **5.11** and **5.12** are further supported by variable temperature NMR (VT NMR) studies (Figure 5.5).

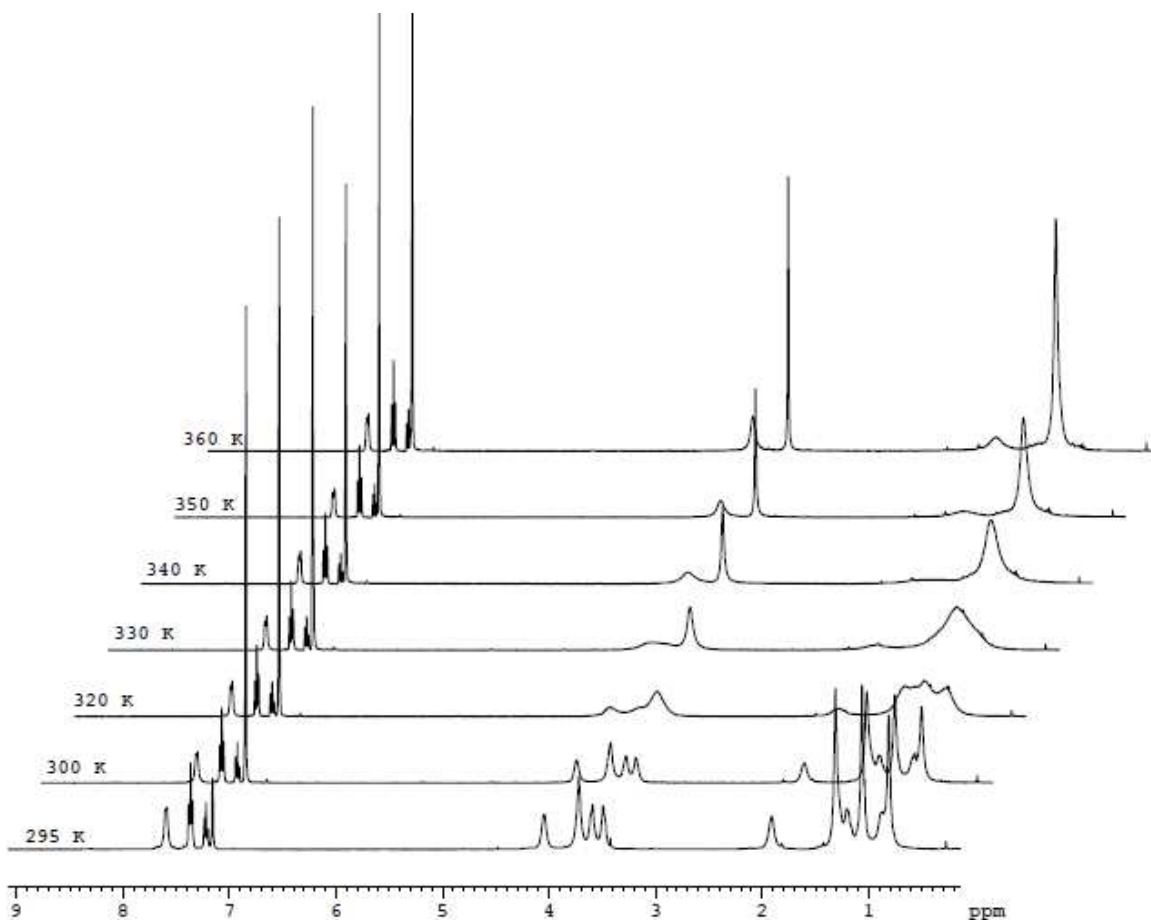


**Figure 5.5.**  $^1\text{H}$  NMR spectra of  $\text{To}^{\text{M}}\text{Ir}(\eta^4\text{-C}_8\text{H}_{12})$  (**5.11**) showing coalesce of oxazoline resonances as temperature is increased.

The variable temperature  $^1\text{H}$  NMR spectra of **5.11** acquired from 295 K to 360 K in benzene- $d_6$  showed resonances of oxazolines and cyclopentadiene that broaden as the temperature was increased. At 340 K, the three sets of oxazoline resonances coalesced into one set. At 360 K, one sharp singlet at 1.12 ppm for methyl and one singlet at 3.63 ppm for methylene groups of oxazolines suggest that **5.11** is  $C_{3v}$ -symmetric. The VT NMR experiments suggest that the rapid exchange between pendent oxazoline and coordinated oxazolines is faster than  $^1\text{H}$  NMR time scale above coalesce temperature that make the three oxazolines of  $\text{To}^{\text{M}}$  ligand indistinguishable.

In the solid state, the  $\text{To}^{\text{M}}$  ligand in **5.11** and **5.12** is bidentate, as evident by two  $\nu_{\text{CN}}$  bands in IR spectra corresponding to coordinated (**5.11**:  $1558\text{ cm}^{-1}$ ; **5.12**:  $1567\text{ cm}^{-1}$ ) and uncoordinated (**5.11**:  $1607\text{ cm}^{-1}$ ; **5.12**:  $1611\text{ cm}^{-1}$ ) oxazolines. X-ray quality single crystals of **5.12** are obtained by vapor diffusion of pentane into a toluene solution at  $-30\text{ }^{\circ}\text{C}$ . The solid state structure of **5.12** is established by X-ray crystallography, which also reveals  $\kappa^2\text{-To}^{\text{M}}$  coordination (Figure 5.6). Rhodium is coordinated to nitrogens of two oxazolines and to 1,5-cyclooctadiene. The six-membered chelate ring in **5.12** forms the boat configuration. The phenyl group is pseudoaxial, and the pendant oxazoline is pseudoequatorial.

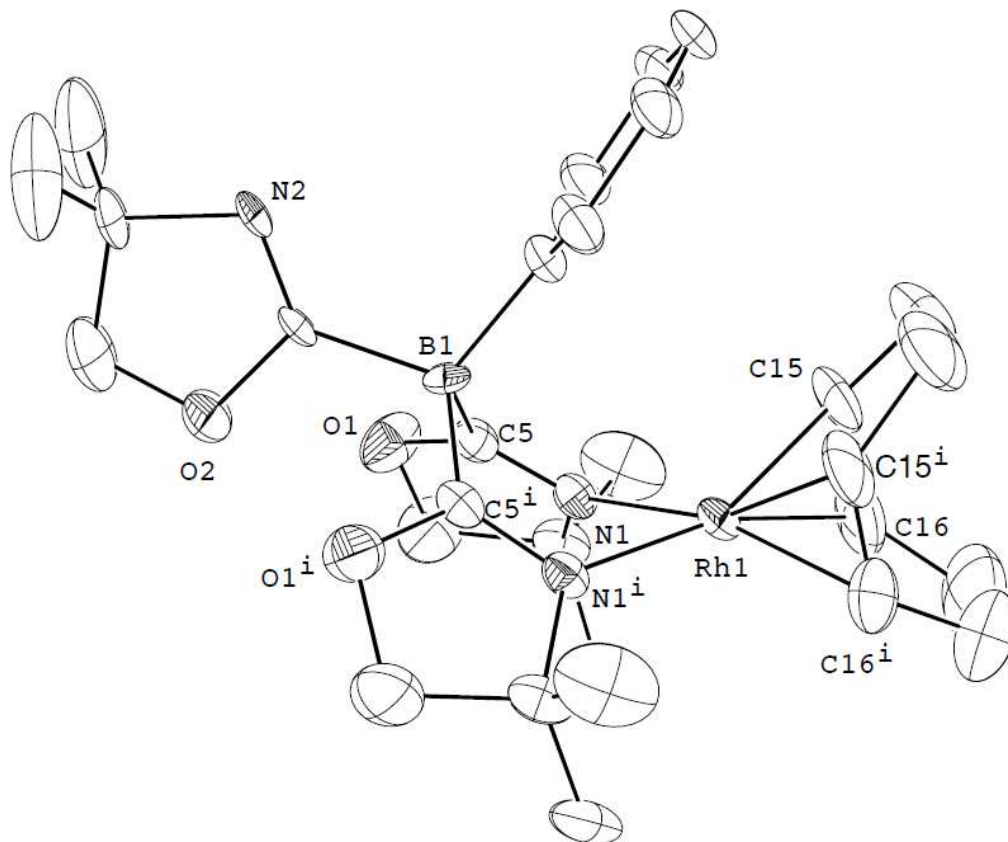


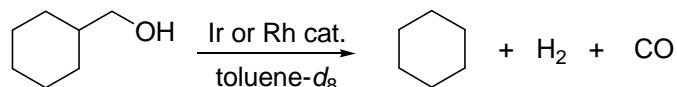
**Figure 5.6.** ORTEP diagram of  $\text{To}^{\text{M}}\text{Rh}(\eta^4\text{-C}_8\text{H}_{12})$  (**5.12**). Ellipsoids are plotted at 50% probability, and hydrogen atoms are not illustrated for clarity. Selected bond distances ( $\text{\AA}$ ): Rh1–N1, 2.116(6); Rh1–C15, 2.099(9); Rh1–C16, 2.120(10).

### *Catalytic alcohol decarbonylations*

All the above bis- and tris(oxazolanyl)borato iridium and rhodium complexes are tested as precatalysts for thermal decarbonylation of primary alcohols without any CO acceptor. Our effort to develop a direct acceptorless thermal decarbonylation of alcohols began with studies of the reaction of cyclohexanemethanol (CyCH<sub>2</sub>OH) as the substrate with 10 mol % of iridium or rhodium complexes in toluene-*d*<sub>8</sub>. These screening reactions were conducted in milligram scale within a sealed J-Young style NMR tube by gradual increment of temperature ranging from 60 °C to 180 °C. The progress of the reaction was monitored by <sup>1</sup>H NMR spectroscopy and the analysis by GC-MS. Selected results of these experiments are shown in Table 5.2.

The previous findings from our group that To<sup>M</sup>Rh(H)<sub>2</sub>CO and To<sup>M</sup>Rh(CO)<sub>2</sub> catalyze the photolytic decarbonylation of CyCH<sub>2</sub>OH to cyclohexane led us first to test the identical reaction under thermal conditions.<sup>12</sup> The mixture of CyCH<sub>2</sub>OH and 10 mol % of To<sup>M</sup>Rh(H)<sub>2</sub>CO or To<sup>M</sup>Rh(CO)<sub>2</sub> in toluene was heated at 120 °C for 48 h, however the resulting mixture contained only the alcohol starting material and a black precipitate due to the catalyst decomposition (Table 5.2, entries 1–2). We then investigated several other known rhodium and iridium carbonyl and chloride complexes in this reaction. Unfortunately, none of these complexes showed any activity for the conversion of CyCH<sub>2</sub>OH (Table 5.2, entries 3–7). Reaction of CyCH<sub>2</sub>OH with 10 mol % of either [IrCl(η<sup>4</sup>-C<sub>8</sub>H<sub>12</sub>)]<sub>2</sub> or [RhCl(η<sup>4</sup>-C<sub>8</sub>H<sub>12</sub>)]<sub>2</sub> at 180 °C contain a small amount of cyclohexane and some black precipitate (Table 5.2, entries 8 & 9). This finding motivated to screen several known or newly synthesized iridium and rhodium cyclooctadienyl complexes for CyCH<sub>2</sub>OH decarbonylation (Table 5.2, entries 10 & 21). Tp\*Ir(η<sup>4</sup>-C<sub>8</sub>H<sub>12</sub>) [Tp\* = tris(3,5-dimethylpyrazolyl)borate] fails to convert alcohol to alkane, even after prolonged heating at 180 °C (Table 5.2, entry 10).



**Table 5.2.** Conditions and catalysts tested for the catalytic decarbonylation of CyCH<sub>2</sub>OH.<sup>a</sup>

Entry	Catalyst	Temperature	Time (days)	Yield (%) <sup>b</sup>
1	To <sup>M</sup> Rh(H) <sub>2</sub> CO	120 °C	2	0
2	To <sup>M</sup> Rh(CO) <sub>2</sub>	180 °C	4	0
3	To <sup>M</sup> Ir(CO) <sub>2</sub>	180 °C	4	0
4	[Rh(dppp) <sub>2</sub> Cl]	180 °C	4	0
5	[Rh(CO)Cl(dppp)] <sub>2</sub>	180 °C	4	0
6	[Rh(dppe) <sub>2</sub> Cl]	180 °C	4	0
7	[Rh(dppe)ClCO]	180 °C	4	0
8	[IrCl(η <sup>4</sup> -C <sub>8</sub> H <sub>12</sub> ) <sub>2</sub> ]	180 °C	4	<10
9	[RhCl(η <sup>4</sup> -C <sub>8</sub> H <sub>12</sub> ) <sub>2</sub> ]	180 °C	4	<10
10	Tp*Ir(η <sup>4</sup> -C <sub>8</sub> H <sub>12</sub> )	180 °C	4	0
11	PhClB(Ox <sup>Me2</sup> ) <sub>2</sub> Ir(η <sup>4</sup> -C <sub>8</sub> H <sub>12</sub> ) ( <b>5.4</b> )	130 °C	4	<10
12	PhClB(Ox <sup>Me2</sup> ) <sub>2</sub> Rh(η <sup>4</sup> -C <sub>8</sub> H <sub>12</sub> ) ( <b>5.5</b> )	130 °C	2	<10
14	PhClB(Ox <sup>Me2</sup> ) <sub>2</sub> Rh(CO) <sub>2</sub> ( <b>5.6</b> )	130 °C	4	0
15	Ph(Ph <sub>3</sub> SiO)B(Ox <sup>Me2</sup> ) <sub>2</sub> Rh(η <sup>4</sup> -C <sub>8</sub> H <sub>12</sub> ) ( <b>5.7</b> )	130 °C	2	0
16	Ph <sub>2</sub> B(Ox <sup>Me2</sup> ) <sub>2</sub> Ir(η <sup>4</sup> -C <sub>8</sub> H <sub>12</sub> ) ( <b>5.9</b> )	130 °C	2	54
17	ClB(Ox <sup>Me2</sup> ) <sub>3</sub> Rh(CO) <sub>2</sub> ( <b>5.10</b> )	130 °C	4	0
18	To <sup>M</sup> Ir(η <sup>4</sup> -C <sub>8</sub> H <sub>12</sub> ) ( <b>5.11</b> )	130 °C	4	0
19		180 °C	4	86
20	To <sup>M</sup> Rh(η <sup>4</sup> -C <sub>8</sub> H <sub>12</sub> ) ( <b>5.12</b> )	130 °C	4	0
21		180 °C	4	10

<sup>a</sup> Reaction conditions: 10 mol % catalyst, toluene as the solvent, <sup>b</sup> NMR yield.

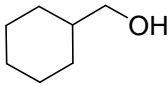
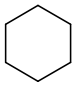
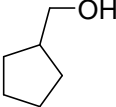
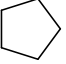
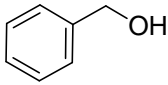
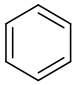
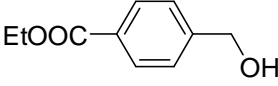
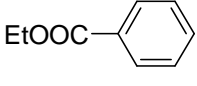
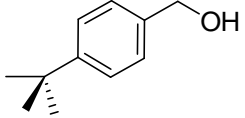
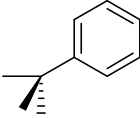
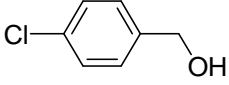
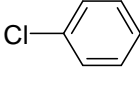
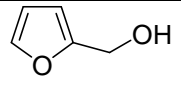
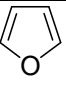
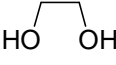
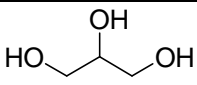
PhClB(Ox<sup>Me2</sup>)<sub>2</sub>Ir(η<sup>4</sup>-C<sub>8</sub>H<sub>12</sub>) (**5.4**) and PhClB(Ox<sup>Me2</sup>)<sub>2</sub>Rh(η<sup>4</sup>-C<sub>8</sub>H<sub>12</sub>) (**5.5**) display small activity in alcohol decarbonylation at 130 °C, however rapid decomposition of catalysts hinder

further conversion. Notably, 10 mol %  $\text{Ph}_2\text{B}(\text{Ox}^{\text{Me}_2})_2\text{Ir}(\eta^4\text{-C}_8\text{H}_{12})$  (**5.10**) catalyzes decarbonylation of  $\text{CyCH}_2\text{OH}$  to  $\text{CyH}$ ,  $\text{CO}$ , and  $\text{H}_2$  with 54% conversion after heating at  $130\text{ }^\circ\text{C}$  for two days (Table 5.2, entries 17). During the course of the reaction although no black precipitate of iridium is formed, however complex **5.10** is slowly convert to catalytically inactive unidentified complex that precipitates out from the reaction mixture. We then examined the catalytic activity of  $\text{To}^{\text{M}}\text{Ir}(\eta^4\text{-C}_8\text{H}_{12})$  (**5.11**), which is more thermally stable in toluene than  $\text{Ph}_2\text{B}(\text{Ox}^{\text{Me}_2})_2\text{Ir}(\eta^4\text{-C}_8\text{H}_{12})$  (**5.10**). Surprising,  $\text{To}^{\text{M}}\text{Ir}(\eta^4\text{-C}_8\text{H}_{12})$  **5.11** is inert to react with  $\text{CyCH}_2\text{OH}$  at temperatures up to  $150\text{ }^\circ\text{C}$ . However, **5.11** is an active precatalyst for decarbonylation of  $\text{CyCH}_2\text{OH}$  at  $180\text{ }^\circ\text{C}$  in toluene.  $\text{CyCH}_2\text{OH}$  is converted to cyclohexane,  $\text{CO}$ , and  $\text{H}_2$  by 10 mol % of **5.11** in 86% conversion after heating at  $180\text{ }^\circ\text{C}$  for 4 days (Table 5.2, entries 19). GC analysis of the gas mixture collected from the head space of the J-Young NMR tube confirmed the formation of  $\text{CO}$  and  $\text{H}_2$  in the reaction. Interestingly, in contrast to  $\text{Ph}_2\text{B}(\text{Ox}^{\text{Me}_2})_2\text{Ir}(\eta^4\text{-C}_8\text{H}_{12})$  (**5.10**) and  $\text{To}^{\text{M}}\text{Ir}(\eta^4\text{-C}_8\text{H}_{12})$  (**5.11**), all bis- and tris(oxazolinyl)borato rhodium complexes don't provide detectable quantity of cyclohexane from  $\text{CyCH}_2\text{OH}$ .

We then investigated the decarbonylation of a series of primary alcohols using 5 mol % of  $\text{To}^{\text{M}}\text{Ir}(\eta^4\text{-C}_8\text{H}_{12})$  (**5.11**) and  $\text{Ph}_2\text{B}(\text{Ox}^{\text{Me}_2})_2\text{Ir}(\eta^4\text{-C}_8\text{H}_{12})$  (**5.10**), and the results are summarized in Table 5.3. Complexes **5.11** and **5.10** catalyze the conversion of cyclopentanemethanol to cyclopentane in 73% and 45% yield respectively (Table 5.2, entries 3 and 4). Several benzyl alcohols, the central components of lignin,<sup>18</sup> are also decarbonylated to provide corresponding arenes. Notably,  $\text{To}^{\text{M}}\text{Ir}(\eta^4\text{-C}_8\text{H}_{12})$  (**5.11**) tolerates ether, ester, oxo, and chloro functional groups. Furfuryl alcohol is transformed to furan by **5.11** at  $180\text{ }^\circ\text{C}$  in 45% yield (Table 5.2, entry 13). Importantly, **5.11** also catalyzes decarbonylation of polyols such as ethylene glycol and glycerol

into syngas at 180 °C (Table 5.2, entries 15 and 17). More than 90% conversion of ethylene glycol was achieved by heating with 10 mol % **5.11** in toluene at 180 °C over 4 days.

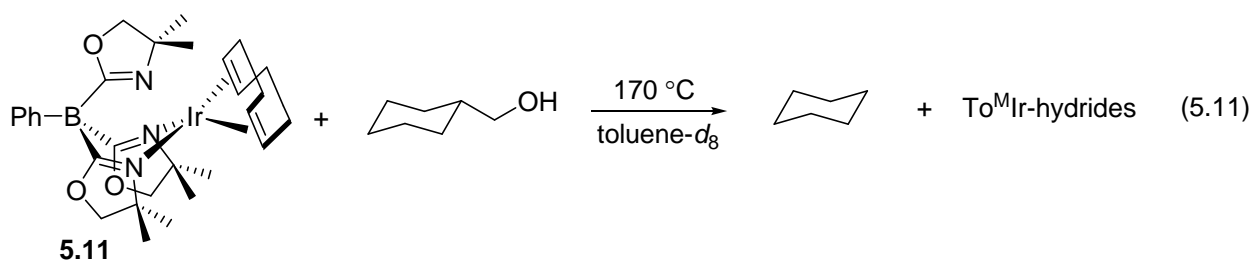
**Table 5.3.**  $\text{To}^{\text{M}}\text{Ir}(\eta^4\text{-C}_8\text{H}_{12})$  (**5.11**) and  $\text{Ph}_2\text{B}(\text{Ox}^{\text{Me}_2})_2\text{Ir}(\eta^4\text{-C}_8\text{H}_{12})$  (**5.10**) catalyzed alcohol conversion into RH,  $\text{H}_2$ , and  $\text{CO}$ .<sup>a</sup>

Substrate	Product	Entry	Catalyst	Time (days)	Yield (%) <sup>b,c</sup>
		1	$\text{To}^{\text{M}}\text{Ir}(\eta^4\text{-C}_8\text{H}_{12})$	4	84
		2	$\text{Ph}_2\text{B}(\text{Ox}^{\text{Me}_2})_2\text{Ir}(\eta^4\text{-C}_8\text{H}_{12})$	2	52
		3	$\text{To}^{\text{M}}\text{Ir}(\eta^4\text{-C}_8\text{H}_{12})$	4	73 (65)
		4	$\text{Ph}_2\text{B}(\text{Ox}^{\text{Me}_2})_2\text{Ir}(\eta^4\text{-C}_8\text{H}_{12})$	2	45
		5	$\text{To}^{\text{M}}\text{Ir}(\eta^4\text{-C}_8\text{H}_{12})$	4	85
		6	$\text{Ph}_2\text{B}(\text{Ox}^{\text{Me}_2})_2\text{Ir}(\eta^4\text{-C}_8\text{H}_{12})$	2	41
		7	$\text{To}^{\text{M}}\text{Ir}(\eta^4\text{-C}_8\text{H}_{12})$	4	81
		8	$\text{Ph}_2\text{B}(\text{Ox}^{\text{Me}_2})_2\text{Ir}(\eta^4\text{-C}_8\text{H}_{12})$	4	25
		9	$\text{To}^{\text{M}}\text{Ir}(\eta^4\text{-C}_8\text{H}_{12})$	4	72 (66)
		10	$\text{Ph}_2\text{B}(\text{Ox}^{\text{Me}_2})_2\text{Ir}(\eta^4\text{-C}_8\text{H}_{12})$	2	33
		11	$\text{To}^{\text{M}}\text{Ir}(\eta^4\text{-C}_8\text{H}_{12})$	4	67
		12	$\text{Ph}_2\text{B}(\text{Ox}^{\text{Me}_2})_2\text{Ir}(\eta^4\text{-C}_8\text{H}_{12})$	4	10
		13	$\text{To}^{\text{M}}\text{Ir}(\eta^4\text{-C}_8\text{H}_{12})$	4	45
		14	$\text{Ph}_2\text{B}(\text{Ox}^{\text{Me}_2})_2\text{Ir}(\eta^4\text{-C}_8\text{H}_{12})$	4	0
	$\text{CO} + \text{H}_2$	15	$\text{To}^{\text{M}}\text{Ir}(\eta^4\text{-C}_8\text{H}_{12})$	4	90
		16	$\text{Ph}_2\text{B}(\text{Ox}^{\text{Me}_2})_2\text{Ir}(\eta^4\text{-C}_8\text{H}_{12})$	4	0
	$\text{CO} + \text{H}_2$	17	$\text{To}^{\text{M}}\text{Ir}(\eta^4\text{-C}_8\text{H}_{12})$	4	n.a.
		18	$\text{Ph}_2\text{B}(\text{Ox}^{\text{Me}_2})_2\text{Ir}(\eta^4\text{-C}_8\text{H}_{12})$	4	0

<sup>a</sup> Reaction conditions: 5 mol % catalyst, toluene as the solvent, 180 °C. <sup>b</sup> % yield was determined by GC using cyclooctane as an internal standard. <sup>c</sup> Isolated yield.

### *Preliminary investigations of catalytic pathways*

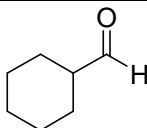
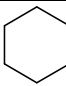
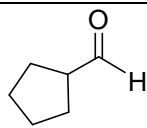
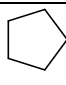
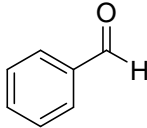
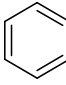
The interesting thermal decarbonylation of alcohols without any CO acceptor catalyzed by  $\text{To}^{\text{M}}\text{Ir}(\eta^4\text{-C}_8\text{H}_{12})$  (**5.11**) led us to investigate the possible catalytic pathways.  $\text{CyCH}_2\text{OH}$  is inert to react with catalytic or stoichiometric amount of **5.11** at temperatures up to 160 °C, however, reaction initiates at 170 °C. During the course of the catalytic decarbonylation reaction, a small quantity of aldehyde was always observed as detected by  $^1\text{H}$  NMR spectroscopy and GC-MS analysis. This observation suggests that the dehydrogenation of alcohol to an aldehyde is likely involved in the first step of dehydrogenative decarbonylation of alcohol as mentioned before. We therefore performed a stoichiometric decarbonylation reaction to identify intermediate of this dehydrogenative process.  $\text{CyCH}_2\text{OH}$  is completely converted into cyclohexane, when a mixture of equivalent amounts of  $\text{To}^{\text{M}}\text{Ir}(\eta^4\text{-C}_8\text{H}_{12})$  (**5.11**) and  $\text{CyCH}_2\text{OH}$  in toluene- $d_8$  was heated at 180 °C for 6 h. In  $^1\text{H}$  NMR spectroscopy, four iridium hydride resonances were detected at -15.87, -16.62, -18.53 and -20.37 ppm. No free 4,4-dimethyl-2-oxazoline ( $2\text{H-Ox}^{\text{Me}_2}$ ) was observed. Structural assignment of any  $\text{To}^{\text{M}}\text{Ir}$ -species was impossible from this  $^1\text{H}$  NMR spectrum due to the overlapping resonances.  $^{11}\text{B}$  NMR spectrum showed one broad peak at -17.9 ppm.



We then investigated the interaction of aldehyde with **5.11**.  $\text{CyCHO}$  is converted to cyclohexane in 84% yield after heating at 180 °C for 2 days by 10 mol % **5.11** (Table 5.4; Entry 1). Likewise, **5.11** also catalyzes the decarbonylation of cyclopentane aldehyde (Table 5.4; Entry 2) and benzaldehyde (Table 5.4; Entry 3). Although full conversion of aldehydes is not achieved,

however, the decarbonylation of an aldehyde is much faster than the dehydrogenation/decarbonylation of an alcohol under the identical reaction conditions. The above observations *i.e.* the formation of aldehyde during catalysis and the fast decarbonylation of aldehyde suggest a sequential dehydrogenation/decarbonylation pathway of an alcohol in the catalytic cycle.

**Table 5.4.**  $\text{To}^{\text{M}}\text{Ir}(\eta^4\text{-C}_8\text{H}_{12})$  (**5.11**) catalyzed decarbonylation of aldehydes. <sup>a</sup>

Entry	Substrate	Product	Time (days)	Yield (%) <sup>b</sup>
1			2	84
2			2	81
3			2	72

<sup>a</sup>Reaction conditions: 10 mol % catalyst, toluene as the solvent, 180 °C. <sup>b</sup>NMR yield

## Conclusion

We have demonstrated a catalytic acceptorless thermal dehydrogenative decarbonylation of alcohols.  $\text{To}^{\text{M}}\text{Ir}(\eta^4\text{-C}_8\text{H}_{12})$  (**5.11**) is an active precatalyst for decarbonylation of several aliphatic and aromatic primary alcohols containing ether, ester, oxo, and chloro functional groups. Polyols such as ethylene glycol and glycerol are decarbonylated to syngas by  $\text{To}^{\text{M}}\text{Ir}(\eta^4\text{-C}_8\text{H}_{12})$ . Although the mechanism of catalytic decarbonylation is not entirely studied, our preliminary mechanistic investigations suggest a pathway involving dehydrogenation of alcohol to aldehyde, followed by decarbonylation of aldehyde in the catalytic cycle. Therefore, our

current efforts are focused on identifying and synthesizing possible intermediates, and study the mechanism *via* kinetics.

### Experiment details.

**General Procedures.** All reactions were performed under a dry argon atmosphere using standard Schlenk techniques or under a nitrogen atmosphere in a glove box unless otherwise indicated. Dry, oxygen-free solvents were used throughout. Benzene, toluene, pentane and tetrahydrofuran were degassed by sparging with nitrogen, filtered through activated alumina columns, and stored under N<sub>2</sub>. Benzene-*d*<sub>6</sub>, toluene-*d*<sub>8</sub> and tetrahydrofuran-*d*<sub>8</sub> were vacuum transferred from Na/K alloy and stored under N<sub>2</sub> in a glove box. All organic reagents were purchased from Aldrich. Tl[ToM],<sup>15</sup> PhB(Ox<sup>Me</sup>)<sub>2</sub>,<sup>13</sup> [Ir(μ-Cl)(η<sup>4</sup>-C<sub>8</sub>H<sub>12</sub>)<sub>2</sub>],<sup>19</sup> [Rh(μ-Cl)(η<sup>4</sup>-C<sub>8</sub>H<sub>12</sub>)<sub>2</sub>],<sup>20</sup> [Rh(μ-Cl)(CO)<sub>2</sub>]<sub>2</sub>,<sup>21</sup> and PhLi<sup>22</sup> were prepared by published procedures. <sup>1</sup>H, <sup>13</sup>C{<sup>1</sup>H}, <sup>11</sup>B NMR spectra were collected either on a Bruker DRX-400 spectrometer, Bruker Avance III 700 spectrometer or an Agilent MR 400 spectrometer. <sup>15</sup>N chemical shifts were determined by <sup>1</sup>H-<sup>15</sup>N HMBC experiments either on a Bruker Avance III 700 spectrometer or on a Bruker Avance III 600 spectrometer. <sup>15</sup>N chemical shifts were originally referenced to liquid NH<sub>3</sub> and recalculated to the CH<sub>3</sub>NO<sub>2</sub> chemical shift scale by adding -381.9 ppm. <sup>11</sup>B NMR spectra were referenced to an external sample of BF<sub>3</sub>·Et<sub>2</sub>O. GC-MS was conducted with Agilent 6890 GC system equipped with Agilent DB-5 column. Mass detection is processed by Micromass GCT. Elemental analysis was performed using a Perkin-Elmer 2400 Series II CHN/S by the Iowa State Chemical Instrumentation Facility.

**B(Ox<sup>Me2</sup>)<sub>3</sub> (5.1).** A 250 mL Schlenk flask was charged with 4,4-dimethyl-2-oxazoline (3.00 mL, 28.4 mmol), which was then degassed by three freeze-pump-thaw cycles. The degassed oxazoline was dissolved in 150 mL of THF and the flask was cooled to  $-78\text{ }^{\circ}\text{C}$ . *n*BuLi (12.0 mL, 30.0 mmol) was added *via* syringe to the reaction flask, and the resulting solution was stirred for 45 min at  $-78\text{ }^{\circ}\text{C}$ . Trichloroborane (1.0 M in heptanes) (9.18 mL, 9.18 mmol) was added slowly *via* syringe into the flask, which was then allowed to gradually warm to room temperature. After stirring for 36 h at room temperature, a white precipitate formed, which was separated from the solution. The white solid was washed with THF (3  $\times$  50 mL) and dried *in vacuo* to afford tris(oxazoliny)borane [B(Ox<sup>Me2</sup>)<sub>3</sub>] (2.03 g, 6.64 mmol, 72.3%). <sup>1</sup>H NMR (methanol-*d*, 400 MHz):  $\delta$  1.22 (s, 6 H,  $\overline{\text{CNCMe}_2\text{CH}_2\text{O}}$ ), 3.78 (s, 18 H,  $\overline{\text{CNCMe}_2\text{CH}_2\text{O}}$ ). <sup>13</sup>C{<sup>1</sup>H} NMR (methanol-*d*, 150 MHz):  $\delta$  78.08 ( $\overline{\text{CNCMe}_2\text{CH}_2\text{O}}$ ), 66.41 ( $\overline{\text{CNCMe}_2\text{CH}_2\text{O}}$ ), 27.83 ( $\overline{\text{CNCMe}_2\text{CH}_2\text{O}}$ ). <sup>11</sup>B NMR (methanol-*d*, 128 MHz):  $\delta$  -8.6. IR (KBr, cm<sup>-1</sup>): 2962 s, 2935 s, 2876 s, 1608 s, 1464 s, 1385 w, 1364 m, 1342 w, 1258 s, 1193 m, 1158 m, 1128 s, 1093 s, 1000 s, 975 s, 944 m, 917 w, 883 s, 831 m, 796 m.

**H[Ph<sub>2</sub>B(Ox<sup>Me2</sup>)<sub>2</sub>] (5.2).** A Schlenk flask was charged with PhB(Ox<sup>Me2</sup>)<sub>2</sub> (2.00 g, 7.04 mmol) and PhLi (0.455 g, 5.41 mmol) in the glove box. Then, THF (50 mL) was added to the flask to form a light brown solution. The flask was sealed and the resulting solution was stirred overnight. The solvent was removed under reduced pressure to afford a light yellow solid. This crude product was purified by silica gel column chromatography (hexane:CH<sub>2</sub>Cl<sub>2</sub>:Et<sub>3</sub>N = 5:5:1; R<sub>f</sub> = 0.72) to afford H[Ph<sub>2</sub>B(Ox<sup>Me2</sup>)<sub>2</sub>] (0.750 g, 2.07 mmol, 38.3%). The off white solid was dissolved in benzene and stirred over P<sub>2</sub>O<sub>5</sub> to dry without any reduction in yield. <sup>1</sup>H NMR (benzene-*d*<sub>6</sub>, 700

MHz):  $\delta$  7.86 (d,  $^3J_{\text{HH}} = 5.6$  Hz, 4 H, *ortho*-C<sub>6</sub>H<sub>5</sub>), 7.42 (m, 4 H, *meta*-C<sub>6</sub>H<sub>5</sub>), 7.25 (m, 2 H, *para*-C<sub>6</sub>H<sub>5</sub>), 3.36 (s, 4 H,  $\overline{\text{CNCMe}_2\text{CH}_2\text{O}}$ ), 0.85 (s, 12 H,  $\overline{\text{CNCMe}_2\text{CH}_2\text{O}}$ ).  $^{13}\text{C}\{^1\text{H}\}$  NMR (benzene-*d*<sub>6</sub>, 150 MHz):  $\delta$  194.78 (br s,  $\overline{\text{CNCMe}_2\text{CH}_2\text{O}}$ ), 150.20 (br s, *ipso*-C<sub>6</sub>H<sub>5</sub>), 135.06 (*ortho*-C<sub>6</sub>H<sub>5</sub>), 128.00 (*meta*-C<sub>6</sub>H<sub>5</sub>), 126.05 (*para*-C<sub>6</sub>H<sub>5</sub>), 80.19 ( $\overline{\text{CNCMe}_2\text{CH}_2\text{O}}$ ), 63.36 ( $\overline{\text{CNCMe}_2\text{CH}_2\text{O}}$ ), 28.00 ( $\overline{\text{CNCMe}_2\text{CH}_2\text{O}}$ ).  $^{11}\text{B}$  NMR (benzene-*d*<sub>6</sub>, 128 MHz):  $\delta$  -14.5.  $^{15}\text{N}$  NMR (benzene-*d*<sub>6</sub>, 71 MHz):  $\delta$  -170.5 ( $\overline{\text{CNCMe}_2\text{CH}_2\text{O}}$ ). IR (KBr, cm<sup>-1</sup>): 3044 w, 3015 w, 2996 w, 2967 s, 2928 m, 2871 w, 1580 s, 1490 m, 1460 s, 1431 m, 1415 m, 1383 m, 1317 m, 1261 s, 1195 m, 1172 w, 1135 w, 1105 w, 1022 w, 964 s, 888 w, 866 w, 841 w, 803 m, 739 s, 703 s, 642 w, 620 w. Anal. Calcd for C<sub>22</sub>H<sub>27</sub>BO<sub>2</sub>N<sub>2</sub>: C, 72.94; H, 7.51; N, 7.73. Found: C, 72.76; H, 7.31; N, 7.23. Mp: 146-152 °C.

**Tl[Ph<sub>2</sub>B(Ox<sup>Me2</sup>)<sub>2</sub>] (5.3).** A Schlenk flask was charged with H[Ph<sub>2</sub>B(Ox<sup>Me2</sup>)<sub>2</sub>] (0.214 g, 0.611 mmol) and dissolved in Et<sub>2</sub>O (7 mL). To the solution, thallium(1) ethoxide (86.5  $\mu\text{L}$ , 1.22 mmol) was added by a microliter syringe. The resulting solution was stirred at room temperature for 8 h. During stirring, a yellow solid crushed out from the solution. The solution was decanted to get the white solid precipitation in the glove box. The solid was washed with Et<sub>2</sub>O and dried *in vacuo* to give Tl[Ph<sub>2</sub>B(OX<sup>Me2</sup>)<sub>2</sub>] as a white solid (0.420 g, 0.555 mmol, 90.8%), which was stored in glove box.  $^1\text{H}$  NMR (benzene-*d*<sub>6</sub>, 400 MHz):  $\delta$  7.79 (d,  $^3J_{\text{HH}} = 6.4$  Hz, 4 H, *ortho*-C<sub>6</sub>H<sub>5</sub>), 7.39 (t,  $^3J_{\text{HH}} = 7.2$  Hz, 4 H, *meta*-C<sub>6</sub>H<sub>5</sub>), 7.22 (t,  $^3J_{\text{HH}} = 7.2$  Hz, 2 H, *para*-C<sub>6</sub>H<sub>5</sub>), 3.45 (s, 4 H,  $\overline{\text{CNCMe}_2\text{CH}_2\text{O}}$ ), 0.93 (s, 12 H,  $\overline{\text{CNCMe}_2\text{CH}_2\text{O}}$ ).  $^{13}\text{C}\{^1\text{H}\}$  NMR (benzene-*d*<sub>6</sub>, 700 MHz):  $\delta$  195.57 (br s,  $\overline{\text{CNCMe}_2\text{CH}_2\text{O}}$ ), 154.12 (br s, *ipso*-C<sub>6</sub>H<sub>5</sub>), 136.12 (*ortho*-C<sub>6</sub>H<sub>5</sub>), 127.80 (*meta*-C<sub>6</sub>H<sub>5</sub>), 125.81 (*para*-C<sub>6</sub>H<sub>5</sub>), 79.69 ( $\overline{\text{CNCMe}_2\text{CH}_2\text{O}}$ ), 66.75 ( $\overline{\text{CNCMe}_2\text{CH}_2\text{O}}$ ), 28.99 (



$\overline{\text{CNCMe}_2\text{CH}_2\text{O}}$ ).  $^{11}\text{B}$  NMR (benzene- $d_6$ , 128 MHz):  $\delta$  -13.1.  $^{15}\text{N}$  NMR (benzene- $d_6$ , 71 MHz):  $\delta$  -107.1 ( $\overline{\text{CNCMe}_2\text{CH}_2\text{O}}$ ). IR (KBr,  $\text{cm}^{-1}$ ): 3063 w, 3041 w, 3017 w, 2992 w, 2962 s, 2926 w, 2888 w, 2868 w, 1593 s, 1581 s, 1488 w, 1460 m, 1430 w, 1384 w, 1366 m, 1345 w, 1251 m, 1186 m, 1129 m, 1095 s, 1066 w, 990 s, 963 s, 877 m, 828 w, 787 w, 742 s, 731 s, 705 s. Anal. Calcd for  $\text{C}_{22}\text{H}_{26}\text{BO}_2\text{N}_2\text{Ti}$ : C, 46.71; H, 4.63; N, 4.95. Found: C, 46.44; H, 4.91; N, 4.58. Mp: 182-187 °C, dec.

#### **PhClB(Ox<sup>Me2</sup>)<sub>2</sub>Ir( $\eta^4$ -C<sub>8</sub>H<sub>12</sub>) (5.4).**

In a glove box, PhB(Ox<sup>Me2</sup>)<sub>2</sub> (0.460 g, 1.62 mmol) and [Ir( $\eta^4$ -C<sub>8</sub>H<sub>12</sub>)Cl]<sub>2</sub> (0.340 g, 0.506 mmol) were placed in a vial. The solids were dissolved in methylene chloride (15 mL), and the solution was stirred overnight. The resultant orange solution was filtered to another vial and the filtrate was concentrated under reduced pressure. Few drops of pentane were added to the solution and cooled to -30 °C. Orange crystals precipitated out, which was isolated from the rest of the solution and was dried under vacuum to afford PhClB(Ox<sup>Me2</sup>)<sub>2</sub>Ir( $\eta^4$ -C<sub>8</sub>H<sub>12</sub>) as an orange solid (0.570 g, 0.919 mmol, 91.0%).  $^1\text{H}$  NMR (benzene- $d_6$ , 400 MHz):  $\delta$  7.58 (m, 2 H, *ortho*-C<sub>6</sub>H<sub>5</sub>), 7.36 (m, 2 H, *meta*-C<sub>6</sub>H<sub>5</sub>), 7.24 (m, 1 H, *para*-C<sub>6</sub>H<sub>5</sub>), 4.04 (br s, 2 H, C<sub>8</sub>H<sub>12</sub>), 3.70 (br s, 2 H, C<sub>8</sub>H<sub>12</sub>), 3.57 (d, 2 H,  $^2J_{\text{HH}} = 4.8$  Hz,  $\overline{\text{CNCMe}_2\text{CH}_2\text{O}}$ ), 3.39 (d, 2 H,  $^2J_{\text{HH}} = 4.8$  Hz,  $\overline{\text{CNCMe}_2\text{CH}_2\text{O}}$ ), 1.89 (br s, 2 H, C<sub>8</sub>H<sub>12</sub>), 1.20 (br m, 4 H, C<sub>8</sub>H<sub>12</sub>), 1.01 (s, 6 H,  $\overline{\text{CNCMe}_2\text{CH}_2\text{O}}$ ), 0.88 (m, 2 H, C<sub>8</sub>H<sub>12</sub>), 0.80 (s, 6 H,  $\overline{\text{CNCMe}_2\text{CH}_2\text{O}}$ ).  $^{13}\text{C}\{^1\text{H}\}$  NMR (benzene- $d_6$ , 400 MHz):  $\delta$  187.95 (br,  $\overline{\text{CNCMe}_2\text{CH}_2\text{O}}$ ), 148.35 (*ipso*-C<sub>6</sub>H<sub>5</sub>), 133.89 (*ortho*-C<sub>6</sub>H<sub>5</sub>), 128.68 (*meta*-C<sub>6</sub>H<sub>5</sub>), 126.39 (*para*-C<sub>6</sub>H<sub>5</sub>), 82.70 ( $\overline{\text{CNCMe}_2\text{CH}_2\text{O}}$ ), 69.72 ( $\overline{\text{CNCMe}_2\text{CH}_2\text{O}}$ ), 63.86 (C<sub>8</sub>H<sub>12</sub>), 60.30 (C<sub>8</sub>H<sub>12</sub>), 31.47 (C<sub>8</sub>H<sub>12</sub>), 30.24 (C<sub>8</sub>H<sub>12</sub>), 28.16 ( $\overline{\text{CNCMe}_2\text{CH}_2\text{O}}$ ), 27.20 ( $\overline{\text{CNCMe}_2\text{CH}_2\text{O}}$ ).  $^{15}\text{N}$  NMR (benzene-

$d_6$ , 71 MHz):  $\delta$ -182.5 ( $\overline{\text{CNCMe}_2\text{CH}_2\text{O}}$ ).  $^{11}\text{B}$  NMR (benzene- $d_6$ , 128 MHz):  $\delta$ -7.6. IR (KBr,  $\text{cm}^{-1}$ ): 3061 w, 3000 m, 2964 m, 2942 m, 2927 m, 2881 m, 2831 m, 1564 s, 1464 m, 1431 m, 1390 w, 1371 m, 1288 s, 1201 s, 1157 s, 1048 m, 990 s, 965 s, 914 w, 893 m, 867 w, 846 m, 820 w, 765 m, 724 s, 706 s. EA: Anal. Calcd for  $\text{C}_{24}\text{H}_{33}\text{BClIrN}_2\text{O}_2(\text{CH}_2\text{Cl}_2)_{0.33}$ : C, 45.08; H, 5.23; N, 4.32. Found: C, 45.08; H, 5.12; N, 4.21. Mp: 189-191 °C.

**PhClB(Ox<sup>Me2</sup>)<sub>2</sub>Rh( $\eta^4$ -C<sub>8</sub>H<sub>12</sub>) (5.5).** In the glove box, methylene chloride (15 mL) was added to a vial containing PhB(Ox<sup>Me2</sup>)<sub>2</sub> (0.560 g, 1.95 mmol) and [RhCl( $\eta^4$ -C<sub>8</sub>H<sub>12</sub>)]<sub>2</sub> (0.300 g, 0.608 mmol). The resultant yellow solution was stirred overnight. The solution was filtered and the filtrate was concentrated under reduced pressure. Few drops of pentane were added to the solution and then cooled to -30 °C. Deep yellow crystals precipitated out, which was isolated and dried *in vacuo* to afford PhClB(Ox<sup>Me2</sup>)<sub>2</sub>Rh( $\eta^4$ -C<sub>8</sub>H<sub>12</sub>) as a deep yellow solid (0.560 g, 1.06 mmol, 87.0%). Crystals suitable for X-ray diffraction were grown from toluene/pentane solution at -30 °C.  $^1\text{H}$  NMR (benzene- $d_6$ , 400 MHz):  $\delta$  7.74 (br s, 2 H, *ortho*-C<sub>6</sub>H<sub>5</sub>), 7.41 (br s, 2 H, *meta*-C<sub>6</sub>H<sub>5</sub>), 7.29 (t, 1 H, *para*-C<sub>6</sub>H<sub>5</sub>), 4.21 (br m, 2H, C<sub>8</sub>H<sub>12</sub>), 3.92 (br m, 2H, C<sub>8</sub>H<sub>12</sub>), 3.55 (br s, 2 H,  $\overline{\text{CNCMe}_2\text{CH}_2\text{O}}$ ), 3.37 (d, 2 H,  $^2J_{\text{HH}} = 8.4$  Hz,  $\overline{\text{CNCMe}_2\text{CH}_2\text{O}}$ ), 1.97 (br m, 2 H, C<sub>8</sub>H<sub>12</sub>), 1.33 (br m, 4 H, C<sub>8</sub>H<sub>12</sub>), 1.03 (s, 6 H,  $\overline{\text{CNCMe}_2\text{CH}_2\text{O}}$ ), 0.87 (m, 2 H, C<sub>8</sub>H<sub>12</sub>), 0.72 (s, 6 H,  $\overline{\text{CNCMe}_2\text{CH}_2\text{O}}$ ).  $^{13}\text{C}\{1\text{H}\}$  NMR (methylene chloride- $d_2$ , 100 MHz):  $\delta$  187.76 (br,  $\overline{\text{CNCMe}_2\text{CH}_2\text{O}}$ ), 151.67 (*ipso*-C<sub>6</sub>H<sub>5</sub>), 133.71 (*ortho*-C<sub>6</sub>H<sub>5</sub>), 128.40 (*meta*-C<sub>6</sub>H<sub>5</sub>), 126.58 (*para*-C<sub>6</sub>H<sub>5</sub>), 82.02 ( $\overline{\text{CNCMe}_2\text{CH}_2\text{O}}$ ), 79.935, 79.814 (d,  $J_{\text{Rh-C}} = 12.1$  Hz, C<sub>8</sub>H<sub>12</sub>), 77.045, 76.919 (d,  $J_{\text{Rh-C}} = 12.1$  Hz, C<sub>8</sub>H<sub>12</sub>), 69.31 ( $\overline{\text{CNCMe}_2\text{CH}_2\text{O}}$ ), 30.60 (C<sub>8</sub>H<sub>12</sub>), 29.23 (C<sub>8</sub>H<sub>12</sub>), 28.46 ( $\overline{\text{CNCMe}_2\text{CH}_2\text{O}}$ ), 27.73 ( $\overline{\text{CNCMe}_2\text{CH}_2\text{O}}$ ).  $^{15}\text{N}$  NMR (benzene- $d_6$ , 71 MHz):  $\delta$  -180.5 (

$\overline{\text{CNCMe}_2\text{CH}_2\text{O}}$ ).  $^{11}\text{B}$  NMR (benzene- $d_6$ , 128 MHz):  $\delta$ -6.8. IR (KBr,  $\text{cm}^{-1}$ ): 3063 w, 3043 w, 3001 m, 2966 s, 2967 s, 2875 m, 2831 w, 1578 s, 1460 m, 1431 m, 1389 w, 1366 m, 1334 w, 1280 s, 1196 s, 1156 s, 1020 w, 987 s, 961 s, 912 w, 896 w, 865 w. EA: Anal. Calcd for  $\text{C}_{24}\text{H}_{33}\text{BClRhN}_2\text{O}_2(\text{CH}_2\text{Cl}_2)_{0.33}$ : C, 52.28; H, 6.07; N, 5.01. Found: C, 52.65; H, 6.04; N, 4.97. Mp: 152-156 °C.

**PhClB(Ox<sup>Me2</sup>)<sub>2</sub>Rh(CO)<sub>2</sub> (5.6).** In the glove box, PhB(Ox<sup>Me2</sup>)<sub>2</sub> (0.483 g, 1.70 mmol) and [Rh(CO)<sub>2</sub>Cl]<sub>2</sub> (0.300 g, 0.772 mmol) were weighing out in two different vials. [Rh(CO)<sub>2</sub>Cl]<sub>2</sub> was dissolved in methylene chloride (15 mL), and was transferred to the vial containing PhB(Ox<sup>Me2</sup>)<sub>2</sub>. The solution mixture was stirred for 6 h. The resultant deep brown solution was filtered, and the volume of the filtrate was reduced under vacuo. Pentane was added to the solution and then the solution was recrystallized at -30 °C overnight to obtain deep brown crystals of PhClB(Ox<sup>Me2</sup>)<sub>2</sub>Rh(CO)<sub>2</sub> (0.320 g, 0.666 mmol, 86.3%).  $^1\text{H}$  NMR (methylene chloride- $d_2$ , 400 MHz):  $\delta$  7.33 (d,  $^3J_{\text{HH}} = 7.0$  Hz, 2 H, *ortho*-C<sub>6</sub>H<sub>5</sub>), 7.25 (t, 2 H, *meta*-C<sub>6</sub>H<sub>5</sub>), 7.19 (t, 1 H, *para*-C<sub>6</sub>H<sub>5</sub>), 4.23 (d, 2 H,  $^2J_{\text{HH}} = 8.4$  Hz,  $\overline{\text{CNCMe}_2\text{CH}_2\text{O}}$ ), 4.18 (d, 2 H,  $^2J_{\text{HH}} = 8.4$  Hz,  $\overline{\text{CNCMe}_2\text{CH}_2\text{O}}$ ), 1.41 (s, 6 H,  $\overline{\text{CNCMe}_2\text{CH}_2\text{O}}$ ), 1.32 (s, 6 H,  $\overline{\text{CNCMe}_2\text{CH}_2\text{O}}$ ).  $^{13}\text{C}\{^1\text{H}\}$  NMR (methylene chloride- $d_2$ , 150 MHz):  $\delta$  190.31 (br,  $\overline{\text{CNCMe}_2\text{CH}_2\text{O}}$ ), 184.95 (CO), 184.57 (CO), 149.22 (*ipso*-C<sub>6</sub>H<sub>5</sub>), 132.89 (*ortho*-C<sub>6</sub>H<sub>5</sub>), 128.05 (*meta*-C<sub>6</sub>H<sub>5</sub>), 126.97 (*para*-C<sub>6</sub>H<sub>5</sub>), 80.95 ( $\overline{\text{CNCMe}_2\text{CH}_2\text{O}}$ ), 68.90 ( $\overline{\text{CNCMe}_2\text{CH}_2\text{O}}$ ), 28.94 ( $\overline{\text{CNCMe}_2\text{CH}_2\text{O}}$ ), 28.77 ( $\overline{\text{CNCMe}_2\text{CH}_2\text{O}}$ ).  $^{15}\text{N}$  NMR (methylene chloride- $d_2$ , 71 MHz):  $\delta$ -199.0 (s,  $\overline{\text{CNCMe}_2\text{CH}_2\text{O}}$ ).  $^{11}\text{B}$  NMR (methylene chloride- $d_2$ , 128 MHz):  $\delta$ -8.3. IR (KBr,  $\text{cm}^{-1}$ ): 3076 w, 3053 w, 3037 w, 3008 m, 2963 s, 2929 m, 2895 m, 2872 m, 2076 s, 1993 s, 1580 s, 1551 m, 1493 w, 1460 s, 1431 m, 1390 w, 1370 s,

1290 s, 1257 w, 1204 s, 1163 m, 1085 w, 1025 w, 993 m, 961 s, 949 s, 926 w, 892 w, 841 w, 804 m, 782 w, 728 m, 704 m. EA: Anal. Calcd for  $C_{18}H_{23}BClN_2O_4Rh$ : C, 44.99; H, 4.82; N, 5.83. Found: C, 44.54; H, 4.44; N, 5.25. Mp: 107-111 °C.

**Ph(Ph<sub>3</sub>SiO)B(Ox<sup>Me2</sup>)<sub>2</sub>Rh( $\eta^4$ -C<sub>8</sub>H<sub>12</sub>) (5.7).** In the glove box, PhClB(Ox<sup>Me2</sup>)<sub>2</sub>Rh( $\eta^4$ -C<sub>8</sub>H<sub>12</sub>) (0.050 g, 0.087 mmol) and Ph<sub>3</sub>SiOK (0.027 g, 0.087 mmol) were placed in a vial. The solids were dissolved in benzene (15 mL), and the solution was stirred for 36 h. The resultant yellow solution was filtered. The filtrate was concentrated and recrystallized at -30 °C to afford Ph(Ph<sub>3</sub>SiO)B(Ox<sup>Me2</sup>)<sub>2</sub>Rh( $\eta^4$ -C<sub>8</sub>H<sub>12</sub>) as a yellow solid (0.063 g, 0.082 mmol, 94.2 %). <sup>1</sup>H NMR (benzene-*d*<sub>6</sub>, 400 MHz):  $\delta$  8.06-7.14 (20 H, C<sub>6</sub>H<sub>5</sub>; overlapped), 4.27 (br s, 2H, C<sub>8</sub>H<sub>12</sub>), 3.98 (br s, 2H, C<sub>8</sub>H<sub>12</sub>), 3.45 (d, 2 H, <sup>2</sup>*J* = 8.4 Hz,  $\overline{CNCMe_2CH_2O}$ ), 3.22 (d, 2 H, <sup>2</sup>*J* = 8.4 Hz,  $\overline{CNCMe_2CH_2O}$ ), 2.02 (m, 2H, C<sub>8</sub>H<sub>12</sub>), 1.48-1.40 (m, 4 H, C<sub>8</sub>H<sub>12</sub>), 1.14 (m, 2 H, C<sub>8</sub>H<sub>12</sub>), 1.05 (s, 6H,  $\overline{CNCMe_2CH_2O}$ ), 0.75 (s, 6H,  $\overline{CNCMe_2CH_2O}$ ). <sup>13</sup>C{<sup>1</sup>H} NMR (benzene-*d*<sub>6</sub>, 100 MHz):  $\delta$  193.59 (br,  $\overline{CNCMe_2CH_2O}$ ), 141.21 [*ipso*-(C<sub>6</sub>H<sub>5</sub>)B], 136.65 [(C<sub>6</sub>H<sub>5</sub>)<sub>3</sub>Si], 134.89 [(C<sub>6</sub>H<sub>5</sub>)B], 129.66 [(C<sub>6</sub>H<sub>5</sub>)B], 128.91 [d, 2 H, <sup>2</sup>*J* = 2.2 Hz, *ipso*-(C<sub>6</sub>H<sub>5</sub>)<sub>3</sub>Si], 128.86 [(C<sub>6</sub>H<sub>5</sub>)B], 127.63 [(C<sub>6</sub>H<sub>5</sub>)<sub>3</sub>Si], 126.03 [(C<sub>6</sub>H<sub>5</sub>)<sub>3</sub>Si], 80.85 ( $\overline{CNCMe_2CH_2O}$ ), 79.584- 79.464 (d, *J*<sub>Rh-C</sub> = 12.0 Hz, C<sub>8</sub>H<sub>12</sub>), 75.840-75.713 (d, *J*<sub>Rh-C</sub> = 12.7 Hz, C<sub>8</sub>H<sub>12</sub>), 68.18 ( $\overline{CNCMe_2CH_2O}$ ), 30.78 (C<sub>8</sub>H<sub>12</sub>), 29.59 (C<sub>8</sub>H<sub>12</sub>), 28.05 ( $\overline{CNCMe_2CH_2O}$ ), 27.78 ( $\overline{CNCMe_2CH_2O}$ ). <sup>15</sup>N NMR (benzene-*d*<sub>6</sub>, 71 MHz):  $\delta$  -185.5 ( $\overline{CNCMe_2CH_2O}$ ). <sup>11</sup>B NMR (benzene-*d*<sub>6</sub>, 128 MHz):  $\delta$  -4.5. IR (KBr, cm<sup>-1</sup>): 3065 m, 3044 m, 2997 m, 2963 s, 2918 w, 2880 w, 2834 w, 1575 s, 1483 w, 1459 w, 1428 s, 1386 w, 1365 m, 1333 w, 1303 w, 1279 s, 1199 s, 1156 s, 1113 s, 1099 s, 1029 w, 995 m, 979 m, 894 w, 878 w, 836 w, 798 w, 742 m, 704 s. EA:

Anal. Calcd for  $C_{42}H_{48}BN_2O_3RhSi$ : C, 65.46; H, 6.28; N, 3.64. Found: C, 65.18; H, 6.0; N, 3.53.

Mp: 193-197 °C, dec.

**Ph(Ph<sub>3</sub>SiO)B(Ox<sup>Me2</sup>)<sub>2</sub>Li(THF)<sub>2</sub> (5.8).** A Schlenk flask was charged with PhB(Ox<sup>Me2</sup>)<sub>2</sub> (1.00 g, 3.52 mmol) and Ph<sub>3</sub>SiOLi (0.621 g, 2.20 mmol) in the glove box. The flask was attached to a Schenk manifold and THF (60 mL) was added to form a yellow solution. The flask was sealed and the resulting solution was stirred overnight. The solution was filtered to remove a precipitate that appeared overnight, and then the solvent was removed under reduced pressure to afford a light yellow solid. This solid was dissolved in toluene and layered with pentane and kept at -30 °C to afford Ph(Ph<sub>3</sub>SiO)B(Ox<sup>Me2</sup>)<sub>2</sub>Li(THF)<sub>2</sub> as colorless crystals (1.290 g, 1.82 mmol, 83.0%).

<sup>1</sup>H NMR (acetonitrile-*d*<sub>3</sub>, 400 MHz): δ 7.66 {m, 6 H, *ortho*-(C<sub>6</sub>H<sub>5</sub>)<sub>3</sub>Si}, 7.50 (d, <sup>3</sup>J<sub>HH</sub> = 6.4 Hz, 2 H, *ortho*-C<sub>6</sub>H<sub>5</sub>), 7.30 {m, 9 H, *meta*-(C<sub>6</sub>H<sub>5</sub>)<sub>3</sub>Si, *para*-(C<sub>6</sub>H<sub>5</sub>)<sub>3</sub>Si}, 7.06 (t, 2 H, *meta*-C<sub>6</sub>H<sub>5</sub>), 6.97 (t, 1 H, *para*-C<sub>6</sub>H<sub>5</sub>), 3.64 (m, 8 H, THF), 3.38 (d, 2 H, <sup>2</sup>J<sub>HH</sub> = 8.0 Hz,  $\overline{CNCMe_2CH_2O}$ ), 3.06 (d, 2 H, <sup>2</sup>J<sub>HH</sub> = 8.0 Hz,  $\overline{CNCMe_2CH_2O}$ ), 1.80 (m, 8 H, THF), 1.05 (s, 6 H,  $\overline{CNCMe_2CH_2O}$ ), 1.04 (s, 6 H,  $\overline{CNCMe_2CH_2O}$ ). <sup>13</sup>C{<sup>1</sup>H} NMR (acetonitrile-*d*<sub>3</sub>, 150 MHz): δ 186.34 (br,  $\overline{CNCMe_2CH_2O}$ ), 156.10 (*ipso*-C<sub>6</sub>H<sub>5</sub>), 141.28 {*ipso*-(C<sub>6</sub>H<sub>5</sub>)<sub>3</sub>Si}, 136.76 {*ortho*-(C<sub>6</sub>H<sub>5</sub>)<sub>3</sub>Si}, 132.53 (*ortho*-C<sub>6</sub>H<sub>5</sub>), 129.75 {*meta*-(C<sub>6</sub>H<sub>5</sub>)<sub>3</sub>Si}, 128.39 (*meta*-C<sub>6</sub>H<sub>5</sub>), 127.67 {*para*-(C<sub>6</sub>H<sub>5</sub>)<sub>3</sub>Si}, 125.56 (*para*-C<sub>6</sub>H<sub>5</sub>), 77.32 ( $\overline{CNCMe_2CH_2O}$ ), 68.69 ( $\overline{CNCMe_2CH_2O}$ , THF), 67.35 ( $\overline{CNCMe_2CH_2O}$ ), 29.19 ( $\overline{CNCMe_2CH_2O}$ ), 28.77 ( $\overline{CNCMe_2CH_2O}$ ), 26.65 (THF). <sup>15</sup>N NMR (acetonitrile-*d*<sub>3</sub>, 71 MHz): δ -151.1 (s,  $\overline{CNCMe_2CH_2O}$ ). <sup>11</sup>B NMR (acetonitrile-*d*<sub>3</sub>, 128 MHz): δ -6.1. IR (KBr, cm<sup>-1</sup>): 3064 m, 3048 m, 2967 s, 2929 m, 2883 m, 1601 s, 1586 m, 1484 w, 1461 m, 1428 s, 1381 w, 1362 m, 1347 w, 1259 s, 1186 s, 1160 s, 1113 s, 1055 s, 1029 w, 991 s, 972

m, 881 m, 830 w, 796 w, 740 m, 731 m, 703 s. EA: Anal. Calcd for.  $C_{42}H_{52}BLiN_2O_5Si$ : C, 70.98; H, 7.37; N, 3.94. Found: C, 70.67; H, 7.45; N, 3.94. Mp: 137-141 °C.

**$Ph_2B(Ox^{Me_2})_2Ir(\eta^4-C_8H_{12})$  (5.9).** In a glove box, a vial was charged with  $PhClB(Ox^{Me_2})_2Ir(\eta^4-C_8H_{12})$  (0.160 g, 0.258 mmol) and  $PhLi$  (0.022 g, 0.258 mmol). The solids were dissolved in benzene (7 mL), and the solution was stirred for 2 h. The resultant yellow solution was filtered to remove the  $LiCl$  precipitate. The filtrate was evaporated to dryness *in vacuo*, affording  $Ph_2B(Ox^{Me_2})_2Ir(\eta^4-C_8H_{12})$  as an orange solid (0.171 g, 0.231 mmol, 89.5%).  $^1H$  NMR (benzene- $d_6$ , 400 MHz):  $\delta$  7.57-7.25 (m, 10 H,  $C_6H_5$  overlapped), 4.09 (br s, 2 H,  $C_8H_{12}$ ), 3.76 (br s, 2 H,  $C_8H_{12}$ ), 3.41 (m, 4 H,  $\overline{CNCMe_2CH_2O}$ ), 1.94 (br s, 2 H,  $C_8H_{12}$ ), 1.33 (br s, 2 H,  $C_8H_{12}$ ), 1.23 (br m, 2 H,  $C_8H_{12}$ ), 1.08 (s, 6 H,  $\overline{CNCMe_2CH_2O}$ ), 0.93 (m, 2 H,  $C_8H_{12}$ ), 0.81 (s, 6 H,  $\overline{CNCMe_2CH_2O}$ ).  $^{13}C\{1H\}$  NMR (benzene- $d_6$ , 400 MHz):  $\delta$  193.18 (br,  $\overline{CNCMe_2CH_2O}$ ), 133.83 (*ortho*- $C_6H_5$ ), 126.53 (*meta*- $C_6H_5$ ), 125.23 (*para*- $C_6H_5$ ), 82.73 ( $\overline{CNCMe_2CH_2O}$ ), 68.84 ( $\overline{CNCMe_2CH_2O}$ ), 64.02 ( $C_8H_{12}$ ), 60.52 ( $C_8H_{12}$ ), 31.44 ( $C_8H_{12}$ ), 30.23 ( $C_8H_{12}$ ), 28.10 ( $\overline{CNCMe_2CH_2O}$ ), 27.14 ( $\overline{CNCMe_2CH_2O}$ ).  $^{15}N$  NMR (benzene- $d_6$ , 71 MHz):  $\delta$  -152.2 ( $\overline{CNCMe_2CH_2O}$ ).  $^{11}B$  NMR (benzene- $d_6$ , 128 MHz):  $\delta$  -12.8. IR (KBr,  $cm^{-1}$ ): 3037m, 3000 m, 2963 s, 2927 s, 2881 s, 2834 m, 1588 m, 1555 s, 1463 m, 1431 m, 1389 w, 1370 m, 1330 w, 1285 s, 1197 s, 1157 s, 1078 w, 1022 w, 991 m, 965 s, 892 m, 841 w, 785 w, 703 s, 678 s. EA: Anal. Calcd for  $C_{30}H_{38}BIrN_2O_2$ : C, 54.46; H, 5.79; N, 4.23. Found: C, 54.21; H, 5.63; N, 3.78. Mp: 97-102 °C.

**$ClB(Ox^{Me_2})_3Rh(CO)_2$  (5.10).** In a glove box, THF (10 mL) was added to a vial containing  $B(Ox^{Me_2})_3$  (200 mg, 0.655 mmol) and  $[Rh(CO)_2Cl]_2$  (120 mg, 0.308 mmol). The resultant

mixture was stirred at room temperature for 3 h. Then, the mixture was filtered and the filtrate was evaporated to dryness providing a white solid. The solid was washed with pentane (3 x 5 mL) and dried under vacuum yielding  $\text{ClB}(\text{Ox}^{\text{Me}_2})_3\text{Rh}(\text{CO})_2$  as a white powder (0.308 g, 0.617 mmol, 94.2%).  $^1\text{H}$  NMR (tetrahydrofuran- $d_8$ , 400 MHz):  $\delta$  3.75 (s, 6 H,  $\overline{\text{CNCMe}_2\text{CH}_2\text{O}}$ ), 1.29 (s, 18 H,  $\overline{\text{CNCMe}_2\text{CH}_2\text{O}}$ ).  $^{13}\text{C}\{^1\text{H}\}$  NMR (tetrahydrofuran- $d_8$ , 150 MHz):  $\delta$  186.53 (br,  $\overline{\text{CNCMe}_2\text{CH}_2\text{O}}$ ), 80.01 ( $\overline{\text{CNCMe}_2\text{CH}_2\text{O}}$ ), 67.16 ( $\overline{\text{CNCMe}_2\text{CH}_2\text{O}}$ ), 27.96 ( $\overline{\text{CNCMe}_2\text{CH}_2\text{O}}$ ).  $^{11}\text{B}$  NMR (benzene- $d_6$ , 128 MHz):  $\delta$  -9.3. IR (KBr,  $\text{cm}^{-1}$ ): 2917 w, 2847 w, 2237 s, 2082 s, 1599 m, 1462 w, 1370 w, 1272 w, 1162 s, 1100 s, 1049 s, 991 m, 842 s, 750 m.

**To<sup>M</sup>Ir( $\eta^4$ -C<sub>8</sub>H<sub>12</sub>) (5.11).** A Schlenk flask was charged with TITo<sup>M</sup> (0.700 g, 1.19 mmol) and  $[\text{IrCl}(\eta^4\text{-C}_8\text{H}_{12})]_2$  (0.411 g, 0.611 mmol) in the glove box. Then, benzene (20 mL) was added to the flask. The flask was sealed and the resulting solution was heated for 4 h at 60 °C. The solvent was filtered and the residue was extracted with benzene. The solvent was removed under reduced pressure to afford To<sup>M</sup>Ir( $\eta^4$ -C<sub>8</sub>H<sub>12</sub>) as a deep yellow solid (0.758 g, 1.11 mmol, 93.3%).  $^1\text{H}$  NMR (benzene- $d_6$ , 400 MHz):  $\delta$  7.59 (d,  $^3J_{\text{HH}} = 6.4$  Hz, 2 H, *ortho*-C<sub>6</sub>H<sub>5</sub>), 7.37 (t,  $^3J_{\text{HH}} = 7.2$  Hz, 2 H, *meta*-C<sub>6</sub>H<sub>5</sub>), 7.22 (t,  $^3J_{\text{HH}} = 7.2$  Hz, 1 H, *para*-C<sub>6</sub>H<sub>5</sub>), 4.05 (br m, 2 H, C<sub>8</sub>H<sub>12</sub>), 3.72 (br m, 4 H,  $\overline{\text{CNCMe}_2\text{CH}_2\text{O}}$ , C<sub>8</sub>H<sub>12</sub> overlapped), 3.59 (s, 2 H,  $\overline{\text{CNCMe}_2\text{CH}_2\text{O}}$ ), 3.49 (s, 2 H,  $\overline{\text{CNCMe}_2\text{CH}_2\text{O}}$ ), 1.91 (br m, 2 H, C<sub>8</sub>H<sub>12</sub>), 1.31 (s, 6 H,  $\overline{\text{CNCMe}_2\text{CH}_2\text{O}}$ ), 1.21 (br m, 4 H, C<sub>8</sub>H<sub>12</sub>), 1.06 (s, 6 H,  $\overline{\text{CNCMe}_2\text{CH}_2\text{O}}$ ), 0.81 (s, 8 H,  $\overline{\text{CNCMe}_2\text{CH}_2\text{O}}$ , C<sub>8</sub>H<sub>12</sub> overlapped).  $^{13}\text{C}\{^1\text{H}\}$  NMR (benzene- $d_6$ , 150 MHz):  $\delta$  193.92 (br,  $\overline{\text{CNCMe}_2\text{CH}_2\text{O}}$ ), 152.44 (*ipso*-C<sub>6</sub>H<sub>5</sub>), 134.48 (*ortho*-C<sub>6</sub>H<sub>5</sub>), 127.39 (*meta*-C<sub>6</sub>H<sub>5</sub>), 125.10 (*para*-C<sub>6</sub>H<sub>5</sub>), 82.62 (2  $\overline{\text{CNCMe}_2\text{CH}_2\text{O}}$  overlapped), 77.05 ( $\overline{\text{CNCMe}_2\text{CH}_2\text{O}}$ ), 68.26 (2  $\overline{\text{CNCMe}_2\text{CH}_2\text{O}}$ , overlapped), 62.77 (C<sub>8</sub>H<sub>12</sub>), 59.25 (C<sub>8</sub>H<sub>12</sub>), 31.18 (2

$C_8H_{12}$ , overlapped), 29.90 ( $C_8H_{12}$ ), 29.15 ( $\overline{CNCMe_2CH_2O}$ ), 27.80 ( $\overline{CNCMe_2CH_2O}$ ), 26.78 ( $\overline{CNCMe_2CH_2O}$ ).  $^{15}N$  NMR (benzene- $d_6$ , 71 MHz):  $\delta$  -154.9, -192.9 ( $\overline{CNCMe_2CH_2O}$ ).  $^{11}B$  NMR (benzene- $d_6$ , 128 MHz):  $\delta$  -16.4. IR (KBr,  $cm^{-1}$ ): 3063 w, 3036 w, 3000 m, 2965 s, 2928 s, 2881 s, 2835 m, 1607 m, 1558 s, 1462 m, 1433 w, 1388 w, 1370 m, 1329 w, 1284 s, 1254 w, 1198 s, 1158 s, 1131 m, 1002 s, 967 s, 892 w, 875 w, 839 w, 817 w, 785 w, 739 m, 704 m. EA: Anal. Calcd for  $C_{29}H_{41}BIrN_3O_3$ : C, 51.02; H, 6.05; N, 6.16. Found: C, 51.00; H, 5.53; N, 6.03. Mp: 175-180 °C.

**To<sup>M</sup>Rh( $\eta^4$ -C<sub>8</sub>H<sub>12</sub>) (5.12).** A Schlenk flask was charged with TITo<sup>M</sup> (0.440 g, 0.749 mmol) and [RhCl( $\eta^4$ -C<sub>8</sub>H<sub>12</sub>)]<sub>2</sub> (0.189 g, 0.384 mmol) in the glove box. Then, benzene (20 mL) was added to the flask. The flask was sealed and the resulting solution was stirred for 4 h at room temperature. The solvent was filtered and the residue was extracted with benzene. The solvent was removed under reduced pressure to afford To<sup>M</sup>Rh( $\eta^4$ -C<sub>8</sub>H<sub>12</sub>) as a deep yellow solid (0.205 g, 0.345 mmol, 90.3%).  $^1H$  NMR (benzene- $d_6$ , 400 MHz):  $\delta$  7.75 (d,  $^3J_{HH} = 6.4$  Hz, 2 H, *ortho*-C<sub>6</sub>H<sub>5</sub>), 7.43 (t,  $^3J_{HH} = 7.6$  Hz, 2 H, *meta*-C<sub>6</sub>H<sub>5</sub>), 7.28 (t,  $^3J_{HH} = 7.6$  Hz, 1 H, *para*-C<sub>6</sub>H<sub>5</sub>), 4.24 (br m, 2H, C<sub>8</sub>H<sub>12</sub>), 3.96 (br m, 2 H, C<sub>8</sub>H<sub>12</sub>), 3.73 (s, 2 H,  $\overline{CNCMe_2CH_2O}$ ), 3.57 (s, 2 H,  $\overline{CNCMe_2CH_2O}$ ), 3.46 (s, 2 H,  $\overline{CNCMe_2CH_2O}$ ), 1.99 (br s, 2 H, C<sub>8</sub>H<sub>12</sub>), 1.37 (br s, 4H, C<sub>8</sub>H<sub>12</sub>), 1.32 (s, 6 H,  $\overline{CNCMe_2CH_2O}$ ), 1.08 (s, 8 H,  $\overline{CNCMe_2CH_2O}$ , C<sub>8</sub>H<sub>12</sub> overlapped), 0.72 (s, 6 H,  $\overline{CNCMe_2CH_2O}$ ).  $^{13}C\{1H\}$  NMR (benzene- $d_6$ , 150 MHz):  $\delta$  192.77 (br,  $\overline{CNCMe_2CH_2O}$ ), 135.41 (*ortho*-C<sub>6</sub>H<sub>5</sub>), 127.84 (*meta*-C<sub>6</sub>H<sub>5</sub>), 125.57 (*para*-C<sub>6</sub>H<sub>5</sub>), 81.78 ( $\overline{CNCMe_2CH_2O}$ ), 79.33 (C<sub>8</sub>H<sub>12</sub>), 77.39 ( $\overline{CNCMe_2CH_2O}$ ), 75.65 (C<sub>8</sub>H<sub>12</sub>), 68.46 ( $\overline{CNCMe_2CH_2O}$ ), 67.61 ( $\overline{CNCMe_2CH_2O}$ ), 30.81 (C<sub>8</sub>H<sub>12</sub>), 29.50 (C<sub>8</sub>H<sub>12</sub>,



( $\overline{\text{CNCMe}_2\text{CH}_2\text{O}}$  overlapped), 28.13 ( $\overline{\text{CNCMe}_2\text{CH}_2\text{O}}$ ), 27.55 ( $\overline{\text{CNCMe}_2\text{CH}_2\text{O}}$ ).  $^{15}\text{N}$  NMR (benzene- $d_6$ , 71 MHz):  $\delta$ -161.1, -169.2 ( $\overline{\text{CNCMe}_2\text{CH}_2\text{O}}$ ).  $^{11}\text{B}$  NMR (benzene- $d_6$ , 128 MHz):  $\delta$ -16.3. IR (KBr,  $\text{cm}^{-1}$ ): 3063 w, 3042 w, 2999 m, 2963 s, 2927 s, 2879 s, 2834 m, 1611 m, 1567 s, 1485 w, 1461 m, 1432 w, 1387 w, 1365 m, 1335 w, 1303 w, 1276 s, 1252 m, 1194 s, 1155 m, 1130 w, 995 s, 968 s, 894 w, 874 w, 838 w, 816 w, 775 w, 729 m, 704 m. EA: Anal. Calcd for  $\text{C}_{29}\text{H}_{41}\text{BN}_3\text{O}_3\text{Rh}$ : C, 58.70; H, 6.96; N, 7.08. Found: C, 58.57; H, 6.77; N, 7.01. Mp: 180-185 °C, dec.

**Representative example of catalytic alcohol decarbonylation.** A mixture of cyclohexanemethanol (0.09 mmol),  $\text{To}^{\text{M}}\text{Ir}(\eta^4\text{-C}_8\text{H}_{12})$  (**5.11**) (0.005 mmol), cyclooctane (0.09 mmol) as an internal standard and toluene- $d_8$  (0.6 mL) was loaded into a J-Young style NMR tube. The tube was sealed and heated at 180 °C for 4 days. The progress of the reaction was monitored by  $^1\text{H}$  NMR spectroscopy. After the reaction, the solution was diluted with  $\text{CH}_2\text{Cl}_2$  and the yield of cyclohexane was determined by GC-MS from a calibration curve.

**Procedure for Preparative Scale Catalysis.** A Schlenk tube was charged with the  $\text{To}^{\text{M}}\text{Ir}(\eta^4\text{-C}_8\text{H}_{12})$  (**5.11**) (0.11 mmol), substrate (2.1 mmol), and toluene (10 mL). The tube was heated at 180 °C for 4 days. After the catalysis, the products were purified either by fractional distillation *in vacuo*, or by silica gel column chromatography.

**Cyclopentane from cyclopentanemethanol** (Table 5.3; entry 3). The product (0.138 g, 1.38 mmol) was isolated by fractional distillation (47-50 °C) in 65.7% yield.

***tert*-Butylbenzene from 4-(*tert*-butyl)benzylalcohol** (Table 5.3; entry 9). The product (0.187 g, 1.39 mmol) was purified by silica gel column chromatography (hexane:EtOAc = 3:1;  $R_f$  = 0.93) in 66.2% yield.

## References

- (1) Klass, D. L. *Biomass for Renewable Energy, Fuels and Chemicals*; Academic Press: San Diego, 1998.
- (2) Huber, G. W.; Iborra, S.; Corma, A. *Chem. Rev.* **2006**, *106*, 4044-4098.
- (3) (a) Cook, G. K.; Andrews, M. A. *J. Am. Chem. Soc.* **1996**, *118*, 9448-9449. (b) Ziegler, J. E.; Zdilla, M. J.; Evans, A. J.; Abu-Omar, M. M. *Inorg. Chem.* **2009**, *48*, 9998-10000. (c) Schlaf, M.; Ghosh, P.; Fagan, P. J.; Hauptman, E.; Bullock, R. M. *Adv. Synth. Catal.* **2009**, *351*, 789-800. (d) Vkuturi, S.; Chapman, G.; Ahmad, I.; Nicholas, K. M. *Inorg. Chem.* **2010**, *49*, 4744-4746. (e) Ahmad, I.; Chapman, G.; Nicholas, K. M. *Organometallics* **2011**, *30*, 2810-2818. (f) Stanowski, S.; Nicholas, K. M.; Srivastava, R. S. *Organometallics* **2012**, *31*, 515-518.
- (4) Bond energy references: (a) Sanderson, R. T. *Polar covalence*; Academic Press: New York, 1983. (b) Sanderson, R. T. *Chemical bonds and bond energy*, 2<sup>nd</sup> ed.; Academic Press: New York, 1976.
- (5) (a) Huber, G. W.; Chheda, J. N.; Barrett, C. J.; Dumesic, J. A. *Science* **2005**, *308*, 1446-1450. (b) de Lasa, H.; Salices, E.; Mazumder, J.; Lucky, R.; *Chem. Rev.* **2011**, *111*, 5404-5433. (c) Matson, T. D.; Barta, K.; Iretskii, A. V.; Ford, P. C. *J. Am. Chem. Soc.* **2011**, *133*, 14090-14097.
- (6) (a) Vaska, L.; DiLuzio, J. W. *J. Am. Chem. Soc.* **1961**, *83*, 2784-2785. (b) Chaudret, B. N.; Cole-Hamilton, D. J.; Nohr, R. S.; Wilkinson, G. *J. Chem. Soc., Dalton Trans.* **1977**, 1546-1557. (c) Kawai, T.; Sakata, T.; *J. Chem. Soc., Chem. Commun.* **1980**, 694-695. (d) Morton, D.; Cole-Hamilton, D. J.; Utuk, I. D.; Paneque-Sosa, M.; Lopez-Poveda, M. *J. Chem. Soc., Dalton Trans.* **1989**, 489-495. (e) Chen, Y.-Z.; Chan, W. C.; Lau, C. P.; Chu, H. S.; Lee, H.

- L.; Jia, G. *Organometallics* **1997**, *16*, 1241-1246. (f) Coalter, J. N.; Huffman, J. C.; Caulton, K. G. *Organometallics* **2000**, *19*, 3569-3578. (g) Morales-Morales, D.; Redón, R.; Wang, Z.; Lee, D. W.; Yung, C.; Magnuson, K.; Jensen, C. M. *Can. J. Chem.* **2001**, *79*, 823-829. (h) Klei, S. R.; Golden, J. T.; Tilley, T. D.; Bergman, R. G. *J. Am. Chem. Soc.* **2002**, *124*, 2092-2093. (i) Boaretto, R.; Paolucci, G.; Sostero, S.; Traverso, O. *J. Mol. Catal. A: Chem.* **2003**, *204-205*, 253-258. (j) Dinger, M. B.; Mol, J. C. *Organometallics* **2003**, *22*, 1089-1095. (k) Kloek, S. M.; Heinekey, D. M.; Goldberg, K. I. *Organometallics* **2006**, *25*, 3007-3011. (l) Bolton, P. D.; Grellier, M.; Vautravers, N.; Vendier, L.; Sabo-Etienne, S. *Organometallics* **2008**, *27*, 5088-5093. (m) Melnick, J. G.; Radosevich, A. T.; Villagrán, D.; Nocera, D. G. *Chem. Commun.* **2010**, *46*, 79-81.
- (7) (a) Charman, H. B.; *J. Chem. Soc. Phys. Org.* **1967**, 629-632. (b) Morton, D.; Cole-Hamilton, D. J. *J. Chem. Soc. Chem. Commun.* **1988**, 1154-1156. (c) Zhang, J.; Gandelman, M.; Shimon, L. J. W.; Rozenberg, H.; Milstein, D. *Organometallics* **2004**, *23*, 4026-4033. (d) Fujita, K.-I.; Tanino, N.; Yamaguchi, R. *Org. Lett.* **2007**, *9*, 109-111. (e) Kawahara, R.; Fujita, K.-I.; Yamaguchi, R. *J. Am. Chem. Soc.* **2012**, *134*, 3643-3646.
- (8) (a) Ohno, K.; Tsuji, J. *J. Am. Chem. Soc.* **1968**, *90*, 99-107. (b) Doughty, D. H.; Pignolet, L. H. *J. Am. Chem. Soc.* **1978**, *100*, 7083-7085. (c) Abu-Hasanayn, F.; Goldman, M. E.; Goldman, A. S.; *J. Am. Chem. Soc.* **1992**, *114*, 2520-2524. (d) Beck, C. M.; Rathmill, S. E.; Park, Y. J.; Chen, J.; Crabtree, R. H.; Liable-Sands, L. M.; Rheingold, A. L. *Organometallics* **1999**, *18*, 5311-5317. (e) Kreis, M.; Palmelund, A.; Bunch, L.; Madsen, R. *Adv. Synth. Catal.* **2006**, *348*, 2148-2154. (f) Iwai, T.; Fujihara, T.; Tsuji, Y. *Chem. Commun.* **2008**, 6215-6217. (g) Roa, A. E.; Salazar, V.; López-Serrano, J.; Oçate, E.; Paneque, M.; Poveda, M. L. *Organometallics* **2012**, *31*, 716-721.

- (9) (a) Delgado-Lieta, E.; Luke, M. A.; Jones, R. F.; Cole-Hamilton, D. J. *Polyhedron* **1982**, *1*, 836-838. (b) Morton, D.; Cole-Hamilton, D. J. *J. Chem. Soc. Chem. Commun.* **1987**, 248-249. (c) Morton, D.; Cole-Hamilton, D. J.; Utuk, I. D.; Paneque-Sosa, M.; Lopez-Poveda, M. *J. Chem. Soc. Dalton Trans.* **1989**, 489-495.
- (10) Park, J. H.; Cho, Y.; Chung, Y. K. *Angew. Chem.* **2010**, *122*, 5264-5267; *Angew. Chem. Int. Ed.* **2010**, *49*, 5138-5141.
- (11) Ruberu, T. P. A.; Nelson, N. C.; Slowing, I. I.; Vela, J. *J. Phys. Chem. Lett.* **2012**, *3*, 2798-2802.
- (12) Ho, H.-A.; Manna, K.; Sadow, A. D. *Angew. Chem.* **2012**, *124*, 8735-8738; *Angew. Chem. Int. Ed.* **2012**, *51*, 8607-8610.
- (13) Dunne, J. F.; Manna, K.; Wiench, J. W.; Ellern, A.; Pruski, M.; Sadow, A. D. *Dalton Trans.* **2010**, *39*, 641-653.
- (14) Dunne, J. F.; Su, J.; Ellern, A.; Sadow, A. D. *Organometallics* **2008**, *27*, 2399-2401.
- (15) Ho, H.-A.; Dunne, J. F.; Ellern, A.; Sadow, A. D. *Organometallics* **2010**, *29*, 4105-4114.
- (16) (a) Yang, X.; Stern, C. L.; Marks, T. J. *J. Am. Chem. Soc.* 1994, *116*, 10015-10031. (b) Yang, X.; Stern, C. L.; Marks, T. J. *J. Am. Chem. Soc.* 1991, *113*, 3623-3625. (c) Chen, E. Y.-X.; Marks, T. J. *Chem. Rev.* 2000, *100*, 1391-1434.
- (17) Pawlikowski, A. V.; Gray, T. S.; Schoendorff, G.; Baird, B.; Ellern, A.; Windus, T. L.; Sadow, A. D. *Inorg. Chim. Acta* **2009**, *362*, 4517-4525.
- (18) Zakzeski, J.; Bruijninx, P. C. A.; Jongerius, A. L.; Weckhuysen, B. M. *Chem. Rev.* **2010**, *110*, 3552-3599.
- (19) Herde, J. L.; Lambert, J. C.; Senoff, C. V. *Inorg. Synth.* **1974**, *15*, 18-20.
- (20) Giordano, G.; Crabtree, R. H. *Inorg. Synth.* **1990**, *28*, 88-90.

- (21) McCleverty, J. A.; Wilkinson, G. *Inorg. Synth.* **1966**, 8, 211.
- (22) Reich, H. J., Borst, J. P.; Dykstra, R. R.; Green, D. P. *J. Am. Chem. Soc.* **1993**, 115, 8128-8741.

## Chapter 6 – Conclusion

The design and synthesis of chiral ligands remain an important area of developing metal-catalyzed asymmetric transformations. In particular, developing ligands for enantioselective olefin hydroamination has seen tremendous growth in the past two decades. Despite significant advances, enantioselective hydroamination catalysts are typically limited by poor substrate scopes, low enantioselectivity and diastereoselectivity. We have synthesized a new class of chiral ligands cyclopentadienyl-bis(oxazolanyl)borates and their yttrium and zirconium complexes for enantioselective hydroamination of aminoolefins.

Our cyclopentadienyl-bis(oxazolanyl)borato zirconium and hafnium complexes are unusually active for catalytic cyclization of aminoolefins at room temperature or even at  $-30\text{ }^{\circ}\text{C}$ , in contrast to other group 4 hydroamination catalysts that requires elevated temperature. Both zirconium and hafnium precatalysts provide several 2-methyl-pyrrolidines with very high enantiomeric excesses up to 99%. The zirconium precatalysts is also oxo- and halogen-functional group tolerant. Additionally, the zirconium precatalyst cyclizes aminoheptenes at room temperature affording optically active seven-membered azepanes with greater than 90% ee. Our mechanistic investigations suggest a non-insertive mechanism involving concerted C–N/C–H bond formation in the turn-over limiting step of the catalytic cycle.

$\{\text{PhB}(\text{C}_5\text{H}_4)(\text{Ox}^{4S\text{-iPr,Me}_2})_2\}\text{Zr}(\text{NMe}_2)_2$  also desymmetrizes olefin moieties of achiral non-conjugated aminodienes and aminodiyne during cyclization. The dsymmetrization of aminodienes affords diastereomeric mixture of *cis* and *trans* cyclic amines with high diastereomeric ratios and excellent enantiomeric excesses. Similarly, the desymmetrization of alkyne moieties in  $\{S\text{-2}\}\text{Zr}(\text{NMe}_2)_2$ -catalyzed cyclization of aminodiyne provides

corresponding cyclic imines bearing quaternary stereocenters with enantiomeric excesses up to 93%. The *cis/trans* ratio can be systematically tuned in favor of either *cis* or *trans* diastereomer by controlling the concentration of the substrate, temperature, *N*-deuteration of the substrate, and the primary amine additive.

Cyclopentadienyl-bis(oxazoliny)borato yttrium complex  $\{\text{PhB}(\text{C}_5\text{H}_4)(\text{Ox}^{4S-t\text{Bu}})_2\}\text{YCH}_2\text{SiMe}_3$  displays highly enantioselective in the cyclization of aminoalkenes at room temperature affording cyclic amines with enantiomeric excesses up to 96%. The yttrium precatalyst provides cyclic amines with *S*-configuration, whereas *R*-configured amines are obtained by the corresponding zirconium precatalysts even though the identical chiral ancillary ligand is present. A noninsertive mechanism involving a six-membered transition state by a concerted C–N bond formation and N–H bond cleavage is proposed for  $\text{PhB}(\text{C}_5\text{H}_4)(\text{Ox}^{4S-t\text{Bu}})_2\}\text{YCH}_2\text{SiMe}_3$ -catalyzed hydroamination based on the kinetic, spectroscopic, and stereochemical features.

Cyclopentadienyl-bis(oxazoliny)borates have been proven as superior chiral ancillary ligands in asymmetric olefin hydroamination. The group 3 and group 4 complexes containing cyclopentadienyl-bis(oxazoliny)borates could be useful catalyst to prepare various azacycles that are important building blocks for synthesizing natural products and drug molecules. Additionally, several other cyclopentadienyl-bis(oxazoliny)borate containing main group and transition metal complexes could be synthesized, which might find application as catalysts in various industrially important processes such as stereoselective olefin copolymerization and olefin hydrosilation.

In this thesis, we have also reported several bis- and tris(oxazoliny)borato iridium and rhodium complexes for acceptorless dehydrogenative decarbonylation of primary alcohols. Our

catalysts survey shows that the compound  $\text{To}^{\text{M}}\text{Ir}(\eta^4\text{-C}_8\text{H}_{12})$  is the most active for the conversion of primary alcohols into alkane,  $\text{H}_2$ , and  $\text{CO}$  at  $180\text{ }^\circ\text{C}$  in toluene. Several aliphatic and aromatic primary alcohols are decarbonylated in the catalytic conditions. Furthermore,  $\text{To}^{\text{M}}\text{Ir}(\eta^4\text{-C}_8\text{H}_{12})$  is also able to decarbonylate polyols such as ethylene glycol and glycerol to syngas ( $\text{H}_2$  and  $\text{CO}$ ) at  $180\text{ }^\circ\text{C}$ .

In industry, the production of syngas from biomass relies on gasification at high temperature (above  $400\text{ }^\circ\text{C}$ ). In this respect, the decarbonylation of polyols to syngas catalyzed by  $\text{To}^{\text{M}}\text{Ir}(\eta^4\text{-C}_8\text{H}_{12})$  at  $180\text{ }^\circ\text{C}$  is remarkable. Therefore,  $\text{To}^{\text{M}}\text{Ir}(\eta^4\text{-C}_8\text{H}_{12})$  will be tested as catalysts for conversion of cellulose and sugars to syngas at low temperature. Additionally, the future directions will be continued on grafting the oxazolinylborato iridium catalysts on mesoporous silica nanoparticles for developing heterogeneous catalysts for acceptorless decarbonylation of alcohols .



## VITA

NAME OF AUTHOR: Kuntal Manna

PLACE OF BIRTH: Ghatal, West Midnapur, W.B., India.

### DEGREES AWARDED:

- B.S. Chemistry (Hons.), Vidyasagar University, India, 2004.
- M. S. Chemistry, Indian Institute of Technology, Kanpur, 2006.

### HONORS AND AWARDS:

- Graduate and Professional Student Senate Peer Research Award, Iowa State University, 2012.
- ACS-DIC Student Travel Award, American Chemical Society, 2012.
- The Henry Gilman Fellowship, Iowa State University, 2011.
- The Frank J. Moore and Thoreen Beth Moore Fellowship, Iowa State University, 2010.
- Chevron Phillips and P&G travel award, 2012, 2010.
- Junior Research Fellowship, CSIR (Council of Scientific and Industrial Research), India, 2006.
- 'First Class First' in B.Sc. (Honors in Chemistry), Vidyasagar University, W.B., India, 2004.
- Pitambar Das Memorial Scholarship with silver medal, Banamalichatta High School, India, 1999.
- SBI scholarship, State Bank of India, India, 1994-2004.

### PROFFESIONAL EXPERIENCE:

Teaching and Research Assistant, Department of Chemistry, Iowa State University, 2007-2012

### PROFESSIONAL PUBLICATIONS:

- Ho, H.-A., **Manna, K.**, Sadow, A. D. "Acceptorless Photocatalytic Dehydrogenation for Alcohol Decarbonylation and Imine Synthesis" *Angew. Chem., Int. Ed.* **2012**, *51*, 8607-8610.
- **Manna, K.**; Kruse, M. L.; Sadow, A. D. "Concerted C–N/C–H Bond Formation in Highly Enantioselective Yttrium(III)-Catalyzed Hydroamination" *ACS Catalysis* **2011**, *1*, 1637-1642.
- **Manna, K.**; Xu, S.; Sadow, A. D. "A Highly Enantioselective Zirconium Catalyst for Intramolecular Alkene Hydroamination: Significant Isotope Effects on Rate and Stereoselectivity" *Angew. Chem., Int. Ed.* **2011**, *50*, 1865-1868.
- **Manna, K.**; Ellern, A.; Sadow, A. D. "A Zwitterionic Zirconium Complex that Catalyzes Hydroamination of Aminoalkenes at Room Temperature" *Chem. Commun.* **2010**, *46*, 339-341.
- Dunne, J. F.; **Manna, K.**; Wiench, J. W.; Ellern, A.; Pruski, M.; Sadow, A. D. "Bis(oxazolinyl)phenylborane: A Lewis Acid-containing Ligand for Methide Abstraction-based Coordination to Aluminum(III)" *Dalton Trans.* **2010**, *39*, 641-653.
- **Manna, K.**; Ellern, A.; Sadow, A. D. "Neutral Cyclopentadienyl-bis(oxazolinyl)borato Group 4 Complexes as Catalysts for Enantioselective Hydroamination of Aminoolefins" *submitted.*

- **Manna, K.;** Ellern, A.; Sadow, A. D. “Acceptorless Thermal Decarbonylation of Alcohols Catalyzed by Oxazolinyborato Iridium Complexes” *manuscript in preparation.*
- **Manna, K.;** Sadow, A. D. “The Desymmetrization of Non-Conjugated Aminodienes and Aminodiynes through Enantioselective and Diastereoselective Hydroamination” *manuscript in preparation.*
- **Manna, K.;** Sadow, A. D. “Chiral Cyclopentadienyl-bis(oxazoliny)borato Lanthanide Catalysts for Enantioselective Hydroamination” *manuscript in preparation.*